

Design and Biological Evaluation of Novel *Staphylococcus aureus* DNA GyrB Inhibitors to Treat Pathogenic Infections

THESIS

Submitted in partial fulfillment
of the requirements for the degree of
DOCTOR OF PHILOSOPHY

by

RENUKA J

ID No 2011PHXF422H

Under the Supervision of

Prof. D. SRIRAM



BITS Pilani

BITS Pilani | Dubai | Goa | Hyderabad

BIRLA INSTITUTE OF TECHNOLOGY AND SCIENCE, PILANI

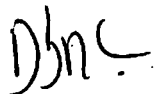
2016

BIRLA INSTITUTE OF TECHNOLOGY AND SCIENCE, PILANI

CERTIFICATE

This is to certify that the thesis entitled “**Design and biological evaluation of novel *Staphylococcus aureus* DNA GyrB inhibitors to treat pathogenic infections**” submitted by **RENUKA J** ID No. **2011PHXF422H** for award of Ph.D. of the Institute embodies original work done by he under my supervision.

Signature of the Supervisor:



Name in capital letters:

D. SRIRAM

Designation:

Professor

Date:

07.04.16

ACKNOWLEDGEMENT

Desire and determination- the foundation of all success

Ute Wieczorek-King

I might not be able to do adequate justice in this task of acknowledging my indebtedness to all those who have directly as well as indirectly made it possible to complete my thesis. I am going to try anyway, and if your name is not listed, rest assured that my gratitude is not less than for those listed below.

First and foremost, I would like to thank God Almighty, who has given me this opportunity.

*It's a fact that every mission needs a right spirit of hard work and dedication, but it needs to be put on the right path to meet its destination and in my case this credit goes to my esteemed supervisor respected **Prof. D. Sriram**, for his encouragement, continuous support, valuable suggestion and timely advice, without whom my thesis would not have been a success. This has thus been a memorable phase of about three and a half years and he shall always remain my greatest inspiration. I am short of words to thank him for his patience throughout the duration of the thesis work.*

*I deeply acknowledge and convey my heartfelt thanks to **Prof. P. Yogeeswari**, Department of Pharmacy, BITS, Pilani-Hyderabad campus, for her valuable suggestions, guidance and precious time which she offered me throughout my research as one of my DAC member.*

*With immense pleasure and profound sense of gratitude, I take this golden opportunity to express my heartfelt and sincere indebtedness to my other DAC member **Prof. A. Sajeli Begum**, Department of Pharmacy, BITS, Pilani-Hyderabad campus, for the precious suggestions and guidance during my research work.*

I am grateful to Prof. Bijendra Nath Jain, Vice-Chancellor (BITS) and Director Prof. V.S.Rao (Hyderabad campus), for allowing me to carry my doctoral research work in the institute.

I would like to express my gratitude towards Prof. Shrikant Yashwant Charde, Head of the department, Pharmacy, for providing me competent laboratory facilities and for having helped me at various stages of my research work.

I am thankful to Prof. S. K. Verma, Dean, Academic Research Division, BITS-Pilani and Prof. Vidya Rajesh, Associate Dean, Academic Research Division, BITS-Pilani, Hyderabad campus for their cooperation and encouragement at every stage of research work.

I sincerely acknowledge the help rendered by Prof. Punna Rao Ravi, Dr. V. Vamsi Krishna, Dr. Swati Biswas, Dr. Onkar Prakash Kulkarni, Dr. Arti Dhar faculties at the BITS-Pilani, Hyderabad campus.

I am extremely grateful to our laboratory assistants, Mr. Srinivas, Mrs. Saritha, Mr. Rajesh, and Mrs. Rekha of the animal house.

I would like to render my special thanks to my friends Shalini Saxena, Bobesh Andrews, Bhramam, Jean Kumar, Vijay Soni, Pushkar Kulkarni, Mallika, Nikhila, Brindha and Priyanka Suryadevara for their kind support and help towards completion of my work.

I would also like to thank all my colleagues, Ganesh P, Ganesh S, Priyanaka P, Reshma R, Prashanthi, Srikanth R, Rukkaya, Shubham, Manoj, Radhika, Madhubabu, Praveen, Suman, Poorna, Gangadhar, Saketh, Srikanth, Shailender, Santhosh, Patrish, Priyanka U, Preeti, Prakruti, Submitha, Anup Jose, Omkar.

The good wishes of all my well-wishers not mentioned here are gratefully acknowledged.

My vocab falls short to express my sense of gratitude and indebtedness to my father J. Ram Reddy and my mother Jayamma and my brother Mr. Yogeshwar Reddy for their restless effort and selfless sacrifices in order to fulfil my need and ambitions without which I could never have reached these heights.

*Similarly, I would like to thank my uncle **K. Shekar Reddy** and my aunt **P. Vasumathi** for their immense support throughout my education.*

*My heartfelt thanks to my father-in-law **Mr. P. Upender Reddy**, mother-in-law **P. Nageshwari** and sister-in-law **P. Pravalika** for their support.*

*I would like to dedicate this piece of work to **my parents**, whose dreams had come to life with me getting the highest degree in education. I owe my doctorate degree to **my parents** who kept with their continuous care, support and encouragement my morale high.*

*Most importantly, I would thank my husband, **Mr. Venkat Koushik Pulla**, who has supported me in the darkest times and believed in me even when I did not believe in myself though. Your tireless effort enabled me to take the time necessary to complete this work. This would not have possible without your support. No words can express how grateful I am for your kind support.*

Lastly, I am grateful for the financial assistance given by Under Grant Commission (UGC) and Council of Scientific and Industrial Research (CSIR), Government of India, New Delhi, during the course of this study in the form of Senior Research fellowship (SRF).

Renuka Janupally

ABSTRACT

Staphylococcus aureus remains to be one of the pathogens which can modify its genome easily and undergo multidrug resistance in very short duration. The rate of mutation^{2w} is high and about 30 efflux pumps located on its cell membrane makes it more prone to resistance. Moreover, despite the success of genomics in identifying new essential bacterial genes in these years of drug discovery, yet there is a lack of sustainable leads in antibacterial drug discovery to address increasing multidrug resistance. In the present study, we explored the pharmaceutically underexploited regions of *S. aureus* DNA Gyrase and one of its catalytic domain DNA Gyr B as potential platform for developing novel agents that target multidrug resistant *S. aureus* which is responsible for various infections of different degrees.

Utilizing the *in silico* computational tools of structure based drug design approach, Methyl 3-(2-(4-(5-chloro-1H-benzo[d]imidazol-2-yl)piperidin-1-yl)acetamide)benzoate was identified as potential DNA gyrase NBTI lead which was further optimized to obtain a better compound 2-(4-(5-methyl-1H-benzo[d]imidazol-2-yl)piperidin-1-yl)-N-(6-nitrobenzo[d]thiazol-2-yl)acetamide with IC_{50} of $0.32 \pm 0.17 \mu\text{M}$, almost half the drug concentration of the lead and with improved biological and biophysical properties.

Similarly, two lead molecules were identified against DNA Gyr B domain, these leads obtained from the targets were further customized using a combination of molecular docking and chemical synthesis to develop various analogues that displayed considerable properties. Compounds 6-(4-(1H-benzo[d]imidazol-2-yl)phenyl)-5-oxohexanoic acid and 3-(4-(furan-2-carboxamido)phenyl carbamoyl)propanoic acid which were further lead optimized to get 5-((4-

(5-Fluoro-1H-benzo[d]imidazol-2-yl)phenyl)amino)-5-oxopentanoic acid and N-(4-(4-Hydrazinyl-4-oxobutanamido)phenyl)-5-methylfuran-2-carboxamide which possess better Gyr B and other biological properties compared to the lead molecules. Biological properties include minimum inhibitory concentration of the drugs in MTCC3160 and MTCC96 strains, toxicity studies, inhibition of biofilm formation studies, efflux pump inhibitor studies, T_m studies using biophysical studies.

With new anti-staphylococcal agents desperately needed, we believe that the present class of inhibitors targeting both the DNA gyrase and DNA Gyr B domain presented in this work would be interesting as potential leads further in developing rational drug design against methicillin-resistant *Staphylococcus aureus* (MRSA) strain from pharmaceutical and drug development point of view. ^{what does this mean?}

Table of contents

<i>Contents</i>	<i>Page No.</i>
<i>Certificate</i>	<i>i</i>
<i>Acknowledgements</i>	<i>ii-iv</i>
<i>Abstract</i>	<i>v-vi</i>
<i>List of Tables</i>	<i>xi</i>
<i>List of Figures</i>	<i>xii-xiii</i>
<i>List of Abbreviations</i>	<i>xiv-xv</i>
CHAPTER 1 – INTRODUCTION	1-10
1.1. Epidemiology	1
1.2. The causative agent <i>S. aureus</i>	2
1.3. History of the current drug therapy	4
1.4. Problems with current treatment of <i>S. aureus</i> infections	6
1.5. The current Staphylococcal drugs in pipeline	8
CHAPTER 2 – LITERATURE REVIEW	11-25
2.1. Importance of DNA Gyrase, a type II topoisomerase	12
2.1.1. Structural information	12
2.1.2. DNA Gyrase as a drug target	14
2.1.3. Mechanism of the DNA Gyrase enzyme	15
2.2. Inhibitors available till date targeting the DNA Gyrase enzyme	18
2.2.1. Fluoroquinolones	18
2.3. Inhibitors targeting Gyr B domain of the DNA Gyrase	20
2.3.1. Aminocoumarins	20
2.3.2. Cyclothialidines	22
2.3.3. Pyrrolamides	22
2.3.4. Benzimidazoles	23
2.3.5. Bithiazoles	25
CHAPTER 3 – OBJECTIVES AND PLAN OF WORK	26-33
3.1. Objectives	26
3.2. Plan of work	27
3.2.1. To Design the NBTIs against <i>S. aureus</i> Gyrase and also new potent inhibitors against <i>S. aureus</i> DNA Gyr B domain	27
3.2.2. Cloning, expression and purification of <i>S. aureus</i> Gyr A, Gyr B and <i>E. coli</i> Gyr A proteins	28
3.2.2.1: Cloning, expression and purification of <i>Staphylococcal</i> Gyr A and Gyr B protein	28
3.2.2.2: Cloning, expression and purification of <i>E.coli</i> DNA Gyr A protein	28
3.2.3. Biological assessment of the <i>S. aureus</i> Gyrase enzyme and Gyr B protein with designed inhibitors	28
3.2.3.1. <i>In vitro</i> Gyr B inhibitory potency	28
3.2.3.2. <i>In vitro</i> supercoiling assay	29
3.2.4. Synthesis and characterization	29
3.2.5. <i>In vitro</i> <i>S. aureus</i> screening	29
3.2.5.1. <i>In vitro</i> activity in <i>S. aureus</i> MTCC strain	29

3.2.5.2. <i>In vitro</i> activity in <i>S. aureus</i> MRSA strains	29
3.2.6. <i>In vitro</i> cytotoxicity screening	30
3.2.7. Biofilm Inhibition studies	30
3.2.7.1. Quantitative assay of the biofilm formed on 96 well flat-bottomed microtiter plates	30
3.2.8. Evaluation of protein-inhibitor stability using biophysical technique	32
3.2.9. <i>zERG</i> channel inhibition studies	
3.2.10. Determination of time kill kinetics	33
CHAPTER 4 – MATERIALS AND METHODS	34-53
4.1. Identification of novel inhibitors targeting <i>S. aureus</i> enzymes	34
4.1.1. Identification of novel inhibitors targeting the <i>S. aureus</i> DNA Gyrase as a whole enzyme and DNA Gyr B domain alone	34-52
4.1.1.1. Structure based drug design approach	34
4.1.1.2. DNA Gyrase protein as a target	35
4.1.1.3. Protein and ligand preparation	35
4.1.1.4. Glide XP (Extra-Precision) docking	36
4.1.1.5. E-pharmacophore generation	36
4.1.1.6. Preparation of Asinex commercial database	37
4.1.1.7. High-throughput virtual screening and docking studies	38
4.1.1.8. Molecular docking studies using GOLD	39
4.1.1.9. QikProp analysis	39
4.1.2. Synthesis and characterization	40
4.1.2.1. Synthesis of top lead analogues of DNA gyrase NBTI inhibitor	40
4.1.2.1a. Synthetic protocol adopted for hit expansion of the leads obtained from structure-based virtual screening of DNA Gyrase (2XCS) protein	41
4.1.2.2. Synthesis of two series of the top two leads of DNA Gyr B inhibitor	41
4.1.2.2a. Synthetic protocol adopted for hit expansion of the lead molecule (A1) obtained from structure-based virtual screening of DNA Gyr B (3TTZ) protein.	42
4.1.2.2b. Synthetic protocol adopted for hit expansion of the lead molecule (B1) obtained from structure-based virtual screening of DNA Gyr B (3TTZ) protein.	43
4.1.3. <i>In vitro</i> biological evaluation	44
4.1.3.1. Cloning, expression and purification	45
4.1.3.2. Enzyme kinetics <i>S. aureus</i> Gyr B ATPase activity	46
4.1.3.3. <i>In vitro</i> Gyr B ATPase assay	46
4.1.3.4. <i>In vitro</i> supercoiling assay	47
4.1.3.5. <i>In vitro</i> antibacterial screening	48
4.1.3.6. <i>In vitro</i> cytotoxicity screening	49
4.1.3.7. Biophysical characterization using DSF	50
4.1.3.8. Biofilm inhibition studies	50
4.1.3.9. Quantitative assay of the biofilm formed on 96-well microtiter plates	51
4.1.3.10. <i>zERG</i> channel inhibition studies	52
4.1.3.11. Inhibition of drug efflux pump	53
4.1.3.12. Kill kinetics	53
CHAPTER 5 – RESULTS AND DISCUSSION	55-112
5.1. Development of new class of antibacterial agents against DNA gyrase as potential <i>anti-staphylococcal</i> inhibitors.	55
5.1.1. Novel inhibitors developed using structure based drug design strategy	56

5.1.1.1. Design and development of DNA Gyrase inhibitors based on GSK299423 inhibitor bound protein (PDB ID: 2XCS)	57
5.1.1.1.1. Protein preparation	57
5.1.1.1.2. E-pharmacophore generation	58
5.1.1.1.3. Virtual screening of commercial database	60
5.1.1.2. Biological validation of the virtually screened hits	67
5.1.1.2.1. <i>In vitro S. aureus</i> supercoiling assay	67
5.1.1.3. Hit expansion and lead optimization	69
5.1.1.3.1. Chemical synthesis and characterization	69
5.1.1.3.2. <i>In vitro</i> DNA supercoiling assay of the synthesized compounds with SAR	70
5.1.1.4. Antibacterial potency	71
5.1.1.5. Cytotoxicity studies	72
5.1.1.6. Inhibition of biofilm formation studies	72
5.1.1.7. Efflux pump inhibitor assay	73
5.1.1.8. <i>zERG</i> toxicity studies	73
5.1.1.9. Kill kinetics	74
5.2. Development of <i>S. aureus</i> DNA Gyr B inhibitors as potential inhibitors	77
5.2.1. Design and development of <i>S. aureus</i> DNA Gyr B inhibitors through structure based drug design strategy	77
5.2.2. Enzyme kinetics of <i>S. aureus</i> DNA Gyr B	74
5.2.2.1. <i>S. aureus</i> DNA Gyr B ATPase assay	81
5.2.3. Hit expansion and lead optimization of lead molecule (A1)	82
5.2.4. QikProp results	84
5.2.5. Biological validation	87
5.2.5.1. <i>S. aureus</i> DNA Gyr B ATPase assay with SAR	87
5.2.5.2. <i>S. aureus</i> DNA Gyrase supercoiling assay	88
5.2.5.3. Antibacterial activity	89
5.2.5.4. Cytotoxicity studies	90
5.2.5.5. Differential Scanning Fluorimetry	90
5.2.5.6. Inhibition of biofilm formation studies	92
5.2.5.7. <i>zERG</i> cardiotoxicity studies	94
5.3. Highlights of this study	97
5.4. Lead molecule (B1): Design and development of potential inhibitors of <i>S. aureus</i> DNA Gyr B via hit expansion and lead optimization of 4-((4-(furan-2-carboxamido)phenyl)amino)-4-oxobutanoic acid.	99
5.4.1. Gyr B activity of the synthesized analogues in correlation with the structure based drug design and its structure activity relationship (SAR)	100
5.4.2. Supercoiling assay	105
5.4.3. Antibacterial activity in Staphylococcal strains	106
5.4.4. Inhibition of biofilm formation studies	107
5.4.5. Cytotoxicity studies	108
5.4.6. <i>zERG</i> cardiotoxicity inhibition studies	108
5.4.7. Differential scanning fluorimetry studies	110
5.5. Highlights of this study	112
CHAPTER 6– SUMMARY AND CONCLUSION	113-114
FUTURE PERSPECTIVES	115
REFERENCES	116-125
Annexure-I	126-145
Annexure-II	146-169
Annexure-III	170-183

APPENDIX

List of publications and presentations

Biography of the candidate

Biography of the supervisor

184-189

187

188

189

List of tables

Table No	Description	Page No
Table 5.1	Energy scores of hypothesis in e-pharmacophore	60
Table 5.2	A QikProp analysis of the ADMET properties of the hits.	62
Table 5.3	Docking score, fitness, H-bond interactions and GOLD score of best fit ligands.	64
Table 5.4	Activity of the lead compounds with their DNA supercoiling results	68
Table 5.5	Biological activities of the synthesized compounds	76
Table 5.6	QikProp analysis of the ADMET properties of the synthesized molecules	85
Table 5.7	Biological evaluation of the synthesized compounds	96
Table 5.8	Biological activity data of the synthesized compounds	111

List of Figures

Figure No	Description	Page No
Figure 1.1	Pathogenesis of Staphylococcal Invasion of Tissue	5
Figure 2.1	(a) Different domains of DNA gyrase (b) A structural model for the Gyrase-DNA complex	13
Figure 2.2	Types of topoisomerases and their mode of action	15
Figure 2.3	A cascade of DNA-induced conformational changes prepares gyrase for strand passage	16
Figure 2.4	Model of conformational changes in the catalytic cycle of gyrase and their relation to strand passage	17
Figure 2.5	Chemical structures of quinolones	20
Figure 2.6	Chemical structures of aminocoumarins	21
Figure 2.7	Structure of Cyclothialidine	22
Figure 2.8	Structure of pyrrolamide with space for several substitutions.	23
Figure 2.9	Benzimidazoles targeting the DNA Gyrase and Topoisomerase IV	24
Figure 2.10	4,5'-Bithiazole compounds with available substitutions at R ₁ , R ₂ , R ₃	25
Figure 4.1	Synthetic pathway used to achieve the target compounds (R3-R42).	41
Figure 4.2	Synthetic scheme adopted for the lead derivatization to obtain the target compounds (S5-S44).	42
Figure 4.3	Synthetic scheme adopted for the lead derivatization to obtain the target compounds (T5-T28).	43
Figure 5.1	Superimposed pose of the crystal ligand GSK299423 and the docked pose of the same ligand with an RMSD of 0.95 Å.	58
Figure 5.2	Energy based e-pharmacophore with four features.	59
Figure 5.3	Virtual screening flowchart.	60
Figure 5.4	Top 15 lead molecules identified from Asinex database	63
Figure 5.5	Ligand-protein interactions of all the hits with the active site residues of <i>S. aureus</i> protein	65-66
Figure 5.6	Structure of L15 compound with an IC ₅₀ of 0.79±0.12 μM.	68
Figure 5.7	Synthetic procedure to obtain the final analogues.	70
Figure 5.8	(a) Mean (±S.E.M.) of the heart rate of atria and ventricles of R36 & R20 treatment groups. (*p<0.05, **p<0.01 and ***p<0.001). Statistical significance was analyzed with respect to the control group. (b) Mean (±S.E.M.) score of atrio ventricular ratio of treatment groups. (*p<0.05, **p<0.01 and ***p<0.001). Statistical significance was analyzed comparing control group Vs all the groups	74
Figure 5.9	Time kill kinetics of compound R20 in <i>S. aureus</i> . The MIC in the experiment was 0.03 μM.	75
Figure 5.10	3-point e-pharmacophore of 3TTZ Gyr B protein.	78
Figure 5.11	Crystal ligand interactions with the DNA Gyr B protein in the active site pocket.	79
Figure 5.12	Interaction pattern of crystal ligand with lead molecule A1 (BAS01355130).	79
Figure 5.13	Top twelve hit molecules obtained from Asinex database after virtual screening of 5 lakh molecules.	80
Figure 5.14	Enzyme kinetics of <i>S. aureus</i> Gyr B protein.	81
Figure 5.15	Lead molecule (A1) BAS01355130	82

Figure 5.16	The synthetic scheme used to achieve lead modification	83
Figure 5.17	Outline of the computational and biological work presented in this study.	86
Figure 5.18	Surface interaction picture of compound S10 with conserved amino acids accordance with ligand interaction diagram	87
Figure 5.19	Hill slope of the most active compound S10 with different log concentration of the inhibitor on X-axis % Inh on Y-axis.	88
Figure 5.20	Inhibitory profile of <i>S. aureus</i> DNA gyrase supercoiling activity by compound S10.	89
Figure 5.21	DSF experiment for compound showing an increase in thermal stability between the native G24 protein (blue) and DNA Gyr B protein-compound complex (red).	92
Figure 5.22	Dose-response curve of compound inhibition on <i>S. aureus</i> MRSA96 biofilm formation.	93
Figure 5.23	(a) Mean (\pm S.E.M.) of the heart rates of atria and ventricles of Compound-S10. (* p <0.05, ** p <0.01 and *** p <0.001). b) Mean (\pm S.E.M.) score of atrio ventricular ratio. (* p <0.05, ** p <0.01 and *** p <0.001). Statistical significance was analyzed comparing control group Vs all groups	95
Figure 5.25	Synthetic protocol adopted for the lead derivatization.	100
Figure 5.26	Structure of the identified lead molecule (B1)	102
Figure 5.27	Lead molecule (B1) at <i>S. aureus</i> Gyr B active site (a) Electrostatic surface view of Gyr B its hydrophobic pocket (b) Interaction of lead molecule (B1) at Gyr B pocket (pink lines indicate hydrogen bonds).	102
Figure 5.28	Interaction profile of most active compound T22 (green) showing hydrogen bonds (blue) with active site residues (yellow).	103
Figure 5.29	Dose response curve of compound T22 with log concentration of the inhibitor on X-axis and percentage inhibition Y-axis.	105
Figure 5.30	Depicting the inhibitory profile of <i>S. aureus</i> DNA gyrase supercoiling activity by compound T22 in dose dependent manner	106
Figure 5.31	(a) Mean (\pm SEM) of the heart rates of atria and ventricles of Compound T22. (* p <0.05, ** p <0.01 and *** p <0.001). (b) Mean (\pm SEM) score of atrio ventricular ratio. (* p <0.05, ** p <0.01 and *** p <0.001).	109
Figure 5.32	DSF experiment for compound T22 showing an increase in thermal stability between the native protein (blue with T _m of 45.1 oC) and DNA Gyr B protein-compound T22 complex (red with a T _m of 47.9) with a positive	110

Abbreviations

2D	:	Two-Dimensional
3D	:	Three-Dimensional
A	:	Acceptor
ATP	:	Adenosine triphosphate
AZ	:	AstraZeneca
BITS-Pilani	:	Birla Institute of Technology and Science, Pilani
Bp	:	Basepair
BTZ043	:	Benzothiazinones
¹³ C NMR	:	Carbon Nuclear Magnetic Resonance
CG	:	Conjugate gradient
CTD	:	C-terminal Domain
D	:	Donor
DNA	:	Deoxyribonucleic acid
DMSO	:	Dimethyl sulfoxide
DTT	:	Dithiothreitol
DSF	:	Differential scanning fluorimetry
EDTA	:	Ethylenediaminetetraacetic acid
ELISA	:	Enzyme-linked immunosorbent assay
EF	:	Enrichment factor
e-pharmacophore	:	Energy based pharmacophore
EPI	:	Efflux pump inhibitor
FBS	:	Fetal bovine serum
Gyr A	:	DNA gyrase A subunit
Gyr B	:	DNA gyrase B subunit
GSK	:	GalaxoSmithKline
GH	:	Goodness of hits
GOLD	:	Genetic Optimization for Ligand Docking
HTS	:	High-Throughput Screening
<i>hERG</i>	:	Human Ether-à-go-go-Related Gene
¹ H NMR	:	Proton Nuclear Magnetic Resonance
HPLC	:	High-Performance Liquid Chromatography
HTVS	:	High throughput virtual screening
HY	:	Hydrophobic
HBD	:	Hydrogen bond donor
HBA	:	Hydrogen bond acceptor
HEPES	:	(4-(2-hydroxyethyl)-1-piperazineethanesulfonic acid)
IPTG	:	Isopropyl β-D-1-thiogalactopyranoside
K _i	:	Inhibitor constant
K _d	:	Dissociation constant
KCl	:	Potassium chloride
KOH	:	Potassium hydroxide
LB	:	Luria-Bertani
L	:	Litre
LHS	:	Left hand side
ml	:	Mililiter

µg	:	Microgram
mg	:	Milligram
MIC	:	Minimum inhibitory concentration
µM	:	Micromolar
MTT	:	(4,5-dimethylthiazol-2-yl)-2,5-diphenyltetrazolium bromide
mmol	:	Millimole
M.p	:	Melting point
MgCl ₂	:	Magnesium chloride
MRSA	:	Methicillin resistant <i>Staphylococcus aureus</i>
NBTIs	:	Novel bacterial topoisomerase inhibitors
NTD	:	N-terminal Domain
nM	:	Nanomolar
NAD	:	Nicotinamide adenine dinucleotide
NADH	:	Nicotinamide adenine dinucleotide (reduced form)
N	:	Negative ionizable
NaCl	:	Sodium chloride
OADC	:	Oleic acid, Albumin, Dextrose, and Catalase
PAS	:	Para-aminosalicylic acid
PTH	:	Prothionamide
PDB	:	Protein Data Bank
PCR	:	Polymerase Chain Reaction
P	:	Positive ionizable
PBS	:	Phosphate buffered saline
RHS	:	Right hand side
RMSD	:	Root mean square deviation
rpm	:	Rotation per minute
rt	:	Room temperature
R	:	Ring aromatic
RPMI	:	Roswell Park Memorial Institute
S. a	:	<i>Staphylococcus aureus</i>
SD	:	Steepest descent
SP	:	Standard precision
SAR	:	Structure activity relationship
T _m	:	Melting temperature
TAE	:	Tris-acetate-EDTA
WHO	:	World Health Organization
XP	:	Extra precision
zERG	:	Zebrafish ether-a-go-go-related gene

Chapter 1

Introduction

Staphylococcus aureus, once considered as a normal flora inhabiting 30% of human population overall had emerged to the status of causative agent of many severe infections of immunocompromised patients and healthy humans in the community [McAdam, P. R., *et al.*, 2012]. In the recent past, *S. aureus* infections are a major cause of human morbidity and mortality in community and hospital settings as well [Lele, A. C., *et al.*, 2013]. Furthermore, *S. aureus* strains that combine resistant and virulent genes have become a major treatment problem in Europe, United States and developing countries like India. The organism is equipped with a cell wall, a capsule, surface proteins, enzymes and toxins [Franklin D. Lowy., *et al.*, 1998]. Usually the pathogenesis of the organism lies in the toxins produced and their mechanism of action. Toxins include the cytotoxins that cause septic syndrome, pyrogenic-toxin results in T-cell proliferation and cytokine release, enterotoxin ends in toxic shock syndrome and food poisoning and the exfoliative toxins causes scalded skin syndrome, although the mechanism of action of these toxins remains controversial [Franklin D. Lowy., *et al.*, 1998]. The diseases associated with *S. aureus* are bacteremia, endocarditis, sepsis, impetigo, scalded skin syndrome, cellulitis, folliculitis and toxic shock syndrome.

1.1. Epidemiology

Staphylococcal infections are common in humans and they are considered as natural reservoir of *S. aureus*. Several of the other Staphylococcal species involved in infections are *S.*

pseudintermedius, *S. epidermidis*, *S. saprophyticus*, *S. lugdunensis*, *S. schleiferi*, and *S. caprae*. Among 30% of the adults colonized, 10 to 20 percent are persistently colonized. Usually, persons colonized with *S. aureus* are at increased risk for subsequent infections. Rates of staphylococcal colonization are high among patients diagnosed with type I diabetes, intravenous drug users, patients undergoing hemodialysis, patients' undergone surgeries and patients with HIV infections. Children are more likely to be persistent carriers of the bacteria; however young women are at a higher risk for toxic shock syndrome [Henry F. Chambers., 2001]. A high percentage of hospital-acquired infections are caused by highly resistant bacteria such as methicillin-resistant *Staphylococcus aureus* (MRSA). Staphylococcal outbreaks result from exposure to a single long-term carrier or other environmental sources, though less common. According to the CDC, between 2005 and 2011, overall rates of invasive MRSA dropped 31%. However the same CDC reports, say over 80,000 invasive MRSA infections and 11,285 related deaths occur every year due to this Staphylococcal diseases.

1.2. The causative agent *S. aureus*

S. aureus are facultative anaerobes that usually form clusters, it is a Gram-positive, catalase positive cocci belonging to the Staphylococcaceae family which are nonmotile, non-spore-forming. *S. aureus* has a diverse arsenal of bacterial components and products that contribute to the pathogenesis of infection. Ideally, these components and products of the bacteria have overlapping roles and can act either in concert or alone. A lot is known about the contribution of these bacterial factors to the development and prognosis of the infections while very little is known about their interaction within the bacterial components and with host factors and their relative importance in infection [Franklin D. Lowy., *et al.*, 1998]. The organism is a commensal that colonizes the nares, axillae, vagina, pharynx and the damaged skin surfaces. The virulence

of *S. aureus* infection is remarkable as the infections are initiated when a breach of the skin or mucosal barrier allows staphylococci access due to a tear or rupture. The spread of the infection depends on a complex interplay between *S. aureus* virulence determinants and host defense mechanisms; however mucin appears to be the critical host surface that is colonized. Several factors contribute to the increased susceptibility to infection. Phagocytic function in the presence of foreign material is seriously impaired. Intravenous catheters are frequently implicated in the pathogenesis of bacteremia and nosocomial endocarditis. Moreover, inactivation of regulatory genes reduces bacterial virulence. *S. aureus* produce various enzymes, such as protease, hyaluronidase and lipase and that destroy the host tissue. β -Lactamase is an enzyme that inactivates penicillin, thus rendering ^{SINGLE ANTIBIOTIC} resistance to the organism against many antibiotics [Helen W. Boucher., *et al.*, 2009]. Statens Serum institut in Copenhagen collected more than 2,000 blood culture isolates of *S. aureus* from 1957 to 1966 for which detailed information on the origin of infection was studied, it was observed that high prevalence of penicillin resistance strains (85% to 90%) emerged from hospital isolates of *S. aureus*. The shocking incidence was that penicillinase producing strains were almost as common in the community; with 65% to 70% of isolates resistant to penicillin and several other antibiotics; however by the end of 1998, almost 50% of them were MRSA [Henry F. Chambers., 2001]. However, MRSA remains to be one of the difficult-to-treat ESKAPE pathogens (*Enterococcus faecium*, *S. aureus*, *Klebsiella pneumoniae*, *Acinetobacter baumannii*, *Pseudomonas aeruginosa*, and *Enterobacter species*) despite the introduction of several new antitherapeutic agents during the past decade [Boucher H. W., et al., 2009]. Further, more people now die of MRSA infection in US hospitals than of HIV/AIDS and tuberculosis combined [Klevens R. M., *et al.*, 2006; Boucher H. W., *et al.*, 2008].

1.3. History of the current drug therapy

Management of any disease usually includes abscess drainage, debridement of necrotic tissue, removal of foreign bodies including the artificially fixed intravascular catheters that lead to infections and use of antibiotics. However, initial choice and dosage of prescribed antibiotics depend on site of infection, the severity of illness and probability that resistant strains are involved [Ball P., *et al.*, 2002]. Thus, it is essential to know local resistance patterns for initial therapy towards a disease. In 1941, a wonder drug penicillin was introduced which served to treat the Staphylococcal infections but very soon in a span of 6 years, 25% of the hospital strains were resistant for this drug. Antibiotics selected based on severity of infection and local resistance patterns. The emergence and prevalence of penicillinase-producing strains of *S. aureus* within hospitals and communities soon began to rise as penicillin became readily available after World War II [Henry F. Chambers., 2001]. Yet penicillin continued to be recommended as an effective anti-staphylococcal agent as late as the 1970's due to lack of any other cost-effective treatment. Later it was observed that community-acquired isolates often were resistant only to penicillin due to production of penicillinase production, whereas nosocomial strains typically were resistant to multiple antibiotics [George H. Talbot., *et al.*, 2006]. By mid-1970s, almost about 70% to 85% prevalence of penicillin resistant strains was found regardless of location within and outside the United States. A survey was conducted in the mid-1980s by Center for Disease Control and the National Nosocomial Infections Surveillance (NNIS) data indicated that MRSA was limited within the urban medical centers and that rates were restricted to about 5 to 10%. Gradually, in 1990s, rates increased to 20% in smaller hospital areas, and twice that rate was found in the larger urban centers [Henry F. Chambers., 2001].

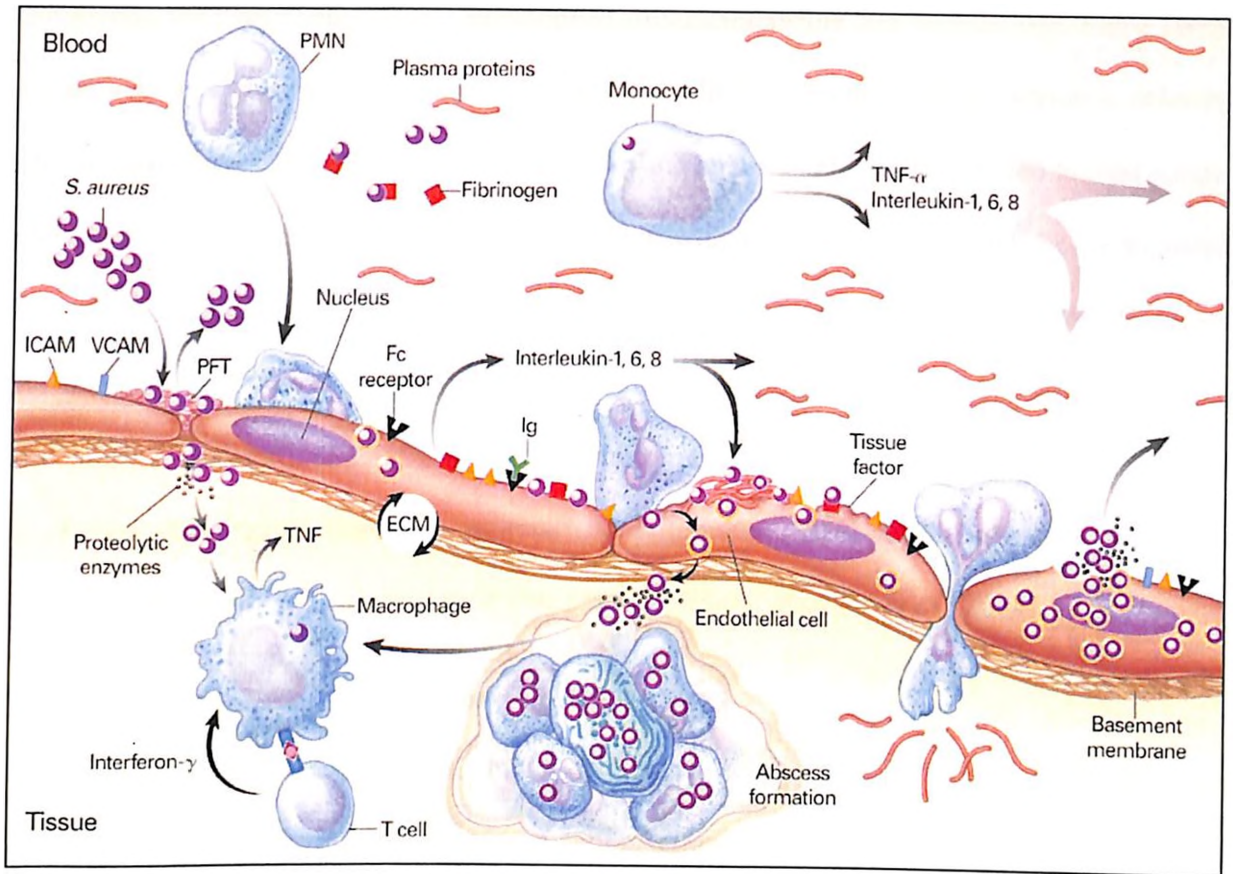


Figure 1.1: Pathogenesis of Staphylococcal Invasion of Tissue [Franklin D. Lowy., *et al.*, 1998]

By 1998, it ^{had} reached 50% with the prevalence of MRSA isolates from intensive care units, thus MRSA is now the etiologic pathogen for the majority of health care and community associated infections. Moreover, nosocomial MRSA infections are associated with higher morbidity, mortality, and medical costs ^{over} this the emergence of community-associated MRSA has raised additional concerns [George H. Talbot., *et al.*, 2006]. The communicability of this MRSA is much rapid because of their production of Panton-Valentine leukocidin, a virulence factor associated with severe, rapidly progressive infection, even in previously healthy individuals [Franklin D. Lowy., *et al.*, 1998]. ^{? How?} Due to relatively short staphylococcal cassette chromosome IV, community-associated MRSA strains possess limited number of resistance genes rendering them susceptible to non-β-lactam antibiotics, including orally bioavailable

compounds, such as clindamycin, trimethoprim-sulfamethoxazole and doxycycline. Since 1960s, vancomycin has been the mainstay of therapy for MRSA infections. Vancomycin is effective against most MRSA strains, but at times rifampin and an aminoglycoside is added to treat serious infections. At times, treatment of MRSA infection with vancomycin can often be complicated, due to its inconvenient route of administration of the drug (intravenously). However, vancomycin-resistant *S. aureus* (VRSA; MIC >16 mcg/mL) and vancomycin-intermediate susceptible *S. aureus* (VISA; MIC 4 to 8 mcg/mL) strains have appeared for which an alternative drugs like daptomycin, linezolid, quinupristin/dalfopristin, TMP-SMX, possibly ceftaroline should be considered to achieve greater success rates [Hiramatsu, K., *et al.*, 2014].

1.4. Problems with current treatment

The available therapies presently, have no longer found fully effective in treating the Staphylococcal infections because of the emerged antibiotic resistance, enzyme and toxins production, biofilm forming capacity and immune evasion capability have combined to accelerate the emergence of *S. aureus* as a globally important human pathogen. While the other ^{what?} failure for developing therapeutics to treat this gram-positive pathogen infections is the formation of biofilm compounded by the existence of multiple biofilm mechanisms in *S. aureus* and high resistant MRSA [Clarissa Pozz., *et al.*, 2012]. Rifampin is no longer recommended for monotherapy of acute bacterial skin and skin structure infections (ABSSSIs) because of the rapid development of resistance. Tetracyclines and TMP-SMX have limited activity against CA-MRSA, that too in the presence of beta-lactam agent, resistance is a concern even in the case of clindamycin. (.) Tetracyclines also have potential photosensitization potential. However, Doxycycline and minocycline also have a limited effect in adolescents and adults due to staining of dental enamel [Keith A., Rodvold., *et al.*, 2014]. In spite of newer therapies, for diagnosis and

treatment of Staphylococcal infections, unfortunately, millions of people are still suffering and dying from this disease. There are several major hindrances associated with the currently available treatment. Vancomycin, though considered as first line therapy yet the emergence of less-susceptible strains, poor clinical outcomes, its side effects mainly the increased nephrotoxicity with high-dose therapy are challenging its current role as first-line therapy [Keith A., Rodvold., *et al.*, 2014]. As MRSA is a major treat to the health care system, a significant risk factor for these healthcare associated infections is the extensive use of implanted prosthetic biomaterials for diagnostic and therapeutic purposes, which can be colonized by staphylococci giving rise to device-related infections (DVI) involving biofilms, current chemotherapeutics for DVI have limited effectiveness against biofilms [O’Gara J. P., *et al.*, 2007]. While novel target identification and validation are important components of drug discovery, success in the antibacterial therapy area is also critically dependent on the attributes of the chemical series synthesized against the target [Ann E. Eakin., *et al.*, 2012]. Successful antibacterial compounds must have appropriate properties to penetrate bacterial cells while also exhibiting *in vivo* and physicochemical properties suitable for achieving relatively high doses with acceptable safety margins. A study in the Journal of the American Medical Association shows a 28% decline in hospital-associated MRSA infections between 2005 and 2008 which is a good sign medically though reasons are unclear. [Anne-Catrin Uhlemann., *et al.*, 2014]. According to the Center for Disease Control and Prevention (CDC) there were estimated 94,360 MRSA infections (invasive) in the US with approx. 18,650 deaths in 2005. With time many bacterial MRSA strains have emerged namely EMRSA15, EMRSA16, MRSA252, CC8 strain, hospital-acquired MRSA (HA-MRSA) and community acquired MRSA (CA-MRSA). Both the EMRSA15 and EMRSA16 strains are resistant to erythromycin and ciprofloxacin indicating the urgency of developing

novel therapeutics [Paul R. McAdam., *et al.*, 2012]. Till date, MRSA stands as one among the top three superbugs which are highly resistant to all the antibiotics available with vancomycin-resistant Enterococcus (VRE) and multi-drug-resistant *Mycobacterium tuberculosis* (MDR-TB) being the other two [WHO, antibacterial resistance, fact sheet N*194]. Also, it is important to achieve shortened therapy to slow down the development of drug resistance in Staphylococcus.

1.5. The current drugs in pipeline

Though many drugs have been in market since decades to treat the Staphylococcal infections, presently none of them provide complete treatment. Hence novel classes of drugs are needed, as the current class of drugs exhibit treatment-limiting toxicities and emerging antibiotic resistance. MRSA came into existence when methicillin-susceptible *S. aureus* (MSSA) has acquired the methicillin-resistance gene *mecA* by horizontal gene transfer that was mediated by a mobile genetic element staphylococcal cassette chromosome (SCC) [Ito T., *et al.*, 1999]. Vancomycin is still the first-line antibiotic against MRSA infection though resistance against it as been reported [Hidayat L, K., *et al.*, 2006; Lodise T. P., *et al.*, 2008]. According to US Food and Drug Administration (FDA), 5 antiinfective agents have been approved for the treatment of MRSA based infections namely linezolid, daptomycin, tigecycline, telavancin, and ceftaroline.

Linezolid is the only available drug for Staphylococcal infections which can be taken in both an oral and an intravenous formulation and could be considered for empiric monotherapy of both CA-MRSA and beta-hemolytic streptococci. However, its clinical use has been limited to selective patients because of its high drug costs. Its mechanism of action is bacteriostatic by protein synthesis inhibition (23S RNA at 50S ribosomal subunit). Treatment is by Intravenous (IV) or by oral therapy (PO). Its side effects include, thrombocytopenia and anemia, peripheral

and optic neuropathy, lactic acidosis, serotonin syndrome. Drug is 100% bioavailable *via* oral formulation.

Daptomycin is a cyclic lipopeptide with activity against gram positive organisms including MRSA and vancomycin-resistant enterococci. It serves as an alternative to vancomycin for patients with MRSA bacteremia. Mechanism of action includes bactericidal effect and membrane depolarization (Ca⁺⁺ dependent). Mode of treatment is *via* Intravenous. Side effects include myopathy, peripheral neuropathy. It is very effective for MRSA bloodstream infections and right-side endocarditis, active against VRE, extensive published literature on treatment experiences for a wide range of MRSA infections. The drug is inactivated by pulmonary surfactant and should not be used to treat pneumonia.

The other drug **Tigecycline** is a semisynthetic derivative of minocycline, the first licensed drug from the glycylcycline class of antimicrobial agents. It has a broad spectrum activity that includes aerobic and anaerobic gram positive and gram negative pathogens as well as atypical pathogens. Mechanism of action is bacteriostatic and by protein synthesis inhibition (at 30S ribosomal subunit). Mode of administration is by Intravenous (IV). Causes GI side effects (nausea and vomiting). Drug is active against VRE bacteriostatic, low serum and ELF drug concentrations, causes high rates of GI adverse events and higher risk of mortality.

Telavancin ^{is} was a once-daily parenteral lipoglycopeptide approved for the treatment of adult patients with complications caused by MSSA and MRSA. Phase 3, randomized, double-blind clinical trials have investigated telavancin for the treatment of nosocomial pneumonia. Mechanism of action is by bactericidal effect, cell wall inhibition and membrane depolarization. Mode of administration is by Intravenous (IV). Side effects include, GI problems, mild QT

prolongation, nephrotoxicity. The drug is rapidly bactericidal against MRSA, VISA, and VRSA, also active against MRSA strains resistant to vancomycin, linezolid, and daptomycin. **Ceftaroline fosamil** is a first FDA-approved cephalosporin with an activity against MRSA. Phase 3, non-inferiority designed clinical trials have demonstrated that 5 to 14 days of intravenous ceftaroline should be administered. Mechanism of action is by bactericidal effect and cell wall inhibition. Mode of administration is by Intravenous. It's a well tolerated drug with <5% incidence of diarrhea, nausea, rash though moderately expensive.

Moreover, **tedizolid**, **dalbavancin**, and **oritavancin** are currently completing phase 3 clinical trials for the treatment of ABSSSIs caused by MRSA.

Chapter 2

Literature Review

Firstly, combating a disease with drug requires the identification of a target either a cellular component which, when acted upon by a drug, will lead to the death or cause an arrest in the growth of the cell. [Anthony Maxwell., 1997]. Importantly, in evolution neither we cannot avoid the emergence of new infectious agents nor the resistance developed against a target, but definitely one can work to mitigate these issues with target based drug designing in research that will yield new agents with novel mechanism in discovering and developing leads for new antimicrobials [Eric D. Brown., *et al.*, 2005]. Secondly, while there is a plethora of new targets with great potential for new drug discovery, the selection of any one of these remains the subject of considerable debate. The targets to be selected are normally validated with *in vitro* genetic methods to determine gene essentiality and its vitality [Bhavsar., *et al.*, 2001] [Guzman., *et al.*, 1995]. One can identify the ideal target such as an enzyme with fully elucidated function and mechanism, easily able to get purified in quantity as a recombinant protein such that it is amenable and subjectable to highthroughput assays and to downstream biochemical characterizations to sort out their mechanism of inhibition including co-structural examinations. Molecular factors that are essential for microbial virulence are also targeted and this is also one of the best strategy. Usually, in this approach, proteins associated with infection and replication are targeted rather than those which are ubiquitously required for growth [[Eric D. Brown., *et al.*, 2005]. In the case of an antibacterial, the ideal target is absent in the human host making this one of the reason, for its exploitation. In this great search for an effective target, one group of

enzymes that have proved their worth are the DNA Gyrase, a type II DNA topoisomerase. Being the only enzyme of this group, able to impart negative coils to the DNA, it occupies a unique position as a drug target as the absence of it induces stress and results in bactericidal activity.

2.1. Importance of DNA Gyrase, a type II topoisomerase

2.1.1. Structural information

The type II topoisomerase possess the following properties [Wang, J. C., 1996]: (a) The enzymes are dimeric with a bound duplex DNA. (b) The breakage and re-union of the strands involves covalent attachment of each subunit of the dimer to the end of the DNA *via* a 3' phosphotyrosine bond (c) Due to this, a conformational change is involved that pulls the two ends of the cleaved duplex DNA apart, resulting in an opening termed as the gated or G-segment DNA. Subsequently, the other region of duplex DNA referred to as the transported or T-segment, passes through the open DNA gate. This mechanism of the topoisomerase explains why the linking number is changed by a factor of two when the supercoiling of a circular DNA is changed [Brown, P. O., *et al.*, 1979; Mizuuchi, K., *et al.*, 1980; Liu, L. F., *et al.*, 1980] (d) The above supercoiling reactions require Mg(II) ions and ATP hydrolysis for enzyme turnover associated with rapid kinetics (e) The crystal structures of several topoisomerases reveal that the active site tyrosine residues are situated in a helix-turn-helix (HTH) motif found within a domain of the catabolite activator protein (CAP) of *E. coli*. In addition, acidic residues of the Rossmann fold appear to collaborate with the HTH region of the CAP-like domain to assemble the active site for catalysis that may be involved in metal ion binding [Nichols, M. D., 1999; Berger, J. M., 1998; Liu, Q. Y., 1999]. This fold was popularly referred as "toprim motif" as it is found in DNA primases as well as the DNA topoisomerases that catalyze phosphotransfers or hydrolyze

phosphodiester bonds [Nichols, M. D., *et al.*, 1999; Aravind, L., *et al.*, 1998] (f) All the type II topoisomerases from prokaryotic domain that were described till date contain two different subunits heterotetrameric in structure, while the eukaryotic enzymes are homodimers. Interestingly, different members of the type II family of topoisomerases can be distinguished by their relative proficiency of action performed at DNA relaxation versus decatenation and this property likely reflects their specialized roles in the cell. Furthermore, among all of the known type II enzymes, DNA gyrase stands alone as the only enzyme capable of introducing negative supercoils energetically driven by the hydrolysis of ATP, catalysed by the Gyr B subunit [Silke Alt., *et al.*, 2011]. The heterotetramer includes two GyrA and two Gyr B subunits. While the GyrA is involved in cleavage and religation of the DNA strands, the Gyr B subunits act as energy providers. For the first time in 2010, the *S. aureus* DNA Gyrase was co-crystallized with an inhibitor complex GSK299423 associated with DNA at 2.10 Å resolution (PDB ID = 2XCS) [Bax B.D., *et al.*, 2010]. Subsequently, in 2011 a group of scientists from AstraZeneca has succeeded in crystallizing *S. aureus* DNA Gyr B with a pyrrolamide inhibitor at a resolution of 1.63 Å (PDB ID = 3TTZ) [Sherer B. A., *et al.*, 2011].

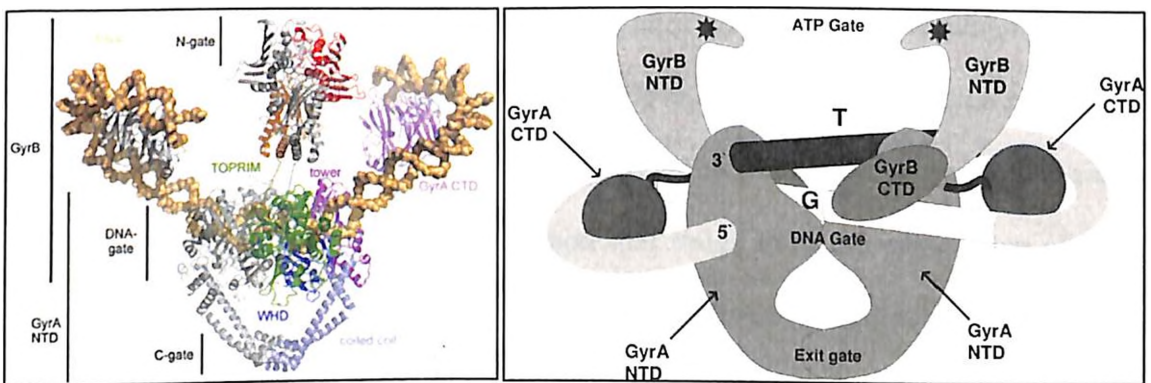


Figure 2.1: (a) Different domains of DNA gyrase [Gubaev et al., 2014] (b) A structural model of the Gyrase-DNA complex [Mark Oram., *et al.*, 2006]

2.1.2. DNA Gyrase as a drug target

Topoisomerases are ubiquitous enzymes present in all cells (prokaryote and eukaryote) have been shown to be essential for the organism survival. As they have important functions in DNA replication, eukaryotic topoisomerases are targets for antitumor agents, exploiting the fact that cancer cells divide more rapidly than other cell types. Camptothecin and etoposide are examples of antitumour drugs targeted to eukaryotic topoisomerases for viability. In the case of prokaryotes, DNA gyrase has been found to be an effective target for therapeutic agents [Anthony Maxwell., 1997]. Although gyrase is evolutionarily related to other topoisomerases, it is the only enzyme of this group that can introduce supercoils into DNA, thus relieving the stress in the bacterial DNA [Reece R. J., *et al.*, 1991; Wigley D. B., 1995]. This complex reaction appears to provide a great deal of scope for drug targeting, and several useful agents are known. In our efforts to find new compounds with activity against *S. aureus*, we have targeted the type IIA bacterial topoisomerase, DNA Gyrase, an essential enzyme involved in bacterial replication, through the ATP-dependent supercoiling of DNA. Bacterial DNA gyrase, a type II topoisomerase from the enzyme family GHKL (Gyrase, HSP 90, histidine kinase, MutL), remains as one of the most investigated and validated target for the development of novel antibacterials. Its absence in the mammals and the crucial role it plays in the bacterial DNA replication cycle, transcription, recombination and chromosome modelling makes this enzyme a very suitable target for the development of potential drugs from the perspective of selective toxicity [Collin F., *et.al.*, 2011]. The main role of this enzyme is the introduction of negative supercoils.

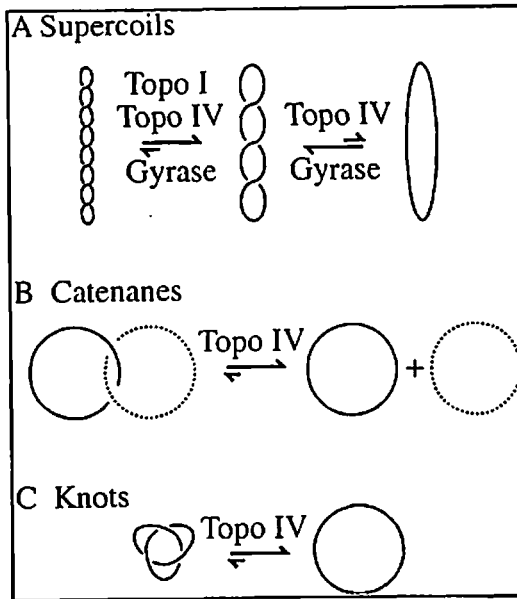


Figure 2.2: Types of topoisomerases and their mode of action [Richard W. Deibler., 2001].

2.1.3. Mechanism of the DNA Gyrase enzyme

Although all type II topoisomerases require ATP hydrolysis for efficient relaxation of supercoils, DNAgyrase is capable of coupling the energy of ATP hydrolysis to the generation of negative supercoils in a plasmid DNA. This property of the enzyme requires the DNA binding region found in the C-terminal domain of the A subunit, since removal of this region produces an enzyme capable of relaxing DNA but incapable of introducing negative supercoils into the DNA. There are two keys to the negative supercoiling reaction catalyzed by DNA gyrase. The first is that the DNA bound to the C-terminal domain is wrapped around the protein with a right-handed writhe. The resulting constrained positive supercoil is associated with approximately 140 bp of DNA. The second key to the reaction relates to the resulting spatial relationship between the enzyme-bound G-segment DNA and the T-segment DNA trapped in the DNA.

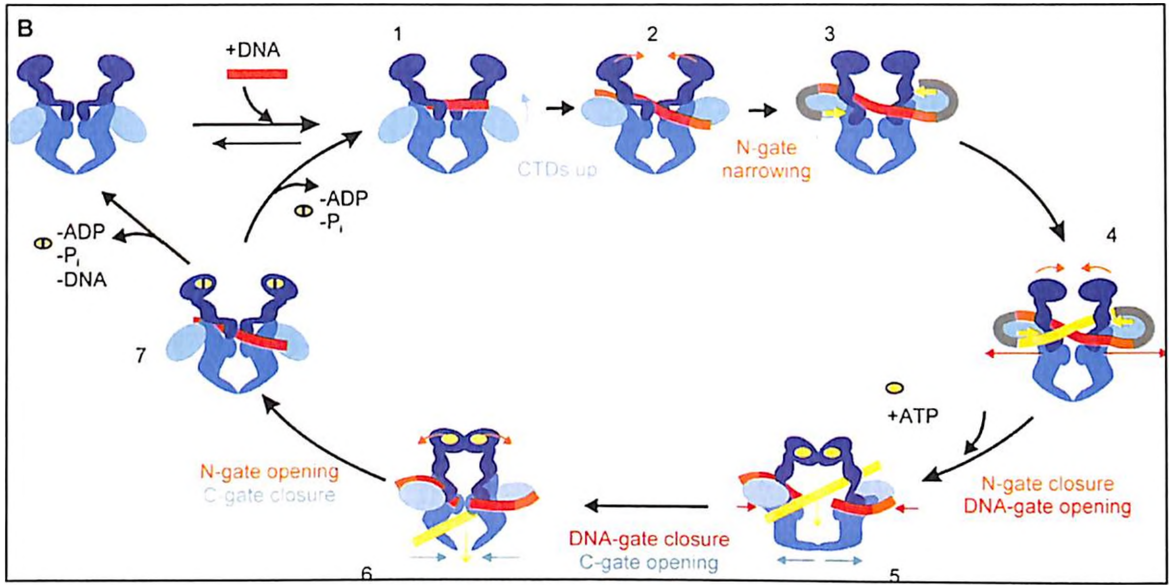


Figure 2.3: A cascade of DNA-induced conformational changes prepares gyrase for strand passage [Gubaev *et al.*, 2014].

The two crossing segments of DNA are referred to as a DNA node that can be either positive or negative in sign, depending on how the two DNA regions of the same molecule lie across each other. For all of the type IIA topoisomerases except DNA gyrase, the sign of the node formed by the bound G- and T-segments is determined by the sense of the supercoiling of the substrate DNA; negatively supercoiled DNAs bind to produce a negative node, and positively supercoiled DNAs bind to produce a positive node. In either case, inversion of the node by the DNA transport reaction relaxes the DNA by canceling out two of the supercoils. On the other hand, for DNA gyrase the right-handed wrap of the DNA around the enzyme must dictate that the nodal arrangement of the G- and T-segments, leading to a productive transport reaction is nearly always a positive one. Thus, one plausible explanation for the directionality of DNA transfer by DNA gyrase is that the C-terminal region delivers the two DNA segments to the enzyme in such a way that only a positive node can be formed prior to cleavage. Based on an analysis of the

topology of the bound DNA at various stages of the reaction [Kampranis S. C., *et al.*, 1999] have proposed a slightly different model for the supercoiling preference of DNA gyrase.

They suggest that two regions of a DNA can potentially associate with the DNA gyrase to produce a node of either sign. The bound T-segment DNA promotes opening of the DNA gate to set up an “on-enzyme” equilibrium in which the T-segment distributes itself either before or after the DNA gate depending on the topology of the DNA. For a positively supercoiled substrate, which is a good substrate for gyrase, the equilibrium position for the T-segment is beyond the gate so that with closure and release two negative supercoils are introduced that offset two of the positive supercoils. For a negatively supercoiled DNA, the equilibrium favors a position for the T-segment before the DNA gate, and therefore a much reduced chance for any change in the supercoiling of the DNA. The right-handed wrap of the DNA around the enzyme must play a critical role in determining the equilibrium position of the two DNA segments.

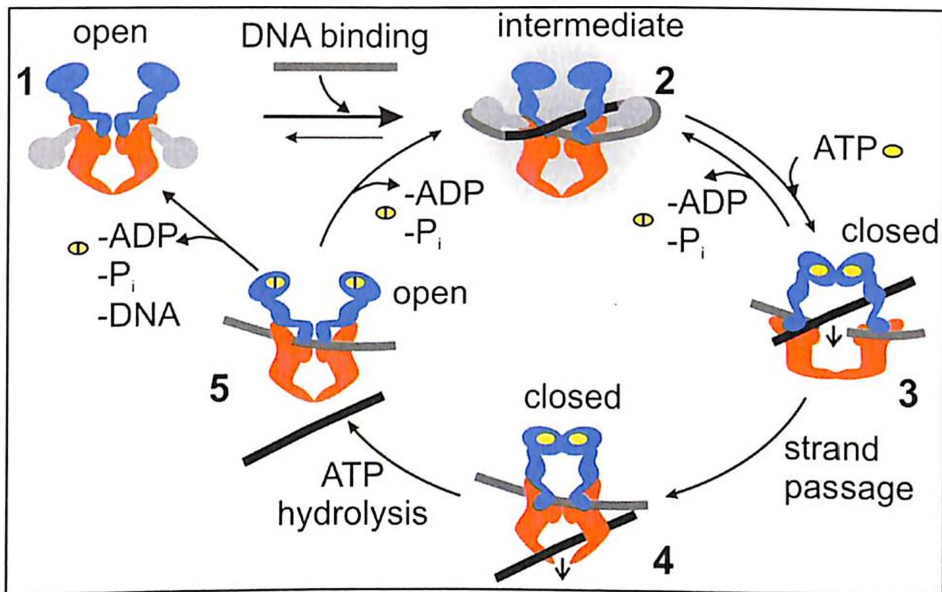


Figure 2.4: Model of conformational changes in the catalytic cycle of gyrase and their relation to strand passage [Airat Gubaev., *et al.*, 2011].

2.2. Inhibitors available till date targeting the DNA Gyrase enzyme

2.2.1. Fluoroquinolones

DNA Gyrase, a type II topoisomerase has been of tremendous interest ever since, it was discovered as the biological target of quinolones. Gyrase enzyme is a lethal antibacterial drug because of certain parameters: (1) They being the necessary components of all bacteria. (2) These proteins viability is a must for the bacterial DNA replication and cell division. (3) Their function is associated with bactericidal activity, (4) These inhibitors show bacterial specificity due to distinct structural differences from that of their mammalian enzyme counterparts. (5) These enzymes possess multiple sites as target [Mdluli K., *et al.*, 2007].

Among the various classes of inhibitors reported till date, for DNA Gyrase quinolones are the most promising leads, displaying broad spectrum antibacterial potency. However, till date not many drugs acting through DNA gyrase are reported except the 6-fluoroquinolone chemical class of molecules. These molecules are the only DNA gyrase inhibitors approved and available for clinical practice [Brvar M., *et al.*, 2012]. The strategy of quinolone inhibition is by binding to the ternary complex formed between the DNA molecule and the DNA Gyr A domain, subsequently stabilizing the formed complex. Overall, this ternary complex helps in preventing the reunion of both the DNA strands and ultimately stopping the bacterial replication cycle. According to Minovski, fluoroquinolones have significant utility in the treatment of respiratory and urinary infections; however, identification and occurrence of some serious side effects calls for novel research in this field [Minovski N., *et al.*, 2012]. Secondly, the other critical drawback of this chemical class of molecules is, they are more potent against the gram negative bacteria when compared with gram positive ones due to the presence of another homologous target, the

Why is this critical?

topoisomerase IV [Fournier B., *et al.*, 2000]. Moxifloxacin, a quinolone currently possess most promising anti-gyrase activity against both drug sensitive and drug resistant strains of *S. aureus*. The targeting of either DNA gyrase or topoisomerase IV as the primary target by fluoroquinolones varies with bacterial species and specific fluoroquinolone; however, dual targeting is of great advantage as it aids in effective bacterial killing. When either DNA gyrase or topoisomerase IV induces transient double-strand DNA breaks, they first bind covalently to the DNA to form drug-enzyme-DNA complex before breaking the bound DNA, thereby passing another segment of DNA through this break, and rejoining the original DNA segment [Drlica K., *et al.*, 2009]. Fluoroquinolones bind to DNA gyrase or topoisomerase IV, which is then unable to re-ligate or re-join the DNA substrate. However, in 1980's when the fluoroquinolones were introduced into medical practice, great expectations were raised because of their potent broad spectrum activity and absence of transferable mechanisms of resistance or inactivating enzymes, it was hoped that clinical resistance to this useful group of drugs would not occur. However, over the years, due to intense selective pressure and relative lack of potency of the available quinolones against some strains, bacteria have evolved various mechanisms of resistance [Rattan A., 1999]. (i) Alteration of molecular targets like mutations in specified regions, mostly in genes coding for the gyrase/topoisomerase leads to clinical resistance [Black M.T., *et al.*, 2008]. (ii) Resistance due to increased drug accumulation which can probably be due to the inability of the drug to cross the bacterial cell wall (permeability barriers) (iii) An efflux pump effective in pumping out hydrophilic quinolones. In addition, QTc interval prolongation by blocking voltage-gated potassium channels ⁱⁿ the heart associated with these classes of drugs has limited their clinical use and future progress, necessitating research into

development of new antibacterial agents that lack cross-resistance mediated by mutations in the bacterial targets.

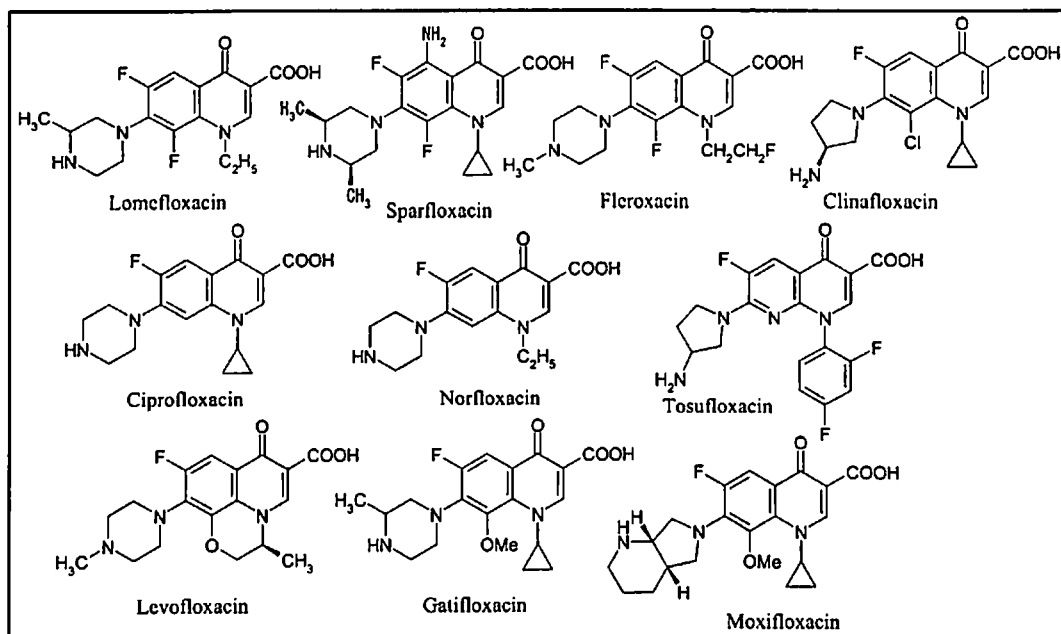


Figure 2.5: Chemical structures of quinolones [Norihiro Hayashi., *et al.*, 2004]

2.3. Inhibitors targeting Gyr B domain of the DNA Gyrase

2.3.1. Aminocoumarins

Aminocoumarins are a well known class of antibiotics that act by inhibition of the DNA gyrase enzyme involved in cell division in the bacteria. The basic skeleton of an aminocoumarins is a 3-amino-4,7-dihydroxycoumarin ring. In comparison with fluoroquinolones, aminocoumarins are regarded as 'Cinderellas' of the gyrase inhibitors. Novobiocin, clorobiocin and coumermycin A1 are the class of aminocoumarins isolated from *Streptomyces* species, however many derivatives of aminocoumarins were made by genetic manipulation, metabolic engineering, and mutasynthesis and also by chemical synthesis. Coumermycin A1 has coumarin rings attached to

TH 6442

either side of a pyrrole group; a substituted sugar is attached to each of the coumarin rings, and a pyrrole group is attached to each noviose sugar. Structurally clorobiocin and novobiocin differ in the substitution of the methyl group at the 8' position of the 13-ringed coumarin with a chlorine atom, and a 5-methyl-pyrrole-2-carboxyl group substitutes the carbamoyl group at the 3' position of the noviose (Figure 2.6). Structure of novobiocin, clorobiocin and coumermycin A1. Simocyclinones are another variety of aminocoumarin moiety with an additional angucyclinone polyketide group. Both aminocoumarins and simocyclinones are two different non-quinolone, gyrase-targeted antibacterials that bind at different subunits and are evolutionarily related also. Though aminocoumarins are potent inhibitors of *S. aureus* DNA Gyr B enzymes *in vitro*, their poor activity against gram negative bacteria, cytotoxicity and poor solubility parameters prevent them from being clinically successful drugs [Brvar M., *et al.*, 2012]. So their further structural exploration is still needed.

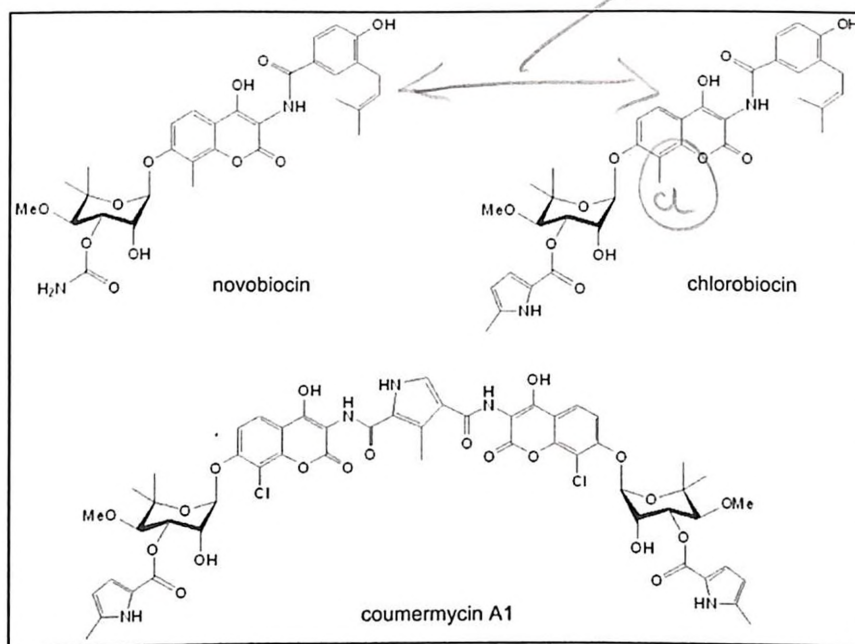


Figure 2.6: Chemical structures of aminocoumarins [Lutz Heide., 2009].

2.3.2. Cyclothialidines

Cyclothialidines include a substituted resorcinol ring with the attached pentapeptide chain (Cys, Ala, Ser, Pro, and Ala). Their mode of action is similar to the aminocoumarin drugs where the Gyr B domain is targeted and not the Gyr A. Cyclothialidines are effective competitive inhibitors to ATP and thus the supercoiling activity of the gyrase is inhibited *via* the inhibition of Gyr B [Naoki Nakada., *et al.*, 1994]. Despite their higher potencies and better selectivity against topoisomerases as well in comparison to the coumarin class, they lack *in vivo* antibacterial activity due to their high lipophilicity nature. Recently, several fruitful attempts are being made to improve their water solubility and permeability characteristics and to increase their *in vivo* activities. (Figure 2.7) depicting the structure of cyclothialidines.

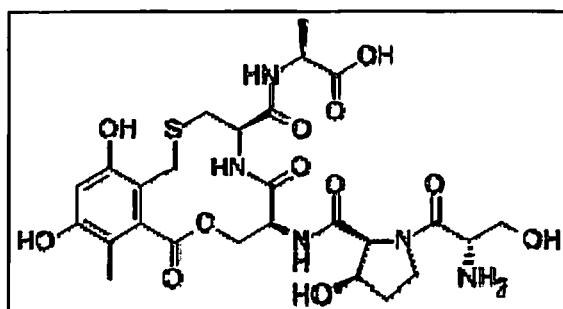


Figure 2.7: Structure of Cyclothialidine [Naoki Nakada., *et al.*, 1994].

2.3.3. Pyrrolamides

Pyrrolamide class of compounds/ were first identified at AstraZeneca as novel DNA Gyr B inhibitors through HTVS screening and structure-guided design strategy, with effective antibacterial activity. However, ^{It} it was found that the pyrrolamides target DNA gyrase ~~an essential enzyme at a broader range~~ across bacterial species and inhibition of it results in the disruption of DNA synthesis and subsequently in cell death. Further, optimization of biochemical

activity and other drug-like properties through various substitutions to the pyrrole, piperidine, and heterocycle portions of the parent molecule resulted in pyrrolamides with improved cellular activity and *in vivo* efficacy as shown in (Figure 2.8). Furthermore, the antibacterial activity, broad spectrum and mode of action of these compounds underscore the promise of the pyrrolamide series as attractive candidates for the treatment of several clinical indications, including respiratory and soft tissue infections [Maria U.N., *et al.*, 2013]. In 2014, Gregory S.B., *et al.*, has developed AZP5099 belonging to pyrrolamide class based on fragment based approach. This compound targets ATP binding site type II topoisomerase and has successfully entered phase I trials for treatment of resistant bacterial infection [Gregory S.B., *et al.*, 2014].

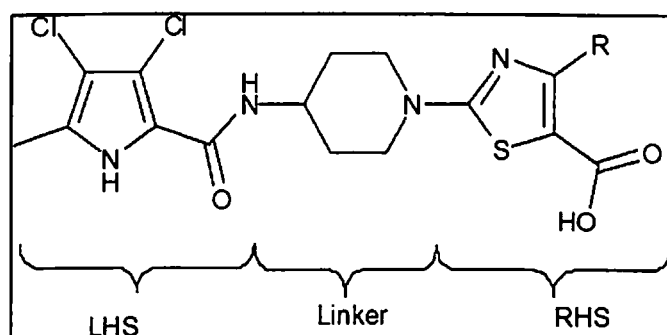


Figure 2.8: Structure of pyrrolamide with space for several substitutions.

2.3.4. Benzimidazoles

Benzimidazole ureas were effective antibacterials developed by Vertex pharmaceuticals by high throughput screening (HTS), these are a novel class of compounds targeting both Gyr B and topoisomerase IV of *S. aureus*. In 2012, benzimidazole ureas were evaluated for Gyr B inhibition potencies with effective IC_{50} in nanomolar range and also active against fluoroquinolone resistant strains and murine models [Chopra S., *et al.*, 2012]. Various substitutions were attempted on the benzimidazole nucleus for generating structure activity relationship. A smaller

alkyl chain was favored at the R₁ position, as it allowed the core moiety to penetrate deeper into the active site pocket, resulting in tighter binding. Secondly, it was observed that the pocket occupied by the ribose of ATP was accessed by the ring attached to the benzimidazole R₂ position. These interactions were considered important for the optimal binding of the ligand in the ATP-binding pocket of Gyr B. However, the pyridyl ring was optimized to be the ideal substituent at this position and with respect to the substituents on the pyridyl ring at the R₃ position, a variety of substituents were well tolerated with respect to gyrase activity, but the presence of a fluoro group enhanced the antibacterial potency almost 6 to 18 times. However, it was confirmed that co-planarity at the R₃ position provided optimal enzyme inhibitory potency; one such compound was the 3-fluoropyridin-2-yl which was optimized to be the ideal substituent at this position.

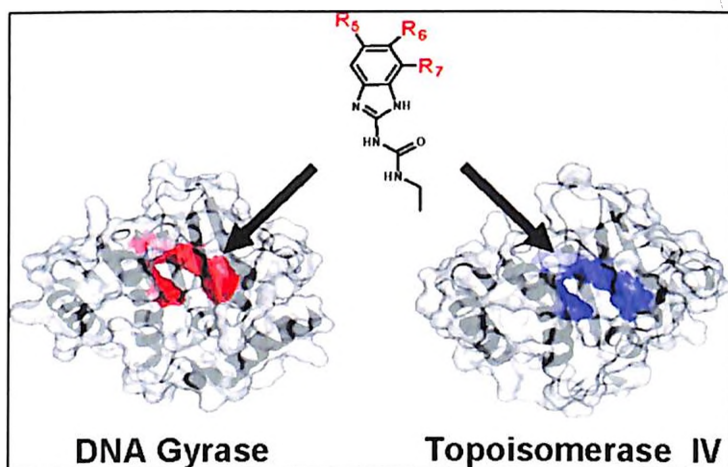


Figure 2.9: Benzimidazoles targeting the DNA Gyrase and Topoisomerase IV [Paul S. Charifson., *et al.*, 2008].

2.3.5. Bithiazoles

Brvar M., and his colleagues from Slovenia, identified and characterized a novel class of 4'-methyl-N2 -phenyl-[4,5'-bithiazole]- 2,2'-diamine as bacterial Gyr B inhibitors. The 2-aminothiazole moiety of these class, were able to fulfill the general prerequisite for gyrase inhibition with acceptor-donor interaction pattern and could be considered a promising starting scaffold. As in their previous studies, they found that the second thiazole ring appeared to be suitable linker between the first thiazole ring and the substituted phenyl ring which was capable of possessing additional hydrophobic interactions. Furthermore, the phenyl ring substitution was shown to be of importance, and the hydrogen bond acceptor on the *para* position of the phenyl ring was apparently crucial for the inhibitory activity of the enzyme. In this case, the carboxyl group was capable of forming additional ionic interactions, which contributed considerably to the strength of binding interactions. Furthermore, in most cases, the 2'-acetyl substitution of the 2'-amino group lead to a higher activity of the inhibitor. The lipophilic part of the 2' substituent is positioned in the hydrophobic pocket of the ATP-binding site and forms favorable hydrophobic interactions.

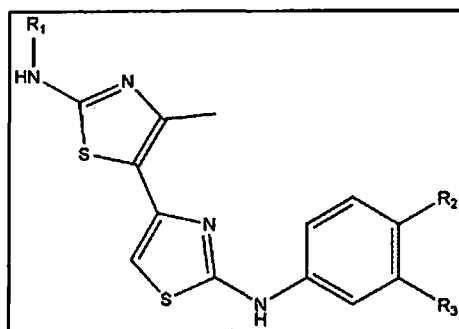


Figure 2.10: 4,5'-Bithiazole compounds with available substitutions at R₁, R₂, R₃ [Brvar M., *et al.*, 2012]

Chapter 3

OBJECTIVES AND PLAN OF WORK

3.1. Objectives

Despite the success of genomics and proteomics in identifying new essential bacterial genes and proteins, a lack of sustainable leads in antibacterial drug discovery to address ever-increasing multidrug resistance mainly in organisms like Staphylococcal species. With an increase in flexibility and complexity of the enzymes, each day, it is a considerable challenge for structural studies of drug action and their mechanism. An intense search of the various literatures available highlighted the importance of Staphylococcal DNA Gyrase and its sub domain DNA Gyr B and their role as tools in changing the topology of the DNA. These enzymes are also considered as validated targets for antibacterial chemotherapy.

The main objective of the proposed work is to:

1. Design and identify Novel Bacterial Type II Topoisomerase Inhibitors (NBTIs) and DNA Gyr B inhibitors of *S. aureus* using structure based drug design strategy in view of understanding the pharmacophoric requirements for their antibacterial activity.
 - a. To evaluate the inhibitory potencies of the identified NBTIs by DNA supercoiling assay, and of Gyr B inhibitors by (i) Gyr B ATPase assay and (ii) DNA Supercoiling assay
2. To evaluate the protein-inhibitor binding affinities using biophysical characterization technique.

3. To carry out *in vitro* antibacterial screening of the identified leads for DNA Gyrase and DNA Gyr B as well in various *S. aureus* and MRSA strains.
4. To perform the cytotoxicity studies in cell lines
5. To evaluate the potencies of the identified leads for inhibition of biofilm formation in strains of *S. aureus* and MRSA.
6. Effect of the compounds on *zERG* channel toxicity studies.
7. Kill kinetic studies of the designed lead compounds.

3.2. Plan of work

Overall the plan of work was classified into the following categories.

3.2.1. To design the NBTIs against *S. aureus* Gyrase and also new potent inhibitors against *S. aureus* DNA Gyr B domain

The strategy for designing the inhibitors was:

- i) The available crystal structure of *S. aureus* in complex with NBTIs was utilized as a structural framework for virtual screening of a commercially available database (Asinex) collection to identify new leads.
- ii) The crystal structure of *S. aureus* DNA Gyr B protein bound to inhibitor was retrieved for virtual screening of the above commercial database was used for identification of new leads.

Aren't aim 1 & 2 same?

3.2.2. Cloning, expression and purification of *S. aureus* Gyr A, Gyr B and *E. coli* Gyr A proteins

3.2.2.1. Cloning, expression and purification of *Staphylococcal* Gyr A and Gyr B protein

The gene RN4220 from *S. aureus* genomic DNA was amplified by using the specified primers. Clones were treated with restriction digestion enzymes and the resulting constructs were transformed into expression vector pQE2 (Qiagen) with a 6-His-tag and was then transformed into BL21-CodonPlus (DE3) cells.

3.2.2.2. Cloning, expression and purification of *E.coli* DNA Gyr A protein

The genomic DNA of *E.coli* DH5 α strain was taken as a template to isolate DNA *gyrA* gene, specified primers were used to amplify the gene of interest. Restriction enzymes were used to obtain the final constructs which were transformed into pQE2 with a His tag. Clones were transformed into BL21-CodonPlus (DE3) cells.

3.2.3. Biological assessment of the *S. aureus* Gyrase enzyme and Gyr B protein with designed inhibitors

3.2.3.1. *In vitro* Gyr B inhibitory potency

The identified Gyrase analogues were further evaluated for their inhibitory potency in *S. aureus* DNA GyrA and Gyr B. The other set of Gyr B analogues were tested in *S. aureus* DNA Gyr B using *E. coli* DNA Gyr A and *S. aureus* DNA Gyr B.

against
What is the other set?
why test them against
E. coli *gyrA*?

3.2.3.2. *In vitro* supercoiling assay

The identified inhibitors are screened with the DNA gyrase enzyme to know their efficiency. In this assay DNA Gyr A, DNA Gyr B along with relaxed DNA is used in the presence of assay buffer *for 10 min*.

3.2.4. Synthesis and characterization

The designed molecules were commercially obtained from Asinex database and the leads were further derivatized and were synthesized in our laboratory utilizing novel/previously reported methodology available in literature for structurally related molecules. All the feasible reactions were monitored using thin layer chromatography and LCMS. The synthesized compounds were fully characterized using modern analytical techniques. LCMS, $^1\text{H-NMR}$ and $^{13}\text{C NMR}$ were recorded and analyzed to confirm the structure of the compounds. Purity of the compounds was evaluated by elemental analysis and HPLC.

3.2.5. *In vitro S. aureus* screening

3.2.5.1. *In vitro* activity in *S. aureus* MTCC strain *against*

All the molecules were screened for their *in vitro* antibacterial activity against *S. aureus* MTCC3160 by microplate broth dilution method.

3.2.5.2. *In vitro* activity in *S. aureus* MRSA strains *against*

Estimation of the test compounds activity against MRSA96 strains of *S. aureus* was performed tested by most probable number (MPN) assay.

3.2.6. *In vitro* cytotoxicity screening

Compounds were also tested for *in vitro* cytotoxicity against RAW 264.7 cells at 50 μM concentration using MTT assay to evaluate their selectivity index and toxicity profiles.

3.2.7. Biofilm Inhibition studies

Biofilm formation assay was carried in 96-well tissue culture plate (TCP) method as described in earlier protocol [Christensen G. D., *et al.*, 1985]. Detection of the biofilm formation by the MRSA 96 strain was done as reported earlier by Congo red agar (CRA) method [Freeman D. J., *et al.*, 1989]. Though certain disadvantages are associated with this method, yet it was followed due to its simple, economic and efficient process. The screening was done using specially prepared Brain Heart Infusion broth (BHI) (Himedia) supplemented with 5% sucrose. A concentrated Congo red stain was prepared and autoclaved at 121 $^{\circ}\text{C}$ for 15 min, diluted and added when the agar had cooled to 55 $^{\circ}\text{C}$ [Freeman D. J., *et al.*, 1989]. The strain was inoculated onto the plates prepared, incubated for 36 h at 37 $^{\circ}\text{C}$ aerobically. The observation of the black colonies has confirmed the biofilm producing nature of the MRSA96 strain. Subsequently, the assay was performed in a 96 well flat-bottom tissue culture plate (NEST) in trypticase soy broth with 1% glucose (TSB) (Himedia).

Why this long?

What is your +ve control?
-ve control?

Why change media?

3.2.7.1. Quantitative assay of the biofilm formed on 96 well flat-bottomed microtiter plates

Isolates from agar plate were inoculated in TSB media and incubated for 18 h at 37 $^{\circ}\text{C}$ with 120 rpm. Later the culture was diluted 1 in 100 with fresh TSB medium and 200 μL of it was aliquoted onto each of the plate wells along with the test compounds at different concentrations of 100–1.56 μM , while the control was incubated with DMSO solvent, though the DMSO usage was limited to 4% during the assay. The plates were incubated for 24h at 37 $^{\circ}\text{C}$ in stationary

phase with the lid closed. The contents of each well was gently removed by tapping the plates inverted, the plates were washed thrice with 0.2 mL of phosphate buffered saline (PBS) of pH 7.2 to remove an unattached, dead and free floating planktonic bacteria. The biofilm formed by adherent sessile *S. aureus* MRSA96 strain was fixed with sodium acetate (2%) and stained with (0.1% w/v) crystal violet. As crystal violet stains the dead and live cells, it is limited to certain use, but in this assay the wells were washed thrice so the chance of unattached dead cells staining was almost neglected [Freeman D., *et al.*, 1989]. Excess stain was rinsed off by thorough washing with running water and plates were dried in a hot air oven. The plates were photographed. For the quantitative estimation, absorbance was read at 570 nm by Perkin Elmer Victor X3 plate reader. The optical density (OD) values reflected an index of the *S. aureus* bacteria adhering to surface and in forming the biofilm. The experiment was performed in triplicates, the background absorbance was compensated by reading the OD from sterile medium, fixative used, auto absorbance and dye which were averaged and subtracted from all test values, and this mean OD was also subtracted from the control well. The control well OD was 0.28 which indicated that the MRSA96 strain was a strong biofilm producer. In general, OD values above 0.2 are considered as strong biofilm producers [Mathur T., *et al.*, 2006]. The percentage of inhibition of the test compounds was calculated by using the formula.

$$\% \text{ Inhibition} = \frac{\text{control reading} - \text{blank reading}}{\text{control reading}} * 100$$

Further, the dry crystal violet stained plates were treated with 200 μ L of 33% glacial acetic acid, given a brief shake in orbital shaker and the plates were read at 570 nm in a Perkin Elmer Victor X3 96-well plate reader. The OD gives us the approximate count of the cells involved in the biofilm formation.

3.2.8. Evaluation of protein-inhibitor stability using biophysical technique

Biophysically, the binding affinity of the potent Gyr B analogues was evaluated by differential scanning fluorimetry experiment using Bio-Rad CFX Real Time PCR.

3.2.9. *zERG* channel inhibition studies

zERG studies were conducted using zebrafish larvae model. Zebrafish were procured commercially from Vikrant Aquaculture, Mumbai, India. They were maintained in a recirculatory system containing 0.06% sea salt under 14 h light and 10 h dark cycle and 28 °C water temperature [Banote R. K., *et al.*, 2013]. Males and females were maintained in different tanks before they were allowed to breed. Breeding of zebrafish were allowed in the ratio of 2 females: 3 males under the sudden stimulation of light. Subsequently, embryos were collected into petridish containing E3 medium (5 mM NaCl, 0.17 mM KCl, 0.33 mM CaCl₂ and 0.33 mM MgSO₄) incubated at 28 °C temperature. In this assay, 3 dpf embryos were distributed in a 24-well plate along with 250 µL of 0.1% DMSO solution, while the stocks were prepared in 100% DMSO, working concentrations of the compound was prepared by serial dilutions. Each well containing 5 embryos were treated with each required concentration of the solution and incubated at 28 °C for 4 h. Later, individual embryo of each well was focused under light microscope (Leica) and heartbeat was observed (i.e., atrial and ventricular beats). The time taken for 30 beats was measured with the help of stopwatch while the mean for the time taken by 5 embryos was calculated for each well. Subsequently, the number of heart beats per minute was calculated as follows:

$$1800/X = \text{beats/minute (where X = time in seconds)}$$

3.2.10. Determination of time kill kinetics

Time kill kinetic studies are done to know the bactericidal effect of the compounds. The 0.5x, 1x, 2x, 4x and 8x times of their MIC concentrations of the drugs are incubated with the bacterial culture to evaluate their bactericidal effect at different time points [Sheo B. S., *et al.*, 2014].

Chapter 4

MATERIALS AND METHODS

4.1. Identification of novel inhibitors targeting *S. aureus* enzymes

4.1.1. Identification of novel inhibitors targeting the *S. aureus* DNA Gyrase as a whole enzyme and DNA Gyr B domain alone

In order to identify Staphylococcal inhibitors targeting DNA Gyrase protein and also one of its domain Gyr B protein, we utilized the following design strategy.

4.1.1.1. Structure based drug design approach

As the *S. aureus* DNA Gyrase and DNA Gyr B domain were our target proteins, we describe here a novel protocol for generating energy-optimized pharmacophore (e-pharmacophore) based on mapping of the energetic terms obtained from the Glide XP scoring function onto atom centers. Beginning with a ligand-receptor complex we refined the ligand pose, computed the Glide XP scoring terms, and mapped the energies onto atoms. Then, pharmacophore sites were generated, and the Glide XP energies from the atoms that comprised each pharmacophore site were summed. The sites are then ranked based on these energies, and the most favorable sites were selected for the pharmacophore hypothesis [Salam N.K., *et al.*, 2009]. Finally, this e-pharmacophores were used as queries for virtual screening.

4.1.1.2. DNA Gyrase protein as a target

In the present study, crystal structure of *S. aureus* Gyrase in complex with GSK299423 and DNA (PDB code: 2XCS) was retrieved from protein data bank (PDB) and was utilized for structure-based drug design [Bax B. D., *et al.*, 2010]. Hydrogen atoms, bond orders and formal charges were added using the protein preparation wizard application of the maestro software package. Water molecules were removed from the atomic co-ordinates $>5\text{\AA}$ distance. The resulting output structure was energy minimized using minimization wizard. Interaction of the GSK299423 ligand with the protein residue and DNA wrapped around at the active site were visualized using ligand-interaction diagram in Schrodinger suite version 9.3.

Similarly, crystal structure of *S. aureus* DNA Gyr B in complex with pyrrolamide (PDB code: 3TTZ) was retrieved from protein data bank to subject it to structure-based drug design [Sherer B. S., *et al.*, 2011]. Using the protein preparation wizard the hydrogen bonds, the bond orders and the formal charges were added. After the removal of the water molecules from the atomic coordinates the structure was energy minimized. Interactions of the pyrrolamide with the protein were examined using the Schrodinger software ligand-interaction diagram.

4.1.1.3. Protein and ligand preparation

The protein files were prepared using protein preparation wizard and impact energy minimization was performed using 500 cycles of steepest descent (SD) and 5000 cycles of conjugate gradient (CG) methods. Optimized potential for liquid simulations (OPLS) 2005 force field was attained. The active site of the proteins was defined and grid files were generated using receptor grid generation panel [McCarthy J.D., 1999]. The reference ligand structures of the protein was downloaded from PDB and minimized using impact energy minimization wizard

with 100 cycles of SD and 500 cycles of CG. The three dimensional structure of five lakh compounds were retrieved from Asinex and were employed for the virtual screening. The database compounds were energy minimized and were used as a single file using LigPrep module (LigPrep v2.2, Schrodinger, LLC, New York).

4.1.1.4. Glide XP (Extra-Precision) docking

The generated grid files from the prepared proteins were used for Glide XP docking calculations. The grid size or the binding site of the ligand with the protein was defined by a rectangular box of 20 Å in the x-ray structure, while the others were kept at default setting. The grid size of the protein 2XCS was restricted to 20 Å as well. Thus the minimized conjugate gradient output of the reference ligands was used. In the Schrodinger software, the “Write XP descriptor information” option and “Compute RMSD” option were enabled and the settings were kept default for the rest of the parameters. The XP Glide scoring function aided in ordering the best ranked compounds, the specific interactions like π -cation and π - π stacking were simultaneously analyzed using XP visualizer in Glide module. The input RMSD of the ligand was also ascertained.

4.1.1.5. E-pharmacophore generation

The pharmacophore hypotheses was created for the reference ligands GSK299423 and the pyrrolamide of both proteins by using the Xpdes file of the Glide XP output, located in the docking post processing tool of the scripts module by using default settings for refinement and scoring. Starting with the refined crystal ligand GSK299423 of 2XCS, pharmacophoric sites were automatically generated with Phase module using a default set of four chemical features for the NBTIs: three aromatic rings and a positive ionizable (P) group. In this e-pharmacophore, the

positive ionisable group showed an interaction with the single hydrogen bond, whereas the ring aromatic structures were involved in the hydrophobic interactions at the active site pocket. All these projected points allowed the possibility for the structurally dissimilar active compounds to form hydrogen bonds in the same location, regardless of their point of origin and directionality [Singh K.D., *et al.*, 2012]. The other crystal ligand, generated e-pharmacophore with 3 chemical features: one donor (D), an acceptor (A) and a negative ionisable group (N). The reference ligands were docked with Glide XP and the docked poses were refined and the Glide XP scoring terms were computed to map energies onto the atoms. Finally, the pharmacophore sites were generated, and the Glide XP energies from the atoms that comprised each of the pharmacophore sites were summed up later ranked them based on the individual energies, and the most favorable sites were selected for the pharmacophore hypotheses.

4.1.1.6. Preparation of Asinex commercial database

Asinex database (www.asinex.com) containing 5,00,000 unique structures was used in this study. The database molecules were prepared using LigPrep and Epik application to expand protonation and tautomeric states at pH 7.0. All the molecules were subjected to conformational sampling using the ConfGen search algorithm. In our laboratory, ConfGen with OPLS_2005 force field was employed and a duplicate pose elimination criterion of 1Å RMSD was used to remove redundant conformers. Simultaneously, a distance-dependent dielectric solvation treatment was used to screen electrostatic interactions. In order to eliminate the high energy structures, maximum relative energy difference of 10.0 kcal/mol was chosen. Using Phase module, the database was indexed with the automatic creation of pharmacophore sites for each conformer to allow rapid database alignments and screening of the molecules.

4.1.1.7. High-throughput virtual screening and docking studies

For the structure-based e-pharmacophore approach, explicit matching was required for the most energetically favourable site (scoring better than 1.0 kcal/mol) that finds matching pharmacophores in the given set of ligands. For filtering the database molecules, a minimum of 3-5 sites were required to match for hypotheses with 3-7 sites. The above criterion was followed in the present work to screen the commercial Asinex database. The database hits were ranked in the order of their fitness scores and it also gave an idea of how well the aligned ligand conformer matched with the hypothesis based on RMSD score, its site matching parameter, the vector alignments with the volume terms. The shortlisted database ligands after the application of the e-pharmacophore filter were docked into the binding sites of their respective 2XCS and 3TTZ proteins utilizing high-throughput virtual screening (HTVS) scoring function to estimate their protein-ligand binding affinities. Subsequently, the ligands filtered from HTVS were subjected to Glide SP (standard precision) docking. Default settings of the software were used for both the grid generation and docking too. Based on the position of the co-crystallized ligand, the center of the Glide grid was defined. Further, to optimize the ligand geometries, post docking minimization was done and then the compounds with best docking and Glide scores were subjected to Glide XP (extra precision) docking. At this point, the final shortlisting of possible hit compounds was based on visual inspection of parameters like the important amino acid residues at the active site cleft involved in binding, the hydrophobic interactions and the RMSD values.

4.1.1.8. Molecular docking studies using GOLD

Once the molecules were shortlisted using the Schrodinger software, another molecular docking software GOLD; a Genetic Optimisation for Ligand Docking software (GOLD 5.2) was used to check the accuracy and validity of the structure-based approach of both the proteins [Marcel, L. V., *et al.*, 2003]. The molecular docking studies were carried out to understand the binding modes of the DNA Gyrase NBTI's and DNA Gyr B inhibitors using the GOLD software on a Windows-based PC, which allowed partial flexibility of the protein along with the full flexibility of the ligands. The reported crystal structure of GSK299423 bound DNA Gyrase and secondly pyrrolamide bound DNA Gyr B ATPase protein (PDB ID: 2XCS and 3TTZ) was downloaded from the PDB. Initially, the protein alone was considered with the removal of ligand for the purpose of docking studies. The above proteins were minimized up to a gradient of 0.01 kcal/mol Å and hydrogens were added using the CHARMM force field available in the Discovery studio 3.5 software. The energy-minimized structures were further used for analysis. In this software, the default parameters used were the population size (100), the selection-pressure (1.1), number of operations (10,000), number of islands (1), niche size (2) and operator weights of migrate (0), mutate (100) and crossover (100) were applied. Subsequently, the active site was defined within 10Å, while the Goldscore (GS) and Chemscore (CS) were used to analyse the ligand-binding interactions .

4.1.1.9. QikProp analysis

The selected compounds after virtual screening were further selected for in-silico prediction of their pharmacokinetic properties like the absorption, distribution, metabolism, excretion and toxicity (ADMET) using Quick QikProp 3.5 module of Schrodinger software. QikProp

efficiently evaluates pharmaceutically relevant properties of over half a million compounds in an hour, making it an indispensable tool in lead generation and lead optimization. Moreover, the greatest advantage of this tool is its accurate prediction of absorption, distribution, metabolism, elimination (ADME) properties prior to expensive experimental procedures, such as High-Throughput Screenings (HTS), which would eliminate unnecessary testing on compounds that would ultimately fail in clinical trials; the other advantage of ADME prediction was to focus mainly on lead optimization efforts in order to enhance the desired properties of given compounds. The ADME properties of the synthesized compounds were also predicted using QikProp. Here compounds prepared were subjected to druglikeness filter. The criteria of the filter was limited to molecular weight of 160-480, number of heavy atoms 20-70, lipophilicity 40-52, number of hydrogen bond acceptors 8-12, number of hydrogen bond donors 4-7, percentage of human oral absorption, cell permeability, solubility, etc.

4.1.2. Synthesis and characterization

4.1.2.1. Synthesis of top lead analogues of DNA gyrase NBTI inhibitor

One of the top active lead identified using the NBTI template, from a set of shortlisted twenty compounds obtained from commercial Asinex database in terms of better activity in DNA Gyrase supercoiling assay, was further taken up for further lead optimization *via* synthesis.

4.1.2.1a. Synthetic protocol for hit expansion of the leads obtained from structure-based virtual screening of DNA Gyrase (2XCS) protein

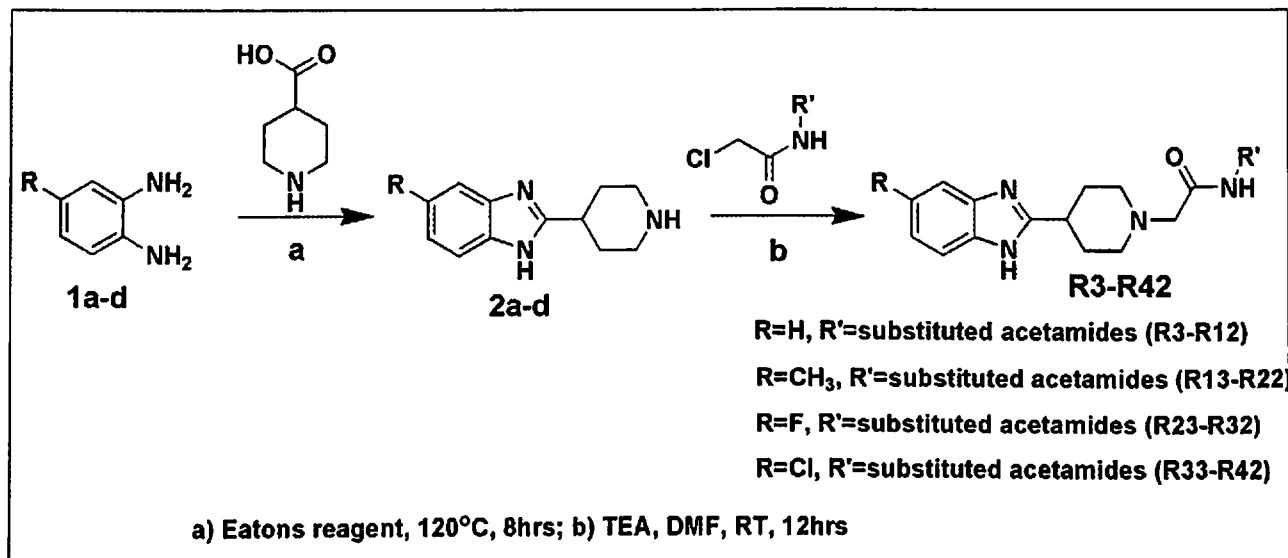


Figure 4.1: Synthetic pathway used to achieve the target compounds (R3-R42).

4.1.2.2. Synthesis of two series of the top two leads of DNA Gyr B inhibitor

Similarly, among the twelve identified hits obtained from another crystal structure from Asinex for 3TTZ target protein, two of the best top active lead compounds; lead molecule (A1) and lead molecule (B1) identified were taken up for further lead optimization through synthesis. Hit expansion of the various leads identified were achieved using the following synthetic protocols.

4.1.2.2a. Synthetic protocol adopted for hit expansion of the lead molecule (A1) obtained from structure-based virtual screening of DNA Gyr B (3TTZ) protein.

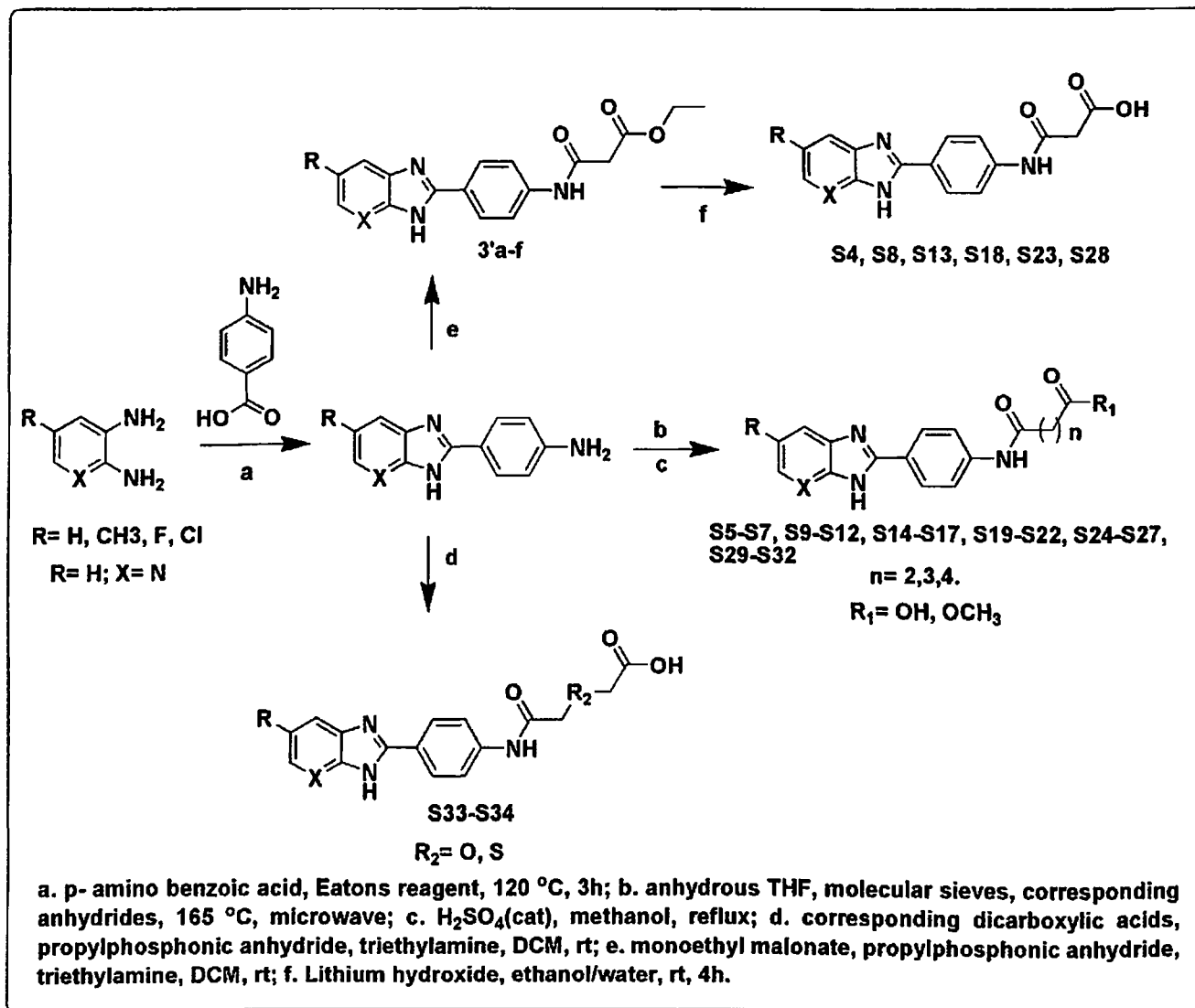


Figure 4.2: Synthetic protocol adopted for the lead derivatization to obtain the target compounds (S5-S44).

4.1.2.2b. Synthetic protocol adopted for hit expansion of the lead molecule (B1) obtained from structure-based virtual screening of DNA Gyr B (3TTZ) protein.

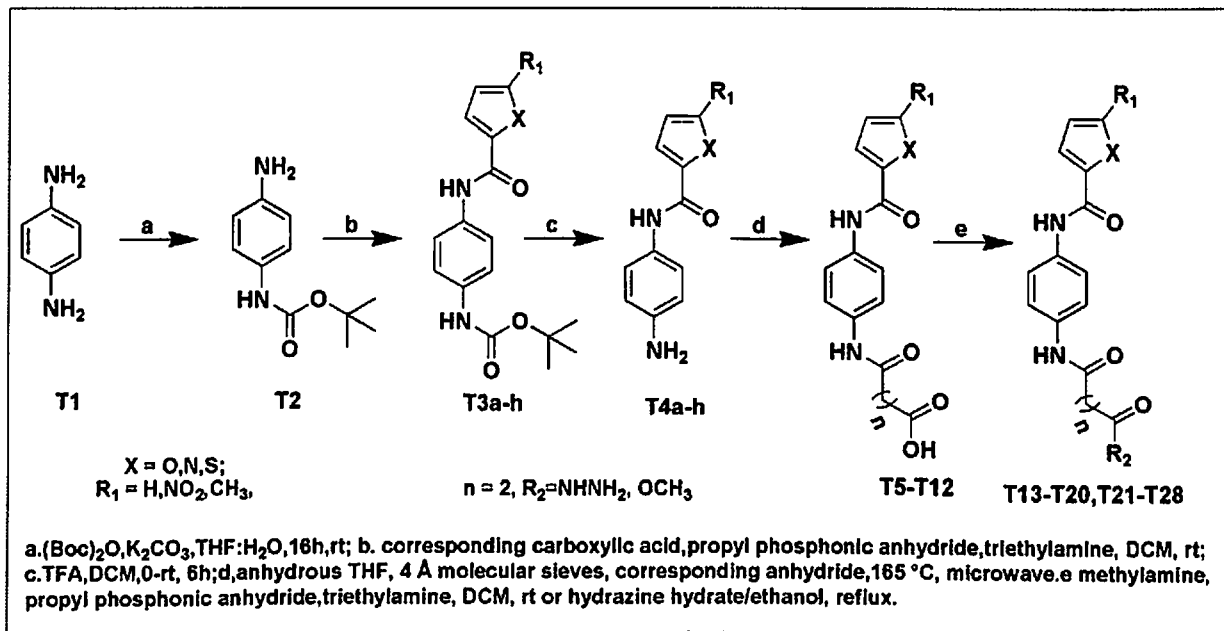


Figure 4.3: Synthetic protocol for the lead derivatization to obtain the target compounds (T5-T28).

All commercially available chemicals and solvents were used without further purification. TLC experiments were performed on alumina-backed silica gel 40 F254 plates (Merck, Darmstadt, Germany). The homogeneity of the compounds was monitored by thin layer chromatography (TLC) on silica gel 40 F254 coated on aluminum plates, visualized by UV light and $KMnO_4$ treatment. Purifications were done on Biotage Isolera purification system on silica gel (MPLC grade) by using either hexane: ethylacetate or dichloromethane: methanol as eluent. All 1H and ^{13}C NMR spectra were recorded on a Bruker AM-300 (300.12 MHz, 75.12 MHz) NMR spectrometer, Bruker BioSpin Corp. Germany. Chemical shifts are reported in ppm (δ) with reference to the internal standard TMS. The signals were designated as follows: s, singlet; d,

doublet; dd, doublet of doublets; t, triplet; m, multiplet. Molecular weights of the synthesized compounds were checked by LCMS 6100B series Agilent Technology. Elemental analyses were carried out on an automatic Flash EA 1112 Series, CHN Analyzer (Thermo). The purity of the final compounds was examined by HPLC (Shimadzu, Japan, (on Phenomenex C8 (150 * 4.6 mm, 5 μ m, 100 Å) double end-capped RPHPLC column)) and was greater than 95%. Detailed synthetic protocols are included in Annexure-I.

4.1.3. *In vitro* biological evaluation

All the identified leads and the synthesized analogues of GSK299423 ligand and pyrrolamide ligand were evaluated for their *in vitro* gyrase inhibitory potencies. The analogues of GSK299423 ligand were evaluated by DNA Gyrase supercoiling assay, whereas the analogues of the pyrrolamide ligand of 3TTZ protein were evaluated initially by the DNA Gyr B ATPase assay followed by the DNA supercoiling assay. Further, the binding affinities of the potent ligands of the Gyr B assay were evaluated by biophysical differential scanning fluorimetry experiments (DSF) from ^{using} Bio-Rad CFX real-time PCR machine. To know the insights of the inhibitor potency against the organism, the compounds were ~~also~~ subjected ^{to} for antibacterial activity study against *S. aureus* MTCC3160 strain obtained from Microbial Type Culture Collection and Gene Bank, Chandigarh, India and ~~also~~ against the MRSA96 strain obtained from Sir Ronald Ross Institute of Tropical and Communicable Diseases (Nallakunta, India) by agar dilution method. [Pandeya S., *et al.*, 1999]. Thus the inhibitory profiles of the inhibitors were also understood by performing the inhibition of the biofilm formation studies quantitatively followed by mammalian cytotoxicity studies against HEK-293 cell lines using MTT assay [Sriram D., *et al.*, 2007]. Furthermore, *zERG* (orthologous to human ether-a-go-go-related gene)

channel inhibition studies were also examined to test the cardio-toxicity of the designed inhibitors in zebra fish model [Banote R. K., *et al.*, 2013].

4.1.3.1. Cloning, expression and purification

The vectors used were from Qiagen, the primers from Sigma–Aldrich and all the enzymes unless otherwise mentioned were from New England Biolabs. *E. coli* DNA Gyr A gene was amplified using a forward primer 5' CACCCATATGCTACGTTATGGTTTACCGGC 3' and a reverse primer 5' AGCTGCGGCCGCCCACTGCCAGCATATTGCA 3' from the genomic DNA of *E. coli* DH5 α strain. Subsequently, the amplified PCR products were further digested with NdeI and NotI and cloned into NdeI and NotI sites of pQE2 vector under T5 promoter with His tag at N-terminal. Similarly, the gene encoding *S. aureus* DNA Gyr B was amplified from *S. aureus* RN4220 genomic DNA by using the forward primer 5' CACCCATATGGTGACTGCATTGTCAGA 3' and a reverse primer 5' AGCTAAGCTTTTAGAAGTCTAAGTTTGCAT 3' flanked with NdeI and HindIII sites. These digested products were ligated at the same site of the pQE2 vector, downstream of the T5 promoter with an N-terminal His tag, the clone was later authenticated by sequencing ~~using a sequencer. Final clones were confirmed by sequencing in a sequencer.~~ Further, for expression of these clones, they were transformed into BL21-codon plus (DE3) cells of *E. coli*. Transformants were grown in Luria Bertani (LB) broth (Himedia) at 37 °C, shaking (rpm 140), in the presence of ampicillin (100 g/mL) ^{ug/ml} (Sigma) until the starting optical density of 0.1 reached the value of 0.4-0.6. The protein expression was induced with 0.2 mM IPTG (Himedia) and further grown overnight for induction of the protein/ at 18 °C. Cells were harvested by centrifugation (5500 rpm, 4 °C, 15 min) and suspended in lysis buffer containing 20 mM Tris–HCl (pH 7.4), 0.1 M NaCl, 2 mM KCl, 10 mM Na₂HPO₄, 1.3 mM K₂HPO₄, 5% Glycerol, 1 mM DTT, 1:200 μ L

protease inhibitor cocktail. The mixture was further sonicated (amplitude 35%, 1 s on 2 s off for 4 min) and was centrifuged (12,000 rpm, 4 °C, 20 min). To the supernatant, pre-equilibrated Ni-NTA beads (GE Healthcare) were mixed and swirled for 1 h at cold room, centrifuged at 500 rpm for 5 min at 4 °C, the pellets were re-dissolved in lysis buffer and loaded onto the Bio-Rad column, each loaded fraction was washed with 50 mL Tris-HCl (pH 7.4), 500 mM NaCl, 2 mM KCl, 10 mM Na₂HPO₄, 1.3 mM K₂HPO₄, 5% Glycerol, 1 mM DTT. Protein was eluted with 25 mM Tris-HCl (pH 8), 140 mM NaCl, 5% Glycerol, 1 mM DTT, and 1 mM PMSF. Initial wash was done with elution buffer without imidazole (Himedia). Subsequently, various imidazole concentration gradients were included from 5 mM to 500 mM. Samples were collected in autoclaved 2 mL eppendorf tubes. Dialysis was performed 4 times overnight against (25 mM Tris-HCl pH 7.4, 140 mM NaCl, 15% glycerol, 2 mM dithiothreitol, 1 mM EDTA), and dialyzed protein was concentrated at (3000 rpm, 4 °C) to a final concentration of 2.5 mg/mL. Later the purity of the protein was analyzed by SDS PAGE method. A 20 µL volume of the dialyzed protein was applied on the polyacrylamide gel (1 mm, 10%), and 5 µL of a commercially available protein molecular weight marker (Bio-Rad) was added. The electrophoresis was run in 1X TBE buffer (Tris-HCl pH 7.5, 1 mM boric acid, 1 mM EDTA) for a period of 90 min at a constant voltage. Later the gel was transferred to a solution of Coomassie Brilliant Blue dye mixed with 20% acetic acid. After 20 min of shaking in an orbital shaker, it was destained several times with 10% acetic acid in 30% methanol and 60% of water until the complete staining was lost and transparency of the gel was achieved. Subsequently, the purity of the protein was determined to be >90% as only single bands corresponding to its molecular weight of *S. aureus* Gyr B was observed between 70 and 80 kDa, while that of *E. coli* Gyr A was observed between 90 and 99 kDa. ? ^{NOT possible.} Why are they different?

4.1.3.2. Enzyme kinetics of *S. aureus* Gyr B ATPase enzyme

The rate of *S. aureus* DNA Gyr B was slow, and the reaction continued for long time. Whereas in the presence of Gyr A subunit the reaction takes place much faster as it stimulates the Gyr B. Substitution of *E. coli* Gyr A with *S. aureus* Gyr A stimulate the reaction by 20-fold. Addition of DNA increases the reaction rate by 620-fold [Eakin A., *et al.*, 2007]. The ATPase activity of enzyme followed the first-order kinetics.

↳ Is this your data or Eakin's data?

4.1.3.3. *In vitro* Gyr B ATPase assay

Purified *S. aureus* Gyr B does not have a highly active ATPase activity naturally like *E. coli* Gyr B [Blanche F., *et al.*, 1996]. Hence Gyr B assay was done with recombinant proteins of *E. coli* Gyr A and *S. aureus* Gyr B [Sherer B. A., *et al.*, 2011; Eakin A., *et al.*, 2007]. As per the reports, the reaction was activated to about 620 fold with incorporation of small molecular weight DNA, in the assay as it is reported to stimulate the protein [Eakin A., *et al.*, 2007]. Initially, equimolar quantities of about 0.5 μM each of *E. coli* Gyr A and *S. aureus* Gyr B were incubated for a period of 45 min with salmon sperm DNA (Sigma) in 50 mM Tris (pH 7.5), 75 mM ammonium acetate buffer for the reconstitution of the hybrid topoisomerases at 4 $^{\circ}\text{C}$. Later the assay was performed in a 96-well microtiter plate [Green O. M., *et al.*, 2010]. The assay buffer includes 50 mM Tris (pH 7.5), 75 mM ammonium acetate, 5% w/ v glycerol, 0.5 mM EDTA, 6 mM magnesium chloride, 0.001% Triton X-100, 1 mM dithiothreitol, DNA of 2 $\mu\text{g}/\text{mL}$ ($\sim 3 \mu\text{M}$ base pairs), 250 μM ATP, 2.2 nM of *E. coli* Gyr A and *S. aureus* Gyr B. Reactions were performed with various drug concentration ranges for the calculation of IC_{50} , with a negative moxifloxacin and positive novobiocin control as standards. The reaction was allowed to proceed for 60 min and was quenched by addition of 20 μL of malachite green reagent (POMG-25H, Bioassay

systems, USA) subsequently absorbance was read at 650 nm after 20 min incubation. Triton X-100 acts as a surfactant to prevent aggregation of molecules during the assay.

4.1.3.4. *In vitro* supercoiling assay

Supercoiling assay was performed using the commercially available kit (*S. aureus* DNA Gyrase supercoiling assay kit: SAS4001) from Inspiralis Pvt. limited, Norwich, UK. The assay was performed in 1.5 mL eppendorf tubes at room temperature. 1 U of *S. aureus* DNA gyrase was incubated with 0.5 µg of relaxed pBR 322 DNA in 30 µL reaction volume at 37 °C for 30 min with 40 mM HEPES. KOH (pH 7.6), 10 mM magnesium acetate, 10 mM DTT, 2 mM ATP, 500 mM potassium glutamate, 0.05 mg/mL albumin (BSA). Standard compound novobiocin was the positive control and 4% DMSO was considered as negative control. Subsequently, each reaction was stopped by the addition of 30 µL of stop dye [40% sucrose, 100 mM Tris-HCl (pH 7.5), 1 mM EDTA and 0.5 mg/mL bromophenol blue] [Hallett P., *et al.*, 1990], briefly centrifuged for 45 s and was run in 1% agarose gel in 1X TAE buffer (40 mM Tris acetate, 2 mM EDTA). Furthermore, concentration of the range of compounds that inhibits 50% of supercoiling activity (IC₅₀) was determined using densitometry and NIH image through Bio-Rad GelDoc image viewer.
what is this?

4.1.3.5. *In vitro* antibacterial screening

The *S. aureus* ~~bacterial cultures~~ MTCC3160 was obtained from Microbial Type Culture Collection and Gene Bank, Chandigarh, India whereas the MRSA96 strain was obtained from Sir Ronald Ross Institute of Tropical and Communicable Diseases (Nallakunta, India). Minimum inhibitory concentrations (MIC) for the test compounds was determined by the agar dilution method according to Clinical and Laboratory Standards Institute Guidelines [Pandeya S., *et al.*,

1999; Jorgensen J. H., *et al.*, 2000]. The antibacterial activity study for all the compounds was performed at the Department of Pharmacy, Birla Institute of Technology and Science, Hyderabad on both the strains separately. Fresh overnight colonies from Mueller–Hinton agar (Hi-Media) medium were suspended to a turbidity of approximately 10^6 colony forming units (cfu)/mL. Stock solutions of tested compounds and standards (ciprofloxacin and ofloxacin) were prepared in 0.9% saline. A control was set for the comparison of the test compounds. A total of 1 mL of the bacterial suspension was added to plates containing 19 mL of the media, so the test range was about 10 doubling dilutions from 100 μ M to 0.1 μ M. The plates were incubated at 35 °C in ambient air for about 16-20 h. The minimum inhibitory concentration (MIC) for the compounds was considered to be the lowest drug concentration that prevented the visible growth of the bacteria on the plates.

4.1.3.6. *In vitro* cytotoxicity screening

A diploid human embryonic kidney cell line (HEK-293) from ATCC was used to assess the cytotoxicity of all the compounds by Promega Cell Titer 96 non-radioactive cell proliferation assay. [Sriram D., *et al.*, 2007]. Briefly, HEK-293 cells were seeded at 5000 cells per well in a 96-well microtiter plate (NEST). After 24 h incubation, the cells were washed with PBS and 2-fold dilutions of the drug was made in 200 μ L of standard culture medium (RPMI + 5% FBS + 1% penicillin and streptomycin) were added, while the final DMSO concentration of the culture ^{What?} was limited to 0.5%. Further, the cells were incubated with a drug concentration of 100 μ M at 37 °C in 5% CO₂/95% air for 72 h. Untreated cells with DMSO were included as controls. The viability of the cells was assessed on the basis of cellular conversion of the dye MTT (Methylthiazol-tetrazolium) into formazan crystals using Perkin Elmer Victor X3 Titre 96 plate

is this correct?

reader at 570 nm. Ciprofloxacin (3% inhibition) and novobiocin (9.8% inhibition) were used as a positive controls.

4.1.3.7. Biophysical characterization using DSF

incomplete of 2021?

Few active compounds of the chemical class of molecules were further investigated using a biophysical technique, differential scanning fluorimetry. The ability of the compounds to stabilize the catalytic domain of the gyrase protein was assessed by the DSF technique by which the thermal stability of the catalytic domain of Gyr B native protein and of the protein with the ligand is measured [Brvar M., *et al.*, 2012]. Gyr B protein with ligands were heated stepwise from 25 °C to 95 °C in steps of 0.6 °C in the presence of the fluorescent dye, whose fluorescence increases as it interacts with hydrophobic residues of the Gyr B protein. Due to increase in the temperature gradually, the protein gets denatured as the amino acid residues become exposed to the dye [Brvar M., *et al.*, 2012]. A right side positive shift of T_m in comparison to native protein reveals the higher stabilization of the protein-ligand complexes, which is a consequence of the inhibitor binding [Niesen F. H., *et al.*, 2007].

4.1.3.8. Biofilm inhibition studies

Biofilm assay was carried out in 96-well tissue culture plate (TCP) method as described by [Christensen G. D., *et al.*, 1985]. Detection of the biofilm formation by the MRSA 96 strain was done as reported earlier by the Congo red agar media (CRA) method. Though certain disadvantages are associated with this method, yet it was followed due to its simple, economic and efficient process. The screening was done using specially prepared solid medium that is brain heart infusion broth (BHI) (Himedia) supplemented with 5% sucrose. Congo red stain was prepared as concentrated solution and autoclaved at 121 °C for 15 min, ^{and} added when the agar had

cooled to 55 °C. The strain was inoculated on to the plates prepared, incubated for 36 h at 37 °C aerobically. The observation of the black colonies has confirmed the biofilm producing nature of the MRSA strain. Subsequently, the assay was performed in a 96-well flat bottom tissue culture plate in trypticase soy broth with 1% glucose (TSB) (Himedia).

4.1.3.9. Quantitative assay of the biofilm formed on 96-well microtiter plates:

Isolates from agar plate were inoculated in TSB media and incubated for 18 h at 37 °C with 120 rpm. Later the culture was diluted 1 in 100 measure with fresh TSB medium and 200 µL of it was aliquoted into each of the wells along with the test compounds at different concentrations of 100-1.56 µM, while the control was incubated with DMSO solvent, though the DMSO usage was limited to 4% during the assay. ^{too high, max is 2.5%} The plates were incubated for 24 h at 37 °C in stationary phase with the lid closed. The contents of each well were gently removed by tapping the plates inverted, the plates were washed thrice with 0.2 mL of phosphate buffer saline (PBS) at pH 7.2 to remove unattached, dead and free floating planktonic bacteria. The biofilm formed by adherent sessile *S. aureus* MRSA 96 was fixed with sodium acetate (2%) and stained with (0.1% w/v) crystal violet. As the crystal violet stains the dead and live cells, it is limited to certain use, but in this assay the wells were washed thrice so the chance of unattached dead cells staining is almost neglected [Freeman D. J., Falkiner F. R., Keane C. T., 1989]. Excess stain was rinsed off by thorough washing with water and plates were dried in an hot air oven. The plates were photographed. For the quantitative estimation, absorbance was read at 570 nm by Perkin Elmer Victor X3 plate reader. The optical density (OD) values reflected an index of the *S. aureus* bacteria adhering to surface and forming biofilm. The experiment was performed in triplicates, the background absorbance was compensated by reading the OD from sterile medium, fixative used, auto absorbance and dye which were averaged and subtracted from all test values, and this

mean OD was also subtracted from the control well too. The control well OD was 0.28 which indicated that the MRSA 96 strain was a strong biofilm producer. In general, OD values above 0.2 are considered as strong biofilm producers. The inhibition percentage of the tested compounds was calculated by the formula.

$$\% \text{ Inhibition} = \frac{\text{Control reading} - \text{blank reading}}{\text{control reading}} * 100$$

Further, the dry crystal violet stained plates were treated with 200 μ L of 33% glacial acetic acid, given a brief shake in orbital shaker and the plates were read at 570 nm in a Perkin Elmer Victor X3 96-well plate reader. The OD gives us the approximate count of the cells involved in the biofilm formation.

4.1.3.10. *zERG* channel inhibition studies

zERG studies were conducted using zebrafish larval model. Zebrafish were procured commercially from Vikrant Aquaculture, Mumbai, India. They were maintained in a recirculatory system containing 0.06% sea salt under 14 hrs light and 10 hrs dark cycle and 28°C water temperature. Males and females were maintained in different tanks before they were allowed to breed. Breeding of zebrafish were allowed in the ratio of 2 females: 3 males under the sudden stimulation of light. Subsequently, embryos were collected into petridish containing E3 media (5 mM NaCl, 0.17 mM KCl, 0.33 mM CaCl₂ and 0.33 mM MgSO₄) and incubated at 28°C temperature [Koutarapu S., Chennubhotla K.S., Chatti K., Kulkarni P., 2013]. In this assay 3 dpf embryos were distributed in a 24 well-plate along with 250 μ l of 0.1% DMSO solution, while the stocks were prepared in 100% DMSO, working concentrations of the compound was prepared by serial dilutions. Each well containing 5 embryos were treated with each required concentration of the solution and incubated at 28 °C for 4 hrs. Later, individual embryo of each

well was focused under light microscope (Leica) and heartbeat was observed (i.e. atrial and ventricular beats). The time taken for 30 beats was measured with the help of stopwatch while the mean for the time taken by 5 embryos was calculated for each well. Subsequently, the number of heart beats per minute was calculated as follows:

$$1800/X = \text{beats /minute (where X = time in seconds).}$$

4.1.3.11. Inhibition of drug efflux pump

S. aureus owes its resistance to many antibiotics by various mechanisms. Among them the efflux pump inhibitors (EPI) occupies the main position. There are about 30 EPI/ altogether in the *S. aureus* membrane. Bacterial strain MTCC96 was used, and the reaction was carried in a 96-flat-bottomed well plate in Muller–Hinton Broth (MHB). The assay was carried out by broth dilution method in 96 flat-bottomed well plate in the presence of increasing amounts of efflux pump inhibitors piperine and verapamil in combination by checkerboard synergy method using two-fold serial dilutions. EPI in combination was tested at seven concentrations (100–1.56 µg/mL). Moxifloxacin was set as standard. The plates were incubated for 18 h at 37 °C and the wells were assessed visually for growth [Sheo B. S., *et al.*, 2014].

incorrect
What is the concentration of EPI tested?

4.1.3.12. Kill kinetics

S. aureus MTCC3160 and MRSA96 strains were used for time kill kinetics of top active compounds at 0.5X, 1X, 2X, 4X, and 8X of their respective MIC (determined by agar dilution method) by CLSI guidelines [Clinical and Laboratory Standards Institute, 1999]. A stock solution of moxifloxacin was prepared in DMSO. The *S. aureus* culture was grown on a TSA/5% sheep blood plate. An inoculum suspension was prepared from the plates to equal the turbidity of a 0.5 McFarland Standard in Mueller Hinton II Broth (MHBII, Himedia), further it was diluted in

→ why changing medium 53
from TSA to MHA/MHB?

1:3, grown in fresh MHBII at 35 °C, incubated in shaker at 150 rpm for a span of 2 hr, the suspension was again adjusted to equal a 0.5 McFarland standard, diluted 1:2 in fresh MHBII and 1 mL was used to inoculate each 125 mL flasks containing 8.75 mL of sterile MHBII media. However, the final target cell density was approximately $10^6 - 10^7$ CFU/mL. Just prior to time T0, 0.25 mL of the appropriate concentration of moxifloxacin solution was added to each flask, gently mixed, followed by 1 mL of the above diluted inoculum. Thus, test drug vessels contained 8.75 mL MHBII, 1.0 mL inoculum, and 0.25 mL drug solution. A total of 22 vessels were prepared in this fashion, immediately swirled to mix, and 0.03 mL was removed from the initial 0.5 McFarland standard tube for determination of the viable count at baseline (time T0) by serial ten-fold dilution in MHB II. All vessels were incubated at 35°C in a Shaker rotating at 150 rpm to provide gentle mixing. The vessels were sampled at a span of 2 hr (T2), 4 hr (T4), 6 hr (T6), 8 hr (T8) and 24 hr (T24) for determination of bacterial viable count which were determined by removing 0.3 mL from each vessel and serially diluting 10-fold in 0.27 mL of MHBII, then plating 10 µL samples onto TSA with 5% sheep blood plates using the track dilution method. All plates were incubated for 20-24 hr at 35°C. Colonies were manually counted, and the CFU/ml was determined from the average count from the duplicate plates, followed by calculation of the log10 CFU/ml. A bactericidal effect was measured as decreased in viable count at 24 hr relative to the starting inoculum.

↓
Incomplete definition!

Why do u keep changing the medium?

Chapter 5

RESULTS AND DISCUSSIONS

5.1. Development of new class of antibacterial agents against DNA gyrase as potential *anti-staphylococcal* inhibitors

Bacterial type IIA topoisomerases are a class of enzymes which are A_2B_2 tetramers that cleave and reseal DNA to transform its topology, including, the case with DNA gyrase, involved in the introduction of negative supercoils [Schoeffler A. J., *et al.*, 2008; Nollmann M., *et al.*, 2007]. The mechanism of change in the topology is by covalent bond formation between a tyrosine moiety of the Gyr A subunit of DNA gyrase and a 5' phosphate that generates a 4-base-pair (bp) staggered break in the DNA, rendering the passage of another DNA duplex through this break thus changing the topology. Structurally, DNA Gyrase was observed to possess three protein 'gates' T, DNA and G. These gates can open and close to allow the passage of the transport (T) segment, DNA duplex, and how the gate (G) segment is bent by the enzyme to allow this process to happen. In contrast, inhibitors target this cleavage and religation processes. Fluoroquinolones, bind and stabilize the double-stranded cleaved DNA complexes inhibition. In the present study, we focused on novel bacterial topoisomerase inhibitors (NBTIs), unlike the fluoroquinolones which target mainly the Gyr A domain. NBTI's generally are not associated with stabilization of double-strandedly cleaved DNA complexes rather a protein–DNA–NBTI complex is formed. In the present study, we utilized the computational structure based drug design strategy for

developing NBTI's as described in the material and method section which possessed novel mechanism of action on *S. aureus* DNA Gyrase unlike the known inhibitors till date.

5.1.1. Novel inhibitors developed using structure based drug design strategy

X-ray crystallography is a basic tool used for identifying the atomic and molecular structure of a crystal. Computationally, structure-based drug design relies on this knowledge of the three dimensional structure of the biological target, a protein obtained through the above X-ray crystallography or NMR spectroscopy [McCarthy J.D., 1999]. Using the *in silico* structure of the biological target, candidate drugs that are predicted to bind to the active site of the biological target with high affinity and specificity may be designed using interactive graphics and the intellect of a medicinal chemist. Alternatively, few other automated computational procedures are available to suggest new drug candidates with drug likeliness. Further, receptor-based approach *via* Computer Aided Drug Design (CADD) can be used when a reliable model of the receptor (preferentially complexed with a ligand) is available from x-ray diffraction studies. However, if a receptor structure is available, a primary challenge in lead identification and optimization is to predict both the ligand orientation and binding affinity *via* 'molecular docking' for the former one and through 'scoring' for the latter one. [Taylor R.D., *et al.*, 2002].

NBTI's occupy a unique position as inhibitors of DNA Gyrase with novel mechanism of action, as inhibition by this class of compounds is generally not associated with stabilization of double-strandedly cleaved DNA complexes. A crystal structure of *S. aureus* gyrase co-complexed with 6-methoxy-4-(2-{4-[[[1,3]oxathiol[5,4-C]pyridin-6-ylmethyl)amino]piperidin-1-yl}ethyl)quinoline-3-carbonitrile and DNA was retrieved from the protein data bank with a DNA Gyrase IC₅₀ of 14 nM. A crystal structure of *S. aureus* DNA gyrase with a resolution of 2.1

A° with NBTI in a pre-cleavage complex was achieved associated with a 20-bp DNA duplex, as well as a 3.35 A° structure complex with a fluoroquinolone (ciprofloxacin), including details of the role of the metal-binding TOPRIM domains in catalysis. The C-terminus Gyr B fused to N-terminus Gyr A was involved [Bax B. D., *et al.*, 2010]. This template was used as a structural framework for structure based virtual screening of a commercial database Asinex, to explore newer class of inhibitors.

5.1.1.1. Design and development of DNA Gyrase inhibitors based on GSK299423 inhibitor bound protein (PDB ID: 2XCS)

5.1.1.1.1. Protein preparation

The 2.1 A° crystal structure of *S. aureus* DNA Gyrase in complex with GSK299423 was retrieved from protein data bank and structure-based pharmacophore modelling was performed. The DNA Gyrase protein was a heterotetramer of A₂B₂ subunits, represented as A, B, C, D, chains. The B and the D chains were involved in co-crystallization with the inhibitor which was bound in association with the Gyr B C-terminal 27 KDa domain, residues 410-543 and 580-644, Gyr A N-terminal 56 KDa domain, residues 2-491. The reference inhibitor showed a single key interaction with the surrounding amino acid residues. The ([1,3]oxathio[5,4-c]pyridine-6-yl)methanamine group of the inhibitor interacted with Asp1083 residue of the B chain with a distance of 3.64 A°. This interaction was a crucial one as no other interactions were involved with the protein and the inhibitor. Further, for the validation of active site cavity of the protein, the reference inhibitor bound to the protein was extracted and prepared using Ligprep module and redocked with the active site residues of the same *S. aureus* protein. The re-docked ligand exhibited Glide score of -9.36 kcal/mol and was found to be in the vicinity of the important

amino acids like Met1121, Met1075, Gly1072, Ala1068 of both the B and the D chains. Thus, on re-docking separately the ligand exhibited similar interactions as that of the original crystal structure with RMSD of 0.95 Å thus confirming the position of the ligand within the pocket as shown in (Figure 5.1).

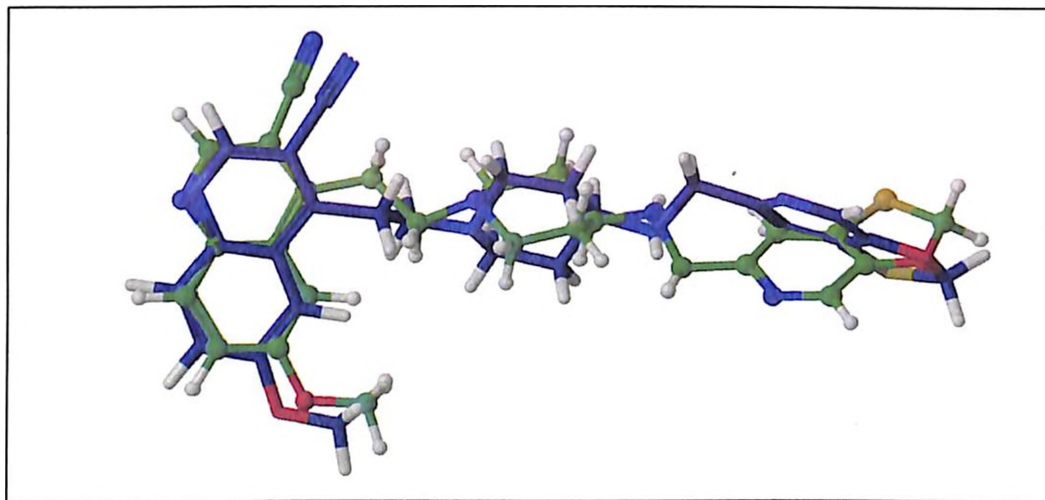


Figure 5.1: Superimposed pose of the crystal ligand GSK299423 and the docked pose of the same ligand with an RMSD of 0.95 Å.

5.1.1.1.2. E-pharmacophore generation

Based on the interaction pattern of the generated e-pharmacophore, the binding mode of the inhibitor within the *S. aureus* protein was defined. Initially, a pharmacophore hypotheses was developed by mapping Glide XP energetic scores onto the pharmacophore sites, calculated based on the structural and energetic information in between the protein and ligand using Phase module, with default set of chemical features within it. Hydrogen-bond donors (D) were represented as projected points if any, located at the corresponding hydrogen-bond acceptor (A) positions in the binding site. The initial number of pharmacophoric sites was set up to 8 for the crystal structure during the pharmacophore generation. Docking results (Xpdes) were then

imported to find the structure-based pharmacophoric features, which would help in finding the best featured functional groups among the ligand. The maximum number of pharmacophoric sites derived for the reference inhibitor was four points with three aromatic rings (R) and one positive ionisable group (P) as shown in (Figure 5.2). The important sites obtained in e-pharmacophore model such as N, were found to correspond to the important amino acid residue Asp1083, while R11, R12 and R13 was not involved in any interaction but these features were inserted into the hydrophobic cavity which was considered to be very crucial for retaining the activity. Energy score of all the four point features is represented in (Table 5.1). The table also shows the R11, P10, R13 and R12 showed energy scores in the increasing order. Though we tried to generate different combinations of pharmacophores yet we could not generate as most of the features were ring aromatics.

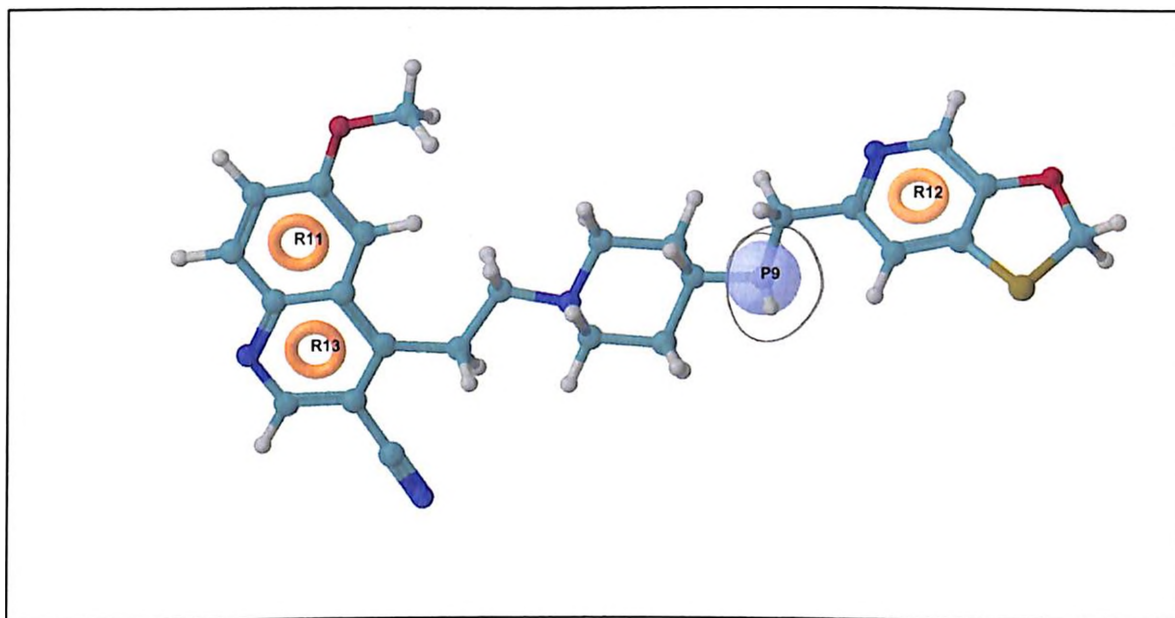


Figure 5.2: Energy based e-pharmacophore with four features.

Table 5.1: Energy scores of hypothesis in e-pharmacophore.

Rank	Feature Lable	Score	Type
1	R11	-1.78	R
2	P10	-1.27	P
3	R13	-1	R
4	R12	-1.34	R

R- ring aromatic; P-Positive ionisable group.

5.1.1.1.3. Virtual screening of commercial database

The implementation of virtual screening protocol is basically to reduce the enormous virtual chemical space of small organic molecules to a manageable/limited number of compounds that were expected to inhibit the desired protein based on selected pharmacophore features. The best pharmacophore model after validation was subjected to virtual screening of commercially available database (Asinex) following a protocol as shown in (Figure 5.3).

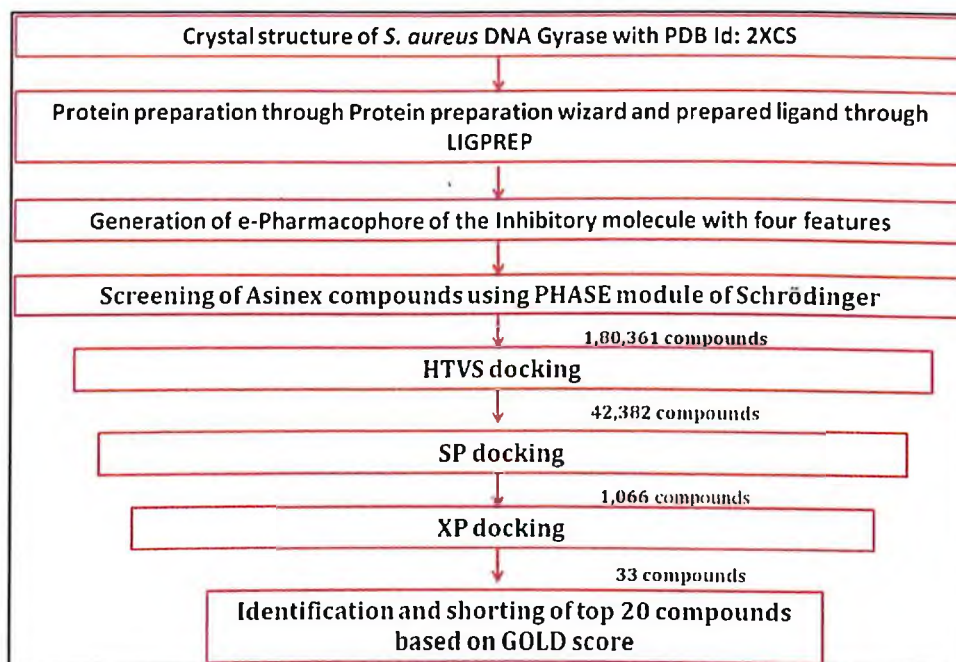


Figure 5.3: Virtual screening flowchart.

Using the pharmacophore model with four features, “find matches” option was used from the Phase module of the Maestro to screen the Asinex database. Compounds showing fitness value above 1.5 were regarded as potential hits. A total of 1,80,361 compounds from 5,00,000 compounds were selected in this step. Further, these compounds were carried forward for HTVS and top 42,382 compounds were selected and were redocked to another round of docking by Glide SP application. Finally, best 1,066 compounds with a score of ≤ -6.5 kcal mol⁻¹ possessing the important hydrogen bond with Asp1083 were further subjected to one more round of docking by Glide XP since Glide XP is associated with accurate, physics-based scoring terms with thorough sampling, gave scores ranging from -8.24 to -10.72 kcal mol⁻¹. A final short listing of possible 33 lead compounds was based on visual inspection of the important amino acid residues involved in binding that included hydrogen bonding with Asp1083; that which was analogous to the one observed with the crystal ligand. To analyse the binding pattern of the ligand with the enzyme, final hit molecules obtained from Glide XP of Schrodinger, were further evaluated with GOLD 5.1.2 software to confirm their potency. Top hits were selected, considering both the results obtained. These hits were filtered based on drug-likeness, by using a Qikprop module of Schrodinger, and the results are presented in the (Table 5.2). Molecules that passed the drug-likeness filter ^{were} having a good permeability, solubility, absorption and those compounds that were not violating the lipinsky rule of five were selected. Thus, we had selected top twenty compounds from the Glide XP docking study with no violations of drug likeliness properties with the best Glide scores (-8.2 to -11.72 kcal mol⁻¹) and GOLD scores (67.49-89.09), suggesting strong protein-ligand interactions. The chemical structures of these twenty compounds illustrated in (Figure 5.4). The compiled results of the docking scores, important amino acid interactions of these hits along with there fitness value is shown in (Table 5.3). The

in silico predicted binding pose of the all the identified hits with key interactions in the binding site of gyrase is represented in (Figure 5.5).

Table 5.2: A QikProp analysis of the ADMET properties of the hits.

Ligand	QLogPo/w	QLogS	QPPCaco	QLogBB	Percent Human Oral Absorption	Rule of Five
L1	4.73	-6.809	1537.512	-0.054	100	0
L2	3.346	-5.887	120.482	-0.716	83.779	0
L3	1.463	-2.513	261.54	0.051	78.78	0
L4	4.714	-5.597	757.226	-0.079	100	0
L5	5.192	-5.607	2937.552	-0.381	100	1
L6	1.711	-2.711	44.907	-0.474	66.534	0
L7	5.211	-4.79	604.404	1.05	94.281	1
L8	3.853	-5.596	483.255	-0.116	100	0
L9	3.778	-6.279	148.479	-0.7	87.935	0
L10	3.824	-5.562	443.321	-0.049	96.708	0
L11	3.25	-5.653	167.834	-0.713	85.799	0
L12	3.241	-5.651	163.187	-0.727	85.528	0
L13	4.243	-5.852	671.704	0.281	100	0
L14	3.788	-5.297	584.144	0.062	100	0
L15	3.453	-5.619	220.348	-0.36	89.103	0
L16	4.469	-5.789	707.831	0.474	100	0
L17	5.074	-6.695	515.661	-0.102	92.241	1
L18	3.995	-3.725	101.115	-0.063	86.221	0
L19	3.995	-5.439	549.53	0.049	100	0
L20	3.326	-4.486	246.037	-0.173	89.213	0

Parameter range indicating value desired for drug like compound: QPPCaco – Predicted apparent Caco-2 cell (model for gut-blood barrier) permeability in nm/s (Range<25 poor, >500 great). QLogBB – Predicted brain/blood partition coefficient (Range -3.0 to 1.2). QLogpo/w- Predicted octanol/water partition co-efficient log p (Range -2.0 to 6.5). QLogS-- Predicted solubility (Range <5.0). Percentage of human oral absorption (Range >80% high <25% poor) Rule of 5 violations – an orally active drug has no more than one violation of the rule of 5 criteria (Range Concern above 1). Range indicates the values desired for drug-like compound.

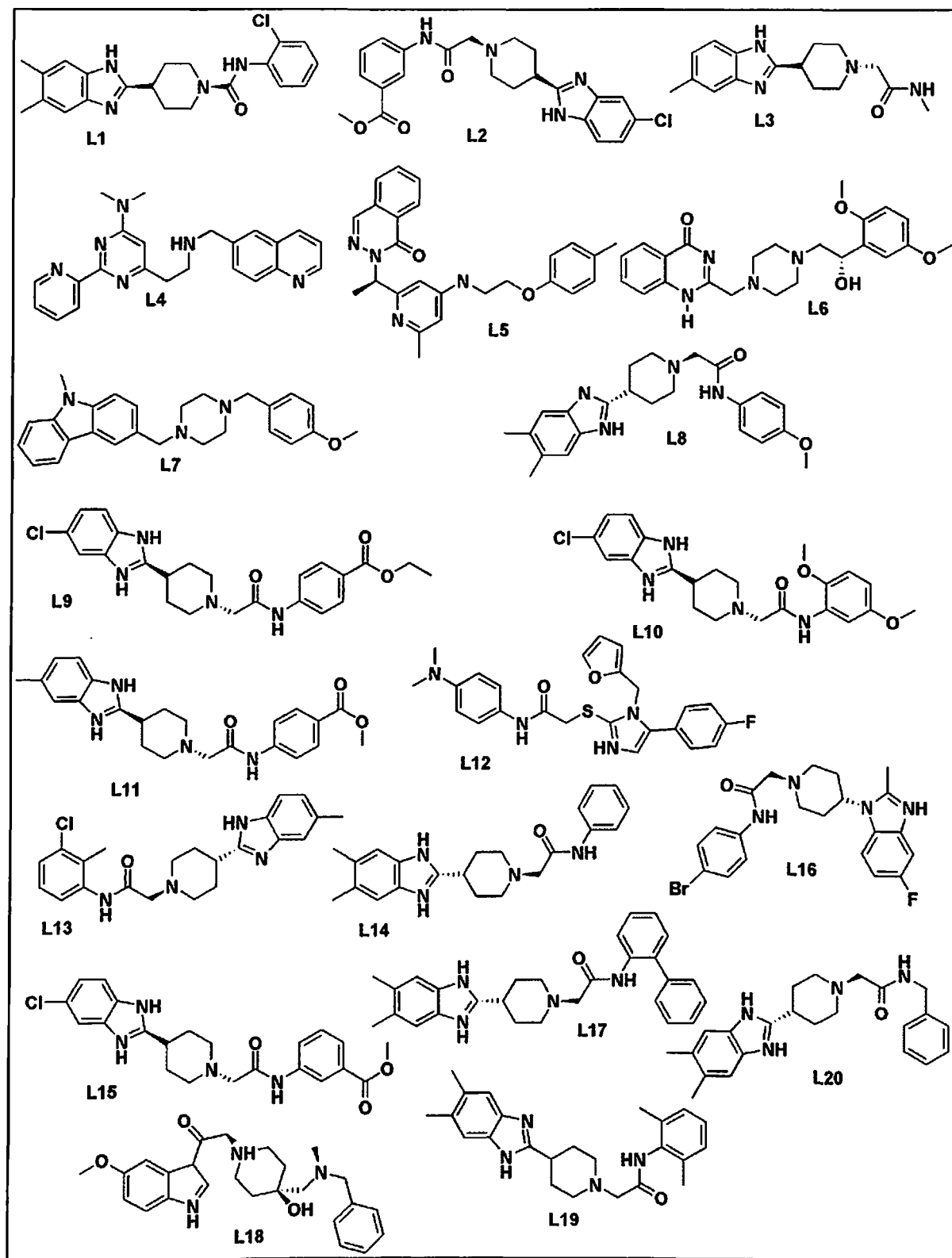


Figure 5.4: Top 15 lead molecules identified from Asinex database

Table 5.3: The docking score, fitness, H-bond interactions and GOLD score of best fit ligands.

Compound Name	Docking score	Interactions	Fitness value	GOLD score
L1	-10.46	Asp1083(B), Asp1082(D)	1.46	73.8
L 2	-10.16	Asp1083(B), Asp1082(D)	1.56	85.31
L 3	-10.33	Asp1083(B), Asp1082(D)	1.55	81.58
L4	-8.65	Asp1083(B)	2.02	-8.65
L 5	-8.00	Asp1083(B), Asp1082(D)	1.40	88.33
L 6	-8.45	Asp1083(B), Asp1082(D)	1.09	70.25
L 7	-8.37	Asp1083(B)	2.01	86.53
L 8	-10.25	Asp1083(B), Asp1082(D)	1.66	77.92
L9	-10.15	Asp1083(B), Asp1082(D)	1.64	82.55
L 10	-10.28	Asp1083(B), Asp1082(D)	1.59	78.87
L 11	-10.12	Asp1083(B), Asp1082(D)	1.65	84.8
L12	-8.87	Asp1083(B)	1.11	73.03
L 13	-10.39	Asp1083(B), Asp1082(D)	1.52	80.8
L14	-10.38	Asp1083(B), Asp1082(D)	1.59	77.56
L 15	-10.26	Asp1083(B), Asp1082(D)	1.57	82.2
L 16	-9.54	Asp1083(B)	1.92	67.49
L17	-10.75	Asp1083(B), Asp1082(D)	1.63	79.4
L 18	-11.17	Asp1083(B)	1.54	70.5
L 19	-9.82	Asp1083(B), Asp1082(D)	1.07	89.09
L 20	-10.33	Asp1083(B), Asp1082(D)	1.27	80.8

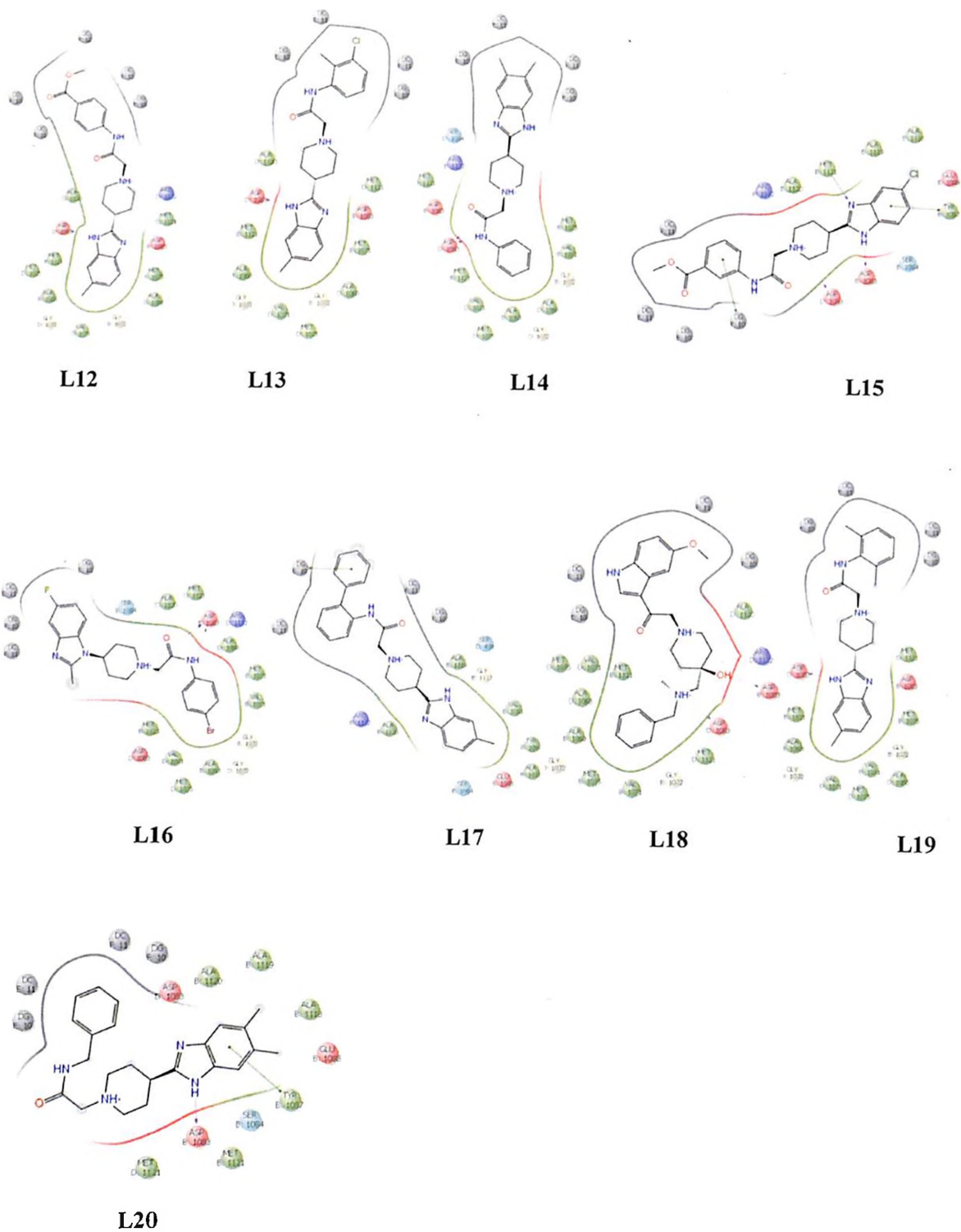


Figure 5.5: Ligand-protein interactions of all the hits with the active site residues of *S. aureus* protein

5.1.1.2. Biological validation of the virtually screened hits

These top twenty selected hits retrieved from the Asinex database were screened biologically in supercoiling assay to check for their inhibition potencies against *S. aureus* DNA Gyrase.

5.1.1.2.1. *In vitro S. aureus* supercoiling assay

All the twenty compounds were further evaluated for their supercoiling inhibition. Initially, the assay was carried at an inhibitor concentration of 100 μM against *S. aureus* DNA Gyrase as illustrated in the material and method section. Those compounds that displayed >50% inhibition were further screened at a lower concentration of 50 μM . Out of 20 compounds fourteen compounds exhibited promising activity less than 10 μM and were studied in more detail and further evaluated at lower concentrations of 5 and 1 μM . A dose response curve was carried out for three of the most active compounds in the supercoiling assay to visualize their inhibitory profile. Novobiocin was used as a positive control in these assays as it was shown to be a potent inhibitor of DNA supercoiling of Staphylococcal DNA Gyrase species with an IC_{50} of about 14 nM. The most active **L15**, had an IC_{50} of 0.79 ± 0.12 nM as shown in ~~the~~ (Figure 5.6). The top three leads **L15**, **L16** and **L18** were also retaining the important hydrogen bonding interactions with Asp1083 amino acid residue. Further, compound **L15** also interacted with another hydrogen bonding interaction with Met1121. Apart from this, the compound was further stabilized by additional *pi-pi* interactions with D10 and Tyr108. The compound also was inserted well into the hydrophobic cavity where it makes various hydrophobic interactions with Ala1068, Met1071, Val1071 amino acid residues. Because of its interaction and binding pattern associated with biological activity, we have taken for further lead optimization and synthesis of its analogues to trace the structure activity relationship because information on the common properties of the

binding groups was essential for resolving the type of inhibitor binding to the target protein. The activity data of all the twenty leads is presented in (Table 5.4).

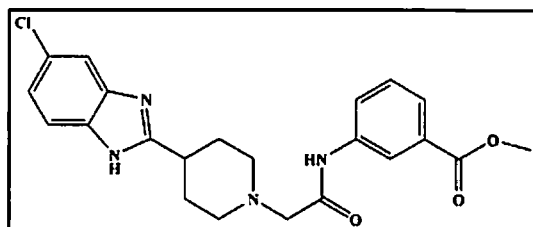


Figure 5.6: Structure of **L15** compound with an IC_{50} of $0.79 \pm 0.12 \mu M$.

Table. 5.4: Activity table of the lead compounds with their DNA supercoiling results

S. No	Asinex Number	Supercoiling assay IC_{50}
Novobiocin	-	0.014 ± 0.01
L1	ASN 06579379	26.72 ± 0.32
L2	ASN 06579315	23.98 ± 0.21
L3	ASN 06579596	6.25 ± 0.16
L4	SYN 22399039	19.44 ± 0.34
L5	SYN 23064783	15.23 ± 0.29
L6	SYN 19978333	4.26 ± 0.18
L7	BAS 01234893	2.28 ± 0.16
L8	ASN 06579259	15.46 ± 0.27
L9	ASN 06579303	2.36 ± 0.16
L10	ASN 06579213	1.96 ± 0.18
L11	ASN 06579291	7.55 ± 0.22
L12	ASN 03017282	3.89 ± 0.34
L13	ASN 06579434	4.22 ± 0.35
L14	ASN 06579121	1.9 ± 0.24
L15	ASN 06579309	0.79 ± 0.12
L16	ASN 06360797	0.83 ± 0.15
L17	ASN 06581953	19.54 ± 0.28
L18	LEG 20477521	0.92 ± 0.14
L19	ASN 06579175	15.24 ± 0.38
L20	ASN 06579127	3.12 ± 0.24

5.1.1.3. Hit expansion and lead optimization

Among the twenty compounds that were obtained from Asinex database through structure based virtual screening, the top three most active compounds were selected based on their inhibitory profile in *S. aureus* DNA gyrase supercoiling assay. Among the three molecules, **L15**, **L16** and **L18** which possess an IC_{50} in nanomolar range, **L15** was taken up for further synthesis and lead optimization based on the feasibility of the chemical reaction and availability of the chemicals. Thus, for lead optimization we have taken most active compound from structure based virtual screening.

5.1.1.3.1. Chemical synthesis and characterization

Taking **L15** compound as a lead, we designed a limited library of forty molecules with the goal of obtaining a pool of analogues with tracable SAR and a better potencies than the previously identified virtual screening hit. All these analogues was synthesized with various substitutions. The core moiety 2-(piperidin-4-yl)-1H-benzo[d]imidazole from the **L15** was retained in all the analogues. In order to explore the structure activity relation, both left hand side as well as the right hand side was varied with different substituents keeping the core benzimidazole group intact. Left hand side was substituted with various electron withdrawing groups like chloro, fluoro as well as electron donating substituents like methyl, hydrogen to check the effect of those groups on the activity. In this way, we obtained four scaffolds with various substituted acetyl chlorides, to modify the right hand side which helped in bringing structural diversity. The synthetic strategy followed is sketched in **(Figure 5.7)**. Synthesis was started with the construction of benzimidazole moiety. This was achieved by condensation between commercially available substituted 1,2 phenylenediamines with 4- aminobenzoic acid

using Eaton's reagent to obtain compound **2** in good yields. Eaton's reagent provides an efficient way to get the condensation product in excellent yield compared to other reagents. In the second step so obtained, benzimidazole scaffolds were treated with various substituted acetyl chlorides in the presence of triethylamine to get corresponding N- substituted acetamides as final molecules (**4-43**) in good yields. The general procedure and spectral analysis of all the forty compounds are represented in Annexure-I.

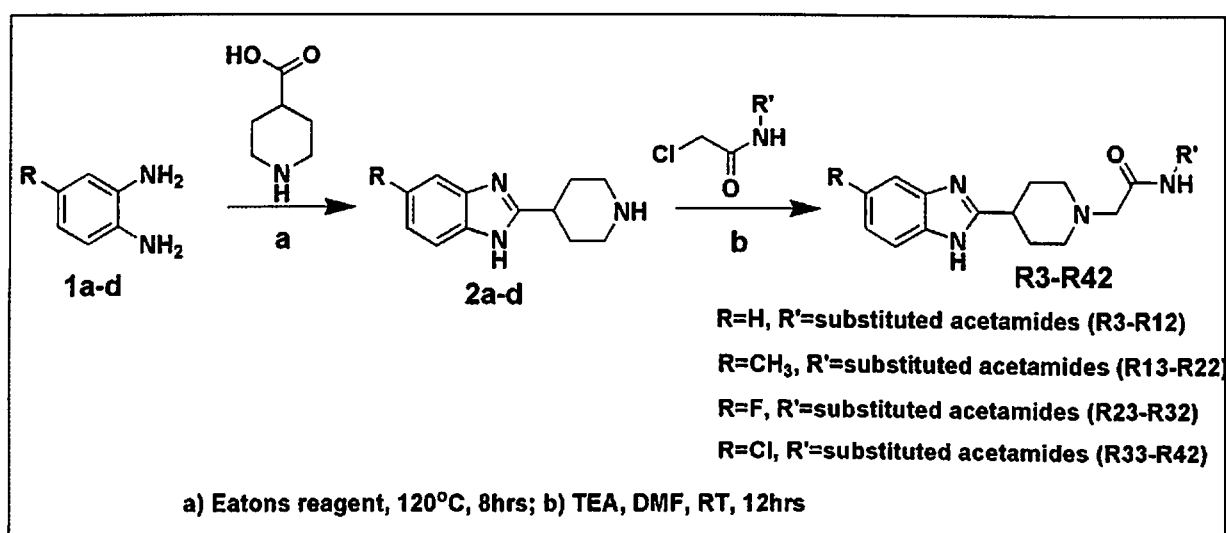


Figure 5.7: Synthetic procedure to obtain the final analogues.

5.1.1.3.2. *In vitro* DNA supercoiling assay of the synthesized compounds with SAR

DNA supercoiling assay was carried for all the synthesized forty molecules. Among the forty molecules thirteen molecules showed inhibitions of less than 5 μM concentration proving the efficiency of this NBTI class of inhibitors. In the first set of compounds **R** group was substituted with H and different **R**¹ substitutions, like phenyl, 2-chloro-5-(trifluoromethyl)phenyl, 6-chloro pyridyl, benzyl, 3-acetyl phenyl, 5-nitrothiazole, benzothiazole, 6-nitro benzothiazole, furyl methyl and 4-methoxy phenyl. Compound **R8** with 3-acetyl phenyl, was the most active

compound with an IC_{50} of $0.62 \pm 0.14 \mu M$. The second set of compounds had an R group of methyl and different substitutions at R^1 as above, compounds **R20** and **R21** was showing good IC_{50} 's of 0.32 ± 0.17 and 2.31 ± 0.32 respectively. Compound **R20** was one of most active compound in this series. The compound substituted with methyl group at R position and benzothiazole groups at R' position emerged as a most potent compound compared to other compounds from this series. This was well supported by the interaction profile of the molecules in the docking studies. With highest docking score of -10.50 kcal/mol which correlated well with its potency in the enzyme assay with an IC_{50} of $0.32 \pm 0.17 \mu M$. Binding analysis of this compound in the active site of protein showed hydrogen bonding interactions with the Asp1083 analogous to crystal ligand and also essential for retaining the activity of compound. The compound also showed hydrophobic interaction with Met1121, Val1071, Met1075, Ala1068, Ala1068 amino acid residues which are equally important for the biological activity. Final set of compounds had R position containing fluoro and chloro groups, while the R^1 had the above mentioned substitutions. Compounds **R25, R29, R30, R31, R36, R38, R39** and **R41** showed better inhibitory profiles compared to the other compounds in the series.

5.1.1.4. Antibacterial potency

NO mention of Table 5-5

Have these strains been validated for resistance?

All the forty compounds were evaluated for their *in vitro* antibacterial inhibition studies. The compounds were tested in 2 strains, **MTCC3160** and **MTCC96**. All the compounds were tested in a range of $125-0.1 \mu M$ in a 96 flat-bottomed well plate. Novobiocin was set as a standard drug with an MIC of $1.23 \mu M$ in **MTCC3160** and $6.51 \mu M$ in **MTCC96** strains, while compounds **R8, R11, R12, R20, R21, R22, R29, R30, R36** and **R41** showed an inhibition less than $10 \mu M$ in **MTCC3160** strain. Subsequently, all the compounds were also tested in **multiresistant MTCC96** strain to check the efficiency of the drug. Seven compounds **R8, R11, R12, R20, R21, R30** and

any 2 or 3

R36 showed inhibitions less than 10 μM . With these studies, it was clear that these class of NBTI's have a good antibacterial potency against different strains of *S. aureus* organisms.

5.1.1.5. Cytotoxicity studies

How is this non toxic?

Cytotoxicity studies were carried on the RAW 264.7 cell line. All the different analogues were tested for their toxicity nature on eukaryotic mouse embryonic cell lines. The range of inhibition of the cells was 0.28-14.32 μM highlighting the non-toxicity of this group of compounds on eukaryotic cells. The assay was carried by using the MTT dye. Among the forty compounds, twenty six compounds inhibition range was below 10 μM . Novobiocin which was considered as a standard, showed an inhibition of 14.66 μM . All the compounds showed less than the standard drug inhibition profile.

Is this CC_{50} ? or CC_{90} ? or CC_{99} ?

Moxifloxacin?

5.1.1.6. Inhibition of biofilm formation studies

incorrect statement?

S. aureus resistance is owed mainly to the biofilm formation nature of the organism. All the compounds which showed a good enzyme inhibition studies and better MIC profile were further taken up for the inhibition of the biofilm formation assays by crystal violet staining. Though the concentration of the compounds required to inhibit the biofilm formation were more than the respective MIC's, yet these analogues can be considered as good scaffolds for further optimization studies. Compound R20 showed a good inhibitory profile at 9.09 μM . All the tested compounds showed biofilm inhibitions less than 70 μM concentration which is an indication of the efficiency of this class of compounds.

Against which strain?

How? what is your cut off for this assay?
What is the +ve control?

5.1.1.7. Efflux pump inhibitor assay

This assay was performed to evaluate the antibiotic resistance created due to the efflux pumps located on the *S. aureus* cell membrane. MTCC96, a multiresistant strain was used to perform the assay. As the evaluated MIC's were high when compared to the enzyme inhibitions, piperine and verapamil (Nor A efflux pump inhibitors) were used in combination to check the effect of the efflux pump in antibiotic removal. Top nine compounds **R8, R12, R20, R21, R25, R29, R30, R36, R41** along with **novobiocin** were selected and assay was performed in a microtitre plates.

Many of the compounds showed 2-3 fold reduction in the MIC's except **R25, R29 and R41** revealing that the efflux pump plays a major role in pumping the antibacterials.

5.1.1.8. zERG toxicity studies

The zERG toxicity studies were carried on zebra fish. In this assay, 3dpf embryos were distributed in a 24 well plate along with 250 μ l of 0.1% DMSO solution and working concentrations of the compounds **R20** and **R36** was prepared by serial dilutions. The wells containing 5 embryos each were treated with required concentration of the drug solution and incubated. In this assay Terfenadine (20 μ M) was used as a positive control and concentrations of the drug compounds was 1, 3, 10 and 30 μ M. Both the compounds showed no toxicity at 1 and 3 μ M whereas at a higher concentration of 10 and 30 μ M toxicity was seen as the embryos died, as shown in the (Figure 5.8). All the statistical analysis was done using GraphPad Prism® software using one way ANOVA followed by Dunnet's post test.

How come MIC of R29/R30/R41 increases in presence of ERP's?

a)

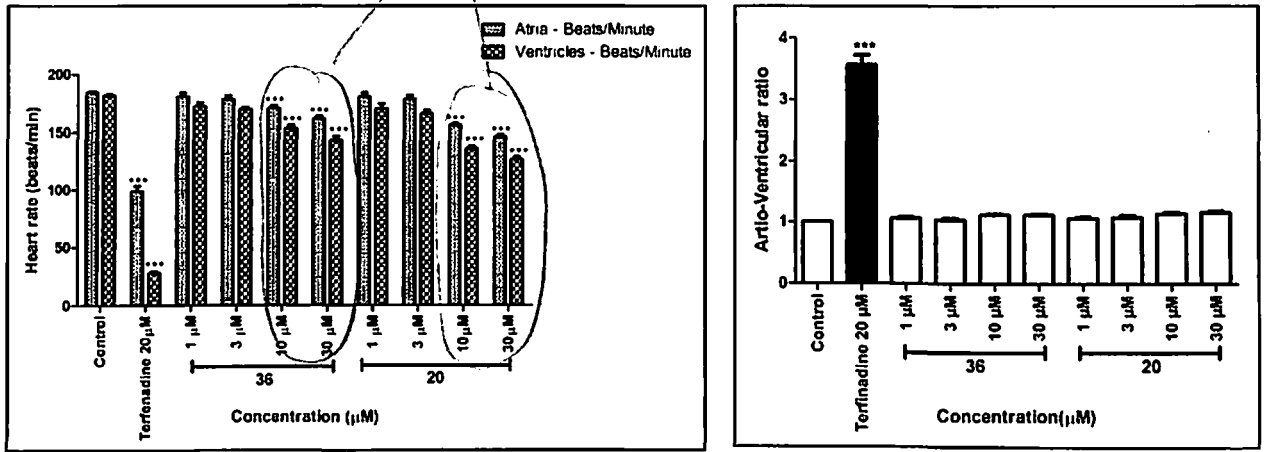


Figure 5.8: (a) Mean (\pm S.E.M.) of the heart rates of atria and ventricles of R36 & R20 treatment groups. (* $p < 0.05$, ** $p < 0.01$ and *** $p < 0.001$). Statistical significance was analyzed with respect to the control group. (b) Mean (\pm S.E.M.) score of atrio ventricular ratio of treatment groups. (* $p < 0.05$, ** $p < 0.01$ and *** $p < 0.001$). Statistical significance was analyzed comparing control group Vs all groups

5.1.1.9. Kill kinetics

Kill kinetic studies were carried for the top compound with good enzymatic and better MIC profiles, we selected compound R20 to perform kill kinetic study using MTCC96 strain by broth dilution method at a drug concentrations of 0.5x, 1x, 2x 4x, and 8x of MIC that was 3.03 μM, 6.06 μM, 12.12 μM, 24.24 μM and 48.48 μM respectively by CLSI guidelines. Reduction of colony forming units (CFU) of *S. aureus* in an *in vitro* time kill kinetic experiment was evaluated (>10⁵ CFU/mL inoculum) at >2x of MIC (0.03 μM) confirming bactericidal effect of this compound.

Handwritten notes:
 - incorrect.
 - what is the definition of bactericidal?
 - This 5.1.1.9 is incorrect. Here, we are saying MIC is 6.06 μM. R20 MIC as per table 5.5 is 3.03 μM.
 - 2x MIC there is no effect whatsoever?

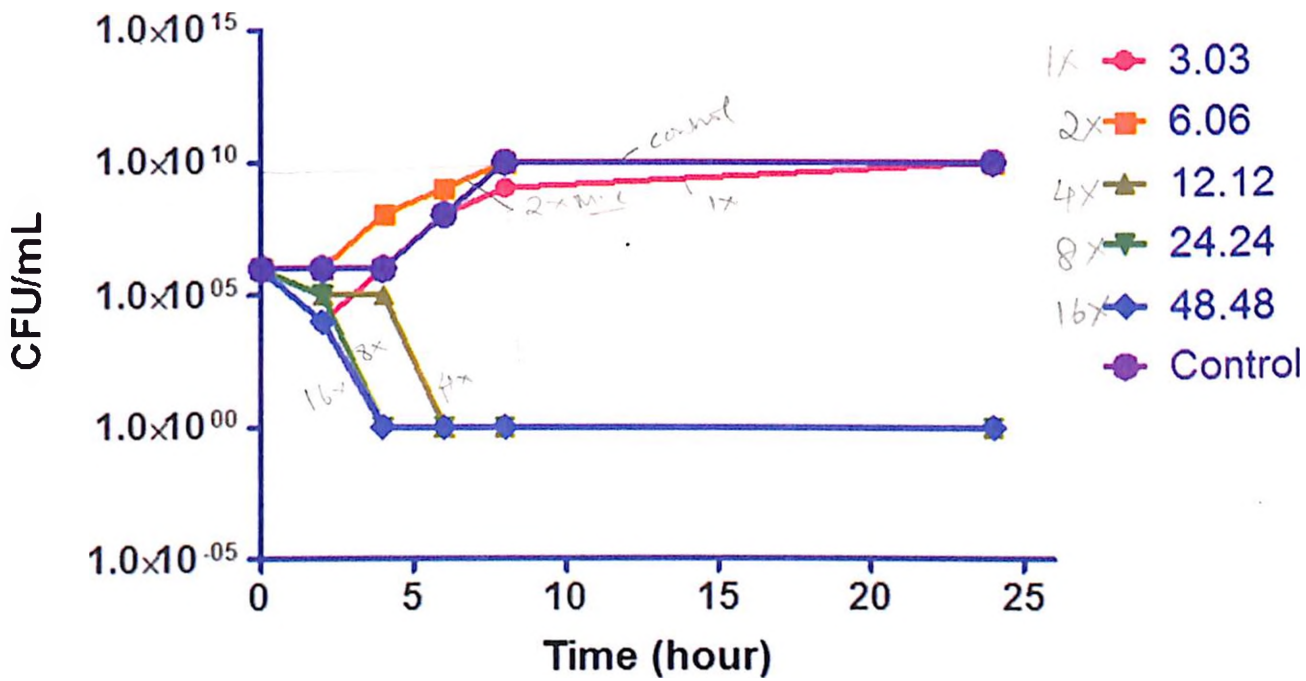


Figure 5.9: Time kill kinetics of compound R20 in *S. aureus*. The MIC in the experiment was

0.03 μM .

How is this MIC?

Against which strain?

differ from data in Table 5.5?

which strain?

— control antibiotic is missing?

— this graph is weird. Your control reaches 10^9 in 9 hrs & then is flat? How is this possible?

— How did you compensate for % DMSO?

Table 5.5: Biological activities of the synthesized compounds

Comp no.	R	R'	Supercoiling Assay (μM)	MIC MTCC 3160 (μM)	MIC MTCC96 (μM)	Efflux pump Inhibitor (μM)	Biofilm IC_{50} (μM)	Cytotoxicity in RAW 264.7 cells at 100 μM
R4	H	Phenyl	21.29 \pm 0.37	37.67	37.67	NA	NA	6.32
R5	H	2-Chloro-5-(trifluoromethyl)phenyl	18.22 \pm 0.29	14.30	28.61	NA	NA	10.95
R6	H	6-Chloro pyridyl	13.99 \pm 0.35	16.28	32.56	NA	NA	7.11
R7	H	Benzyl	19.24 \pm 0.81	35.87	35.87	NA	NA	14.26
R8	H	3-Acetyl phenyl	0.62 \pm 0.14	4.14	8.28	4.14	12.41	6.23
R9	H	5-Nitrothiazole	16.92 \pm 0.39	32.34	32.34	NA	NA	2.80
R10	H	Benzothiazole	12.25 \pm 1.27	63.84	31.92	NA	NA	0.73
R11	H	6-Nitro benzothiazole	2.21 \pm 0.24	7.14	7.14	NA	14.28	1.24
R12	H	Furyl methyl	1.89 \pm 0.26	4.65	18.42	4.65	13.86	2.98
R13	H	4-Methoxy phenyl	8.91 \pm 0.41	17.14	17.14	NA	NA	11.81
R14	CH ₃	Phenyl	13.79 \pm 0.49	71.74	35.87	NA	NA	9.26
R15	CH ₃	2-Chloro-5-(trifluoromethyl)phenyl	16.82 \pm 0.53	55.44	55.44	NA	NA	14.23
R16	CH ₃	6-Chloro pyridyl	19.34 \pm 0.77	62.82	62.82	NA	NA	10.77
R17	CH ₃	Benzyl	14.44 \pm 0.18	34.48	34.48	NA	NA	9.86
R18	CH ₃	3-Acetyl phenyl	21.89 \pm 0.27	32.01	64.02	NA	NA	7.89
R19	CH ₃	5-Nitrothiazole	18.44 \pm 1.82	31.23	62.47	NA	NA	13.21
R20	CH ₃	Benzothiazole	0.32 \pm 0.17	6.03	12.12	3.03	9.09	7.82
R21	CH ₃	6-Nitro benzothiazole	2.31 \pm 0.32	6.92	13.92	6.92	13.84	8.82
R22	CH ₃	Furyl methyl	5.16 \pm 0.27	8.68	17.37	NA	17.37	6.92
R23	CH ₃	4-Methoxy phenyl	21.66 \pm 0.39	33.02	33.02	NA	NA	0.78
R24	F	Phenyl	7.81 \pm 0.83	17.73	35.47	NA	35.47	0.28
R25	F	2-Chloro-5-(trifluoromethyl)phenyl	3.46 \pm 0.41	13.45	13.45	13.45	26.90	1.78
R26	F	6-Chloro pyridyl	8.94 \pm 0.29	31.10	62.20	NA	62.20	12.22
R27	F	Benzyl	9.15 \pm 0.66	17.05	68.22	NA	68.22	10.11
R28	F	3-Acetyl phenyl	16.32 \pm 0.38	63.38	63.38	NA	NA	14.32
R29	F	5-Nitrothiazole	2.44 \pm 0.44	7.72	15.45	15.45	15.45	11.52
R30	F	Benzothiazole	1.17 \pm 0.15	3.85	15.22	7.61	15.22	5.42
R31	F	6-Nitro benzothiazole	4.29 \pm 0.62	13.75	13.75	NA	13.75	4.35
R32	F	Furyl methyl	10.16 \pm 0.59	17.17	17.17	NA	NA	2.29
R33	F	4-Methoxy phenyl	9.21 \pm 1.22	16.34	16.34	NA	32.68	3.13
R34	Cl	Phenyl	11.91 \pm 0.66	16.94	33.88	NA	NA	13.92
R35	Cl	2-Chloro-5-(trifluoromethyl)phenyl	18.16 \pm 1.52	26.52	53.04	NA	NA	9.42
R36	Cl	6-Chloro pyridyl	0.39 \pm 0.14	7.45	14.90	7.45	29.8	5.34
R37	Cl	Benzyl	13.18 \pm 0.68	21.76	21.76	NA	NA	14.19
R38	Cl	3-Acetyl phenyl	4.98 \pm 0.51	14.89	14.89	NA	29.78	1.82
R39	Cl	5-Nitrothiazole	4.16 \pm 0.79	14.54	14.54	NA	29.78	0.29
R40	Cl	Benzothiazole	13.21 \pm 1.23	14.67	29.34	NA	NA	10.67
R41	Cl	6-Nitro benzothiazole	0.57 \pm 0.14	6.49	12.99	12.99	12.98	13.21
R42	Cl	Furyl methyl	19.15 \pm 1.82	33.52	33.52	NA	NA	2.73
R43	Cl	4-Methoxy phenyl	22.31 \pm 1.34	41.78	41.78	NA	NA	3.98
Moxifloxacin			0.019 \pm 0.04	1.23	3.69	3.69	6.15	14.66

5.2. Development of *S. aureus* DNA Gyr B inhibitors as potential inhibitors

Though *S. aureus* DNA Gyrase is a well validated target to treat pathogenic and respiratory diseases, the Gyr B portion remains unexploited compared to the Gyr A domain. Since, the Gyr B is an ATPase catalytic core, this domain remains to be a perfect target for the drug development. Since very few inhibitors were reported till date against DNA Gyr B, in the present work we took an effort to design some novel inhibitors for Gyr B domain.

5.2.1. Design and development of *S. aureus* DNA Gyr B inhibitors through structure based drug design strategy

In the present study, we utilized the structure based virtual screening protocol described in the material and method section, to identify newer scaffolds as potential *S. aureus* DNA Gyr B leads. Initially, we started with e-pharmacophore approach, a combination of both the aspects of structure-based and ligand-based techniques using the crystal structure of DNA Gyr B protein–ligand complex retrieved from the PDB as a template (PDB code: 3TTZ) [Sherer B. A., *et al.*, 2011]. Later, pharmacophore hypothesis was established by mapping the energetic terms from the extra precision Glide scoring function (Glide XP) onto the atom centres (Glide, version 5.7, Schrödinger, LLC, New York, NY, 2011) [Friesner R. A., *et al.*, 2006; Poyraz O. M., *et al.*, 2013]. Structural and energetic information between the protein and ligand were also evaluated by using Phase module (Phase, v3.3, Schrödinger, LLC, New York, NY). As shown in (Figure 5.10), a three-point e-pharmacophore model was generated with ATPase DNA Gyr B domain. The pharmacophoric sites established included one donor (D), one acceptor (A) and one negative ionisable group (N), which was further utilised for virtual screening of commercially available database (Asinex) of five lakh molecules using the protocol as described in material and

methods. Initially, the compounds were retrieved by the three-point e-pharmacophore filter using phase module and those with fit value above 2 were regarded as potential hits. These were further subjected to high throughput virtual screening. Compounds having good fitness score, similar docking pose, possessing two or more hydrogen bonds and a Glide score of $5.8 \text{ kcal mol}^{-1}$ were subjected to another round of docking by Glide XP. The Glide XP module has been reported to be a precise tool as it combines accurate, well defined physics based scoring terms and thorough sampling of the available terms. The final output file resulted in scores ranging from -11.81 to $-6.93 \text{ kcal mol}^{-1}$. Shortlisting of the molecules was based on the protein-ligand interaction at the active site cleft through hydrogen bonding with Asp81, Arg144 and via π -stacking with Arg84. Gyr B consisted of a hydrophobic pocket, surrounded by the amino acid residues like Ser55, Thr173, Val79, Gly85, Pro87, Glu58, Asn54, and Ile86 in the vicinity as shown in (Figure 5.11). *None of these are in R5 5.11* Finally, top twelve hits were selected from the Asinex database and were evaluated biologically (Figure 5.12).

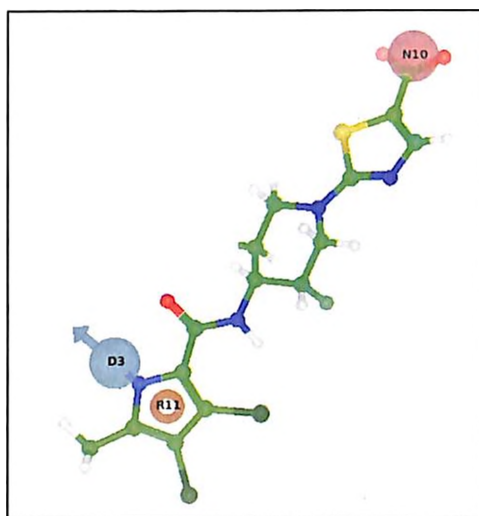


Figure 5.10: 3-point e-pharmacophore of 3TTZ Gyr B protein.

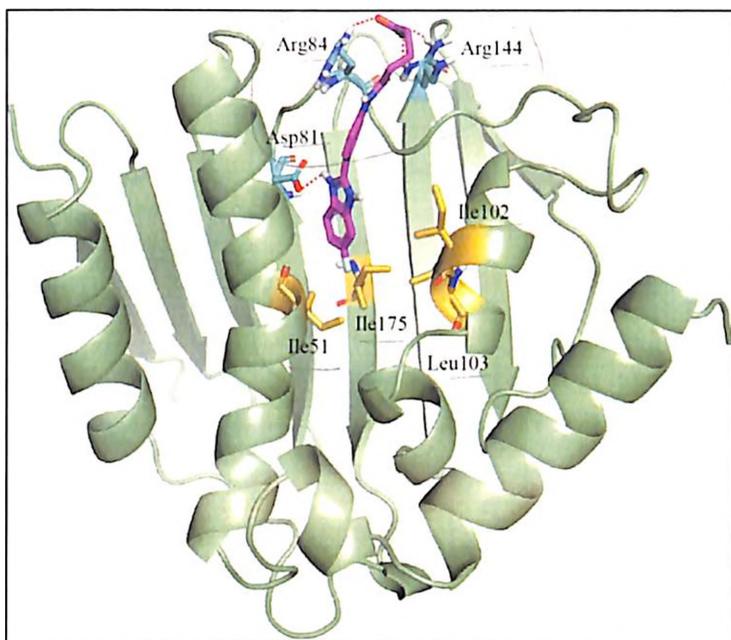


Figure 5.11: Crystal ligand interactions with the DNA Gyrase B protein in the active site pocket.

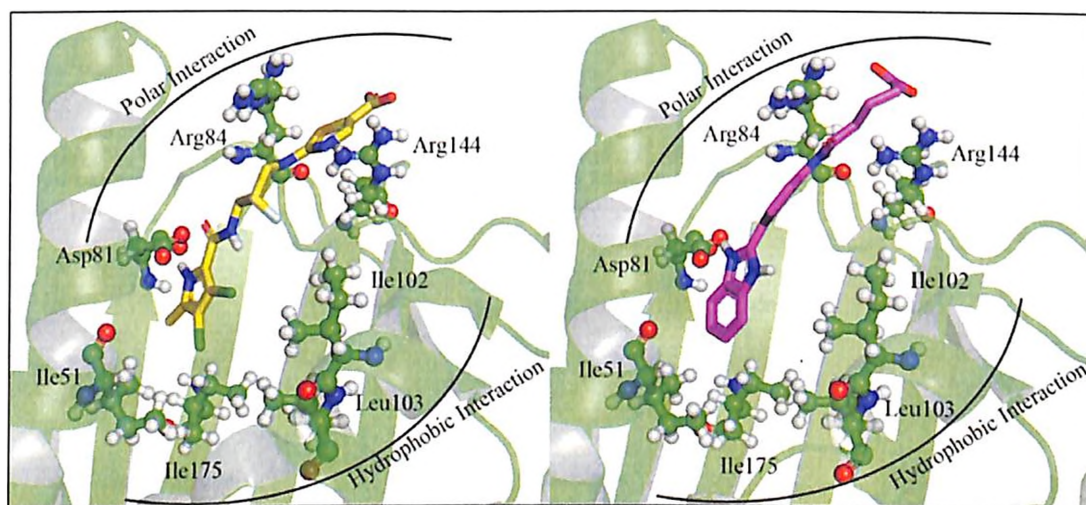


Figure 5.13: Interaction pattern of crystal ligand with lead molecule A1 (BAS01355130).

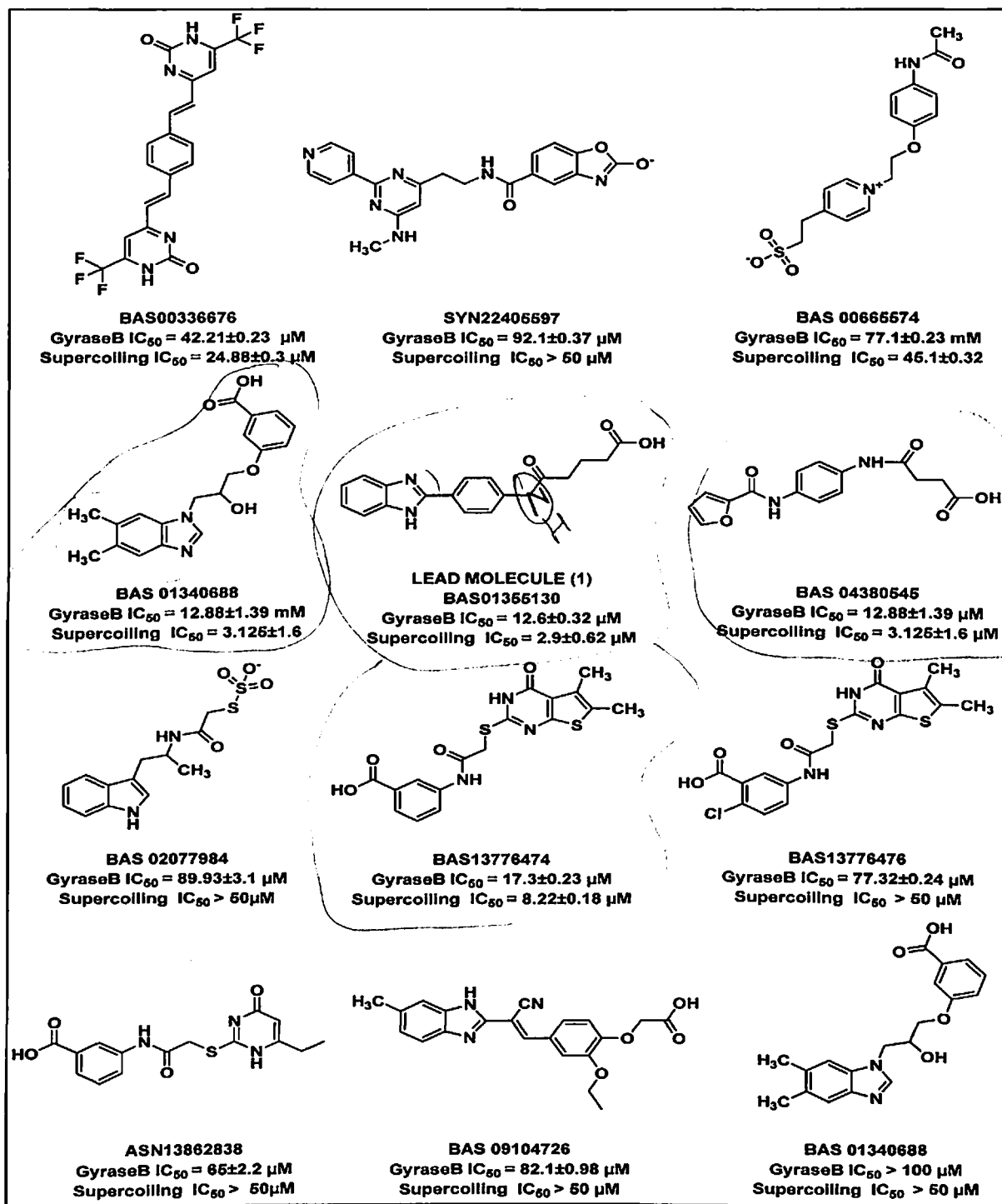


Figure 5.12: The twelve hit molecules retrieved from Asinex database after virtual screening.

5.2.2. Enzyme kinetics of *S. aureus* DNA Gyr B

As per literature, the rate of the reaction of *S. aureus* DNA Gyr B was very slow, and the reaction continued for long time. Whereas in the presence of Gyr A subunit the reaction takes place much faster as it stimulates the Gyr B. Substitution of *E. coli* Gyr A with *S. aureus* Gyr A stimulates the reaction by 20-fold. Addition of DNA increases the reaction rate by 620-fold. The ATPase activity of enzyme followed the first-order kinetics. The K_m and V_{max} was determined experimentally and was found to be 0.0625 mM and 0.47 $\mu\text{mol}/\text{sec}$ respectively.

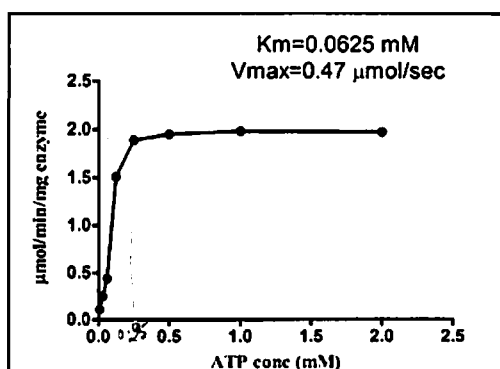


Figure 5.14: Enzyme kinetics of *S. aureus* Gyr B protein.

5.2.2.1. *S. aureus* DNA Gyr B ATPase assay

Among the ^{15 hits} twelve hits shown in ^{5.12} ~~(Figure 5.4)~~ four compounds (BAS01340688, BAS01355130, BAS04380545, and BAS3776474) showed DNA Gyr B IC_{50} of less than 20 μM whereas the others showed an IC_{50} less than 100 μM . All these compounds were also tested for the DNA supercoiling assay and only six compounds showed bioactivity with IC_{50} less than 50 μM and the compounds BAS01340688, BAS01355130, BAS04380545 and BAS3776474 were found to be promising as revealed in the Gyr B inhibition assay. Among the active compounds, the hits BAS01340688 and BAS01355130 possess benzimidazole nucleus and the most active compound

was found to be 4-[4-(1H-benzimidazol-2-yl)-phenylcarbamoyl] butanoic acid (BAS01355130), which showed significant activity in the Gyr B assay with an IC_{50} of $12.6 \pm 0.32 \mu M$ and supercoiling assay IC_{50} of $2.9 \mu M$. The docking orientation of this compound BAS01355130 hereafter represented as lead A1, when compared with the crystal ligand, revealed important polar contacts with Asp81, Arg84 and Arg144 similar to that of the crystal ligand of *S. aureus* Gyr B. The docking score of A1 was found to be -6.58 and a strong non-polar interaction by the benzimidazole moiety at the adenine binding position of ATP with Ile51, Ile102 and Ile175.

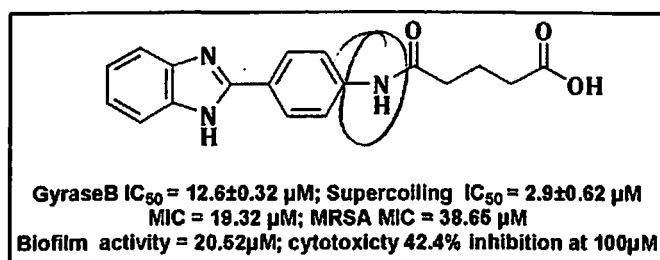


Figure 5.15: Lead molecule (A1) BAS01355130

The structure drawn here is different from that in fig 5.12.

5.2.3. Hit expansion and lead optimization of lead molecule (A1)

The lead molecule A1 (BAS01355130) has a benzimidazole nucleus on the left hand core that run through a 4-aminophenyl linker, to a right handed alkyl side chain as per (Figure 5.15). The promising results of the virtual screening hits encouraged us to design a library of benzimidazole scaffold with a goal of obtaining a series of analogues with tractable SAR and potencies better than the identified virtual screening lead. Considering the input from protein–ligand interactions observed with the crystal structure of Gyr B and the A1, the following modifications were attempted as a first ligand expansion step which included (i) exploring the effect of various substituent's on benzimidazole nucleus (ii) extending the length of acyl side chain and converting the carboxylic acid group into their corresponding ester as shown in (Table

5.6), to identify the ideal sites for introducing chemical diversity and to have a clearer understanding of the role of these substituent as determinants of inhibitory potency. The synthetic pathway used to achieve lead modifications is delineated in (Figure 5.16).

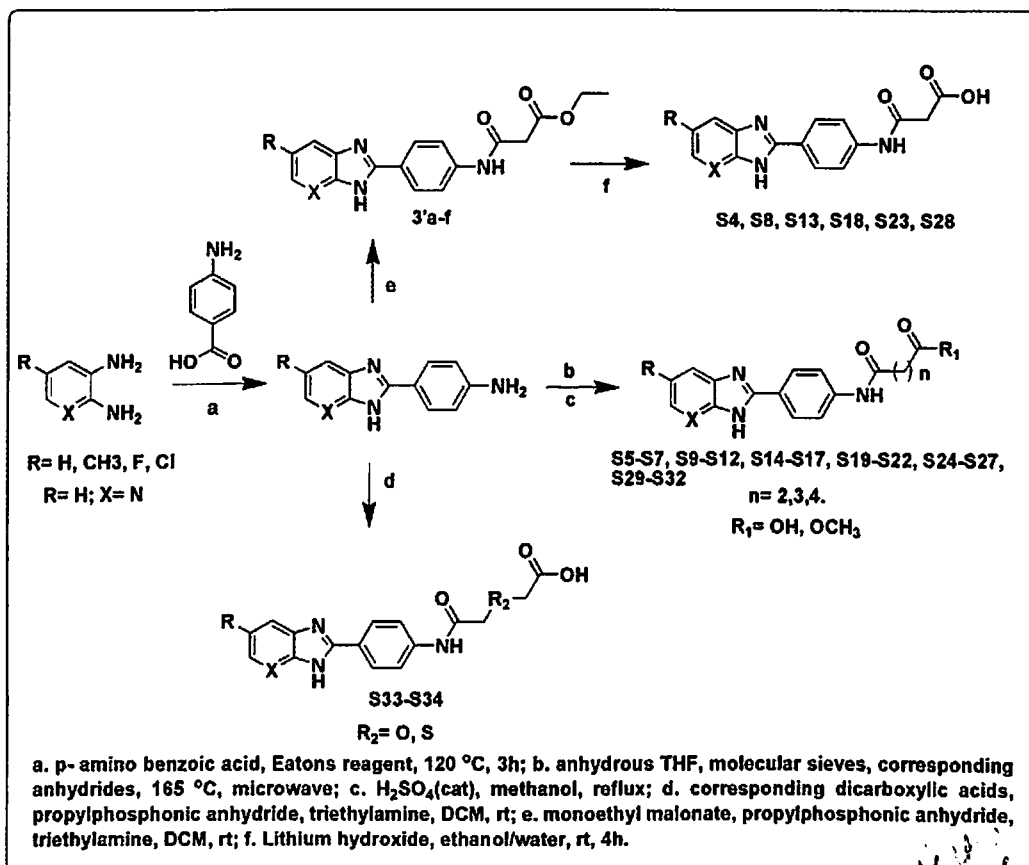


Figure 5.16: The synthetic pathway used to achieve lead modifications

The synthesis of target molecules began with the condensation of commercially available substituted 1,2 phenylenediamine (compounds 2a-e) with 4-aminobenzoic acid in the presence of Eaton's reagent to yield the corresponding 4-(substituted-1H-benzo[d]imidazol-2-yl) aniline (compounds 3a-e) in good yields. This method utilizing Eaton's reagent was highly beneficial in improving the yields of the so obtained 1H-benzo[d]imidazol-2-yl) aniline analogues, when compared to other reagents/protocols available in literature. A similar strategy was adopted to

develop 4-(3H-imidazo [4,5-b]pyridin-2-yl)aniline nucleus (3f) as well, starting from 1,2-diaminopyridine (2f). Functionalization of 4-aminophenyl linker was then brought about by treatment with various acid anhydrides to yield compounds S4–S32. Further, the carboxylic acid side chains of few selected analogues (S5, S10, S15, S20, S25 and S30) were converted into their corresponding esters (S6, S11, S16, S21, S26 and S31) as an effort to improve the bacterial cell wall permeability of these compounds. The oxygen and thio-substituted acyl derivatives (S33–S44) were prepared by coupling 4-(sub:-1Hbenzo[d]imidazol-2-yl)aniline/4-(3H-imidazo[4,5-b]pyridin-2-yl)aniline nucleus (3a–f) with diglycolic acid and 2,20-thiodiacetic acid respectively. Overall, a library of forty one derivatives were synthesized S4–S44, as shown in **Table 5.6**, characterized and evaluated for their ability to inhibit the Gyr B activity as an effort towards the derivatization of structure–activity relationships and lead optimization.

5.2.4. QikProp results

Further, to analyse various pharmacokinetic properties of these forty one compounds QikProp 3.5 module of Schrodinger software was utilized. A preliminary examination of the ADMET results showed that all the desired hits obey Lipinski's rule of five showing their drug-like nature. Compounds with favourable activity against *S. aureus* DNA Gyr B (S10, S44, S41 and S32) showed parameters within desirable range as shown in the Supplementary information **MISSING !!**

Table 1. Interestingly the inactive compound S6 showed poor range values for QPPCaco and QPPMDCK properties. As these two properties were important pharmacokinetic determining parameters for absorption and distribution fate of any drug-like compound. Additionally, percentage human oral absorption range was up to the mark for all active compounds considered, whereas compound S6 values were unacceptable for oral absorption. Thus according to the ADMET analysis, we can conclude that all the active compounds showed characteristics of a

promising drug candidature which can be worked for rational drug design against *S. aureus* DNA Gyr B enzyme from pharmaceutical point of view.

Table 5.6: A QikProp analysis of the ADMET properties of the hits.

Properties ^a	S10	S44	S41	S32	S6	Range ^b
QPlogHERG	-4.574	-4.416	-4.353	-4.687	-4.511	Concern below -5
QPPCaco	41.875	22.037	45.679	22.438	4.914	<25 poor, >500 great
QPlogBB	-1.627	-1.918	-1.676	-2.144	-2.799	-3.0 to 1.2
QPPMDCK	36.875	15.74	22.392	10.385	3.097	<25 poor, >500 great
QPlogKp	-3.428	-3.974	-3.361	-3.848	-5.234	-8.0 to -1.0
QPlogKhsa	-0.068	-0.353	-0.426	-0.192	-0.207	-1.5 to 1.5
Percentage of human oral absorption	73.702	62.982	68.584	65.516	51.229	>85% high <25% poor

^a Parameter range indicating value desired for drug like compound: **QPlogHERG** – Predicted IC₅₀ value for *zERG* K⁺ channels. **QPPCaco** – Predicted apparent Caco-2 cell (model for gut-blood barrier) permeability in nm/s. **QPlogBB** – Predicted brain/blood partition coefficient. **QPPMDCK** – Predicted apparent MDCK cell (model for blood-brain barrier) permeability in nm/s. **QPlogK_p** – Predicted skin permeability. **QPlogKhsa** – Prediction of binding to human serum albumin. ^b Range indicates the values desired for drug-like compound.

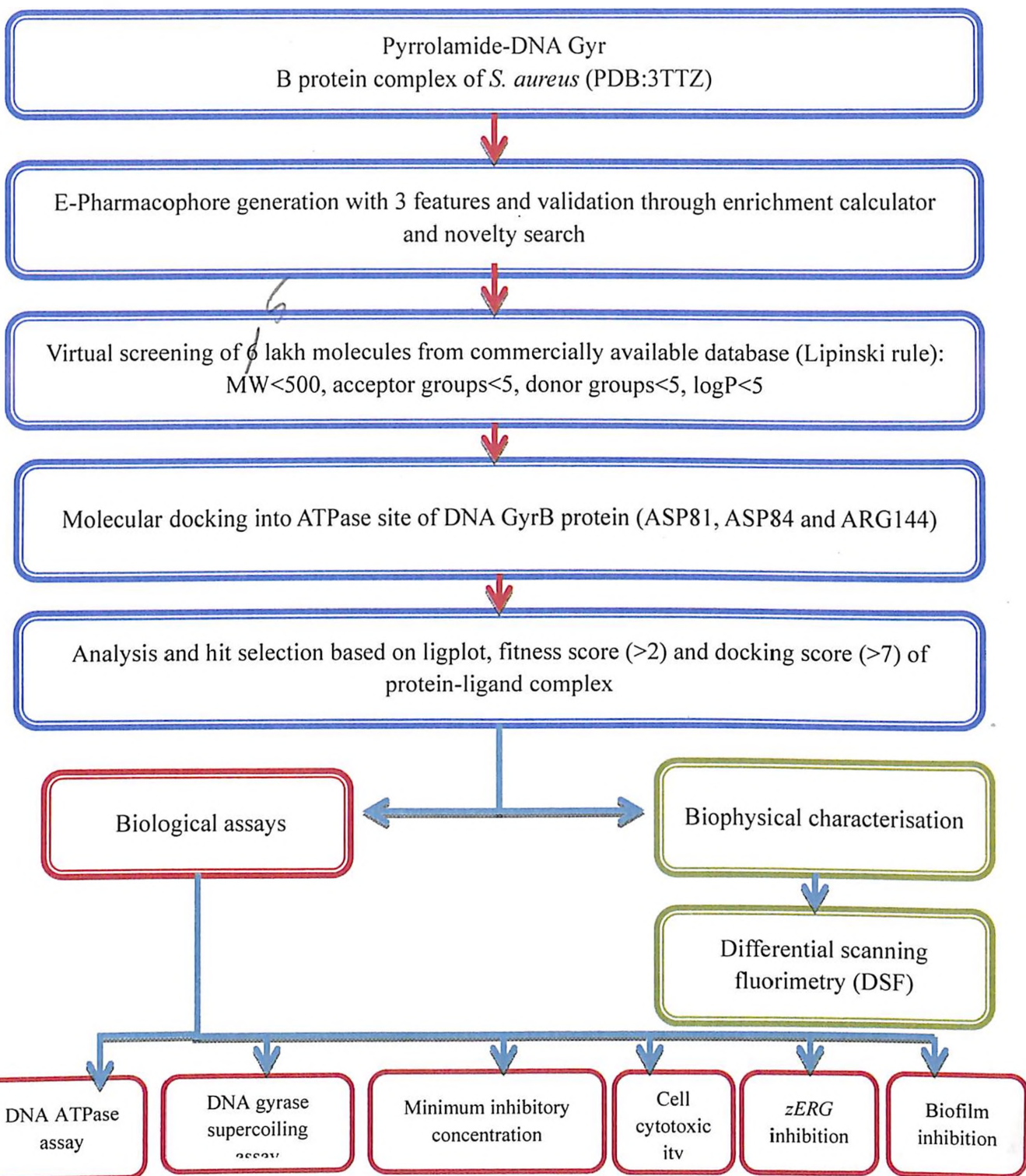


Figure 5.17: Outline of the computational and biological work presented in this study.

5.2.5. Biological validation

5.2.5.1. *S. aureus* DNA Gyr B ATPase assay with SAR

A library of forty one compounds synthesized, were screened for the Gyr B activity and compared with novobiocin as a standard positive control with an IC_{50} of 15 nM. Among the forty one compounds tested, thirty two compounds showed a good inhibitory potency of > 80% at 50 μ M and 20 μ M concentrations. Subsequently, these thirty two compounds were rescreened at lower concentrations of 10 μ M and 5 μ M, in which four compounds showed > 65% inhibition. A final compound concentration of 1 μ M for the four potent compounds was performed, and IC_{50} (Table 5.7) were calculated by GraphPad Prism software, by evaluating the compounds in the above five concentrations for the final time in duplicates. The assay was performed in the presence of detergent to rule out the artifacts like aggregation of molecules.

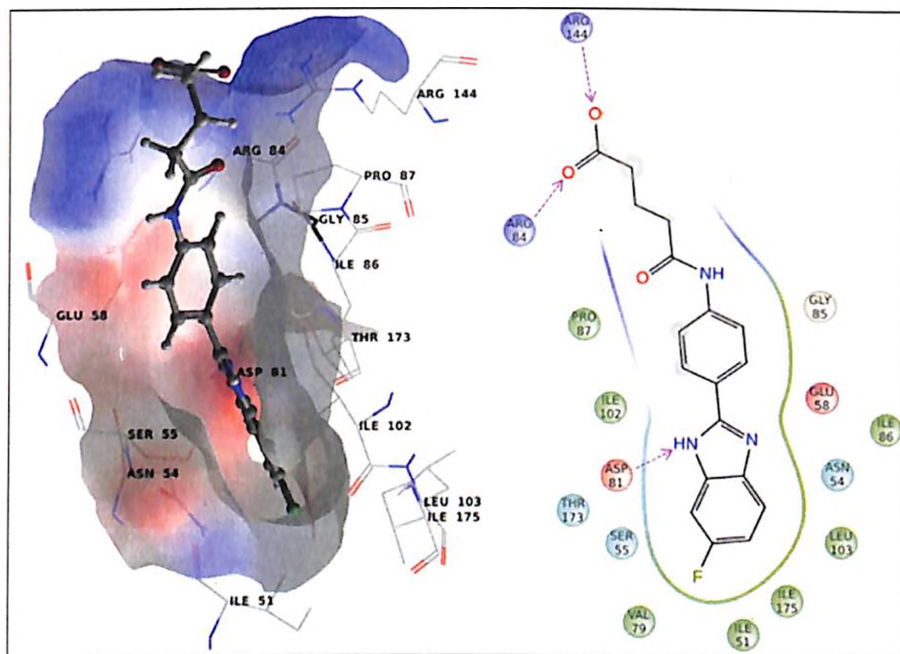


Figure 5.18: Surface interaction picture of compound S10 with conserved amino acids accordance with ligand interaction diagram

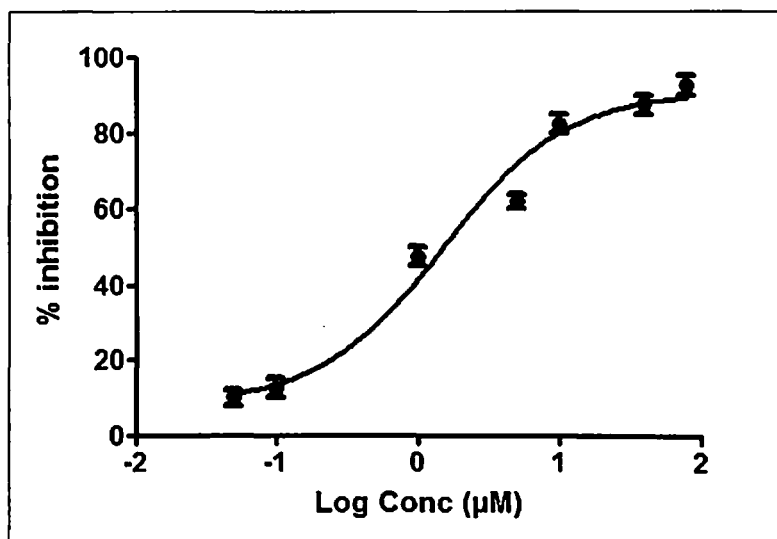


Figure 5.19: Hill slope of the most active compound S10 with different log concentration of the inhibitor on X-axis against percentage inhibition on Y-axis.

5.2.5.2. *S. aureus* DNA Gyrase supercoiling assay

Supercoiling of the DNA occurs in the presence of Gyr A and Gyr B subunits. Targeting either of the domains may result in loss of supercoiling activity. The DNA supercoiling assay was performed using a commercially available Inspiralis kit (Inspiralis Limited, Norwich, UK) with a positive control, moxifloxacin having an IC_{50} of $11.2 \pm 1.8 \mu\text{M}$. The kit included the assay buffer, relaxed pBR 322 DNA as substrate, *S. aureus* DNA with A2B2 subunits. A library of the above forty one synthesized compounds when screened initially at $50 \mu\text{M}$ and $25 \mu\text{M}$ concentrations, we found thirty nine compounds with percentage inhibition $>60\%$. These compounds were repeated at lower concentrations of $12.5 \mu\text{M}$ and $6.25 \mu\text{M}$ subsequently, resulting in eleven compounds that exhibited $>50\%$ relative inhibition profile. These potent inhibitory compounds were finally screened at $1.56 \mu\text{M}$ and $0.75 \mu\text{M}$ and IC_{50} values are reported in ~~Table 5.7~~. As observed in the Gyr B assay results, compound S10 was found to be the most potent exhibiting

an IC_{50} value of $1.13 \pm 0.34 \mu\text{M}$ as depicted in (Figure 5.20). Thus the Gyr B assay results well correlated with the supercoiling activity profile.

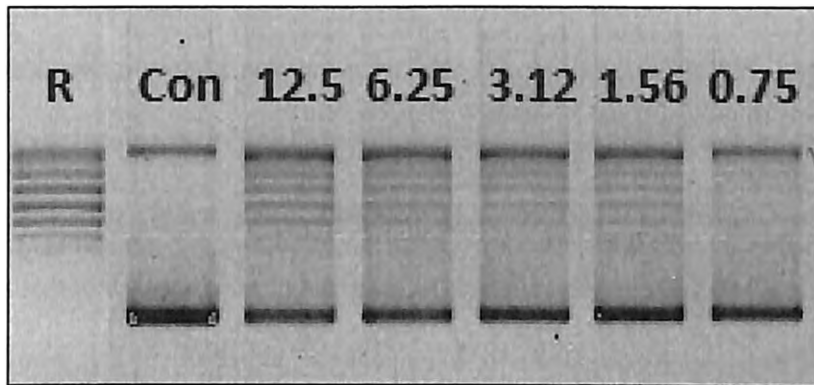


Figure 5.20: Inhibitory profile of *S. aureus* DNA gyrase supercoiling activity by compound **S10**. A representative gel obtained from the analysis of the inhibition of DNA gyrase supercoiling activity is shown above. (R) represents relaxed closed circular DNA; (Con) represents the supercoiled relaxed DNA in the presence of gyrase enzyme. Gel data for assays with compound **S10** in different concentrations with novobiocin as positive standard are shown (in μM).

5.2.5.3. Antibacterial activity

All the synthesized compounds (S4-S44) were further tested for their *in vitro* antibacterial activity against two bacterial strains, *S. aureus* MTCC3160 and MRSA 96 using the protocol as described in experimental section 4.6. Ofloxacin and ciprofloxacin were included as reference compounds. The results of the antibacterial screening are presented in (Table 5.9). Compound **S10** which displayed a very good enzyme inhibition also displayed significant *in vitro* antibacterial activity against both the MTCC and MRSA strains indicating its potential as bactericidal *in vitro*, whose MICs were $4.57 \mu\text{M}$ and $9.15 \mu\text{M}$ comparable to the reference compound ofloxacin which showed $4.15 \mu\text{M}$ and $17.29 \mu\text{M}$ in MTCC3160 strain and MRSA 96

Which new strain is this?

Nope?
7

How from MIC are you deducing whether it is cidal?

INDIRECT
STRUCTURE!

strain respectively. Ciprofloxacin displayed an MIC of 9.431 μM against MTCC 3160 and 18.8 μM against MRSA strain. This confirmed the activity profile of the compound S10 with respect to the reference standards ofloxacin and ciprofloxacin as bactericidal. Compounds S38 and S44 also exhibited good antimicrobial properties in both the strains highlighting the efficacy of this chemical class of molecules in inhibiting the microbes. In contrast, few compounds S5-9, S13-17, S25-28 and S43 displayed a weak antibacterial activity against the above bacterial strains, which could be attributed to the permeability issue or efflux pump transportation.

5.2.5.4. Cytotoxicity studies

Further the safety profile of this chemical class, forty one compounds were evaluated by testing for their *in vitro* cytotoxicity against mammalian HEK-293 cell line at 100 μM concentration in triplicates by utilizing (4,5-dimethylthiazol-2-yl)-2,5-diphenyltetrazolium bromide (MTT) assay. The entire series of compounds tested demonstrated a good safety profile range with very low inhibitory potential. These results were gratifying for us as the most potent compound S10 showed only 7% cytotoxicity at the highest concentration tested on par with ciprofloxacin drug which was considered as control and thus these results confirmed the safety profile of compounds. Percentage inhibition of HEK cells by all the forty one compounds is reported in

Why not RAW?

Table 5.7

5.2.5.5. Differential scanning fluorimetry

The active compounds from this series of chemical class of molecules were further investigated using a biophysical technique, differential scanning fluorimetry (DSF). The ability of the compounds to stabilize the catalytic domain of the gyrase protein was assessed utilizing the DSF

technique by which the thermal stability of the catalytic domain of Gyr B native protein and of the protein bound with the ligand was measured. Complexes with three different ligands **S10**, **S32** and **S44** were heated stepwise from 25 to 95 °C in steps of 0.6 °C in the presence of a fluorescent dye, whose fluorescence increased as it interacted with hydrophobic residues of the Gyr B protein. As the protein was denatured, the amino acid residues became exposed to the dye. A right side positive shift of T_m in comparison to native protein meant higher stabilization of the protein-ligand complexes, which was a consequence of the inhibitor binding. In our study, compound **S10** showed significant positive shift confirming the stability of the protein-ligand complex, as it was already reported in literature that the carboxylic group at para position played an important role in the complex stabilization by interacting with amino acid residues like Arg144, Arg84 as shown in our *in silico* model. In addition, the hydrophobic pocket formed around the lipophilic group by Ile102, Ile86, Leu103, Gly85, Ile102, Thr173, Ile175, Ile51 and Pro87 also contributed to the stabilization of this complex. Among the three tested compounds, best improvement in the protein–inhibitor complex stability, as indicated by the positive shift was observed in the case of compound **S10** with the T_m shift of 3.2 °C, followed by compound **S32** and **44**. These results were in accordance with the most potent DNA Gyr B inhibition by compound **S10**, with an IC_{50} of $1.32 \pm 0.17 \mu\text{M}$. (**Figure 5.21**) depicts the curves obtained in the DSF experiment for the native Gyr B protein (red) and protein-compound **S10** complex (blue).

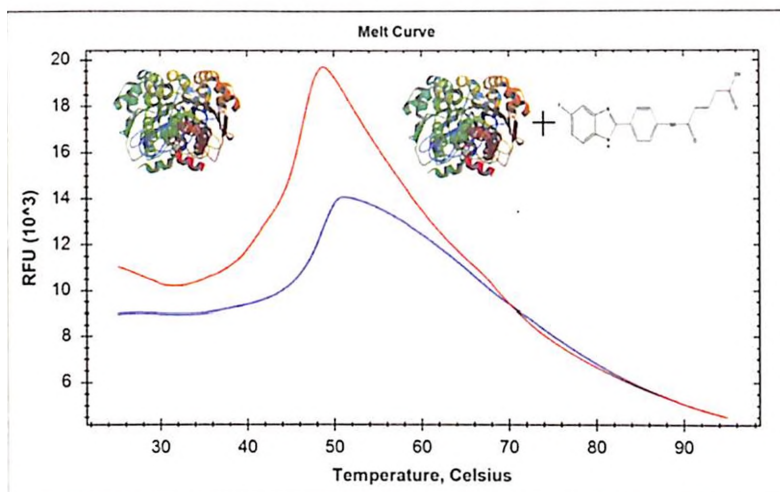


Figure 5.21: DSF experiment for compound showing an increase in thermal stability between the native G24 protein (blue) and DNA Gyr B protein-compound complex (red).

5.2.5.6. Inhibition of biofilm formation studies

Biofilm is an extracellular polysaccharide, produced by staphylococcal species that facilitate attachment and matrix formation that results in alteration in the phenotype of the organism, with respect to gene transcription and growth rate. It was estimated that 65% of all the human bacterial infections were due to biofilms which may result in prolonged and chronic infections leading to death. While recalcitrance of these biofilm-mediated infections has been associated with adverse effect on patient health, the increase in the resistance of *S. aureus* to methicillin resulted in more hysterical condition. The extensive resistance of *S. aureus* biofilms against the antibacterials can be attributed to failure of antibiotics to penetrate the biofilm, the different metabolic states of the cells in the biofilm aggregates, and the differential expression of genes by the bacteria concerned in the same biofilm aggregates One of the novel approach of inhibiting pathogen virulence could be by inhibiting the biofilm formation thus minimizing the selection pressure for resistance as it hold a great promise as an alternative to traditional antibiotic

treatment. We focused our study on inhibition of *S. aureus* biofilm formation by the forty one synthesised small molecule inhibitors. The estimation of inhibition of biofilm formation was monitored quantitatively and qualitatively. Initially, Congo red method was adopted to know the strain's efficiency in biofilm formation [Smith K., et al., 2008]. The MRSA 96 was a strong biofilm producer with >2 OD at 570 nm wavelength. Assays were performed in a 96-well microtiter plate, with different concentrations of the compounds on biofilm producing clinical MRSA96. All the forty one compounds were subjected for biofilm assay and it was gratifying to observe that the most potent compound S10 had good biofilm formation inhibitory profile with an IC_{50} of 9.63 μ M as shown in (Figure 5.22). Ciprofloxacin was used as the standard references whose IC_{50} was 16.89 μ M. In comparison with ciprofloxacin, compound S10 showed two-fold increased efficacy in inhibiting the biofilm formation. Compounds S19, S33, S36, S39, S41 and S45 also displayed appreciable IC_{50} 's, giving enough proof that this class of compounds possess dual effect, as DNA gyrase inhibitors with effective inhibition of biofilm formation too.

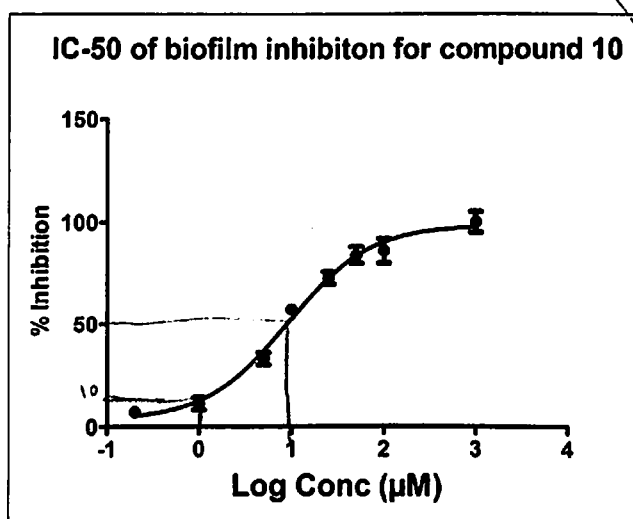


Figure 5.22: Dose-response curve of compound inhibition on *S. aureus* MRSA96 biofilm formation. The data is presented as % inhibition mean \pm standard error of means for 6 samples. Percent inhibition is relative to DMSO control.

5.2.5.7. *zERG* cardiotoxicity studies

Till date the only drugs clinically approved for DNA gyrase inhibition were flouoroquinolones, among which the potent one being moxifloxacin, that suffer from *hERG* toxicity. Also the previously reported antibacterial C and N linked aminopiperidine DNA gyrase inhibitors suffered from serious *zERG* toxicity, we felt it was very important to ensure that the newly designed molecules did not suffer from such drawbacks. Compound **S10** was subjected for *zERG* channel inhibition studies by assessing the arrhythmogenic potential on zebrafish ether-a-go-go-related gene (*zERG*) which was orthologous to the human ether-a-go-go-related gene (*hERG*), due to their homology. This method of study, possessed significant advantage over the current conventional animal models which include ethical issues, low compound requirement, manually less tedious and low cost. Presently, zebrafish (*Danio rerio*) has become an emerging model to study the pro-arrhythmic potential of candidate drugs [Ahuja V., *et al.*, 2013]. Furthermore, Milan *et al.*, 2003 and Mittelstadt *et al.*, 2008 had reported that bradycardia and atrio-ventricular dissociation in zebrafish larvae can be used as a surrogate marker for *hERG* channel inhibition thereby affecting the rapid component of the repolarizing potassium current and inducing arrhythmia. In our study, compound **S10** was subjected to *zERG* channel inhibition in concentrations ranging from 1 μM to 30 μM with 0.1% DMSO as vehicle, the heart rate variations and AV ratio were analysed by using a protocol described in more detail in the experimental section. Compound **S10** was found to be safe when compared to the positive control (20 μM terfenadine), by not showing any significant cardiotoxicity until 30 μM concentration. There was no significant change in the heart rate or AV ratio, in comparison to control group making them relatively safe, a significant breakthrough when compared to otherwise cardiotoxic terfenadine and amiodarone as illustrated in **Figures 5.23a** and **5.23b**.

a)

b)

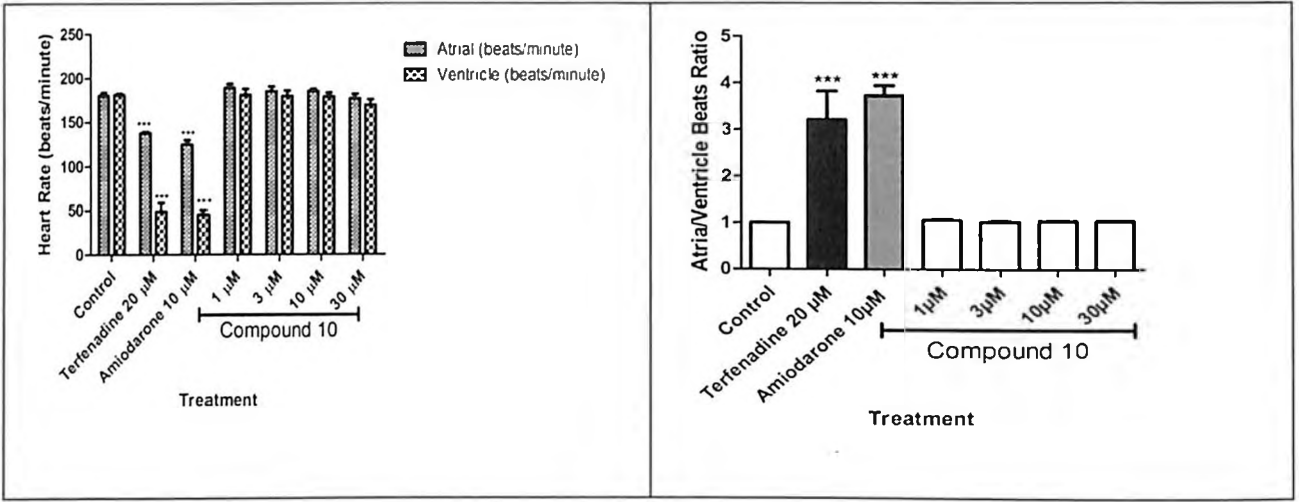
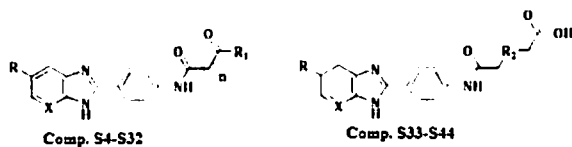


Figure 5.23: (a) Mean (\pm S.E.M.) of the heart rates of atria and ventricles of compound S10. (* p <0.05, ** p <0.01 and *** p <0.001). Statistical significance was analyzed comparing control group *Vs* treated groups. (b) Mean (\pm S.E.M.) score of atrio ventricular ratio. (* p <0.05, ** p <0.01 and *** p <0.001). Statistical significance was analyzed comparing control group *Vs* all groups.

Table 5.7: Biological evaluation of the synthesized compounds

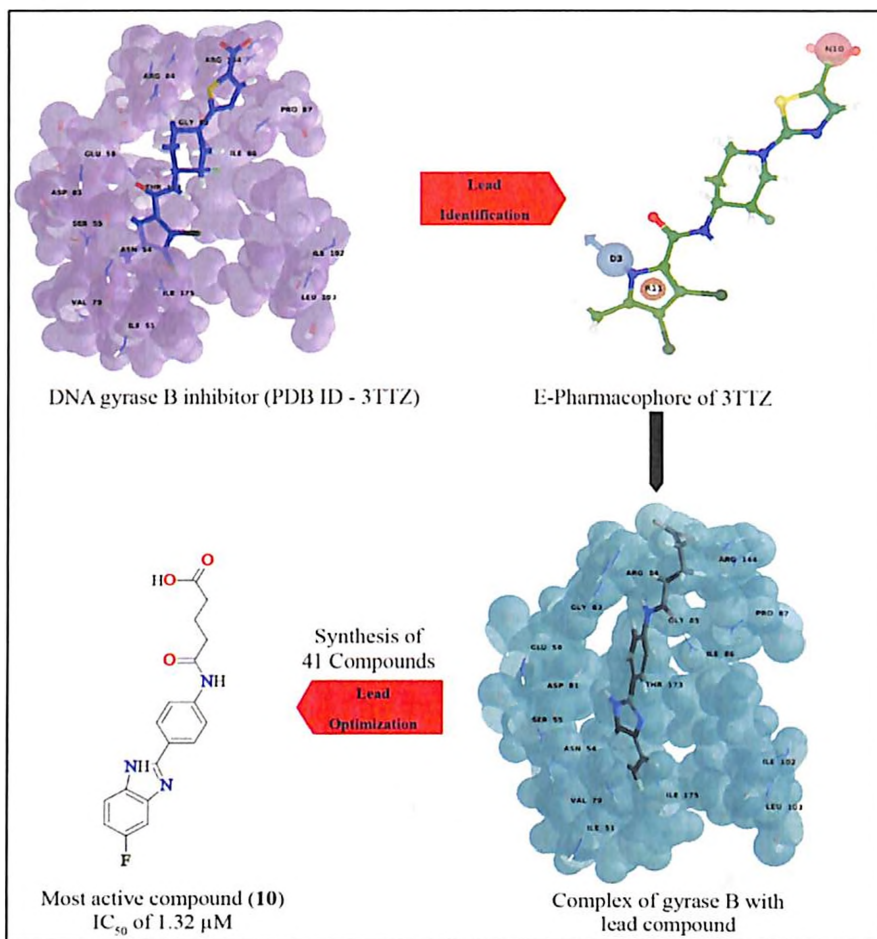


Cmpd.	R	n	X	R ₁	R ₂	Gyr B assay (IC ₅₀)	Supercoiling assay (IC ₅₀)	MIC (μM)	MRSA MIC (μM)	Biofilm Inhibi. (IC ₅₀)	Cytotoxicity in HEK-293 (% inhib:)
S4	H	1	H	OH	-	6.91±0.43	6.125±0.21	42.33	21.16	47.8	7.2
S5	H	2	H	OH	-	7.32±0.83	6.125±0.32	20.205	40.41	88.31	2.9
S6	H	3	H	OCH ₃	-	36.31±0.48	25±0.37	148.2	148.2	>100	9.7
S7	H	4	H	OH	-	5.7±0.16	6.125±0.44	37.05	37.05	81.5	32.06
S8	F	1	H	OH	-	13.43±1.12	16.31±0.21	79.8	79.8	>100	18.06
S9	F	2	H	OH	-	17.6±0.87	12.0±0.26	38.19	38.19	82.7	28.72
S10	F	3	H	OH	-	1.32±0.17	1.13±0.34	4.57	9.15	9.63	7.59
S11	F	3	H	OCH ₃	-	18.6±0.56	10.7±0.11	70.35	32.175	59.33	33.81
S12	F	4	H	OH	-	15.34±0.32	7.1±0.11	35.17	59.3	>100	29.04
S13	Cl	1	H	OH	-	26.35±0.23	18.21±0.71	75.8	75.8	>100	25.62
S14	Cl	2	H	OH	-	11.23±0.85	9.8±0.34	36.36	36.36	53.2	31.66
S15	Cl	3	H	OH	-	9.85±0.31	9.13±0.11	34.9	69.8	>100	45.52
S16	Cl	3	H	OCH ₃	-	35.63±0.76	22.19±1.56	67.23	134.47	>100	27.93
S17	Cl	4	H	OH	-	13.06±1.73	8.91±0.35	33.61	33.61	39.2	39.67
S18	NO ₂	1	H	OH	-	4.932±0.34	2.23±0.51	9.18	18.33	18.35	26.91
S19	NO ₂	2	H	OH	-	17.53±1.41	8.32±0.77	16.96	16.96	27.92	24.57
S20	NO ₂	3	H	OH	-	6.832±0.49	6.12±0.18	33.9	44.12	62.31	27.23
S21	NO ₂	3	H	OCH ₃	-	9.83±1.1	5.3±0.25	32.69	32.69	59.31	35.89
S22	NO ₂	4	H	OH	-	9.823±0.61	6.09±0.42	32.6	32.6	44.2	31.74
S23	OCH ₃	1	H	OH	-	11.06±0.23	18.36±0.33	38.42	76.84	>100	27.35
S24	OCH ₃	2	H	OH	-	13.43±0.85	11.3±0.48	73.67	73.67	>100	26.74
S25	OCH ₃	3	H	OH	-	8.93±0.44	5.32±0.17	35.37	35.37	52.2	22.37
S26	OCH ₃	3	H	OCH ₃	-	21.34±0.34	12.5±0.67	68.04	34.02	63.9	50.48
S27	OCH ₃	4	H	OH	-	22.93±1.33	12.5±0.71	68.04	34.08	71.1	29.36
S28	H	1	N	OH	-	21.8±0.94	8.9±0.38	42.18	42.18	71.9	27.24
S29	H	2	N	OH	-	9.23±0.88	3.125±0.61	20.14	10.07	29.43	31.14
S30	H	3	N	OH	-	18.53±1.44	6.98±0.67	38.54	38.54	88.09	33.81
S31	H	3	N	OCH ₃	-	5.23±0.81	6.8±0.1	36.94	36.94	79.32	57.54
S32	H	4	N	OH	-	2.9±0.4	2.1±0.23	4.61	9.23	15.73	22.72
S33	H	-	H	-	O	6.01±0.41	4.81±0.41	38.42	46.88	68.8	40.02
S34	H	-	H	-	S	22.8±0.14	12.5±0.82	73.3	37.6	82.1	13.07
S35	F	-	H	-	O	6.125±0.23	2.9±0.31	9.102	9.102	19.64	14.47
S36	F	-	H	-	S	6.93±0.83	4.8±0.54	34.78	17.32	59.12	20.63
S37	Cl	-	H	-	O	15.34±0.88	12.5±0.92	34.74	69.49	71.23	29.67
S38	Cl	-	H	-	S	13.83±0.62	12.1±0.95	4.15	4.15	9.72	23.04
S39	NO ₂	-	H	-	O	8.51±0.54	5.8±0.31	33.75	46.98	83.22	31.29
S40	NO ₂	-	H	-	S	3.132±0.24	2.1±0.31	8.087	16.98	10.32	25.21
S41	OCH ₃	-	H	-	O	4.34±0.77	3.062±1.53	17.58	17.58	31.72	23.26
S42	OCH ₃	-	H	-	S	9.31±0.63	15.98±0.28	67.31	67.31	>100	22.63
S43	H	-	N	-	O	6.935±0.25	4.7±0.52	19.15	38.3	82.45	38.71
S44	H	-	N	-	S	2.31±0.48	1.7±0.3	4.55	9.12	11.31	31.86

Control values are not provided?

5.3. Highlights of this study

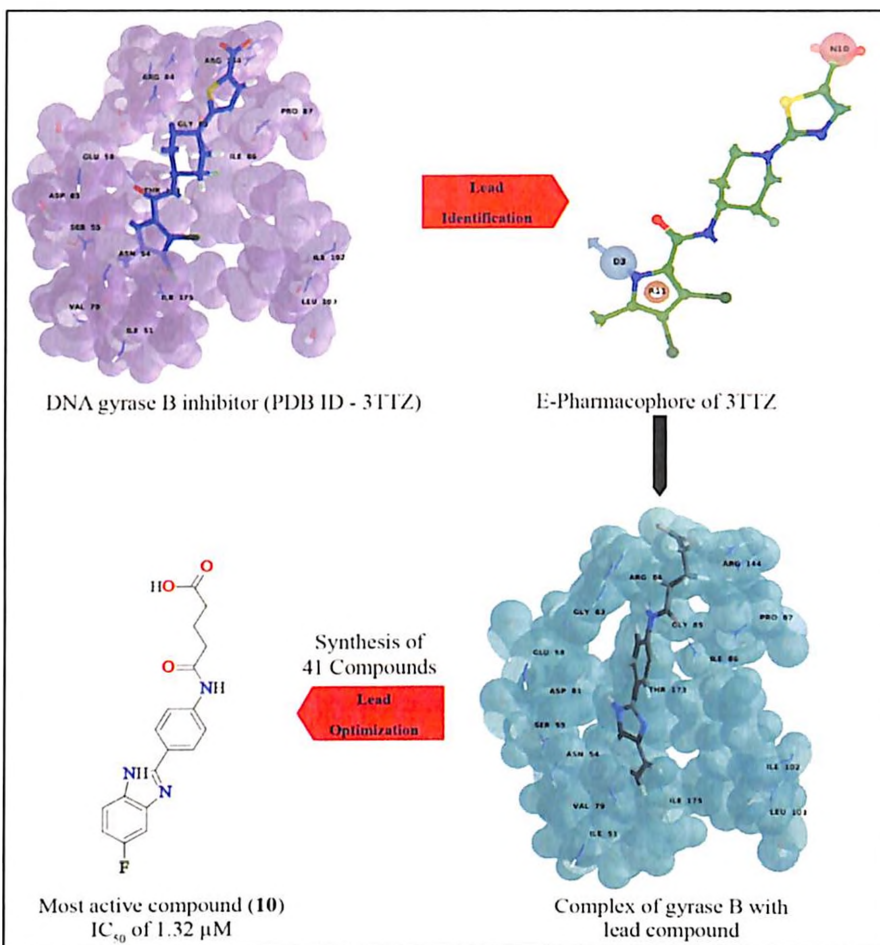
In this study, a structure-based e-pharmacophore modeling has been employed to identify structurally diverse small molecule ligands of *S.aureus* DNA Gyr B based on the crystal structure of the enzyme with a co-crystallized inhibitor. Twelve active compounds of varied structural classes were identified. Out of which three molecules had an *in vitro* Gyr B activity in 5 μ M range, the best molecule **A1** among them was further taken up for synthesis of a library of forty one molecules. All these compounds were subjected to DNA Gyr B assay and DNA supercoiling assay, their binding mode was biophysically confirmed by differential scanning fluorimetry (DSF). It was delighting to see the best compound **S10** in the Gyr B assay had a greater positive shift indicating the highest increase of thermal stability of the complex inhibitor–protein that matched the best *in vitro* antimicrobial activity against the MRSA strain as well. Furthermore, compound **S10** showed better biofilm inhibition profile along with low cell cytotoxicity in mammalian HEK-293 cell line with zero *zERG* inhibition posing no cardiotoxicity makes this compound a potent molecule of this chemical class of DNA Gyr B inhibitors. Furthermore, this class of benzimidazole compounds besets a collection of promising lead compounds for further optimization and development to yield best novel drugs aimed to combat ever present and ever-increasing bacterial infections and also the study provides the basis for further chemical optimization of these potent inhibitors against DNA Gyr B enzyme.



5.4. Lead molecule (B1): Design and development of potential inhibitors of *S. aureus* DNA Gyr B via hit expansion and lead optimization of 4-((4-(furan-2-carboxamido)phenyl)amino)-4-oxobutanoic acid.

Among the twelve compounds that were procured from Asinex database through e-pharmacophore based screening approach using PDB Id: (3TTZ), BAS04380545 was taken up as lead molecule (B1) for further synthesis and lead optimization based on the activity studies against *S. aureus* DNA Gyr B ATPase activity of $12.88 \pm 1.39 \mu\text{M}$ and an MIC of 79.03 μM .

Figure 5.26 depicts the structure of the (B1). Considering this compound as lead in this series and based on the potency and synthetic feasibility; a series of twenty three analogues were designed and synthesized around the (B1) in the ligand expansion step, to trace the structure activity relationship. Considering the important interaction that the *p*-phenylenediamine linker retained with Asp 81, it was decided to retain the linker and explore the right and left hand core as shown in **Table 5.7**. The synthetic pathway used to assemble library has been depicted in **Figure 5.25**. The first step involved, a selective protection of *p*-phenylenediamine using Boc anhydride under controlled conditions by a previously reported protocol. The monoprotected linker was then functionalized with various substituted heterocyclic acids to give the corresponding amide derivatives in excellent yields. Further de-protection and treatment with various anhydrides gave the corresponding acid analogues in moderate yield. The corresponding ester and hydrazide derivative of the acid analogues were also attempted in synthesis, to understand the role of these groups in activity determination.



5.4. Lead molecule (B1): Design and development of potential inhibitors of *S. aureus* DNA Gyr B via hit expansion and lead optimization of 4-((4-(furan-2-carboxamido)phenyl)amino)-4-oxobutanoic acid.

Among the twelve compounds that were procured from Asinex database through e-pharmacophore based screening approach using PDB Id: (3TTZ), BAS04380545 was taken up as lead molecule (B1) for further synthesis and lead optimization based on the activity studies against *S. aureus* DNA Gyr B ATPase activity of $12.88 \pm 1.39 \mu\text{M}$ and an MIC of $79.03 \mu\text{M}$.

{Figure 5.26} depicts the structure of the (B1). Considering this compound as lead in this series and based on the potency and synthetic feasibility; a series of twenty three analogues were designed and synthesized around the (B1) in the ligand expansion step, to trace the structure activity relationship. Considering the important interaction that the *p*-phenylenediamine linker retained with Asp 81, it was decided to retain the linker and explore the right and left hand core as shown in {Table 5.7}. The synthetic pathway used to assemble library has been depicted in (Figure 5.25). The first step involved, a selective protection of *p*-phenylenediamine using Boc anhydride under controlled conditions by a previously reported protocol. The monoprotected linker was then functionalized with various substituted heterocyclic acids to give the corresponding amide derivatives in excellent yields. Further de-protection and treatment with various anhydrides gave the corresponding acid analogues in moderate yield. The corresponding ester and hydrazide derivative of the acid analogues were also attempted in synthesis, to understand the role of these groups in activity determination.

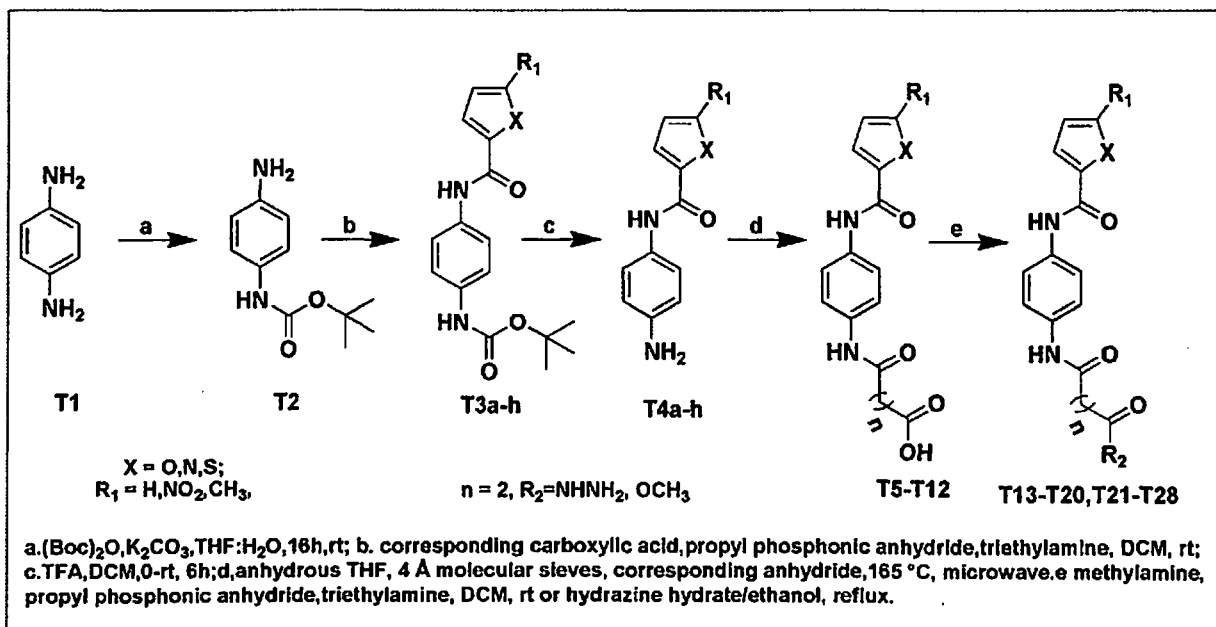


Figure 5.25: Synthetic protocol adopted for the lead derivatization.

5.4.1. Gyr B activity of the synthesized analogues in correlation with the structure based drug design and its structure activity relationship (SAR)

The DNA Gyr B assay was performed as per the protocol described in material and methods section. Absence of highly active DNA Gyr B ATPase activity of the purified *S. aureus* Gyr B in vitro like other bacteria made us use the *E. coli* DNA Gyr A for stimulating the activity of *S. aureus* Gyr B. Subsequently, *E. coli* DNA Gyr A in combination with *S. aureus* DNA Gyr B was used to do the *S. aureus* ATPase activity. As the (B1), showed an IC_{50} of $12.88 \pm 1.39 \mu M$ search was made to obtain a potent ligand with better inhibitory profile, however this compound was found to be in hydrogen bond with residues Gly85 and Arg144 as shown in (Figure 5.27) which was considered as one of the key interaction. Also a cation- π interaction was observed with Arg81 and strong hydrophobic interactions were made by the furan ring with Ile51, Val79, Ile86 and Ile175. Hence, based on these interactions, the compound was further derivatized and was optimized placing the substituents majorly at three positions – substituents over five membered

ring R₁, substituents at oxygen in furan ring (X) and final substitution at the terminal hydroxyl group R₂. The synthesized compounds were docked with the crystal structure of Gyr B of *S. aureus* so as to observe the mode of interaction of the compounds at the active site pocket and to determine its orientation *in silico*, subsequently the biological activity too was performed with different drug concentrations starting from a range of 100 µM to 1.56 µM. Among, the twenty three analogues synthesized, fourteen compounds showed greater than 50% inhibitions at 100 and 50 µM of drug concentration. Further, all these molecules were tested at lower drug concentrations of 25, 12.5, 6.25, 3.12 and 1.56 µM. Initially, substitutions were made at R₂ position replacing hydroxyl group with methoxy T13, and hydrazine T21. These compounds were found to be inactive with docking score of -3.9 and -4.1 respectively, with Gyr B assay values ranging from T27-T36 µM suggesting the favourability of hydroxyl group for the activity as in (B2). Hydroxyl group was involved in hydrogen bonding with Arg144, an important active site residue, deletion of which was found to deplete the activity. The next substitution was done at both R₁ and R₂ positions, where R₁ is occupied by 2-methyl moiety and the R₂ position with hydroxyl T6, methoxy T14 and hydrazine T22 groups. Among these, compound T22, N-(4-(4-hydrazinyl-4-oxobutanamido) phenyl)-5-methylfuran-2-carboxamide emerged as the top hit molecule with a docking score of -8.2 kcal mol⁻¹ with a fitness value of 1.9, a DNA Gyr B IC₅₀ of 5.35±0.44 µM almost one half of the lead molecule, calculated by GraphPad Prism software and an MIC of 18.92 µM. The dose response curve for this compound is shown in (Figure 5.27). S. 29

The binding profile of this compound revealed the presence of four hydrogen bonds at active site with Val79, Asp81, Gly85 and Thr173 as shown in (Figure 5.28). It was found that the presence of hydrazine group at R₂ position contributed for three hydrogen bonds and made the compound orient towards the hydrophobic pocket adding up to non-polar interactions. The compounds were

re-screened for the final time in triplicates to ensure their activity results. The other two molecules were found to be orienting totally in opposite direction.

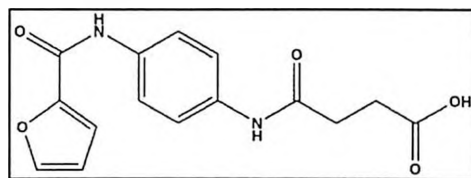


Figure 5.26: Structure of the identified Lead (B1)

The substitutions were further carried out using nitro at R₁ position and the same hydroxyl in T7 with docking score of $-4.61 \text{ kcal mol}^{-1}$, methoxy group in T15 with docking score of $-4.3 \text{ kcal mol}^{-1}$ and hydrazine T23 group at R₂ position with docking score of $-4.9 \text{ kcal mol}^{-1}$. These compounds were found to be inactive against Gyr B (IC_{50} around $27 - 40 \mu\text{M}$). The docking studies of these compounds revealed their orientation with nitro group facing the hydrophobic pocket making it impossible to involve in any hydrophobic contacts resulting in the compounds inactivity.

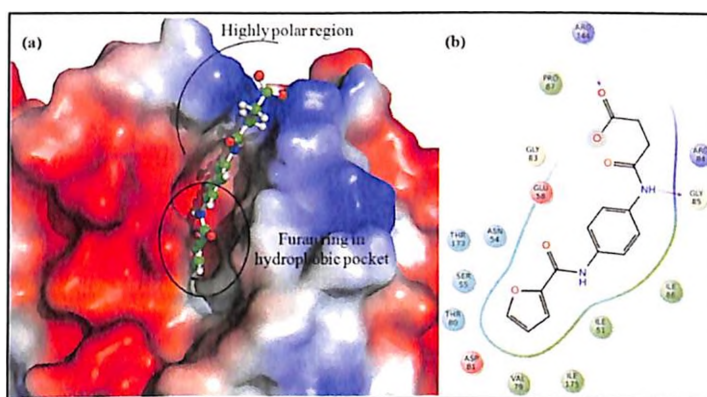


Figure 5.27: Lead molecule (B1) at *S. aureus* Gyr B active site (a) Electrostatic surface view of Gyr B showing its hydrophobic pocket occupied by furan ring (b) Interaction of (B2) at Gyr B pocket (pink lines indicate hydrogen bonds).

Further substitutions were done by replacing the furan ring with thiophene in **8**, **16** and **24** and 2-methyl thiophene in **T9**, **T17** and **T25** with the same three substitutions at R₂ position. All these compounds were found to be inactive (IC₅₀ ranging 21 – >40 μM) except compound **T25** with a docking score of -7.3 kcal mol⁻¹ and a fitness value of 1.9. Potency of this compound (IC₅₀ – 9.71 μM and MIC – 18.04 μM) may be attributed to the presence of hydrazine which was found to be participating in hydrogen bonds with Val79, Asp81 and Thr173 and the carbonyl oxygen next to thiophene ring was found to be in polar contact with Arg144 which were lacking in the remaining compounds. The ethylene linker was found to be involved in strong hydrophobic contacts with Ile51 and Ile175 and thiophene ring with Pro87. The replacement of hydrazine in compound **T9** and **T17** resulted in loss of activity up to five fold showing up the importance of hydrazine for *S. aureus* Gyr B activity.

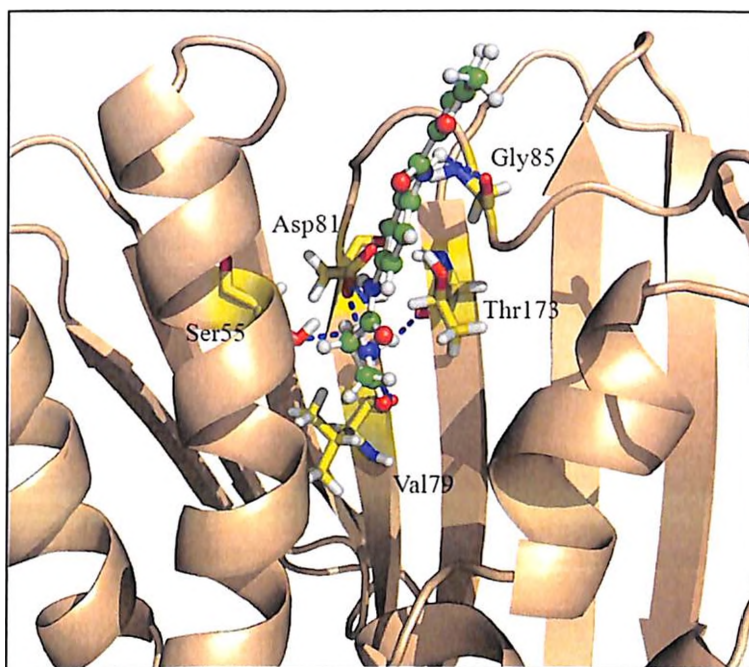


Figure 5.28: Interaction profile of most active compound **T22** (green) showing hydrogen bonds (blue) with active site residues (yellow).

Substitution of furan with 2-nitro thiophene and same three R₂ substitutions in **T10**, **T18** and **T26**, yielded compound **T18** as active one with IC₅₀ of 12.49 μM in Gyr B assay and a docking of -7.8 kcal mol⁻¹ ^{with} and a fitness value of 1.7. This may be reasoned for the hydrogen bond interactions with Asp81 and Arg144. The main reason can be given by non-polar interactions with thiophene ring at the hydrophobic pocket with Ile51 and Ile175. The other two compounds were not involved in hydrogen bonding with Asp81, an important active site residue, as the substitutions at R₂ position oriented the molecules away from Asp81.

The final substitutions were done with tetra hydro furan in **T11**, **T20** and **T28** and pyrrole ring in **T12**, **T19** and **T27** at R₁ position with the same R₂ substitution compounds. Compounds **T11** and **T20** were found to be active with docking scores of -7.3 and -7.7 kcal mol⁻¹ with two hydrogen bonds Asp81 and Arg144 and the hydrophobic interactions with tetrahydrofuran ring. Compound **T28** was inactive with a docking score of -3.9 kcal mol⁻¹ which can be explained by the reversal of binding pattern with the addition of hydrazine as the R₁ position was towards solvent which decreases the activity. All the pyrrole substituted compounds were found to be highly inactive suggesting the un-favourableness of pyrrole ring as it was weakly involved in hydrophobic interactions.

To sum up, it was observed that not all substitutions were favourable for *S. aureus* Gyr B activity. Some of the key features of compounds that are crucial for activity may be (i) a hydrophobic ring (like furan, thiophene, pyrrole) at one terminal of compound is important for the activity and (ii) a combination of substitutions like methoxy over furan or thiophene at one terminal and hydrazine (-NH-NH₂) at the other terminal of the compound is highly fruitful as observed in compounds **T22** and **T25**. Compounds with such above features can be desirable in

drug development process for *S. aureus* targeting Gyr B. Novobiocin, an aminocoumarin was considered as a standard compound in this assay with an IC_{50} of $0.125 \pm 0.24 \mu\text{M}$.

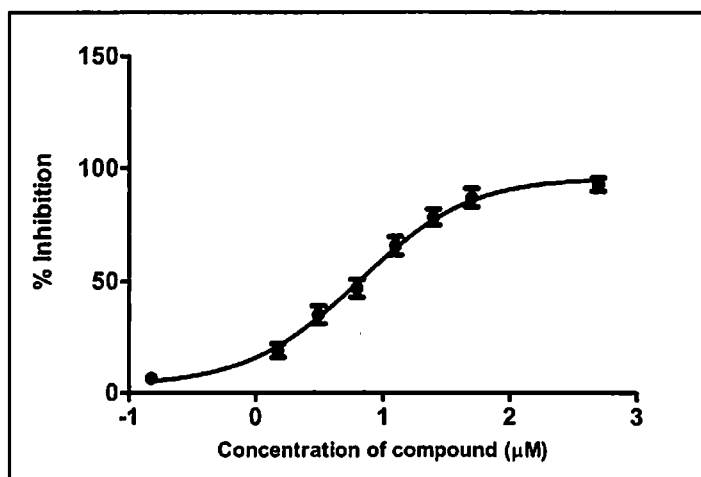


Figure 5.29: Dose response curve of compound T22 with different log concentration of the inhibitor on X-axis against percentage inhibition on Y-axis.

5.4.2. Supercoiling assay

Subsequently, all the molecules were screened for the DNA supercoiling assay as well to confirm the inhibitory profiles of the Gyr B inhibitors. *S. aureus* DNA supercoiling kit was procured from Inspiralis (Inspiralis Pvt. Limited, Norwich) and the different range of drug concentrations were used from 100 to 1 μM . Compounds T9, T6, T7, T25, T10, T11 and T20 showed better inhibitory profiles with an IC_{50} of less than 10 μM . While the (B2) had an IC_{50} of $3.12 \pm 1.6 \mu\text{M}$, the synthesized analogue T22 had a better IC_{50} of $2.79 \pm 0.59 \mu\text{M}$. In this assay too, novobiocin was considered as a standard inhibitor with an IC_{50} of $0.030 \pm 0.01 \mu\text{M}$. The dose dependent inhibitor profile is shown in (Figure 5.30).

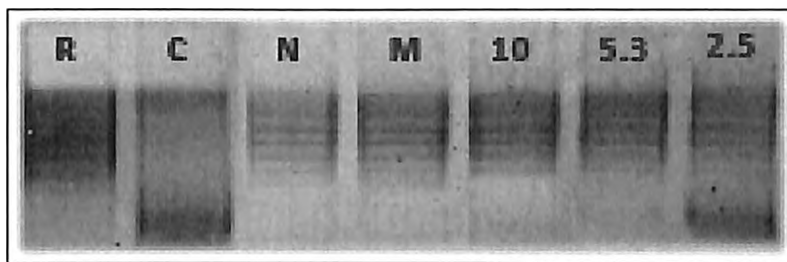


Figure 5.30: Depicting the inhibitory profile of *S. aureus* DNA gyrase supercoiling activity by compound **T22** in dose dependent manner; (R) represents relaxed closed circular DNA; (Con) represents the supercoiled relaxed DNA in the presence of gyrase enzyme. (N) is the novobiocin; (M) is moxifloxacin as standards. Gel data for assays with compound **T22** in different concentrations showing an IC_{50} of $5.35 \mu M$.

5.4.3. Antibacterial activity in Staphylococcal strains

All the synthesized compounds were further screened for their *in vitro* antibacterial activity against two bacterial strains of *S. aureus*, namely *S. aureus* MTCC3160 and MRSA96. The assay was performed according to the Clinical and Laboratory Standards Institute using the protocol as described in material and methods section. The concentration of the drugs used was in a range of $256-0.75 \mu g/mL$. While almost all the compounds showed an MIC less than $100 \mu M$ in MTCC3160 strain, they showed two-three fold higher MIC values in MRSA96 strain elucidating the drugs efficiency to inhibit the multi-resistant strain as well. As per the table, compounds **T22** and **T17** showed better MIC values at $18.92 \mu M$ and $16.56 \mu M$ almost one-fourth less concentration when compared to the (B2). Ofloxacin and ciprofloxacin were included as standard compounds in the assay. The overall results of the antibacterial screening are presented in

(Table 5.7). Few compounds **T6**, **T10**, **T27**, **T5**, **T24**, **T9**, **T19**, **T12** and **T28** exhibited weak

- ⊗ why now report?
- ⊗ they loose efficacy against DR?
- ⊗ Again, control values are not provided

antimicrobial activities which could be attributed to their non-permeability or efflux pump transportation.

5.4.4. Inhibition of biofilm formation studies

All the twenty three analogues were also tested for their biofilm inhibition studies ~~too~~. Being an extracellular polysaccharide produced by *S. aureus* species, biofilm aids in attachment and matrix formation around the bacteria that result in the alteration in the phenotype of the organism, resulting in the development of resistance towards the drugs. According to the recent statistics, it was estimated that 65% of all the human bacterial infections were due to biofilm formation [Donlan R. M., 2001] moreover people with MRSA infections are estimated to be 64% more likely to die than people with a non-resistant form. While the emergence of greater resistance of *S. aureus* biofilms against the antibacterial agents was attributed to failure of antibiotics to penetrate the biofilm, the other important parameter being the existence of different metabolic states of the cells in the biofilm aggregates associated with differential expression of genes by the bacteria concerned in the same biofilm aggregates [Giacometti A.; *et al.*, 2003]. All the synthesized compounds were screened for inhibition of *S. aureus* biofilm formation by a strong biofilm producer MRSA 96 strain. The extent of inhibition and the efficiency of the drugs were monitored quantitatively and qualitatively by the Congo red method [Smith K., *et al.*, 2008]. Assays were performed in a 96 flat-bottomed well plates at different drug concentration range starting from 250 to 0.75 μM . While the potent ligand **T22** showed an IC_{50} of 18.92 μM , all the compounds except **T21**, showed an IC_{50} less than 100 μM indicating the efficiency of these series of compounds towards inhibition of biofilm formation.

How is this any good?
How does this compare with your MRSA biofilm in comparison.

5.4.5. Cytotoxicity studies

All the synthesized compounds were tested for their eukaryotic safety profile information. The compounds were screened for their *in vitro* cytotoxicity against mammalian RAW 264.7 cell line at 100 μ M concentration in triplicates by utilizing (4,5-dimethylthiazol-2-yl)-2, 5-diphenyl tetrazolium bromide (MTT) assay. It was observed that all the twenty three compounds inhibitory range was below 25 μ M. The most potent compound T22 showed only 9.35% cytotoxicity at the highest concentration tested which was on par with novobiocin standard which had 11.4%.

5.4.6. zERG cardiotoxicity inhibition studies

The fluoroquinolones, considered as the only clinically approved DNA gyrase inhibitors till date suffer from zERG toxicity mainly the potent moxifloxacin. As per literature, though many inhibitors were successful at enzyme level studies, previously reported antibacterial C- and N-linked aminopiperidine DNA gyrase inhibitors suffered from serious zERG toxicity, for a safe profile we tested the top hits to ensure that the newly designed molecules did not suffer from such drawbacks. Compound T22 and T25 were subjected for zERG channel inhibition studies by assessing the arrhythmogenic potential on zebra fish ether-a-go-go-related gene (zERG) which was orthologous to the human ether-a-go-go-related gene (*hERG*), due to their conserved homology. This method of assessment, possessed significant advantage over the current conventional animal models which include ethical issues, low compound requirement, manually less tedious and low cost. Furthermore, Milan *et al.*, 2003 and Mittelstadt *et al.*, 2003 had reported that bradycardia and atrio-ventricular dissociation in zebrafish larvae can be used as a surrogate marker for *hERG* channel inhibition thereby affecting the rapid component of the

repolarizing potassium current and inducing arrhythmia in the model. In our study, compound T22 and T25 were subjected to *zERG* channel inhibition in concentrations ranging from 1 μM to 30 μM with 0.1% DMSO as vehicle, the heart rate variations and AV ratio were analysed by using a protocol described in more detail in material and methods section. Both the compounds T22 and T25 were found to be safe when compared to the positive control (20 μM terfenadine), by not showing any significant cardiotoxicity until 30 μM concentration of the drug. Furthermore, there was no significant change in the heart rate or AV ratio, in comparison to control group making them relatively safe, a significant breakthrough when compared to otherwise cardiotoxic terfenadine and amiodarones as illustrated in (Figure 5.31a-5.31b).

a) *if MOXI is zERG toxic, why is it not used as ctrl?* b)

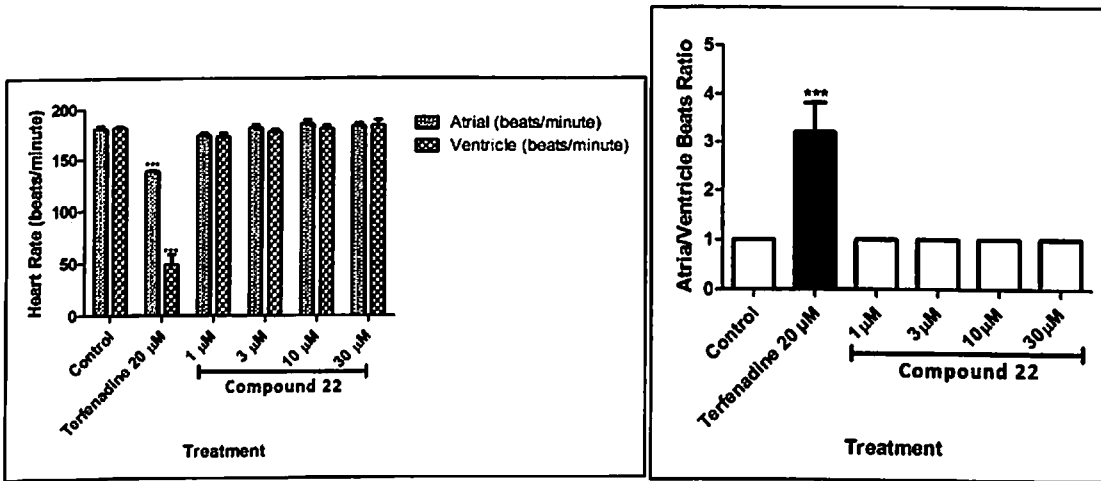


Figure 5.31: (a) Mean (\pm SEM) of the heart rates of atria and ventricles of Compound T22. (* $p < 0.05$, ** $p < 0.01$ and *** $p < 0.001$). Statistical significance was analyzed comparing control group versus treated groups. **Figure 5.31: (b)** Mean (\pm SEM) score of atrio ventricular ratio. (* $p < 0.05$, ** $p < 0.01$ and *** $p < 0.001$). Statistical significance was analyzed comparing control group versus all groups.

5.4.7. Differential scanning fluorimetry studies

To know the thermal stability of the DNA Gyr B protein when associated with the ligand differential scanning fluorimetry (DSF) studies were performed. The most active compound **T22** from this furan/thio-phen-2-carboxamide series was subjected to DSF. Compound **T22** enhanced the thermal stability of the catalytic domain of the Gyr B protein when performed in the presence and absence of the inhibitor. A significant positive shift of 2.9 °C was observed with respect to its T_m of 45.1 °C confirming the stability of the protein–ligand complex as shown in (Figure 5.32).

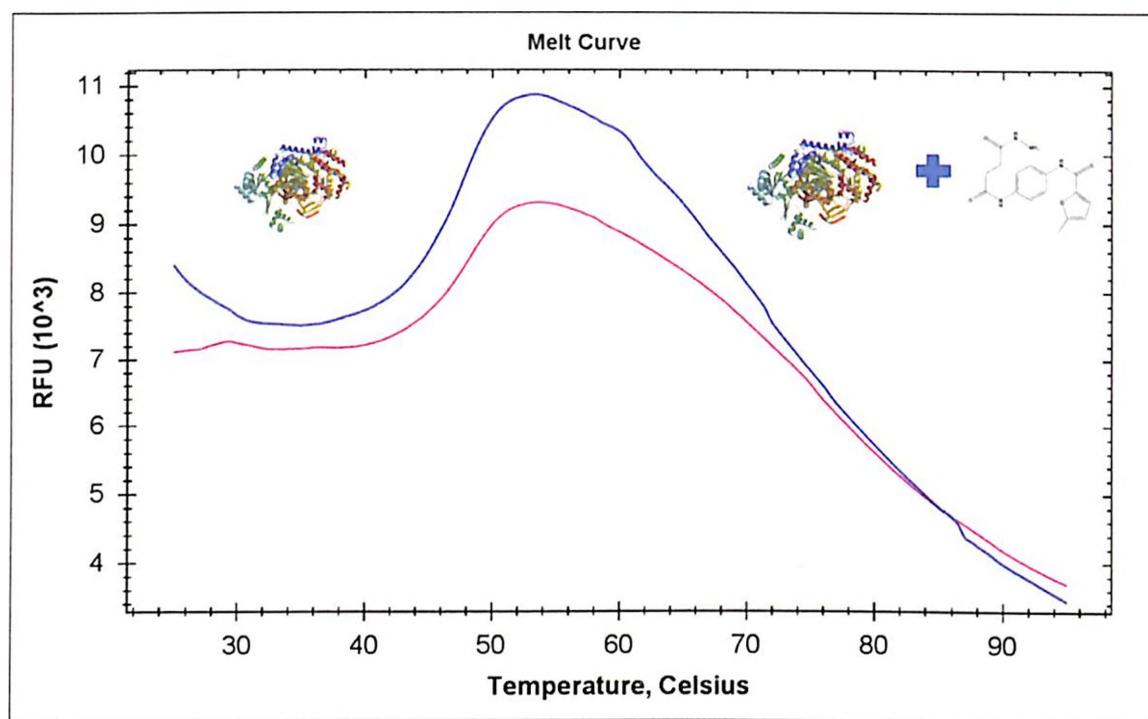
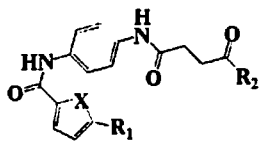


Figure 5.32: DSF experiment for compound **T22** showing an increase in thermal stability between the native protein (blue with T_m of 45.1 °C) and DNA Gyr B protein–compound **T22** complex (red with a T_m of 47.9) with a positive T_m shift of 2.8 °C.

Table 5.8: Biological activity data of the synthesized compounds



*What do the
a f mean?*

Comp	R ₁	R ₂	X	GyraseB assay (IC ₅₀) ^a (μM)	Supercoiling assay (IC ₅₀) ^b (μM)	MIC ATCC (μM) ^c	MRSA MIC (μM) ^d	Biofilm Inhibi (IC ₅₀) ^e	Cytotoxicity (% inhibi.) ^f
T5 (Lead)	H	-OH	O	12.88±1.39	3.12±1.6	79.03	79.03	79.03	15.95
T6	CH ₃	OCH ₃	O	27.63±1.09	26.15±0.3	75.67	75.67	75.67	21.22
T7	NO ₂	OCH ₃	O	22.64±0.66	8.41±0.22	17.29	34.58	34.58	19.88
T8	H	OCH ₃	S	37.63±0.91	11.2±0.69	37.60	75.2	37.60	16.64
T9	CH ₃	OCH ₃	S	37.52±1.22	22.6±0.91	72.17	72.17	72.1	17.34
T10	NO ₂	OCH ₃	S	12.49±0.58	6.12±0.49	16.56	16.56	33.12	17.82
T11	-H	OCH ₃	THF	11.06±0.92	7.5±0.39	40.89	40.89	81.78	15.5
T12	-H	OCH ₃	N	24.86±0.65	13.7±0.77	39.02	78.04	39.02	12.54
T14	CH ₃	-OH	O	10.33±0.51	6.12±0.7	39.51	79.02	39.51	18.33
T15	NO ₂	-OH	O	28.94±0.83	25.8±0.35	35.99	71.98	35.99	13.26
T16	H	-OH	S	21.99±0.74	12.5±0.51	39.26	78.52	39.26	24.62
T17	CH ₃	-OH	S	24.66±0.82	12.5±0.83	39.26	78.52	39.26	18.35
T18	NO ₂	-OH	S	29.49±0.81	26.8±1.25	68.81	68.81	39.26	18.55
T19	-H	-OH	N	42.45±0.88	13.7±0.45	81.61	81.61	81.61	15.22
T20	-H	-OH	THF	11.69±0.5	6.12±0.28	39.02	78.04	39.02	17.06
T21	H	-NH-NH ₂	O	39.41±0.97	23.9±0.4	79.03	79.03	79.03	14.21
T22	CH ₃	-NH-NH ₂	O	5.35±0.44	2.79±0.59	18.92	18.92	18.92	9.35
T23	NO ₂	-NH-NH ₂	O	35.49±1.54	25.1±0.44	34.59	34.59	34.59	22.53
T24	H	-NH-NH ₂	S	32.56±2.41	28.1±0.67	75.23	75.23	75.23	10.22
T25	CH ₃	-NH-NH ₂	S	9.71±0.69	6.12±0.22	18.04	36.08	36.08	19.31
T26	NO ₂	-NH-NH ₂	S	26.44±0.77	19.3±0.88	68.05	68.05	68.05	13.54
T27	-H	-NH-NH ₂	N	54.87±0.84	43.1±0.68	78.03	156.06	156.06	17.33
Novobiocin				0.125 ± 0.24	0.03 ± 0.01	0.25	ND	ND	11.4

There is a log of difference b/w NOV & T22.

This is ridiculous. How can we perform cytotox @ MIC conc only? What about 10x MIC?

5.5. Highlights of this study

A structure based e-pharmacophore model was built and based on the built hypothesis ^{and} twelve molecules were shortlisted. Among them, BAS04380545, 4-((4-(furan-2-carboxamido)phenyl)amino)-4-oxobutanoic acid a compound, which has been synthetically derivitized to obtain another twenty three molecules for which the *in vitro* screening were performed. With hit expansion of this (B2) molecule, a more potent inhibitor T22 with better biological properties was obtained. Further, structural elements were identified that undoubtedly provide the basis for further optimization of the new inhibitors.

Chapter 6

SUMMARY AND CONCLUSION

Efforts since 1950's to discover a drug against DNA Gyr B enzyme have not been fruitful as resistance, a man-made amplification of a natural phenomenon has allowed the resurgence of *S. aureus* in a new virulent forms of MRSA; making the presently available anti-Staphylococcal drug regime inadequate to address the inherent and emerging challenges of treatment. The nosocomial infections along with the development of community associated-methicillin resistant *Staphylococcus aureus* strains has made the the process of drug development an almost impossible mechanism. Thus the targets selected, in this thesis **Staphylococcal DNA gyrase** and **DNA Gyr B** are attractive as they are relatively less exploited targets in the field of drug discovery and hence holds an immense potential for the development of novel agents against them as they are not impacted by target mediated cross-resistance associated with previously reported drugs.

WRONG STATEMENT! RESISTANCE TO GYR B IS VERY WELL CHARACTERIZED!

Utilizing the structure based drug design strategy, a hypothesis was created and validated which was further used to screen the database ^{of} compounds. Among the twenty lead compounds procured, **L15** showed ~~and~~ excellent activity with an IC_{50} of $0.79 \pm 0.12 \mu M$. Further, on lead optimization and synthesis of various analogues of ~~about~~ forty compounds, compound **R20** emerged as the most active with good *in vitro* biological properties with an IC_{50} of $0.32 \pm 0.17 \mu M$, almost half the parent molecule **L15** with no cardio-toxicity nature. The molecule also exhibited good anti-bacterial and potent bactericidal property when tested by the kill kinetic studies. Moreover with

the efflux pump inhibitor assay, the MIC was reduced by half when tried in MTCC3160 and MRSA96 strains.

Secondly, DNA Gyr B domain^{as} the second target, an e-pharmacophore hypothesis was generated by structure based drug discovery strategy via which database screening was done resulting in 12 compounds. On testing the compounds in both the DNA Gyr B ATPase and supercoiling assays, 3 molecules showed very good inhibitory profiles. Among them compound **BAS01355130** was found to be most active with the Gyr B ATPase assay IC_{50} of $12.6 \pm 0.32 \mu M$ and supercoiling assay IC_{50} of $2.9 \mu M$ while the second most active compound **BAS04380545** showed a Gyr B IC_{50} of $12.88 \pm 1.39 \mu M$ whereas the supercoiling IC_{50} was $3.12 \pm 1.6 \mu M$. Thus, these two lead molecules was further taken up and on lead optimization analogues were synthesized. On lead optimization of **BAS01355130** forty one compounds were obtained, **BAS04380545** gave twenty four compounds. All were subjected for their *in vitro* and biophysical characterization studies. From the first series, compound **S10** (5-((4-(5-Fluoro-1H-benzo[d]imidazol-2-yl)phenyl)amino)-5-oxopentanoic acid) was the most active compound whereas from the second series of the derivitized molecules compound **T22** (N-(4-(4-Hydrazinyl-4-oxobutanamido)phenyl)-5-methylfuran-2-carboxamide) was the most active compound with Gyr B IC_{50} of $2.79 \pm 0.59 \mu M$ and supercoiling IC_{50} of $5.35 \mu M$ with no cardiotoxicity and good biofilm inhibitory profile and non-cytotoxic at $25 \mu M$.

The above class of compounds described can be ascertained as promising lead compounds for further optimization and development to yield best antibacterial agents in future to combat ever present and ever-increasing bacterial infections. The study also provides the basis for further chemical optimization of these potent inhibitors as potential anti-bacterial agents.

FUTURE PERSPECTIVES

The Type II topoisomerases of bacteria have a homologous proteins in human beings, but as such DNA Gyrase is absent in humans makes this an attractive target for the development of antibacterials. The present study, focused on utilizing the pharmaceutically unexploited domains of *Staphylococcus aureus* DNA gyrase, the NBTI's and the Gyr B subunit as potential anti-Staphylococcal targets possessing a excellent opportunity to address the ever-increasing problem of the bacterial resistance with a scope to develop an effective treatment for the same.

The study describes the design and development of a chemically diverse series of NBTI molecules as potential DNA gyrase inhibitors followed by two lead series as potential DNA Gyr B inhibitors. The molecules reported here displayed considerable *in vitro* enzyme efficacy and bactericidal activity against *S. aureus* MTCC and MRSA strains while few of them showed submicromolar inhibitory activities. Although these results are encouraging, lead optimization is needed to build in an effective pharmacokinetic and pharmacodynamic profiles in order to achieve an adequate human safety profile to ensure the dose in an acceptable range.

Thus, the advancement of any of the candidate compounds along a drug development path would require a significant investment in medicinal chemistry, preclinical and clinical studies. Thus the work presented in this thesis needs to be looked into the above parameters for further development of them.

REFERENCES

- Ahuja V., Sharma S.J. Drug safety testing paradigm, current progress and future challenges: an overview. *Appl. Toxicol.* **2013**, 34, 576.
- Anthony Maxwell. DNA gyrase as a drug target. *Trends in Microbiology.* **1997**, 5, 102-109.
- Arundhati C. Lele., Nilesh R.Tawari., Mariam S.Degani. Development of pharmacophore model for *S. aureus* DNA gyrase inhibitors. *International Journal of Pharma Bioscience and Technology.* **2013**, 1, 34-39.
- Aravind L., Leipe D.D., Koonin E.V. Toprim a conserved catalytic domain in type IA and II topoisomerases, DnaG-type primases, OLD family nucleases and RecR proteins. *Nucleic Acids Res.* **1998**, 26, 4205–4213.
- Ball P., Baquero F., Cars O., File T., Garau J., Klugman K., Low D.E., Rubinstein E., Wise R. Antibiotic therapy of community respiratory tract infections: strategies for optimal outcomes and minimized resistance emergence. *J Antimicrob Chemother.* **2002**, 49, 31-40.
- Basarab G.S., Hill P.J., Garner C.E., Hull K., Green O., Sherer B.A., Dangel P.B., Manchester J.I., Bist S., Hauck S., Zhou F., Uria-Nickelsen M., Illingworth R., Alm R., Rooney M., Eakin A.E. Optimization of pyrrolamide topoisomerase II inhibitors toward identification of an antibacterial clinical candidate (AZD5099). *J Med Chem.* **2014**, 57, 6060-82.
- Bax B.D., Chan P.F., Eggleston D.S., Fosberry A., Gentry D.R., Gorrec F., Giordano I., Hann M.M., Hennessy A., Hibbs M., Huang J., Jones E., Jones J., Brown K.K., Lewis C.J., May E.W., Saunders M.R., Singh O., Spitzfaden C.E., Shen C., Shillings A., Theobald

A.J., Wohlkonig A., Pearson N.D., Gwynn M.N. Type IIA topoisomerase inhibition by a new class of antibacterial agents. *Nature*. **2010**, 466, 935-40.

Black M.T., Stachyra T., Platel D., Girard A.M., Claudon M., Bruneau J.M., Miossec C. Mechanism of action of the antibiotic NXL101, a novel nonfluoroquinolone inhibitor of bacterial type II topoisomerases. *Antimicrob Agents Chemother*. **2008**, 52, 3339-49.

Banote R.K., Koutarapu S., Chennubhotla K.S., Chatti K., Kulkarni P. Oral gabapentin suppresses pentylenetetrazole-induced seizure-like behavior and cephalic field potential in adult zebrafish. *Epilepsy Behav*. **2013**, 27, 212-9.

Blanche F., Cameron B., Bernard F.X., Maton L., Manse B., Ferrero L., Ratet N., Lecoq C., Goniot A., Bisch D., Crouzet J. Differential behaviors of *Staphylococcus aureus* and *Escherichia coli* type II DNA topoisomerases. *Antimicrob Agents Chemother*. **1996**, 40, 2714-20.

Boucher H.W., Corey G.R. Epidemiology of methicillin-resistant *Staphylococcus aureus*. *Clin Infect Dis*. **2008**, 46, S344-9.

Boucher H.W., Talbot G.H., Bradley J.S., Edwards J.E., Gilbert D., Rice L.B., Scheld M., Spellberg B., Bartlett J. Bad bugs, no drugs: no ESKAPE! An update from the Infectious Diseases Society of America. *Clin Infect Dis*. **2009**, 48, 1-12.

Brown P.O., Cozzarelli N.R. A sign inversion mechanism for enzymatic supercoiling of DNA. *Science*. **1979**, 206, 1081-3.

Brvar M., Perdih A., Renko M., Anderluh G., Turk D., Solmajer T. Structure-based discovery of substituted 4,5'-bithiazoles as novel DNA gyrase inhibitors. *J Med Chem*. **2012**, 55, 6413-26.

Charifson P.S., Grillot A.L., Grossman T.H., Parsons J.D., Badia M., Bellon S., Deininger D.D., Drumm J.E., Gross C.H., LeTiran A., Liao Y., Mani N., Nicolau D.P., Perola E., Ronkin S., Shannon D., Swenson L.L., Tang Q., Tessier P.R., Tian S.K., Trudeau M., Wang T., Wei Y., Zhang H., Stamos D. Novel dual-targeting benzimidazole urea inhibitors of DNA gyrase and topoisomerase IV possessing potent antibacterial activity: intelligent design and evolution through the judicious use of structure-guided design and structure-activity relationships. *J Med Chem.* **2008**, 51, 5243-63.

Christensen G.D., Simpson W.A., Younger J.J., Baddour L.M., Barrett F.F., Melton D.M., Beachey E.H. Adherence of coagulase-negative staphylococci to plastic tissue culture plates: a quantitative model for the adherence of staphylococci to medical devices. *J Clin Microbiol.* **1985**, 22, 996-1006.

Chopra S., Matsuyama K., Tran T., Malerich J.P., Wan B., Franzblau S.G., Lun S., Guo H., Maiga M.C., Bishai W.R., Madrid P.B. Evaluation of gyrase B as a drug target in *Mycobacterium tuberculosis*. *J Antimicrob Chemother.* **2012**, 67, 415-21.

Collin F., Karkare S., Maxwell A. Exploiting bacterial DNA gyrase as a drug target: current state and perspectives. *Appl Microbiol Biotechnol.* **2011**, 92, 479-97.

Deibler R.W., Rahmati S., Zechiedrich E.L. Topoisomerase IV, alone, unknots DNA in *E. coli*. *Genes Dev.* **2001**, 15, 748-61.

Donlan R.M., Biofilm formation: a clinically relevant microbiological process. *Clin. Infect. Dis.* **2001**, 33, 1387.

Drlica K., Hiasa H., Kerns R., Malik M., Mustaev A., Zhao X. Quinolones: action and resistance updated. *Curr Top Med Chem.* **2009**, 9, 981-98.

Eakin A., Ehmann D., Gao N., Karantzeni I., Walkup G. Topoisomerase hybrids and methods of use. United States Patent Application 20070072183. **2007**.

Eakin A.E., Green O., Hales N., Walkup G.K., Bist S., Singh A., Mullen G., Bryant J., Embrey K., Gao N., Breeze A., Timms D., Andrews B., Uria-Nickelsen M., Demeritt J., Loch J.T., Hull K., Blodgett A., Illingworth R.N., Prince B., Boriack-Sjodin P.A., Hauck S., MacPherson L.J., Ni H., Sherer B. Pyrrolamide DNA gyrase inhibitors: fragment-based nuclear magnetic resonance screening to identify antibacterial agents. *Antimicrob Agents Chemother.* **2012**, 56, 1240-6.

Eoghan O'Neill., Clarissa Pozzi., Patrick Houston., Davida Smyth., Hilary Humphreys., D.

Ashley Robinson., James P. O'Gara. *J Clin Microbiol.* **2007**, 45, 1379-1388. *Title is missing*

Eric D.Brown., Wright G.D., New targets and screening approaches in antimicrobial drug discovery. *Chemical reviews.* **2005**, 105, 759-774.

Fournier B., Zhao X., Lu T., Drlica K., Hooper D.C. Selective targeting of topoisomerase IV and DNA gyrase in *Staphylococcus aureus*: different patterns of quinolone-induced inhibition of DNA synthesis. *Antimicrob Agents Chemother.* **2000**, 44, 2160-5.

Franklin D.Lowy., M.D. *Staphylococcus aureus* Infections. *N Engl J Med.* **1998**, 339, 520-532.

Freeman D.J., Falkiner F.R., Keane C.T. New method for detecting slime production by coagulase negative staphylococci. *J Clin Pathol.* **1989**, 42, 872-874.

Gubaev A., Klostermeier D. DNA-induced narrowing of the gyrase N-gate coordinates T-segment capture and strand passage. *Proc Natl Acad Sci.* **2011**, 108, 14085-90.

Gubaev A., Klostermeier D. "The mechanism of negative DNA supercoiling: a cascade of DNA-induced conformational changes prepares gyrase for strand passage". *DNA Repair (Amst)*. **2014**, 130-41.

Hallett P., Grimshaw A.J., Wigley D.B., Maxwell A. Cloning of the DNA gyrase genes under tac promoter control: overproduction of the gyrase A and B proteins. *Gene*. **1990**, 93, 139-42.

Henry F.Chambers. The Changing Epidemiology of *Staphylococcus aureus*? *4th Decennial International Conference on Nosocomial and Healthcare-Associated Infections*. **2001**, 7, 70-78.

Hidayat L.K., Hsu D.I., Quist R., Shriner K.A., Wong-Beringer A. High-dose vancomycin therapy for methicillin-resistant *Staphylococcus aureus* infections: efficacy and toxicity. *Arch Intern Med*. **2006**, 166, 2138-44.

Hiramatsu K., Katayama Y., Matsuo M., Sasaki T., Morimoto Y., Sekiguchi A., Baba T. Multi-drug-resistant *Staphylococcus aureus* and future chemotherapy. *J Infect Chemother*. **2014**, 20, 593-601.

<http://www.who.int/mediacentre/factsheets/fs194/en/> Updated April 2015.

James M.Berger., Deborah Fass., James C.Wang., Stephen C.Harrison. Structural similarities between topoisomerases that cleave one or both DNA strands. *Proc Natl Acad Sci*. **1998**, 95, 7876–7881.

Jorgensen J.H., Ferraro M.J. Antimicrobial susceptibility testing: general principles and contemporary practices. *Clin Infect Dis*. **1998**, 26, 973-80.

Kampranis S.C., Bates A.D., Maxwell A. A model for the mechanism of strand passage by DNA gyrase. *Proc Natl Acad Sci.* **1999**, 96, 8414-9.

Keith A.Rodvold., Kevin W.McConeghy. Methicillin-Resistant *Staphylococcus aureus* Therapy: Past, Present, and Future. *Clin Infect Dis.* **2014**, 58, S20-S27.

Klevens R.M., Edwards J.R., Tenover F.C., McDonald L.C., Horan T., Gaynes R. Changes in the epidemiology of methicillin-resistant *Staphylococcus aureus* in intensive care units in US hospitals, 1992-2003. *Clin Infect Dis.* **2006**, 42, 389-91.

Liu L.F., Liu C.C., Alberts B.M. Type II DNA topoisomerases: enzymes that can unknot a topologically knotted DNA molecule via a reversible double-strand break. *Cell.* **1980**, 19, 697-707.

Lodise T.P., Miller C.D., Graves J., Evans A., Graffunder E., Helmecke M., Stellrecht K. Predictors of high vancomycin MIC values among patients with methicillin-resistant *Staphylococcus aureus* bacteraemia. *J Antimicrob Chemother.* **2008**, 62, 1138-41.

Lutz Heide. The aminocoumarins: biosynthesis and biology. *Nat Prod Rep.* **2009**, 26, 1241-1250.

Marcel L. V., Jason C.C., Micheal J.H., Christopher W.M., Richard D.T., Improved protein-ligand docking using GOLD. *Proteins: Structure, Function and Bioinformatics.* **2003**, 52, 609-623.

Mathur T., Singhal S., S Khan S., Upadhyay D. J., Fatma T., Rattan A. Detection of biofilm formation among the clinical isolates of staphylococci: An evaluation of three different screening methods. **2006**, 24, 25-29.

Journal writing

McAdam P.R., Templeton K.E., Edwards G.F., Holden M.T., Feil E.J., Aanensen D.M., Bargawi H.J., Spratt B.G., Bentley S.D., Parkhill J., Enright M.C., Holmes A., Girvan E.K., Godfrey P.A., Feldgarden M., Kearns A.M., Rambaut A., Robinson D.A., Fitzgerald J.R. Molecular tracing of the emergence, adaptation, and transmission of hospital-associated methicillin-resistant *Staphylococcus aureus*. *Proc Natl Acad Sci*. **2012**, 109, 9107-12.

McCarthy J.D. Computational approaches to structure-based drug design. *Pharma. Thera*. **1999**, 84, 179-191.

Mdluli K., Ma Z. *Mycobacterium tuberculosis* DNA gyrase as a target for drug discovery. *Infect Disord Drug Targets*. **2007**, 7, 159-68.

Milan D.J., Peterson T.A., Ruskin J.N., Peterson R.T., MacRae C.A. Drugs that induce repolarization abnormalities cause bradycardia in zebrafish. *Circulation*. **2003**, 18, 107, 1355-8.

Minovski N., Perdih A., Solmajer T. Combinatorially-generated library of 6-fluoroquinolone analogs as potential novel antitubercular agents: a chemometric and molecular modeling assessment. *J Mol Model*. **2012**, 18, 1735-53.

Mittelstadt S.W., Hemenway C.L., Craig M.P., Hove J.R. Evaluation of zebrafish embryos as a model for assessing inhibition of hERG. *J Pharmacol Toxicol Methods*. **2008**, 57, 100-5.

Mizuuchi K., Fisher L.M., O'Dea M.H., Gellert M. DNA gyrase action involves the introduction of transient double-strand breaks into DNA. *Proc. Nat. Acad. Sci*. **1980**, 77, 1847-1851.

Hayashi N., Nakata Y., Yazaki A. New findings on the structure-phototoxicity relationship and photostability of fluoroquinolones with various substituents at position 1. *Antimicrob Agents Chemother*. **2004**, 48, 799-803.

Nakada N., Gmunder H., Hirata T., Arisawa M. Mechanism of inhibition of DNA gyrase by cyclothialidine, a novel DNA gyrase inhibitor. *Antimicrob Agents Chemother.* **1994**, *38*, 1966-73.

Nichols M.D., DeAngelis K., Keck J.L., Berger J.M. Structure and function of an archaeal topoisomerase VI subunit with homology to the meiotic recombination factor Spo11. *EMBO J.* **1999**, *18*, 6177–6188.

Niesen F.H., Berglund H., Vedadi M. The use of differential scanning fluorimetry to detect ligand interactions that promote protein stability. *Nat Protoc.* **2007**, *2*, 2212-21.

Nöllmann M., Stone M.D., Bryant Z., Gore J., Crisona N.J., Hong S.C., Mittelheiser S., Maxwell A., Bustamante C., Cozzarelli N.R. Multiple modes of Escherichia coli DNA gyrase activity revealed by force and torque. *Nat Struct Mol Biol.* **2007**, *14*, 264-71.

O'Neill E., Pozzi C., Houston P., Smyth D., Humphreys H., Robinson D.A., O'Gara J.P. Association between methicillin susceptibility and biofilm regulation in *Staphylococcus aureus* isolates from device-related infections. *J Clin Microbiol.* **2007**, *45*, 1379-88.

Oram M., Travers A.A., Howells A.J., Maxwell A., Pato M.L. Dissection of the bacteriophage Mu strong gyrase site (SGS): significance of the SGS right arm in Mu biology and DNA gyrase mechanism. *J Bacteriol.* **2006**, *188*, 619-32.

Pandeya S.N., Sriram D., Nath G., De Clercq E. Synthesis and antimicrobial activity of Schiff and Mannich bases of isatin and its derivatives with pyrimidine. *Farmaco.* **1999**, *54*, 624-8.

Pozzi C., Waters E.M., Rudkin J.K., Schaeffer C.R., Lohan A.J., Tong P., Loftus B.J., Pier G.B., Fey P.D., Massey R.C., O'Gara J.P.

Methicillin resistance alters the biofilm phenotype and attenuates virulence in *Staphylococcus aureus* device-associated infections. *PLoS Pathog.* **2012**, *8*, 1002626.

Rattan A. Mechanisms of resistance to fluoroquinolones. *Natl Med J India.* **1999**, *12*, 162-4.

Reece R.J., Maxwell A. DNA gyrase: structure and function. *Crit Rev Biochem Mol Biol.* **1991**, *26*, 335-75.

Salam N.K., Nuti R., Sherman W. Novel Method for Generating Structure-Based Pharmacophores Using Energetic Analysis. *J. Chem. Inf. Model.* **2009**, *49*, 2356–2368.

Schoeffler A.J., Berger J.M. DNA topoisomerases: harnessing and constraining energy to govern chromosome topology. *Q Rev Biophys.* **2008**, *41*, 41-101.

Sherer B.A., Hull K., Green O., Basarab G., Hauck S., Hill P., Loch J.T., Mullen G., Bist S., Bryant J., Boriack-Sjodin A., Read J., DeGrace N., Uria-Nickelsen M., Illingworth R.N., Eakin A.E. Pyrrolamide DNA gyrase inhibitors: optimization of antibacterial activity and efficacy. *Bioorg Med Chem Lett.* **2011**, *21*, 7416-20.

Sheo B.Singh., David E.Kaelin., Jin Wu., Lynn Miesel., Christopher M.Tan., Peter T.Meinke., David Olsen., Armando Lagrutta., Prudence Bradley., Jun Lu., Sangita Patel., Keith W.Rickert., Robert F.Smith., Stephen Soisson., Changqing Wei., Hideyuki Fukuda., Ryuta Kishii., Masaya Takei., Yasumichi Fukuda. Oxabicyclooctane-Linked Novel Bacterial Topoisomerase Inhibitors as Broad Spectrum Antibacterial Agents. *ACS Med Chem Lett.* **2014**, *5*, 609–614.

Silke Alt., Lesley A.Mitchenall., Anthony Maxwell., Lutz Heide. Inhibition of DNA gyrase and DNA topoisomerase IV of *Staphylococcus aureus* and *Escherichia coli* by aminocoumarin antibiotics. *J Antimicrob Chemother.* **2011**, *66*, 1203.

Singh K.D., Kirubakaran P., Nagarajan S., Sakkiyah S., Muthusamy K., Velmurgan D., Jeyakanthan, J. Homology modeling, molecular dynamics, e-pharmacophore mapping and docking study of Chikungunya virus nsP2 protease. *J. Mol. Modeling*. **2012**, 18, 39-51.

Smith K., Perez A., Ramage G., Lappin D., Gemmell C.G., Lang S. Biofilm formation by Scottish clinical isolates of *Staphylococcus aureus*. *J. Med. Microbiol.* **2008**, 1018, 57.

Sriram D., Yogeewari P., Babu N.R., Kurre P.N. Synthesis and in vitro anti-HIV activities of didanosine prodrugs. *J Enzyme Inhib Med Chem*. **2007**, 22, 51-5.

Talbot G.H., Bradley J., Edwards J.E. Jr., Gilbert D., Scheld M., Bartlett J.G. Bad bugs need drugs: an update on the development pipeline from the Antimicrobial Availability Task Force of the Infectious Diseases Society of America. *Clin Infect Dis*. **2006**, 42, 1065.

Taylor R.D., Jewsbury P.J., Essex J.W. A review of protein-small molecule docking methods. *J Comput Aided Mol Des*. **2002**, 16, 151-66.

Uhlemann A.C., Otto M., Lowy F.D., DeLeo F.R. Evolution of community- and healthcare-associated methicillin-resistant *Staphylococcus aureus*. *Infect Genet Evol*. **2014**, 21, 563-74.

Uria-Nickelsen M., Blodgett A., Kamp H., Eakin A., Sherer B., Green O. Novel DNA gyrase inhibitors: microbiological characterisation of pyrrolamides. *Int J Antimicrob Agents*. **2013**, 41, 28-35.

Wang J.C. DNA topoisomerases. *Annu Rev Biochem*. **1996**, 65, 635-92.

Wigley D.B. Structure and mechanism of DNA topoisomerases. *Annu Rev Biophys Biomol Struct*. **1995**, 24, 185-208.

ANNEXURE-I

NBTI synthesis and experimental section:

General procedure for the synthesis of sub:- 2-(Piperidin-4-yl)-1H-benzo[d]imidazole (2a-d): Eaton's reagent (10 vol; wt/vol) was added drop wise to a well pulverised mixture of the corresponding 1,2-phenylenediamine (1a-d) (1 equiv) and piperidine-4-carboxylic acid (1 equiv) at 0°C. The reaction mixture was then heated at 130°C for 5 - 6 h (monitored by TLC and LCMS for completion). The reaction mixture was cooled and neutralised with 10% sodium hydroxide solution to pH of 6-7, the precipitate formed was filtered and washed repeatedly with water and dried. The solid obtained was recrystallized from ethanol to afford the desired product in good yield as described below.

4.2.1 2-(Piperidin-4-yl)-1H-benzo[d]imidazole (2a): The compound was prepared according to the general procedure using 1,2-phenylenediamine 1a (1 g, 9.25 mmol), piperidine-4-carboxylic acid (1.19 g, 9.25 mmol) and eatons reagent (10 mL) to afford 2a (1.42 g, 76% yield) as pale brown solid. M.P - 229 – 231°C. ¹H NMR (DMSO-d₆): δH 1.98-2.81 (m, 9H), 3.21 (b, 1H), 5.05 (b, 1H), 6.89 - 7.62 (m, 4H). ¹³C NMR (DMSO-d₆): δc 142.6, 139.6 (2C), 122.8 (2C), 116.5 (2C), 39.5 (2C), 36.2, 32.5 (2C). EI-MS m/z: 202 (M+H)⁺. Anal Calcd for C₁₂H₁₅N₃: C, 71.61; H, 7.51; N, 20.88. Found: C, 71.64; H, 7.549; N, 20.86.

4.2.2 5-Methyl-2-(piperidin-4-yl)-1H-benzo[d]imidazole (2b): The compound was prepared according to the general procedure using 4-methylbenzene-1,2-diamine 1b (1 g, 8.19 mmol), piperidine-4-carboxylic acid (1.05 g, 8.19 mmol) and eatons reagent (10 mL) to afford 2b (1.02 g, 60% yield) as brown solid. M.P: 222 - 224°C. ¹H NMR (DMSO-d₆): δH 1.95-2.77 (m, 12H), 3.25 (b, 1H), 4.98 (b, 1H), 7.05 - 7.71 (m, 3H). ¹³C NMR (DMSO-d₆): δc 142.6, 140.2, 136.5,

133.5, 124.9, 116.8, 116.2, 39.5 (2C), 36.5, 32.5 (2C), 22.5. EI-MS m/z: 216 (M+H)⁺. Anal Calcd for C₁₃H₁₇FN₃: C, 72.52; H, 7.96; N, 19.52; Found: C, 72.54; H, 7.92; N, 19.50.

4.2.3 5-Fluoro-2-(piperidin-4-yl)-1H-benzo[d]imidazole (2c): The compound was prepared according to the general procedure using 4-fluorobenzene-1,2-diamine 1c (1 g, 7.93 mmol), piperidine-4-carboxylic acid (1.02 g, 7.93 mmol) and eatons reagent (10 mL) to afford 2c (1.1 g, 65% yield) as pale yellow coloured solid. M.P: 231 - 233 °C. ¹H NMR (DMSO-d₆): δH 2.01-2.86 (m, 9H), 3.21 (b, 1H), 4.95 (b, 1H), 6.95 - 7.73 (m, 3H). ¹³C NMR (DMSO-d₆): δc 155.8, 140.2, 139.8, 135.6, 133.2, 110.1, 101.5, 39.5 (2C), 36.5, 32.5 (2C). EI-MS m/z: 220 (M+H)⁺. Anal Calcd for C₁₂H₁₄FN₃: C, 65.73; H, 6.44; N, 19.16; Found C, 65.76; H, 6.46; N, 19.14.

4.2.4 5-Chloro-2-(piperidin-4-yl)-1H-benzo[d]imidazole (3d): The compound was prepared according to the general procedure using 4-chlorobenzene-1,2-diamine 1d (1 g, 7.01 mmol), piperidine-4-carboxylic acid (0.9 g, 7.01 mmol) and eatons reagent (10 mL) to afford 3d (1.2 g, 75% yield) as brown solid. MP: 237 – 239 °C. ¹H NMR (DMSO-d₆): δH 2.04-2.96 (m, 9H), 3.31 (b, 1H), 5.11 (b, 1H), 7.08 – 8.52 (m, 3H). ¹³C NMR (DMSO-d₆): δc 140.3, 139.6, 138.2, 130.1, 125.6, 117.1, 116.3, 39.5 (2C), 36.2, 32.1 (2C). EI-MS m/z: 235 (M)⁺. Anal Calcd for C₁₂H₁₄ClN₃: C, 61.15; H, 5.99; N, 17.83; Found C, 61.14; H, 5.97; N, 17.85.

General procedure for the synthesis of substituted 2-(4-(1H-benzo[d]imidazol-2-yl)piperidin-1-yl)acetamide derivatives (R3-R12): The synthesis followed the literature procedure. To a well stirred solution of the corresponding 2-(piperidin-4-yl)-1H-benzo[d]imidazole (2a) (1 equiv) in anhydrous N,N Dimethyl formamide (1 ml) was added triethylamine (2.5 equiv). The reaction mixture was stirred for 15 mts followed by the addition of corresponding substituted acetyl chlorides (1.2 equiv) and continued the stirring fir 6

h(monitored by TLC and LCMS for completion). Then ice was added to the reaction mixture and extracted repeatedly with ethyl acetate. The combined organic layer was then dried over anhydrous sodium sulphate and concentrated under reduced pressure. The residue obtained was further purified by column chromatography using hexane : ethyl acetate the desired product in good yield and purity as described below.

4.2.1.1. 2-(4-(1H-Benzo[d]imidazol-2-yl)piperidin-1-yl)-N-phenylacetamide (R3): The compound was prepared according to the general procedure using 2-(piperidin-4-yl)-1H-benzo[d]imidazole 2a (0.1 g, 0.49 mmol), triethyl amine (0.13 g, 1.24 mmol), 2-chloro-N-phenylacetamide (0.1 g, 0.59 mmol) to afford 4 (0.11 g, 65% yield) as pale yellow solid. M.P: 249 - 251°C. ¹H NMR (DMSO-d₆): δH 2.05 – 2.89 (m, 9H), 2.99 (s, 2H), 4.6 (b, 1H), 6.95 – 7.62 (m, 9H), 8.21 (b, 1H). ¹³C NMR (DMSO-d₆): δc 169.1, 145.6, 140.2 (2C), 139.2, 130.5 (2C), 129.5, 124.5 (2C), 122.6 (2C), 116.5 (2C), 65.6, 55.2 (2C), 36.3, 30.2 (2C). EI-MS m/z: 335 (M+H) +. Anal Calcd for C₂₀H₂₂N₄O: C, 71.83; H, 6.63; N, 16.75. Found: C, 71.85; H, 6.61; N, 16.72.

4.2.1.2. 2-(4-(1H-Benzo[d]imidazol-2-yl)piperidin-1-yl)-N-(2-chloro-5-(trifluoromethyl)phenyl)acetamide (R4): The compound was prepared according to the general procedure using 2-(piperidin-4-yl)-1H-benzo[d]imidazole 2a (0.1 g, 0.49 mmol), triethyl amine (0.13 g, 1.24 mmol), 2-chloro-N-(2-chloro-5-(trifluoromethyl)phenyl)acetamide (0.16 g, 0.59 mmol) to afford 4 (0.13 g, 60% yield) as white solid. M.P: 269 - 271°C. ¹H NMR (DMSO-d₆): δH 2.01 – 2.85 (m, 9H), 3.02 (s, 2H), 4.8 (b, 1H), 6.91 – 8.15 (m, 7H), 8.18 (b, 1H). ¹³C NMR (DMSO-d₆): δc 169.6, 144.6, 140.5 (2C), 136.5, 130.2 (2C), 126.8, 125.2, 122.1 (2C), 121.5, 119.6, 116.5 (2C), 65.6, 55.2 (2C), 36.2, 30.2 (2C). EI-MS m/z: 336 (M) +. Anal Calcd for C₂₁H₂₀ClF₃N₄O: C, 57.74; H, 4.61; N, 12.82. Found: C, 57.71; H, 4.63; N, 12.85.

4.2.1.3. 2-(4-(1H-Benzo[d]imidazol-2-yl)piperidin-1-yl)-N-((6-chloropyridin-3-yl)methyl)acetamide (R5): The compound was prepared according to the general procedure using 2-(piperidin-4-yl)-1H-benzo[d]imidazole 2a (0.1 g, 0.49 mmol), triethyl amine (0.13 g, 1.24 mmol), 2-chloro-N-((6-chloropyridin-3-yl)methyl)acetamide (0.13 g, 0.59 mmol) to afford 5 (0.12 g, 66% yield) as pale yellow solid. M.P: 235 - 237°C. ¹H NMR (DMSO-d₆): δH 1.98 – 2.75 (m, 9H), 3.05 (s, 2H), 4.46 (s, 2H), 4.72 (b, 1H), 7.01 – 8.56 (m, 8H). ¹³C NMR (DMSO-d₆): δc 172.3, 149.8, 148.2, 140.5, 139.2 (2C), 138.6, 132.2, 122.5, 121.8 (2C), 116.8 (2C), 60.2, 55.8 (2C), 45.6, 37.2, 30.2 (2C). EI-MS m/z: 383 (M) +. Anal Calcd for C₂₀H₂₂ClN₅O: C, 62.58; H, 5.78; N, 18.24. Found: C, 62.60; H, 5.75; N, 18.24.

4.2.1.4 2-(4-(1H-Benzo[d]imidazol-2-yl)piperidin-1-yl)-N-benzylacetamide (R6): The compound was prepared according to the general procedure using 2-(piperidin-4-yl)-1H-benzo[d]imidazole 2a (0.1 g, 0.49 mmol), triethyl amine (0.13 g, 1.24 mmol), N-benzyl-2-chloroacetamide (0.108 g, 0.59 mmol) to afford 6 (0.105 g, 61% yield) as brown solid. M.P: 271 - 273°C. ¹H NMR (DMSO-d₆): δH 1.96 – 2.69 (m, 9H), 3.17 (s, 2H), 4.32 (s, 2H), 4.92 (b, 1H), 6.92 – 7.75 (m, 9H), 8.15 (b, 1H). ¹³C NMR (DMSO-d₆): δc 172.5, 142.3, 140.2 (2C), 138.2, 129.5 (2C), 127.5 (2C), 126.9, 122.2 (2C), 116.2 (2C), 60.5, 55.6 (2C), 45.6, 36.2, 30.2 (2C). EI-MS m/z: 349 (M+H) +. Anal Calcd for C₂₁H₂₄N₄O: C, 72.39; H, 6.94; N, 16.08. Found: C, 72.42; H, 6.96; N, 16.09.

4.2.1.5. 2-(4-(1H-Benzo[d]imidazol-2-yl)piperidin-1-yl)-N-(3-acetylphenyl)acetamide (R7): The compound was prepared according to the general procedure using 2-(piperidin-4-yl)-1H-benzo[d]imidazole 2a (0.1 g, 0.49 mmol), triethyl amine (0.13 g, 1.24 mmol), N-(3-acetylphenyl)-2-chloroacetamide (0.12 g, 0.59 mmol) to afford 7 (0.118 g, 65% yield) as pale yellow solid. M.P: 261 - 263°C. ¹H NMR (DMSO-d₆): δH 1.98 – 2.82 (m, 12H), 3.18 (s, 2H),

4.82 (b, 1H), 6.96 – 8.12 (m, 8H), 8.16 (b, 1H). ¹³C NMR (DMSO-d₆): δ_c 198.2, 170.2, 142.5, 140.6, 139.2 (2C), 137.5, 134.2, 124.5, 122.6 (2C), 119.2, 116.5 (2C), 62.5, 55.6 (2C), 34.8, 30.2 (2C), 25.2. EI-MS m/z: 377 (M+H)⁺. Anal Calcd for C₂₂H₂₄N₄O: C, 70.19; H, 6.43; N, 14.88. Found: C, 70.21; H, 6.45; N, 14.87.

4.2.1.6. 2-(4-(1H-Benzo[d]imidazol-2-yl)piperidin-1-yl)-N-(5-nitrothiazol-2-yl)acetamide (R8): The compound was prepared according to the general procedure using 2-(piperidin-4-yl)-1H-benzo[d]imidazole 2a (0.1 g, 0.49 mmol), triethyl amine (0.13 g, 1.24 mmol), 2-chloro-N-(5-nitrothiazol-2-yl)acetamide (0.13 g, 0.59 mmol) to afford 8 (0.122 g, 64% yield) as yellow solid. M.P: 277 - 279°C. ¹H NMR (DMSO-d₆): δ_H 2.01 – 2.83 (m, 9H), 3.15 (s, 2H), 5.08 (b, 1H), 6.92 – 8.86 (m, 5H), 9.25 (b, 1H). ¹³C NMR (DMSO-d₆): δ_c 170.2, 164.5, 148.5, 142.5, 139.6 (2C), 136.8, 122.5 (2C), 116.2 (2C), 64.5, 55.6 (2C), 36.2, 30.2 (2C).. EI-MS m/z: 387 (M+H)⁺. Anal Calcd for C₁₇H₁₈N₆O₃S: C, 52.84; H, 4.70; N, 21.75. Found: C, 52.86; H, 4.71; N, 21.73.

4.2.1.7. 2-(4-(1H-Benzo[d]imidazol-2-yl)piperidin-1-yl)-N-(benzo[d]thiazol-2-yl)acetamide (R9): The compound was prepared according to the general procedure using 2-(piperidin-4-yl)-1H-benzo[d]imidazole 2a (0.1 g, 0.49 mmol), triethyl amine (0.13 g, 1.24 mmol), N-(benzo[d]thiazol-2-yl)-2-chloroacetamide (0.133 g, 0.59 mmol) to afford 9 (0.136 g, 71% yield) as brown solid. M.P: 247 - 249°C. ¹H NMR (DMSO-d₆): δ_H 2.03 – 2.85 (m, 9H), 3.26 (s, 2H), 4.89 (b, 1H), 7.02 – 8.25 (m, 8H), 9.03 (b, 1H). ¹³C NMR (DMSO-d₆): δ_c 175.6, 169.5, 152.1, 142.3, 140.2 (2C), 131.5, 126.5, 125.2, 122.5 (2C), 121.9, 119.2, 116.5 (2C), 64.5, 55.6 (2C), 36.2, 30.2 (2C). EI-MS m/z: 392 (M+H)⁺. Anal Calcd for C₂₁H₂₁N₅OS: C, 64.43; H, 5.41; N, 17.89. Found: C, 64.44; H, 5.44; N, 17.86.

4.2.1.8. 2-(4-(1H-Benzo[d]imidazol-2-yl)piperidin-1-yl)-N-(6-nitrobenzo[d]thiazol-2-yl)acetamide (R10): The compound was prepared according to the general procedure using 2-(piperidin-4-yl)-1H-benzo[d]imidazole 2a (0.1 g, 0.49 mmol), triethyl amine (0.13 g, 1.24 mmol), 2-chloro-N-(6-nitrobenzo[d]thiazol-2-yl)acetamide (0.16 g, 0.59 mmol) to afford 10 (0.152 g, 71% yield) as yellow solid. M.P: 255 - 257°C. ¹H NMR (DMSO-d₆): δH 1.97 – 2.89 (m, 9H), 3.21 (s, 2H), 4.56 (b, 1H), 6.93 – 8.63 (m, 7H), 9.08 (b, 1H). ¹³C NMR (DMSO-d₆): δc 175.6, 168.2, 160.2, 145.6, 140.2, 139.2 (2C), 130.8, 122.5 (2C), 120.8, 120.2, 118.1, 116.3 (2C), 65.6, 54.5 (2C), 36.2, 30.2 (2C). EI-MS m/z: 437 (M+H) ⁺. Anal Calcd for C₂₁H₂₀N₆O₃S: C, 57.79; H, 4.62; N, 19.25. Found: C, 57.76; H, 4.64; N, 19.24.

4.2.1.9. 2-(4-(1H-Benzo[d]imidazol-2-yl)piperidin-1-yl)-N-(furan-2-ylmethyl)acetamide (R11): The compound was prepared according to the general procedure using 2-(piperidin-4-yl)-1H-benzo[d]imidazole 2a (0.1 g, 0.49 mmol), triethyl amine (0.13 g, 1.24 mmol), 2-chloro-N-(furan-2-ylmethyl)acetamide (0.102 g, 0.59 mmol) to afford 11 (0.113 g, 68% yield) as brown solid. M.P: 215 - 217°C. ¹H NMR (DMSO-d₆): δH 1.96 – 2.73 (m, 9H), 3.31 (s, 2H), 4.82 (b, 1H), 5.62 (s, 2H), 6.43 – 7.82 (m, 7H), 8.15 (b, 1H). ¹³C NMR (DMSO-d₆): δc 172.5, 146.8, 143.5, 142.1, 140.5 (2C), 122.5 (2C), 116.2 (2C), 110.5, 109.9, 60.2, 54.1 (2C), 36.5, 35.8, 30.2 (2C). EI-MS m/z: 339 (M+H) ⁺. Anal Calcd for C₁₉H₂₂N₄O₂: C, 67.44; H, 6.55; N, 16.56. Found: C, 67.42; H, 6.56; N, 16.53.

4.2.1.11. 2-(4-(1H-Benzo[d]imidazol-2-yl)piperidin-1-yl)-N-(4-methoxyphenyl)acetamide (R12): The compound was prepared according to the general procedure using 2-(piperidin-4-yl)-1H-benzo[d]imidazole 2a (0.1 g, 0.49 mmol), triethyl amine (0.13 g, 1.24 mmol), 2-chloro-N-(4-methoxyphenyl)acetamide (0.117 g, 0.59 mmol) to afford 12 (0.125 g, 70% yield) as pale yellow solid. M.P: 238 - 240°C. ¹H NMR (DMSO-d₆): δH 1.97 – 2.81 (m, 9H), 2.95 (s, 2H),

3.75 (s, 3H), 4.96 (b, 1H), 7.03 – 7.68 (m, 8H), 8.03 (b, 1H). ¹³C NMR (DMSO-d₆): δ_c 169.5, 160.2, 140.5, 139.5 (2C), 131.6, 122.5 (2C), 121.8 (2C), 116.5 (2C), 114.9 (2C), 64.5, 55.8, 54.5 (2C), 36.2, 30.2 (2C). EI-MS m/z: 365 (M+H)⁺. Anal Calcd for C₂₁H₂₄N₄O₂: C, 69.21; H, 6.64; N, 15.37. Found: C, 69.20; H, 6.63; N, 15.35.

General procedure for the synthesis of substituted 2-(4-(5-methyl-1H-benzo[d]imidazol-2-yl)piperidin-1-yl)acetamide (R13-R22): The synthesis followed the literature procedure. To a well stirred solution of the corresponding 5-methyl-2-(piperidin-4-yl)-1H-benzo[d]imidazole (2b) (1 equiv) in anhydrous N,N Dimethyl formamide (1 ml) was added triethylamine (2.5 equiv). The reaction mixture was stirred for 15 mts followed by the addition of corresponding substituted acetyl chlorides (1.2 equiv) and continued the stirring for 6 h(monitored by TLC and LCMS for completion). Then ice was added to the reaction mixture and extracted repeatedly with ethyl acetate. The combined organic layer was then dried over anhydrous sodium sulphate and concentrated under reduced pressure. The residue obtained was further purified by column chromatography using hexane : ethyl acetate the desired product in good yield and purity as described below.

4.2.2.1. 2-(4-(5-Methyl-1H-benzo[d]imidazol-2-yl)piperidin-1-yl)-N-phenylacetamide (R13):

The compound was prepared according to the general procedure using 5-methyl-2-(piperidin-4-yl)-1H-benzo[d]imidazole 2b (0.1 g, 0.46 mmol), triethyl amine (0.12 g, 1.16 mmol), 2-chloro-N-phenylacetamide (0.093 g, 0.55 mmol) to afford 13 (0.095 g, 59% yield) as brown solid. M.P: 265 - 267°C. ¹H NMR (DMSO-d₆): δ_H 1.95– 2.72 (m, 12H), 2.98 (s, 2H), 5.02 (b, 1H), 6.98 – 7.82 (m, 8H), 8.13 (b, 1H). ¹³C NMR (DMSO-d₆): δ_c 169.2, 140.2, 139.5, 139.1, 136.2, 131.5, 130.2 (2C), 129.5, 126.2, 120.5 (2C), 116.2 (2C), 65.6, 54.5 (2C), 36.2, 30.2 (2C), 22.5. EI-MS

m/z: 349(M+H) +. Anal Calcd for C₂₁H₂₄N₄O: C, 72.39; H, 6.94; N, 16.08. Found: C, 72.37; H, 6.92; N, 16.09.

4.2.2.2. N-(2-Chloro-5-(trifluoromethyl)phenyl)-2-(4-(5-methyl-1H-benzo[d]imidazol-2-yl)piperidin-1-yl)acetamide (R14): The compound was prepared according to the general procedure using 5-methyl-2-(piperidin-4-yl)-1H-benzo[d]imidazole 2b (0.1 g, 0.46 mmol), triethyl amine (0.12 g, 1.16 mmol), 2-chloro-N-(2-chloro-5-(trifluoromethyl)phenyl)acetamide (0.15 g, 0.55 mmol) to afford 14 (0.146 g, 68% yield) as white solid. M.P: 242 - 244°C. ¹H NMR (DMSO-d₆): δH 1.95 – 2.76 (m, 12H), 3.15 (s, 2H), 5.06 (b, 1H), 6.96 – 8.12 (m, 6H), 8.21 (b, 1H). ¹³C NMR (DMSO-d₆): δc 168.5, 140.2, 139.5, 138.6, 136.2, 133.5, 130.2 (2C), 126.5, 124.9, 123.8, 121.6, 119.5, 117.8, 117.2, 64.5, 55.6 (2C), 36.2, 30.2 (2C), 22.5.. EI-MS m/z: 450 (M) +. Anal Calcd for C₂₂H₂₂ClF₃N₄O: C, 58.60; H, 4.92; N, 12.43. Found: C, 58.63; H, 4.95; N, 12.42.

4.2.2.3. N-((6-Chloropyridin-3-yl)methyl)-2-(4-(5-methyl-1H-benzo[d]imidazol-2-yl)piperidin-1-yl)acetamide (R15): The compound was prepared according to the general procedure using 5-methyl-2-(piperidin-4-yl)-1H-benzo[d]imidazole 2b (0.1 g, 0.46 mmol), triethyl amine (0.12 g, 1.16 mmol), 2-chloro-N-((6-chloropyridin-3-yl)methyl)acetamide (0.12 g, 0.55 mmol) to afford 15 (0.128 g, 68% yield) as pale yellow solid. M.P: 262 - 264°C. ¹H NMR (DMSO-d₆): δH 2.02 – 2.83 (m, 12H), 3.42 (s, 2H), 4.35 (s, 2H), 5.11 (b, 1H), 7.05 – 8.16 (m, 6H), 8.19 (b, 1H). ¹³C NMR (DMSO-d₆): δc 172.3, 149.8, 148.5, 140.2, 139.5, 139.3, 136.5, 134.5, 132.8, 124.6, 123.9, 116.9, 116.4, 60.1, 54.5 (2C), 42.5, 36.8, 30.2 (2C), 22.5.. EI-MS m/z: 397 (M) +. Anal Calcd for C₂₁H₂₄ClN₅O: C, 63.39; H, 6.08; N, 17.60. Found C, 63.42; H, 6.11; N, 17.61.

4.2.2.4. N-Benzyl-2-(4-(5-methyl-1H-benzo[d]imidazol-2-yl)piperidin-1-yl)acetamide (R16):

The compound was prepared according to the general procedure using 5-methyl-2-(piperidin-4-yl)-1H-benzo[d]imidazole 2b (0.1 g, 0.46 mmol), triethyl amine (0.12 g, 1.16 mmol), N-benzyl-2-chloroacetamide (0.1 g, 0.55 mmol) to afford 6 (0.108 g, 64% yield) as light brown solid. M.P: 225 - 227°C. ¹H NMR (DMSO-d₆): δH 1.95 – 2.85 (m, 12H), 3.55 (s, 2H), 4.43 (s, 2H), 4.99 (b, 1H), 6.95 – 7.62 (m, 8H), 8.12 (b, 1H). ¹³C NMR (DMSO-d₆): δc 172.5, 140.2, 139.5, 138.1, 136.2, 133.5, 129.6 (2c), 127.2 (2c), 126.9, 124.9, 116.8, 116.2, 60.2, 54.5 (2c), 44.5, 36.2, 30.2 (2c), 22.5.. EI-MS m/z: 363 (M+H) +. Anal Calcd for C₂₂H₂₆N₄O: C, 72.90; H, 7.23; N, 15.46. Found: C, 72.92; H, 7.21; N, 15.45.

4.2.2.5. N-(3-Acetylphenyl)-2-(4-(5-methyl-1H-benzo[d]imidazol-2-yl)piperidin-1-yl)acetamide (R17):

The compound was prepared according to the general procedure using 5-methyl-2-(piperidin-4-yl)-1H-benzo[d]imidazole 2b (0.1 g, 0.46 mmol), triethyl amine (0.12 g, 1.16 mmol), N-(3-acetylphenyl)-2-chloroacetamide (0.097 g, 0.55 mmol) to afford 17 (0.135 g, 75% yield) as pale yellow solid. M.P: 257 - 259°C. ¹H NMR (DMSO-d₆): δH 1.98 – 2.92 (m, 15H), 3.11 (s, 2H), 4.85 (b, 1H), 7.03 – 8.27 (m, 8H). ¹³C NMR (DMSO-d₆): δc 198.5, 170.2, 140.5, 140.3, 139.6, 137.5, 136.2, 134.5, 134.1, 126.2, 125.8, 124.9, 119.2, 116.8, 116.5, 64.5, 54.5 (2C), 36.2, 30.2 (2C), 26.5, 22.5. EI-MS m/z: 391 (M+H) +. Anal Calcd for C₂₃H₂₆N₄O₂: C, 70.75; H, 6.71; N, 14.35. Found: C, 70.77; H, 6.70; N, 14.35.

4.2.2.6. 2-(4-(5-Methyl-1H-benzo[d]imidazol-2-yl)piperidin-1-yl)-N-(5-nitrothiazol-2-yl)acetamide (R18):

The compound was prepared according to the general procedure using 5-methyl-2-(piperidin-4-yl)-1H-benzo[d]imidazole 2b (0.1 g, 0.46 mmol), triethyl amine (0.12 g, 1.16 mmol), 2-chloro-N-(5-nitrothiazol-2-yl)acetamide (0.12 g, 0.55 mmol) to afford 18 (0.128 g, 68% yield) as yellow solid. M.P: 282 - 284°C. ¹H NMR (DMSO-d₆): δH 2.03 – 2.88 (m,

12H), 3.35 (s, 2H), 5.03 (b, 1H), 7.09 – 9.02 (m, 4H), 9.21(b, 1H). ¹³C NMR (DMSO-d₆): δ_c 169.5, 164.1, 148.5, 140.5, 139.5, 136.2, 135.8, 133.5, 126.2, 116.8, 116.5, 64.5, 55.6 (2C), 36.2, 30.2 (2C), 22.5. EI-MS m/z: 401 (M+H)⁺. Anal Calcd for C₁₈H₂₀N₆O₃S: C, 53.99; H, 5.03; N, 20.99. Found: C, 53.96; H, 5.05; N, 20.98.

4.2.2.7. N-(Benzo[d]thiazol-2-yl)-2-(4-(5-methyl-1H-benzo[d]imidazol-2-yl)piperidin-1-yl)acetamide (R19): The compound was prepared according to the general procedure using 5-methyl-2-(piperidin-4-yl)-1H-benzo[d]imidazole 2b (0.1 g, 0.46 mmol), triethyl amine (0.12 g, 1.16 mmol), N-(benzo[d]thiazol-2-yl)-2-chloroacetamide (0.124 g, 0.55 mmol) to afford 19 (0.142 g, 76% yield) as brown solid. M.P: 233 - 235°C. ¹H NMR (DMSO-d₆): δ_H 2.01 – 2.83 (m, 12H), 3.31 (s, 2H), 4.95 (b, 1H), 7.06 – 8.25 (m, 7H), 9.08 (b, 1H). ¹³C NMR (DMSO-d₆): δ_c 175.6, 169.5, 154.5, 140.5, 139.6, 136.2, 132.8, 131.2, 126.2, 125.8, 124.9, 122.5, 119.2, 116.8, 116.5, 65.6, 54.5 (2C), 36.2, 30.2 (2C), 22.5 EI-MS m/z: 406 (M+H)⁺. Anal Calcd for C₂₂H₂₃N₅OS: C, 65.16; H, 5.72; N, 17.27. Found: C, 65.14; H, 5.75; N, 17.28.

4.2.2.8. 2-(4-(5-Methyl-1H-benzo[d]imidazol-2-yl)piperidin-1-yl)-N-(6-nitrobenzo[d]thiazol-2-yl)acetamide (R20): The compound was prepared according to the general procedure using 5-methyl-2-(piperidin-4-yl)-1H-benzo[d]imidazole 2b (0.1 g, 0.46 mmol), triethyl amine (0.12 g, 1.16 mmol), 2-chloro-N-(6-nitrobenzo[d]thiazol-2-yl)acetamide (0.149 g, 0.55mmol) to afford 20 (0.156 g, 75% yield) as yellow solid. M.P: 269 - 271°C. ¹H NMR (DMSO-d₆): δ_H 1.96 – 2.79 (m, 12H), 3.36 (s, 2H), 4.81 (b, 1H), 6.99 – 8.81 (m, 6H), 9.23 (b, 1H). ¹³C NMR (DMSO-d₆): δ_c 175.6, 169.5, 160.2, 145.6, 140.2, 137.2, 136.2, 133.5, 132.1, 126.2, 122.4, 119.6, 116.8, 116.8, 116.5, 65.6, 54.2 (2C), 36.2, 30.2 (2C), 22.5. EI-MS m/z: 451 (M+H)⁺. Anal Calcd for C₂₂H₂₂N₆O₃S: C, 58.65; H, 4.92; N, 18.65. Found: C, 58.66; H, 4.95; N, 18.66.

4.2.2.9. N-(Furan-2-ylmethyl)-2-(4-(5-methyl-1H-benzo[d]imidazol-2-yl)piperidin-1-yl)acetamide (R21): The compound was prepared according to the general procedure using 5-methyl-2-(piperidin-4-yl)-1H-benzo[d]imidazole 2b (0.1 g, 0.46 mmol), triethyl amine (0.12 g, 1.16 mmol), 2-chloro-N-(furan-2-ylmethyl)acetamide (0.095 g, 0.55 mmol) to afford 21 (0.112 g, 67% yield) as pale brown solid. M.P: 220 - 222°C. ¹H NMR (DMSO-d₆): δH 2.03 – 2.91 (m, 12H), 3.32 (s, 2H), 4.98 (s, 2H), 5.12 (b, 1H), 6.45 – 7.73 (m, 6H), 8.09 (b, 1H). ¹³C NMR (DMSO-d₆): δc 172.1, 146.2, 143.1, 140.5, 139.5, 136.2, 133.5, 126.5, 116.8, 116.5, 110.5, 109.9, 60.2, 55.6 (2C), 38.2, 36.5, 30.2 (2C), 22.5. EI-MS m/z: 353 (M+H) +. Anal Calcd for C₂₀H₂₄N₄O₂: C, 68.16; H, 6.86; N, 15.90. Found: C, 68.17; H, 6.84; N, 15.93.

4.2.2.10. N-(4-Methoxyphenyl)-2-(4-(5-methyl-1H-benzo[d]imidazol-2-yl)piperidin-1-yl)acetamide (R22): The compound was prepared according to the general procedure using 5-methyl-2-(piperidin-4-yl)-1H-benzo[d]imidazole 2b (0.1 g, 0.46 mmol), triethyl amine (0.12 g, 1.16 mmol), 2-chloro-N-(4-methoxyphenyl)acetamide (0.109 g, 0.55 mmol) to afford 22 (0.118 g, 68% yield) as pale yellow solid. M.P: 288 - 290°C. ¹H NMR (DMSO-d₆): δH 1.96– 2.69 (m, 12H), 3.12 (s, 2H), 3.76 (s, 3H), 5.03 (b, 1H), 6.73 – 7.69 (m, 7H), 7.88 (b, 1H). ¹³C NMR (DMSO-d₆): δc 169.6, 160.2, 140.8, 139.5, 136.6, 133.5, 129.9*, 126.5, 123.1 (2C), 116.8, 116.5, 115.2 (2C), 65.68, 56.5, 54.5 (2C), 36.2, 30.2 (2C), 22.5. EI-MS m/z: 379 (M+H) +. Anal Calcd for C₂₂H₂₆N₄O₂: C, 69.82; H, 6.92; N, 14.80. Found: C, 69.84; H, 6.91; N, 14.82.

General procedure for the synthesis of substituted 2-(4-(5-fluoro-1H-benzo[d]imidazol-2-yl)piperidin-1-yl)acetamide (R23-R32): The synthesis followed the literature procedure. To a well stirred solution of the corresponding 5-fluoro-2-(piperidin-4-yl)-1H-benzo[d]imidazole (2c) (1 equiv) in anhydrous N,N Dimethyl formamide (1 ml) was added triethylamine (2.5 equiv). The reaction mixture was stirred for 15 mts followed by the addition of corresponding

substituted acetyl chlorides (1.2 equiv) and continued the stirring for 6 h (monitored by TLC and LCMS for completion). Then ice was added to the reaction mixture and extracted repeatedly with ethyl acetate. The combined organic layer was then dried over anhydrous sodium sulphate and concentrated under reduced pressure. The residue obtained was further purified by column chromatography using hexane : ethyl acetate to give the desired product in good yield and purity as described below.

4.2.3.1. 2-(4-(5-Fluoro-1H-benzo[d]imidazol-2-yl)piperidin-1-yl)-N-phenylacetamide (R23):

The compound was prepared according to the general procedure using 5-fluoro-2-(piperidin-4-yl)-1H-benzo[d]imidazole 2c (0.1 g, 0.456 mmol), triethyl amine (0.12 g, 1.14 mmol), 2-chloro-N-phenylacetamide (0.093 g, 0.55 mmol) to afford 23 (0.101 g, 64% yield) as pale yellow solid. M.P: 241 - 243°C. ¹H NMR (DMSO-d₆): δH 1.96– 2.81 (m, 9H), 2.97 (s, 2H), 4.82 (b, 1H), 7.05 – 7.82 (m, 8H), 8.03 (b, 1H). ¹³C NMR (DMSO-d₆): δc 170.2, 155.2, 140.8, 139.8, 138.6, 135.6, 130.2 (2C), 129.6, 120.8 (2C), 115.8, 110.2, 103.2, 64.5, 54.5 (2C), 36.2, 30.2 (2C). EI-MS m/z: 354(M+H)⁺. Anal Calcd for C₂₀H₂₁N₄O: C, 68.16; H, 6.01; N, 15.90. Found: C, 68.13; H, 6.04; N, 15.88.

4.2.3.2 N-(2-Chloro-5-(trifluoromethyl)phenyl)-2-(4-(5-fluoro-1H-benzo[d]imidazol-2-yl)piperidin-1-yl)acetamide (R24):

The compound was prepared according to the general procedure using 5-methyl-2-(piperidin-4-yl)-1H-benzo[d]imidazole 2c (0.1 g, 0.46 mmol), triethyl amine (0.12 g, 1.16 mmol), 2-chloro-N-(2-chloro-5-(trifluoromethyl)phenyl)acetamide (0.15 g, 0.55 mmol) to afford 24 (0.128 g, 62% yield) as white solid. M.P: 238 - 240°C. ¹H NMR (DMSO-d₆): δH 2.01 – 2.88 (m, 9H), 3.01 (s, 2H), 4.81 (b, 1H), 7.06 – 8.13 (m, 6H), 8.18 (b, 1H). ¹³C NMR (DMSO-d₆): δc 170.2, 155.8, 140.8, 140.2, 138.2, 135.6, 130.2 (2c), 126.2,

124.9, 123.1, 119.1, 116.5, 110.2, 103.5, 64.5, 54.5 (2c), 36.2, 30.2 (2c). EI-MS m/z: 454 (M) +. Anal Calcd for C₂₁H₁₉ClF₄N₄O: C, 55.45; H, 4.21; N, 12.32. Found: C, 55.43; H, 4.19; N, 12.34.

4.2.3.3 N-((6-Chloropyridin-3-yl)methyl)-2-(4-(5-fluoro-1H-benzo[d]imidazol-2-yl)piperidin-1-yl)acetamide (R25): The compound was prepared according to the general procedure using 5-fluoro-2-(piperidin-4-yl)-1H-benzo[d]imidazole 2c (0.1 g, 0.46 mmol), triethyl amine (0.12 g, 1.16 mmol), 2-chloro-N-((6-chloropyridin-3-yl)methyl)acetamide (0.12 g, 0.55 mmol) to afford 25 (0.145 g, 78% yield) as yellow solid. M.P: 281 - 283°C. ¹H NMR (DMSO-d₆): δH 1.96 – 2.76 (m, 9H), 3.34 (s, 2H), 4.32 (s, 2H), 5.03 (b, 1H), 6.95 – 8.95 (m, 7H). ¹³C NMR (DMSO-d₆): δc 172.5, 155.6, 149.8, 149.3, 140.5, 139.8, 137.5, 135.6, 132.5, 124.6, 117.2, 110.2, 103.5, 60.2, 54.5 (2c), 44.5, 36.2, 30.2 (2c). EI-MS m/z: 401 (M) +. Anal Calcd for C₂₀H₂₁ClFN₅O: C, 59.77; H, 5.27; N, 17.43. Found C, 59.79; H, 5.25; N, 17.40.

4.2.3.4. N-Benzyl-2-(4-(5-fluoro-1H-benzo[d]imidazol-2-yl)piperidin-1-yl)acetamide (R26): The compound was prepared according to the general procedure using 5-fluoro-2-(piperidin-4-yl)-1H-benzo[d]imidazole 2c (0.1 g, 0.46 mmol), triethyl amine (0.12 g, 1.16 mmol), N-benzyl-2-chloroacetamide (0.1 g, 0.55 mmol) to afford 26 (0.098 g, 58% yield) as brown solid. M.P: 218 - 220°C. ¹H NMR (DMSO-d₆): δH 1.98 – 2.79 (m, 9H), 3.35 (s, 2H), 4.56 (s, 2H), 4.98 (b, 1H), 7.02 – 7.82 (m, 7H), 8.12 (b, 1H). ¹³C NMR (DMSO-d₆): δc 172.1, 155.8, 140.5, 139.5, 138.5, 135.6, 129.5 (2C), 127.5 (2C), 126.8, 117.2, 110.2, 103.5, 60.2, 55.6 (2C), 44.5, 36.2, 30.2 (2C). EI-MS m/z: 367 (M+H) +. Anal Calcd for C₂₁H₂₃FN₄O: C, 68.83; H, 6.33; N, 15.29. Found: C, 68.80; H, 6.31; N, 15.31.

4.2.3.5. N-(3-Acetylphenyl)-2-(4-(5-fluoro-1H-benzo[d]imidazol-2-yl)piperidin-1-yl)acetamide (R27): The compound was prepared according to the general procedure using 5-

fluoro-2-(piperidin-4-yl)-1H-benzo[d]imidazole 2c (0.1 g, 0.46 mmol), triethyl amine (0.12 g, 1.16 mmol), N-(3-acetylphenyl)-2-chloroacetamide (0.097 g, 0.55 mmol) to afford 27 (0.112 g, 62% yield) as brown solid. M.P: 208 - 210°C. ¹H NMR (DMSO-d₆): δH 1.97 – 2.82 (m, 12H), 2.98 (s, 2H), 5.033 (b, 1H), 7.02 – 8.31 (m, 8H). ¹³C NMR (DMSO-d₆): δc 198.2, 169.5, 155.8, 140.5, 140.1, 139.8, 137.8, 135.6, 134.2, 125.8, 124.3, 119.5, 116.9, 110.2, 103.5, 64.5, 54.5 (2C), 36.2, 30.2 (2C), 25.8. EI-MS m/z: 395 (M+H) +. Anal Calcd for C₂₂H₂₃FN₄O₂: C, 66.99; H, 5.88; N, 14.20. Found: C, 66.96; H, 5.90; N, 14.21.

4.2.3.6. 2-(4-(5-Fluoro-1H-benzo[d]imidazol-2-yl)piperidin-1-yl)-N-(5-nitrothiazol-2-yl)acetamide (R28): The compound was prepared according to the general procedure using 5-fluoro-2-(piperidin-4-yl)-1H-benzo[d]imidazole 2c (0.1 g, 0.46 mmol), triethyl amine (0.12 g, 1.16 mmol), 2-chloro-N-(5-nitrothiazol-2-yl)acetamide (0.12 g, 0.55 mmol) to afford 28 (0.133 g, 72% yield) as yellow solid. M.P: 252 - 254°C. ¹H NMR (DMSO-d₆): δH 2.04 – 2.87 (m, 9H), 3.18 (s, 2H), 4.72 (b, 1H), 7.05 – 9.05 (m, 4H), 9.19 (b, 1H). ¹³C NMR (DMSO-d₆): δc 169.5, 163.5, 157.8, 148.2, 140.8, 140.1, 136.2, 135.8, 117.2, 110.2, 103.5, 64.5, 54.5 (2C), 36.2, 30.2 (2C). EI-MS m/z: 405 (M+H) +. Anal Calcd for C₁₇H₁₇FN₆O₃S: C, 50.49; H, 4.24; N, 20.78. Found: C, 50.46; H, 4.25; N, 20.77.

4.2.3.7. N-(Benzo[d]thiazol-2-yl)-2-(4-(5-fluoro-1H-benzo[d]imidazol-2-yl)piperidin-1-yl)acetamide (R29): The compound was prepared according to the general procedure using 5-fluoro-2-(piperidin-4-yl)-1H-benzo[d]imidazole 2c (0.1 g, 0.46 mmol), triethyl amine (0.12 g, 1.16 mmol), N-(benzo[d]thiazol-2-yl)-2-chloroacetamide (0.124 g, 0.55 mmol) to afford 29 (0.132 g, 70% yield) as pale yellow solid. M.P: 265 - 267°C. ¹H NMR (DMSO-d₆): δH 1.96 – 2.73 (m, 9H), 3.42 (s, 2H), 5.08 (b, 1H), 7.05 – 8.32 (m, 7H), 8.95 (b, 1H). ¹³C NMR (DMSO-d₆): δc 175.6, 169.5, 155.8, 154.2, 140.8, 139.9, 135.6, 133.7, 124.8, 123.9, 120.9, 119.2, 117.5,

110.2, 103.5, 65.6, 54.8 (2C), 36.2, 30.2 (2C). EI-MS m/z : 410 (M+H) $+$. Anal Calcd for $C_{21}H_{20}FN_5OS$: C, 61.60; H, 4.92; N, 17.10. Found: C, 61.62; H, 4.90; N, 17.11.

4.2.3.8. 2-(4-(5-Fluoro-1H-benzo[d]imidazol-2-yl)piperidin-1-yl)-N-(6-nitrobenzo[d]thiazol-2-yl)acetamide (R30): The compound was prepared according to the general procedure using 5-fluoro-2-(piperidin-4-yl)-1H-benzo[d]imidazole 2c (0.1 g, 0.46 mmol), triethyl amine (0.12 g, 1.16 mmol), 2-chloro-N-(6-nitrobenzo[d]thiazol-2-yl)acetamide (0.149 g, 0.55 mmol) to afford 30 (0.162 g, 78% yield) as yellow solid. M.P: 277 - 279°C. 1H NMR (DMSO- d_6): δ H 1.97 – 2.78 (m, 9H), 3.38 (s, 2H), 4.96 (b, 1H), 7.05 – 9.03 (m, 6H), 9.17 (b, 1H). ^{13}C NMR (DMSO- d_6): δ c 175.6, 169.2, 160.2, 155.6, 145.6, 140.2, 139.5, 135.6, 130.9, 120.8, 119.8, 118.3, 117.5, 110.3, 103.5, 64.5, 54.5 (2C), 36.2, 30.2 (2C). EI-MS m/z : 456 (M+H) $+$. Anal Calcd for $C_{21}H_{19}FN_6O_3S$: C, 55.50; H, 4.21; N, 18.40. Found: C, 55.52; H, 4.20; N, 18.43.

4.2.3.9. 2-(4-(5-Fluoro-1H-benzo[d]imidazol-2-yl)piperidin-1-yl)-N-(furan-2-ylmethyl)acetamide (R31): The compound was prepared according to the general procedure using 5-fluoro-2-(piperidin-4-yl)-1H-benzo[d]imidazole 2c (0.1 g, 0.46 mmol), triethyl amine (0.12 g, 1.16 mmol), 2-chloro-N-(furan-2-ylmethyl)acetamide (0.095 g, 0.55 mmol) to afford 31 (0.121 g, 75% yield) as brown solid. M.P: 237 - 239°C. 1H NMR (DMSO- d_6): δ H 1.97 – 2.76 (m, 9H), 3.35 (s, 2H), 4.96 (b, 1H), 5.26 (s, 2H), 6.48 – 7.81 (m, 6H), 7.96 (b, 1H). ^{13}C NMR (DMSO- d_6): δ c 171.9, 155.8, 146.2, 143.1, 140.2, 139.8, 135.6, 117.9, 110.6, 109.8, 109.2, 103.5, 60.2, 54.5 (2C), 38.3, 36.2, 30.2 (2C). EI-MS m/z : 357 (M+H) $+$. Anal Calcd for $C_{19}H_{21}FN_4O_2$: C, 64.03; H, 5.94; N, 15.72. Found: C, 64.05; H, 5.96; N, 15.70..

4.2.3.10. 2-(4-(5-Fluoro-1H-benzo[d]imidazol-2-yl)piperidin-1-yl)-N-(4-methoxyphenyl)acetamide (R32): The compound was prepared according to the general procedure using 5-

fluoro-2-(piperidin-4-yl)-1H-benzo[d]imidazole 2c (0.1 g, 0.46 mmol), triethyl amine (0.12 g, 1.16 mmol), 2-chloro-N-(4-methoxyphenyl)acetamide (0.109 g, 0.55 mmol) to afford 32 (0.126 g, 72% yield) as pale yellow solid. M.P: 265 - 267°C. ¹H NMR (DMSO-d₆): δ_H 2.01– 2.86 (m, 9H), 2.95 (s, 2H), 3.73 (s, 3H), 5.06 (b, 1H), 7.05 – 7.72 (m, 7H), 8.03 (b, 1H). ¹³C NMR (DMSO-d₆): δ_c 169.5, 160.2, 155.8, 140.2, 139.5, 136.2, 129.5, 125.5 (2C), 117.2, 115.6 (2C), 110.2, 103.5, 65.6, 56.2, 54.5 (2C), 36.2, 30.2 (2C).. EI-MS m/z: 383 (M+H) +. Anal Calcd for C₂₁H₂₃FN₄O₂: C, 65.95; H, 6.06; N, 14.65. Found: C, 65.93; H, 6.04; N, 14.64.

General procedure for the synthesis of substituted 2-(4-(5-chloro-1H-benzo[d]imidazol-2-yl)piperidin-1-yl)acetamide (R33-R42): The synthesis followed the literature procedure. To a well stirred solution of the corresponding 5-chloro-2-(piperidin-4-yl)-1H-benzo[d]imidazole (2d) (1 equiv) in anhydrous N,N Dimethyl formamide (1 ml) was added triethylamine (2.5 equiv). The reaction mixture was stirred for 15 mts followed by the addition of corresponding substituted acetyl chlorides (1.2 equiv) and continued the stirring fir 6 h(monitored by TLC and LCMS for completion). Then ice was added to the reaction mixture and extracted repeatedly with ethyl acetate. The combined organic layer was then dried over anhydrous sodium sulphate and concentrated under reduced pressure. The residue obtained was further purified by column chromatography using hexane : ethyl acetate the desired product in good yield and purity as described below.

4.2.4.1. 2-(4-(5-Chloro-1H-benzo[d]imidazol-2-yl)piperidin-1-yl)-N-phenylacetamide (R33):

The compound was prepared according to the general procedure using 5-chloro-2-(piperidin-4-yl)-1H-benzo[d]imidazole (2d) (0.1 g, 0.425 mmol), triethyl amine (0.107 g, 1.06 mmol), 2-chloro-N-phenylacetamide (0.086 g, 0.51 mmol) to afford 33 (0.096 g, 62% yield) as pale yellow solid. M.P: 202 - 204°C. ¹H NMR (DMSO-d₆): δ_H 1.96– 2.85 (m, 9H), 2.96 (s, 2H), 4.96

(b, 1H), 7.09 – 8.43 (m, 9H). ¹³C NMR (DMSO-d₆): δ_c 169.6, 140.8, 139.5, 138.6, 136.2, 130.2, 129.5 (2C), 128.8, 125.6, 122.6 (2C), 116.8, 64.5, 54.5 (2C), 36.2, 30.2 (2C). EI-MS m/z: 369(M+H) +. Anal Calcd for C₂₀H₂₁ClN₄O: C, 65.12; H, 5.74; N, 15.19. Found: C, 65.14; H, 5.71; N, 15.18.

4.2.4.2. 2-(4-(5-Chloro-1H-benzo[d]imidazol-2-yl)piperidin-1-yl)-N-(2-chloro-5-(trifluoromethyl)phenyl)acetamide (R34): The compound was prepared according to the general procedure using 5-chloro-2-(piperidin-4-yl)-1H-benzo[d]imidazole (2d) (0.1 g, 0.425 mmol), triethyl amine (0.107 g, 1.06 mmol), 2-chloro-N-(2-chloro-5-(trifluoromethyl)phenyl)acetamide (0.14 g, 0.51 mmol) to afford 34 (0.132 g, 66% yield) as white solid. M.P: 212 - 214°C. ¹H NMR (DMSO-d₆): δ_H 1.96 – 2.77 (m, 9H), 2.95 (s, 2H), 5.08(b, 1H), 7.11 – 8.53(m, 7H). ¹³C NMR (DMSO-d₆): δ_c 169.5, 140.8, 139.8, 137.5, 136.8, 130.8 (2C), 129.5, 125.6, 125.1, 124.9, 123.2, 119.2, 117.8, 116.2, 64.5, 54.52 (2C), 36.2, 30.2 (2C). EI-MS m/z: 471 (M) +. Anal Calcd for C₂₁H₁₉Cl₂F₃N₄O: C, 53.52; H, 4.06; N, 11.89. Found: C, 53.54; H, 4.04; N, 11.86.

4.2.4.3 2-(4-(5-Chloro-1H-benzo[d]imidazol-2-yl)piperidin-1-yl)-N-((6-chloropyridin-3-yl)methyl)acetamide (R35): The compound was prepared according to the general procedure using 5-chloro-2-(piperidin-4-yl)-1H-benzo[d]imidazole (2d) (0.1 g, 0.425 mmol), triethyl amine (0.107 g, 1.06 mmol), 2-chloro-N-((6-chloropyridin-3-yl)methyl)acetamide (0.11 g, 0.51 mmol) to afford 35 (0.12 g, 68% yield) as brown solid. M.P: 245 - 2247°C. ¹H NMR (DMSO-d₆): δ_H 1.94 – 2.77 (m, 9H), 3.42 (s, 2H), 4.62 (s, 2H), 5.01 (b, 1H), 6.99 – 8.52 (m, 7H). ¹³C NMR (DMSO-d₆): δ_c 172.5, 149.8, 149.1, 140.8, 139.8, 138.6, 136.2, 130.2, 128.5, 125.6, 124.1, 117.2, 116.8, 60.2, 54.5 (2C), 44.5, 36.2, 30.2 (2C) . EI-MS m/z: 418 (M) +. Anal Calcd for C₂₀H₂₁Cl₂N₅O: C, 57.42; H, 5.06; N, 16.74. Found C, 57.43; H, 5.08; N, 16.71.

4.2.4.4. N-Benzyl-2-(4-(5-chloro-1H-benzo[d]imidazol-2-yl)piperidin-1-yl)acetamide (R36):

The compound was prepared according to the general procedure using 5-chloro-2-(piperidin-4-yl)-1H-benzo[d]imidazole (2d) (0.1 g, 0.425 mmol), triethyl amine (0.107 g, 1.06 mmol), N-benzyl-2-chloroacetamide (0.093 g, 0.51 mmol) to afford 36 (0.108 g, 66% yield) as light brown solid. M.P: 236 - 238°C. ¹H NMR (DMSO-d₆): δ_H 2.01 – 2.82 (m, 9H), 3.41 (s, 2H), 4.41 (s, 2H), 5.04 (b, 1H), 7.05 – 8.81 (m, 9H), 8.12 (b, 1H). ¹³C NMR (DMSO-d₆): δ_C 172.1, 140.5, 139.8, 136.5, 135.2, 130.1, 129.6 (2C), 128.5 (2C), 127.9, 125.6, 117.8, 116.9, 60.2, 54.5 (2C), 44.5, 36.2, 30.2 (2C). EI-MS m/z: 383 (M+H) ⁺. Anal Calcd for C₂₁H₂₃ClN₄O: C, 65.87; H, 6.05; N, 14.63. Found: C, 65.89; H, 6.03; N, 14.60.

4.2.4.5. N-(3-Acetylphenyl)-2-(4-(5-chloro-1H-benzo[d]imidazol-2-yl)piperidin-1-yl)acetamide (R37):

The compound was prepared according to the general procedure using 5-chloro-2-(piperidin-4-yl)-1H-benzo[d]imidazole (2d) (0.1 g, 0.425 mmol), triethyl amine (0.107 g, 1.06 mmol), N-(3-acetylphenyl)-2-chloroacetamide (0.107 g, 0.51 mmol) to afford 37 (0.131 g, 75% yield) as brown solid. M.P: 233 - 235°C. ¹H NMR (DMSO-d₆): δ_H 1.97 – 2.71 (m, 12H), 2.95 (s, 2H), 5.12 (b, 1H), 7.03 – 8.71 (m, 8H). ¹³C NMR (DMSO-d₆): δ_C 198.2, 170.2, 140.8, 139.5, 139.1, 138.5, 138.3, 134.5, 130.2, 125.8, 125.1, 124.6, 119.2, 117.2, 116.2, 64.5, 54.5 (2C), 36.2, 30.2 (2C), 26.2. EI-MS m/z: 411 (M+H) ⁺. Anal Calcd for C₂₂H₂₃ClN₄O₂: C, 64.31; H, 5.64; N, 13.64. Found: C, 64.34; H, 5.62; N, 13.63.

4.2.4.6. 2-(4-(5-Chloro-1H-benzo[d]imidazol-2-yl)piperidin-1-yl)-N-(5-nitrothiazol-2-yl)acetamide (R38):

The compound was prepared according to the general procedure using 5-chloro-2-(piperidin-4-yl)-1H-benzo[d]imidazole (2d) (0.1 g, 0.425 mmol), triethyl amine (0.107 g, 1.06 mmol), 2-chloro-N-(5-nitrothiazol-2-yl)acetamide (0.11 g, 0.51 mmol) to afford 38 (0.126 g, 78% yield) as yellow solid. M.P: 274 - 276°C. ¹H NMR (DMSO-d₆): δ_H 1.96 – 2.75

(m, 9H), 3.41 (s, 2H), 4.95 (b, 1H), 7.12 – 8.91 (m, 4H), 9.16 (b, 1H). ¹³C NMR (DMSO-d₆): δ_c 169.5, 162.3, 145.6, 140.8, 139.5, 136.8, 134.9, 130.2, 125.6, 116.5, 115.5, 64.5, 54.5 (2C), 36.2, 30.2 (2C). EI-MS m/z: 421 (M+H) +. Anal Calcd for C₁₇H₁₇ClN₆O₃S: C, 48.51; H, 4.07; N, 19.97. Found: C, 48.53; H, 4.05; N, 19.94.

4.2.4.7. N-(Benzo[d]thiazol-2-yl)-2-(4-(5-chloro-1H-benzo[d]imidazol-2-yl)piperidin-1-yl)acetamide (R39): The compound was prepared according to the general procedure using 5-chloro-2-(piperidin-4-yl)-1H-benzo[d]imidazole (2d) (0.1 g, 0.425 mmol), triethyl amine (0.107 g, 1.06 mmol), N-(benzo[d]thiazol-2-yl)-2-chloroacetamide (0.115 g, 0.51 mmol) to afford 39 (0.128 g, 70% yield) as pale yellow solid. M.P: 225 - 227°C. ¹H NMR (DMSO-d₆): δ_H 1.95 – 2.75 (m, 9H), 3.41 (s, 2H), 5.11 (b, 1H), 7.06 – 8.61 (m, 7H), 9.02 (b, 1H). ¹³C NMR (DMSO-d₆): δ_c 175.6, 169.5, 155.6, 140.5, 139.8, 136.5, 131.5, 130.2, 126.5, 125.2, 124.9, 122.5, 119.1, 117.2, 116.5, 64.5, 54.5 (2C), 36.2, 30.2 (2C). EI-MS m/z: 426 (M+H) +. Anal Calcd for C₂₁H₂₀ClN₅OS: C, 59.22; H, 4.73; N, 16.44. Found: C, 59.24; H, 4.71; N, 16.42.

4.2.4.8. 2-(4-(5-Chloro-1H-benzo[d]imidazol-2-yl)piperidin-1-yl)-N-(6-nitrobenzo[d]thiazol-2-yl)acetamide (R40): The compound was prepared according to the general procedure using 5-chloro-2-(piperidin-4-yl)-1H-benzo[d]imidazole (2d) (0.1 g, 0.425 mmol), triethyl amine (0.107 g, 1.06 mmol), 2-chloro-N-(6-nitrobenzo[d]thiazol-2-yl)acetamide (0.138 g, 0.51mmol) to afford 40 (0.138 g, 69% yield) as yellow solid. M.P: 217 - 219°C. ¹H NMR (DMSO-d₆): δ_H 2.01 – 2.86 (m, 9H), 3.35 (s, 2H), 4.95 (b, 1H), 7.05 – 8.85 (m, 6H), 9.17 (b, 1H). ¹³C NMR (DMSO-d₆): δ_c 174.5, 169.5, 160.5, 145.6, 140.5, 139.5, 138.5, 130.5, 128.5, 125.6, 122.5, 120.5, 118.5, 117.2, 116.8, 64.5, 54.5 (2C), 36.2 30.2 (2C). EI-MS m/z: 471 (M+H) +. Anal Calcd for C₂₁H₁₉ClN₆O₃S: C, 53.56; H, 4.07; N, 17.85. Found: C, 53.57; H, 4.06; N, 17.84.

4.2.4.9. 2-(4-(5-Chloro-1H-benzo[d]imidazol-2-yl)piperidin-1-yl)-N-(furan-2-ylmethyl)acetamide (R41): The compound was prepared according to the general procedure using 5-chloro-2-(piperidin-4-yl)-1H-benzo[d]imidazole (2d) (0.1 g, 0.425 mmol), triethyl amine (0.107 g, 1.06 mmol), 2-chloro-N-(furan-2-ylmethyl)acetamide (0.083 g, 0.51 mmol) to afford 41 (0.106 g, 67% yield) as light brown solid. M.P: 255 - 257°C. ¹H NMR (DMSO-d₆): δH 2.03 – 2.86 (m, 9H), 3.32 (s, 2H), 5.03 (b, 1H), 5.21 (s, 2H), 6.35 – 8.42 (m, 7H). ¹³C NMR (DMSO-d₆): δc 172.1, 146.2, 143.1, 140.5, 139.5, 138.1, 130.2, 125.6, 116.7, 115.9, 110.5, 109.6, 60.2, 54.5 (2C), 38.2, 36.2, 30.2 (2C). EI-MS m/z: 373 (M+H) +. Anal Calcd for C₁₉H₂₁ClN₄O₂: C, 61.21; H, 5.68; N, 15.03. Found: C, 61.23; H, 5.69; N, 15.01.

4.2.4.10. 2-(4-(5-Chloro-1H-benzo[d]imidazol-2-yl)piperidin-1-yl)-N-(4-methoxyphenyl)acetamide (R42): The compound was prepared according to the general procedure using 5-chloro-2-(piperidin-4-yl)-1H-benzo[d]imidazole (2d) (0.1 g, 0.425 mmol), triethyl amine (0.107 g, 1.06 mmol), 2-chloro-N-(4-methoxyphenyl)acetamide (0.101 g, 0.51 mmol) to afford 42 (0.122 g, 72% yield) as pale brown solid. M.P: 219 - 221°C. ¹H NMR (DMSO-d₆): δH 1.96– 2.74 (m, 9H), 2.99 (s, 2H), 3.81 (s, 3H), 4.98 (b, 1H), 7.09 – 8.56 (m, 8H). ¹³C NMR (DMSO-d₆): δc 169.5, 160.2, 140.8, 139.5, 136.8, 129.5, 130.2, 125.6, 123.5 (2C), 117.8, 116.5, 115.6 (2C), 64.5, 56.2, 54.5 (2C), 36.2, 30.2 (2C). EI-MS m/z: 399 (M+H) +. Anal Calcd for C₂₁H₂₃ClN₄O₂: C, 63.23; H, 5.81; N, 14.05. Found: C, 63.22; H, 5.82; N, 14.04.

Annexure-II

Experimental procedure for synthesis of lead (B1):

General procedure for the synthesis of 4-(sub:-1H-Benzo[d]imidazol-2-yl)aniline (3a-e)/4-(3H-imidazo[4,5-b]pyridin-2-yl)aniline (3f). Procedure A: Eaton's reagent (10 vol; wt/vol) was added drop wise to a well pulverised mixture of the corresponding 1,2-phenylenediamine (2a-e)/1,2-diaminopyridine (2f) (1 equiv) and 4-amino benzoic acid (1 equiv) at 0oC. The reaction mixture was then heated at 130oC for 5 - 6 h (monitored by TLC and LCMS for completion). The reaction mixture was cooled and neutralised with 10% sodium hydroxide solution to pH of 6-7, the precipitate formed was filtered and washed repeatedly with water and dried. The solid obtained was recrystallized from ethanol to afford the desired product in good yield as described below.

General procedure for the synthesis of 4-(1H-Benzo[d]imidazol-2-yl)aniline (3a): The compound was prepared according to the general procedure A using 1,2-phenylenediamine 2a (1 g, 9.25 mmol), 4-amino benzoic acid (1.27 g, 9.25 mmol) and eatons reagent (10 mL) to afford 3a (1.42 g, 74% yield) as pale brown solid. M.P - 259 – 261oC. ¹H NMR (DMSO-d₆): δH 6.42 (s, 2H), 6.82-7.98 (m, 8H). ¹³C NMR (DMSO-d₆): δc 153.1, 145.4, 141.5, 128.7, 123.5, 116.7, 115.5. EI-MS m/z: 210.45 (M+H)⁺. Anal Calcd for C₁₃H₁₁N₃: C, 74.62; H, 5.30; N, 20.08. Found: C, 74.64; H, 5.33; N, 20.12.

General procedure for the synthesis of 4-(5-Fluoro-1H-Benzo[d]imidazol-2-yl)aniline (3b): The compound was prepared according to the general procedure A using 4-fluoro-1,2-phenylenediamine 2b (1 g, 7.93 mmol), 4-amino benzoic acid (1.09 g, 7.93 mmol) and eatons

reagent (10 mL) to afford 3b (1.02 g, 56% yield) as brown solid. M.P: 242 - 244°C. ¹H NMR (DMSO-d₆): δ_H 6.33 (s, 2H), 7.00 - 8.09 (m, 7H). ¹³C NMR (DMSO-d₆): δ_C 156.6, 153.3, 145.6, 139.1, 137.8, 128.2, 116.8, 115.6, 110.3, 101.9. EI-MS m/z: 228.26 (M+H)⁺. Anal Calcd for C₁₃H₁₀FN₃: C, 68.71; H, 4.44; N, 18.49; Found: C, 68.73; H, 4.42; N, 18.47.

General procedure for the synthesis of 4-(5-Chloro-1H-Benzo[d]imidazol-2-yl)aniline (3c):

The compound was prepared according to the general procedure A using 4-chloro-1,2-phenylenediamine 2c (1 g, 7.02 mmol), 4-amino benzoic acid (0.96 g, 7.02 mmol) and eatons reagent (10 mL) to afford 3c (1.1 g, 64% yield) as buff coloured solid. M.P: 291 - 293 °C. ¹H NMR (DMSO-d₆): δ_H 6.45 (s, 2H), 7.08 - 8.39 (m, 7H). ¹³C NMR (DMSO-d₆): δ_C 153.1, 145.7, 133.2, 131.2, 129.6, 128.4, 124.3, 116.7, 116.3, 115.9, 115.2. EI-MS m/z: 244.42(M+H)⁺. Anal Calcd for C₁₃H₁₀ClN₃: C, 64.07; H, 4.14; N, 17.24; Found C, 64.11; H, 4.16; N, 17.19;

General procedure for the synthesis of 4-(5-Nitro-1H-Benzo[d]imidazol-2-yl)aniline (3d):

The compound was prepared according to the general procedure A using 4-nitro-1,2-phenylenediamine 2d (1 g, 6.53 mmol), 4-amino benzoic acid (0.9 g, 6.53 mmol) and eatons reagent (10 mL) to afford 3d (1.2 g, 72% yield) as yellowish brown solid. MP: 277 – 278 °C. ¹H NMR (DMSO-d₆): δ_H 6.53 (s, 2H), 7.21 - 8.49 (m, 7H). ¹³C NMR (DMSO-d₆): δ_C 153.3, 148.6, 145.7, 144.6, 140.2, 128.3, 118.9, 116.3, 116.1, 115.3, 113.2. EI-MS m/z: 255.44 (M+H)⁺. Anal Calcd for C₁₃H₁₀N₄O₂: C, 61.41; H, 3.96 N, 22.04; Found C, 61.44; H, 3.94 N, 22.06;

General procedure for the synthesis of 4-(5-Methoxy-1H-benzo[d]imidazol-2-yl)aniline

(3e): The compound was prepared according to the general procedure A using 4-methoxy-1,2-phenylenediamine 2e (1 g, 7.24 mmol), 4-amino benzoic acid (0.99 g, 7.24 mmol) and eatons

reagent (10 mL) to afford 3e (0.91 g, 53%) as reddish brown solid. MP: 162 -165°C. ¹H NMR (DMSO-d₆): δH 3.85 (s, 3H), 6.51 (s, 2H), 7.04 - 8.13 (m, 7H). ¹³C NMR (DMSO-d₆): δc 156.7, 153.4, 145.7, 139.5, 134.5, 128.4, 116.8, 115.3, 112.1, 100.6, 56.1. EI-MS m/z: 240.3 (M+H)⁺. Anal Calcd for C₁₄H₁₃N₃O: C, 70.28; H, 5.48; N, 17.56; Found: C, 70.31; H, 5.47; N, 17.58.

General procedure for the synthesis of 4-(3H-Imidazo[4,5-b]pyridin-2-yl)aniline (3f): The compound was prepared according to the general procedure A using pyridine-2,3-diamine 2f (1 g, 9.16 mmol), 4-amino benzoic acid (1.26 g, 9.16 mmol) and eatons reagent (10 mL) to afford 3f (1.1 g, 58% yield) as pale brown solid. M.P: 265 – 267°C. ¹H NMR (DMSO-d₆): δH 6.43 (s, 2H), 7.03 - 8.22 (m, 7H). ¹³C NMR (DMSO-d₆): δc 162.3, 150.7, 145.6, 145.2, 130.5, 128.3, 124.8, 123.6, 122.8, 115.6. EI-MS m/z: 211.33 (M+H)⁺. Anal Calcd for C₁₂H₁₀N₄: C, 68.56; H, 4.79; N, 26.65; Found: C, 68.59; H, 4.77; N, 26.62.

General procedure for the synthesis of substituted ethyl 3-((4-(1H-benzo[d]imidazol-2-yl)phenyl)amino)-3-oxopropanoate / ethyl 3-((4-(3H-imidazo[4,5-b]pyridin-2-yl)phenyl)amino)-3-oxopropanoate (3'a-f) : The synthesis followed the literature procedure. To a well stirred solution of the corresponding 4-(sub:-1H-benzo[d]imidazol-2-yl) aniline/4-(3H-imidazo[4,5-b]pyridin-2-yl)aniline (3a-f) (1 equiv) in anhydrous dichloromethane was added triethylamine (3 equiv) under 0 °C followed by the addition of monoethyl malonate (1.1 equiv). Then propyphosphonic anhydride (1.5 equiv) was added to the reaction mixture and was stirred at room temperature for 3h (monitored by TLC and LCMS for completion). The solvent was removed under vacuum, diluted with water. The aqueous layer was further washed with dichloromethane. The combined organic layer was then dried over anhydrous sodium sulphate

and concentrated under reduced pressure. The residue obtained was further recrystallized to afford the desired product in good yield and purity as described below.

General procedure for the synthesis of ethyl 3-((4-(1H-benzo[d]imidazol-2-yl)phenyl)amino)-3-oxopropanoate (3'a): The compound was prepared according to the general procedure A using 4-(1H-benzo[d]imidazol-2-yl)aniline 3a (0.4 g, 1.9 mmol), monoethyl malonate (0.278 g, 2.1 mmol) ,triethyl amine (0.58 g, 5.74 mmol) propylphosphonic anhydride (1.22 g, 3.82 mmol) to afford 3'a (0.41 g, 66% yield) as brown solid. M.P - 221 – 223 oC. ¹H NMR (DMSO-d₆): δH1.56-4.53 (m, 7H), 6.15 (s,1H) 7.41 - 8.29 (m, 8H), 10.12 (s, 1H). ¹³C NMR (DMSO-d₆): δc 170.2, 165.2, 155.2, 143.2 (2C), 140.2, 128.5 (2C), 124.2 (2C) 120.8, 118.6 (2C), 55.3, 38.4, 13.2. EI-MS m/z: 324.45 (M+H)⁺. Anal Calcd for C₁₈H₁₇N₃O₃: C, 66.86; H, 5.30; N, 13.00. Found: C, 66.84; H, 5.29; N, 13.01

General procedure for the synthesis of ethyl 3-((4-(5-fluoro-1H-benzo[d]imidazol-2-yl)phenyl)amino)-3-oxopropanoate (3'b): The compound was prepared according to the general procedure A using 4-(5-fluoro-1H-benzo[d]imidazol-2-yl)aniline 3b (0.4 g, 1.76 mmol), monoethyl malonate (0.256 g, 1.93 mmol), triethyl amine (0.53 g, 5.28 mmol) and propylphosphonic anhydride (1.22 g, 3.12 mmol) to afford 3b (0.38 g, 63% yield) as brown solid. M.P: 242 - 244oC. ¹H NMR (DMSO-d₆): δH1.62-4.67 (m, 7H), 6.15 (s,1H) 7.56 - 8.35 (m, 7H), 10.09 (s, 1H). ¹³C NMR (DMSO-d₆): δc 169.2, 165.2, 157.2, 153.2 , 140.2,138.5, 136.5, 128.5 (2C), 122.2 , 118.6 (2C),116.3, 110.5, 102.5, 55.5, 38.2, 13.6. EI-MS m/z: 342.51 (M+H)⁺. Anal Calcd for C₁₈H₁₆FN₃O₃: C, 63.34; H, 4.72; N, 12.31. Found C, 63.37; H, 4.70; N, 12.30.

General procedure for the synthesis of ethyl 3-((4-(5-chloro-1H-benzo[d]imidazol-2-yl)phenyl)amino)-3-oxopropanoate (3'c): The compound was prepared according to the general procedure A using 4-(5-chloro-1H-benzo[d]imidazol-2-yl)aniline 3c (0.4 g, 1.64 mmol), monoethyl malonate (0.239 g, 1.81 mmol), triethyl amine (0.49 g, 4.93 mmol) and propylphosphonic anhydride (1.04 g, 3.29 mmol) to afford 3'c (0.37 g, 63% yield) as pale brown solid. M.P: 242 - 244°C. ¹H NMR (DMSO-d₆): δH 1.52-4.61 (m, 7H), 6.22 (s, 1H) 7.42 - 8.13 (m, 7H), 10.14 (s, 1H). ¹³C NMR (DMSO-d₆): δC 170.2, 165.2, 154.2, 140.2, 134.5, 130.3, 129.5, 128.5 (2C), 124.6, 122.2, 118.6 (2C), 116.3, 114.5, 55.5, 38.2, 13.6. EI-MS m/z: 345.51 (M+H)⁺. Anal Calcd for C₁₈H₁₆ClN₃O₃: C, 60.42; H, 4.51; N, 11.74. Found C, 60.43; H, 4.50; N, 11.76.

General procedure for the synthesis of ethyl 3-((4-(5-nitro-1H-benzo[d]imidazol-2-yl)phenyl)amino)-3-oxopropanoate (3'd): The compound was prepared according to the general procedure A using 4-(5-nitro-1H-benzo[d]imidazol-2-yl)aniline 3d (0.4 g, 1.57 mmol), monoethyl malonate (0.228 g, 1.73 mmol), triethyl amine (0.47 g, 4.72 mmol) and propylphosphonic anhydride (1.00 g, 3.15 mmol) to afford 3'd (0.39 g, 67% yield) as pale orange solid. M.P: 242 - 244°C. ¹H NMR (DMSO-d₆): δH 1.61-4.72 (m, 7H), 6.29 (s, 1H) 7.73 - 8.34 (m, 7H), 10.14 (s, 1H). ¹³C NMR (DMSO-d₆): δC 170.2, 163.2, 154.2, 148.5, 145.6 140.2, 138.6, 128.5 (2C), 122.2, 118.6 (2C), 117.9, 116.3, 114.5, 55.5, 38.2, 13.6. EI-MS m/z: 369.51 (M+H)⁺. Anal Calcd for C₁₈H₁₆N₄O₅: C, 58.69; H, 4.38; N, 15.21. Found C, 58.67; H, 4.39; N, 15.20.

General procedure for the synthesis of ethyl 3-((4-(5-methoxy-1H-benzo[d]imidazol-2-yl)phenyl)amino)-3-oxopropanoate (3'e): The compound was prepared according to the general procedure A using 4-(5-methoxy-1H-benzo[d]imidazol-2-yl)aniline 3e (0.4 g, 1.67

mmol), monoethyl malonate (0.243 g, 1.84 mmol), triethyl amine (0.51 g, 5.02 mmol) and propylphosphonic anhydride (1.06 g, 3.33 mmol) to afford 3'e (0.36 g, 61% yield) as brown solid. M.P: 242 - 244°C. ¹H NMR (DMSO-d₆): δH 1.57-4.64 (m, 10H), 6.26 (s, 1H) 7.67 - 8.29 (m, 7H), 10.14 (s, 1H). ¹³C NMR (DMSO-d₆): δc 170.2, 163.5, 155.2, 153.5, 140.2, 139.5, 134.6, 128.2 (2C), 122.3, 120.1 (2C), 116.5, 111.2, 101.2, 55.5, 53.2, 38.2, 14.5. EI-MS m/z: 354.56 (M+H)⁺. Anal Calcd for C₁₉H₁₉N₃O₄: C, 64.58; H, 5.42; N, 11.89. Found C, 64.56; H, 5.43; N, 11.87.

General procedure for the synthesis of ethyl 3-((4-(3H-imidazo[4,5-b]pyridin-2-yl)phenyl)amino)-3-oxopropanoate (3'f): The compound was prepared according to the general procedure A using 4-(3H-imidazo[4,5-b]pyridin-2-yl)aniline 3f (0.4 g, 1.90 mmol), monoethyl malonate (0.276 g, 2.09 mmol), triethyl amine (0.57 g, 5.71 mmol) and propylphosphonic anhydride (1.21 g, 3.80 mmol) to afford 3'e (0.4 g, 61% yield) as brown solid. M.P: 242 - 244°C. ¹H NMR (DMSO-d₆): δH 1.39-4.33 (m, 7H), 6.53 (s, 1H) 7.73 - 8.21 (m, 7H), 10.16 (s, 1H). ¹³C NMR (DMSO-d₆): δc 170.2, 163.5, 162.2, 150.5, 145.2, 139.5, 129.2 (2C), 128.3, 123.5, 122.1, 119.5 (2C), 111.2, 55.5, 38.2, 14.5. EI-MS m/z: 325.56 (M+H)⁺. Anal Calcd for C₁₇H₁₆N₄O₃: C, 62.95; H, 4.97; N, 17.27. Found C, 62.93; H, 4.95; N, 17.28.

General procedure for the synthesis of acylated derivatives (S4, S8, S13, S18, S23, S28).
Procedure step 1: Substituted ethyl 3-((4-(1H-benzo[d]imidazol-2-yl)phenyl)amino)-3-oxopropanoate (3'a-f) (1 equiv) was dissolved in ethanol and LiOH (2 equiv) in water was added and stirred at room temperature for 4h (monitored by TLC and LCMS for completion). Ethanol was removed under reduced pressure and residue was dissolved in water and acidified with 1.5N HCl. The residue obtained was further recrystallized from ethanol to afford the desired product in good yield and purity as described below.

4.2.1. 3-((4-(1H-Benzo[d]imidazol-2-yl)phenyl)amino)-3-oxopropanoic acid (S4): The compound was prepared according to the general procedure B using ethyl 3-((4-(1H-benzo[d]imidazol-2-yl)phenyl)amino)-3-oxopropanoate 3'a (0.2 g, 0.61 mmol), LiOH (0.051 g, 1.2 mmol) to afford 4 (0.174 g, 61% yield) as pale yellow solid. M.P: 279 - 281°C. ¹H NMR (DMSO-d₆): δH 3.25 (s, 2H), 7.44 - 8.24 (m, 8H), 10.12 (s, 1H), 12.73 (b, 1H). ¹³C NMR (DMSO-d₆): δc 172, 163.3, 153.5, 141.5, 139, 128.3, 123.5, 122.2, 120.6, 115.7, 37.3. EI-MS m/z: 296.4 (M+H)⁺. Anal Calcd for C₁₉H₁₃N₃O₃: C, 65.08; H, 4.44; N, 14.23 Found: C, 65.11; H, 4.47; N, 14.28.

4.2.2. 3-((4-(5-Fluoro-1H-benzo[d]imidazol-2-yl)phenyl)amino)-3-oxopropanoic acid (S8): The compound was prepared according to the general procedure B ethyl 3-((4-(5-fluoro-1H-benzo[d]imidazol-2-yl)phenyl)amino)-3-oxopropanoate 3'b (0.2 g, 0.58 mmol), LiOH (0.049 g, 1.17 mmol) to afford 8 (0.188g, 68% yield) as off white solid. M.P: 210 - 212°C. ¹H NMR (DMSO-d₆): δH 1.71 - 2.39 (m, 2H), 7.03 - 8.25 (m, 7H) 10.16 (s, 1H), 12.68 (b, 1H). ¹³C NMR (DMSO-d₆): δc 172.3, 163.1, 157.2, 153.2, 141.2, 138.7, 137.8, 128.2, 122.3, 120.3, 117.4, 110.3, 102.8, 39.6. EI-MS m/z: 314.3 (M+H)⁺. Anal Calcd for C₁₆H₁₂FN₃O₃: C, 61.34; H, 3.86; N, 13.41; Found: C, 61.38; H, 3.89; N, 13.45.

4.2.3. 3-((4-(5-Chloro-1H-benzo[d]imidazol-2-yl)phenyl)amino)-3-oxopropanoic acid (S13): The compound was prepared according to the general procedure B using ethyl 3-((4-(5-chloro-1H-benzo[d]imidazol-2-yl)phenyl)amino)-3-oxopropanoate 3'c (0.2 g, 0.55 mmol), LiOH (0.046 g, 1.11 mmol) to afford 13 (0.178 g, 66% yield) as pale brown solid. . M.P - 276 - 278 °C. ¹H NMR (DMSO-d₆): δH 3.25 (s, 2H), 7.25 - 8.42 (m, 7H) 10.16 (s, 1H), 12.73 (b, 1H). ¹³C NMR (DMSO-d₆): δc 171.8, 163.2, 153.2, 138.7, 133.2, 131.3, 129.4, 128.2, 124.5, 122.3, 120.3,

116.8, 115.9, 39.6. EI-MS m/z : 330.5 (M+H)⁺. Anal Calcd for C₁₆H₁₂ClN₃O₃: C, 58.28; H, 3.67 N, 12.74; Found: C, 58.29; H, 3.65 N, 12.77.

4.2.4. 3-((4-(5-Nitro-1H-benzo[d]imidazol-2-yl)phenyl)amino)-3-oxopropanoic acid (S18):

The compound was prepared according to the general procedure B ethyl 3-((4-(5-nitro-1H-benzo[d]imidazol-2-yl)phenyl)amino)-3-oxopropanoate 3'd (0.2 g, 0.54 mmol), LiOH (0.045 g, 1.07 mmol) to afford 18 (0.185 g, 69% yield) as pale yellow solid. M.P – 244 - 246 oC. ¹H NMR (DMSO-d₆): δH 3.21 (s, 2H), 7.71 - 8.57 (m, 7H), 10.16 (s, 1H), 12.61 (b, 1H). ¹³C NMR (DMSO-d₆): δc 171.7, 163.5, 153.2, 148.9, 144.6, 140.2, 138.7, 128.3, 122.2, 120.1, 118.8, 116.3, 113.2, 39.8. EI-MS m/z : 341.7 (M+H)⁺. Anal Calcd for C₁₆H₁₂N₄O₅: C, 56.47; H, 3.55; N, 16.46; Found: C, 56.49; H, 3.54; N, 16.48.

4.2.5. 3-((4-(5-Methoxy-1H-benzo[d]imidazol-2-yl)phenyl)amino)-3-oxopropanoic acid (S23):

The compound was prepared according to the general procedure B using ethyl 3-((4-(5-methoxy-1H-benzo[d]imidazol-2-yl)phenyl)amino)-3-oxopropanoate 3'e (0.2 g, 0.56 mmol), LiOH (0.048 g, 1.13 mmol) to afford 23 (0.183 g, 67% yield) as yellow solid. M.P – 277 – 279 oC. ¹H NMR (DMSO-d₆): δH 3.36 (s, 2H), 3.89 (s, 3H), 7.06 - 8.31 (m, 7H) 10.12 (s, 1H), 12.55 (b, 1H). ¹³C NMR (DMSO-d₆): δc 172.5, 162.5, 156.4, 153.2, 140.1, 138.2, 133.8, 127.3, 122.3, 120.1, 115.8, 112.5, 101.2, 56.5, 40.2. EI-MS m/z : 326.4 (M+H)⁺. Anal Calcd for C₁₇H₁₅N₃O₄: C, 62.76; H, 4.65; N, 12.92 Found: C, 62.74; H, 4.68; N, 12.89.

4.2.6. 3-((4-(1H-Imidazo[4,5-b]pyridin-2-yl)phenyl)amino)-3-oxopropanoic acid (S28):

The compound was prepared according to the general procedure B using ethyl 3-((4-(3H-imidazo[4,5-b]pyridin-2-yl)phenyl)amino)-3-oxopropanoate 3'e (0.2 g, 0.61 mmol), LiOH (0.052 g, 1.23 mmol) to afford 28 (0.193 g, 68% yield) as buff coloured solid. M.P – 288 – 290 oC. ¹H

NMR (DMSO-d₆): δ_H 3.36 (s, 2H), 7.01-8.25 (m, 7H) 10.19 (s, 1H), 12.71 (b, 1H). ¹³C NMR (DMSO-d₆): δ_c 172.3, 163.1, 161.9, 150.8, 145.6, 138.6, 130.3, 128.2, 123.7, 122.8, 120.3, 39.8. . EI-MS m/z: 297.5 (M+H)⁺. Anal Calcd for C₁₅H₁₂N₄O₃: C, 60.81; H, 4.08; N, 18.91; Found C, 60.85; H, 4.04; N, 18.90.

General procedure for the synthesis of acylated derivatives (S5-S6, S9-S11, S14-S16, S19-S21, S24-S26, S29-S31, S33.), Procedure B: The synthesis followed the literature procedure. To a well stirred solution of the corresponding 4-(sub:-1H-benzo[d]imidazol-2-yl)aniline /4-(3H-imidazo[4,5-b]pyridin-2-yl)aniline (3a-f) (1 equiv) in anhydrous tetrahydrofuran (0.15 M) with 4 Å molecular sieves in an appropriate sized microwave vial; was added the corresponding anhydride (1 equiv) at room temperature. The reaction mixture was then irradiated in Biotage microwave initiator with stirring at 160 – 170 °C for about 20 – 30 min (monitored by TLC and LCMS for completion). The solvent was removed under vacuum, diluted with water and basified with solid sodium bicarbonate to a pH of 9. The aqueous layer was further washed with dichloromethane, acidified with 2N HCl to a pH of 2, and extracted repeatedly with ethyl acetate. The combined organic layer was then dried over anhydrous sodium sulphate and concentrated under reduced pressure. The residue obtained was further recrystallized from ethanol to afford the desired product in good yield and purity as described below.

4.2.7. 4-(((4-(1H-Benzo[d]imidazol-2-yl)phenyl)amino)-4-oxobutanoic acid (S5): The compound was prepared according to the general procedure B using 4-(1H-benzo[d]imidazol-2-yl)aniline 3a (0.2 g, 0.96 mmol), succinic anhydride (0.096 g, 0.96 mmol) to afford 5 (0.21 g, 71%) as off white solid. M.P: 259 – 261 °C. ¹H NMR (DMSO-d₆): δ_H 2.34 - 2.91 (m, 4H), 7.42 - 8.24 (m, 8H), 10.14 (s, 1H), 12.63 (b, 1H). ¹³C NMR (DMSO-d₆): δ_c 177.5, 174.2, 153.4,

141.4, 139, 127.5, 123.5, 122.1, 120.2, 115.8, 30.9, 29.5. EI-MS m/z: 310.3 (M+H)⁺. Anal Calcd for C₁₇H₁₅N₃O₃: C, 66.01; H, 4.89; N, 13.58. Found: C, 66.05; H, 4.84; N, 13.54.

4.2.8. 6-((4-(1H-Benzo[d]imidazol-2-yl)phenyl)amino)-6-oxohexanoic acid (S7): The compound was prepared according to the general procedure B using 4-(1H-benzo[d]imidazol-2-yl)aniline 3a (0.2 g, 0.96 mmol), adipic anhydride (0.122 g, 0.96 mmol) to afford 7 (0.211 g, 65% yield) as yellow solid. MP: 276 – 278 °C. ¹H NMR (DMSO-d₆): δH 1.34 - 2.42 (m, 8H), 7.48 - 8.32 (m, 8H), 10.11 (s, 1H), 12.53 (b, 1H). ¹³C NMR (DMSO-d₆): δc 180.2, 178.7, 152.7, 142.2, 139.1, 128, 123.3, 122.2, 120.1, 115.8, 37.5, 32.8, 27.9, 24.4. EI-MS m/z: 338.2 (M+H)⁺. Anal Calcd for C₁₉H₁₉N₃O₃: C, 67.64; H, 5.68; N, 12.46; Found: C, 67.61; H, 5.71; N, 12.43.

4.2.9. 4-((4-(5-Fluoro-1H-benzo[d]imidazol-2-yl)phenyl)amino)-4-oxobutanoic acid (S9): The compound was prepared according to the general procedure B using 4-(5-fluoro-1H-benzo[d]imidazol-2-yl)aniline 3b (0.2 g, 0.88 mmol), succinic anhydride (0.088 g, 0.88 mmol) to afford 9 (0.193 g, 67% yield) as off white solid. M.P-297-299 °C. ¹H NMR (DMSO-d₆): δH 2.35 - 2.68 (m, 4H), 7.03 - 8.29 (m, 7H) 10.14 (s, 1H), 12.65 (b, 1H). ¹³C NMR (DMSO-d₆): δc 177.8, 174.2, 156.8, 153.2, 140.8, 138.6, 137.8, 128.3, 122.4, 120.3, 117.4, 110.4, 102.6, 30.5, 28.3. EI-MS m/z: 328.42 (M+H). Anal Calcd for C₁₇H₁₄FN₃O₃: C, 62.38; H, 4.31; N, 12.84; Found: C, 62.35; H, 4.36; N, 12.86.

4.2.10. 5-((4-(5-Fluoro-1H-benzo[d]imidazol-2-yl)phenyl)amino)-5-oxopentanoic acid (S10): The compound was prepared according to the general procedure B using 4-(5-fluoro-1H-benzo[d]imidazol-2-yl)aniline 3b (0.2 g, 0.88 mmol), glutaric anhydride (0.1 g, 0.88 mmol) to afford 10 as off white solid. M.P-282 - 284 °C. ¹H NMR (DMSO-d₆): δH 1.77 - 2.37 (m, 6H),

7.00 - 8.08 (m, 7H), 10.16 (s, 1H), 12.91 (b, 1H). ¹³C NMR (DMSO-d₆): δ_c 174.3, 171.2, 160.2, 157, 152.6, 140.9, 124.4, 119.1, 109.76, 35.5, 33.1, 20.4. EI-MS m/z: 342.56 (M+H)⁺. Anal Calcd for C₁₈H₁₆FN₃O₃: C, 63.34; H, 4.72; N, 12.31; Found: C, 63.36; H, 4.71; N, 12.32

4.2.11. 6-((4-(5-Fluoro-1H-benzo[d]imidazol-2-yl)phenyl)amino)-6-oxohexanoic acid (S12):

The compound was prepared according to the general procedure B using 4-(5-fluoro-1H-benzo[d]imidazol-2-yl)aniline 3b (0.2 g, 0.88 mmol), adipic anhydride (0.113 g, 0.88 mmol) to afford 12 (0.232g, 74% yield) as off white solid. M.P- 282 – 284 °C. ¹H NMR (DMSO-d₆): δ_H 1.35 - 2.48 (m, 8H), 7.05 - 8.31 (m, 7H) 10.16 (s, 1H), 12.62 (b, 1H). ¹³C NMR (DMSO-d₆): δ_c 180.2, 178.9, 156.7, 153.4, 140.6, 138.9, 137.5, 128.4, 122.3, 120.2, 117.2, 110.3, 102.5, 38.2, 33.6, 27.5, 24.2. EI-MS m/z: 356.4 (M+H)⁺. Anal Calcd for C₁₉H₁₈FN₃O₃: C, 64.22; H, 5.11; F, 5.35; N, 11.82; Found: C, 64.25; H, 5.16; F, 5.39; N, 11.87.

4.2.12. 4-((4-(5-Chloro-1H-benzo[d]imidazol-2-yl)phenyl)amino)-4-oxobutanoic acid (S14):

The compound was prepared according to the general procedure B using 4-(5-chloro-1H-benzo[d]imidazol-2-yl)aniline 3c (0.2 g, 0.82 mmol), succinic anhydride (0.082 g, 0.82 mmol) to afford 14 (0.19 g, 68% yield) as pale brown solid. M.P - 288 – 290 °C. ¹H NMR (DMSO-d₆): δ_H 2.37 - 2.68 (s, 4H), 7.23 - 8.36 (m, 7H) 10.15 (s, 1H), 12.69 (b, 1H). ¹³C NMR (DMSO-d₆): δ_c 177.8, 174.2, 153.3, 138.8, 133.2, 131.3, 129.4, 128.2, 124.5, 122.2, 120.2, 116.7, 155.9, 30.5, 28.8. EI-MS m/z: 344.6 (M+H)⁺. Anal Calcd for C₁₇H₁₄ClN₃O₃: C, 59.40; H, 4.10 N, 12.22; Found: C, 59.43; H, 4.12 N, 12.18.

4.2.13. 5-((4-(5-Chloro-1H-benzo[d]imidazol-2-yl)phenyl)amino)-5-oxopentanoic acid (S15):

The compound was prepared according to the general procedure B using 4-(5-chloro-1H-benzo[d]imidazol-2-yl)aniline 3c (0.2 g, 0.82 mmol), glutaric anhydride (0.094 g, 0.82 mmol) to

afford 15 (0.175 g, 59% yield) as off white solid. M.P - 274 - 276 oC. ¹H NMR (DMSO-d₆): δH 1.65-2.28 (m, 6H), 7.23 - 8.46 (m, 7H) 10.21 (s, 1H), 12.85 (b, 1H). ¹³C NMR (DMSO-d₆): δc 180.2, 178.6, 153.2, 138.9, 133.2, 131.2, 129.4, 128.3, 124.5, 122.3, 120.2, 116.8, 115.9, 37.5, 32.8, 20.5. EI-MS m/z: 358.9 (M+H)⁺. Anal Calcd for C₁₈H₁₆N₃O₃: C, 60.42; H, 4.51; N, 11.74; Found C, 60.44; H, 4.49; N, 11.71.

4.2.14. 6-((4-(5-Chloro-1H-benzo[d]imidazol-2-yl)phenyl)amino)-6-oxohexanoic acid (S17):

The compound was prepared according to the general procedure B using 4-(5-chloro-1H-benzo[d]imidazol-2-yl)aniline 3c (0.2 g, 0.82 mmol), adipic anhydride (0.105 g, 0.82 mmol) to afford 17 (0.198g, 65% yield) as pale brown solid. M.P – 255 - 257 oC. ¹H NMR (DMSO-d₆): δH 1.46 - 2.32 (m, 8H), 7.26 - 8.37 (m, 7H) 10.17 (s, 1H), 12.59 (b, 1H). ¹³C NMR (DMSO-d₆): δc 180.2, 178.8, 153.4, 138.7, 134.2, 131.2, 129.5, 128.3, 124.3, 122.3, 120.2, 116.7, 115.9, 38.2, 33.5, 27.3, 24.1. EI-MS m/z: 372.6 (M+H)⁺. Anal Calcd for C₁₉H₁₈N₃O₃: C, 61.38; H, 4.88 N, 11.30; Found: C, 61.36; H, 4.90 N, 11.31.

4.2.15. 4-((4-(5-Nitro-1H-benzo[d]imidazol-2-yl)phenyl)amino)-4-oxobutanoic acid (S19):

The compound was prepared according to the general procedure B using 4-(5-nitro-1H-benzo[d]imidazol-2-yl)aniline 3d (0.2 g, 0.79 mmol), succinic anhydride (0.079 g, 0.79 mmol) to afford 19 (0.195 g, 70% yield) as yellow solid. M.P - 298 – 300 oC. ¹H NMR (DMSO-d₆): δH 2.35 -2.66 (s, 4H), 7.61 - 8.49 (m, 7H) 10.15 (s, 1H), 12.69 (b, 1H). ¹³C NMR (DMSO-d₆): δc 177.8, 174.2, 153.2, 147.9, 144.5, 140.1, 138.8, 127.8, 122.3, 119.9, 118.7, 116.5, 113.2, 30.5, 28.8. . EI-MS m/z: 355.5 (M+H)⁺. Anal Calcd for C₁₇H₁₄N₄O₅: C, 57.63; H, 3.98 N, 15.81; Found: C, 57.66; H, 3.97; N, 15.85.

4.2.16. 5-((4-(5-Nitro-1H-benzo[d]imidazol-2-yl)phenyl)amino)-5-oxopentanoic acid (S20):

The compound was prepared according to the general procedure B using 4-(5-nitro-1H-benzo[d]imidazol-2-yl)aniline 3d (0.2 g, 0.79 mmol), glutaric anhydride (0.09 g, 0.79 mmol) to afford 20 (0.221 g, 76% yield) as yellow solid. ¹H NMR (DMSO-d₆): δH 1.71 -2.36 (m, 6H), 7.73 - 8.57 (m, 7H), 10.16 (s, 1H), 12.56 (b, 1H). ¹³C NMR (DMSO-d₆): δc 180.2, 178.8, 153.4, 148.2, 144.6, 140.2, 138.8, 128.3, 122.2, 120.2, 118.8, 116.3, 133.2, 37.1, 32.5, 20.5. EI-MS m/z: 369.5 (M+H)⁺. Anal Calcd for C₁₈H₁₆N₄O₅: C, 58.69; H, 4.38; N, 15.21; Found: C, 58.72; H, 4.37; N, 15.21.

4.2.17. 6-((4-(5-Nitro-1H-benzo[d]imidazol-2-yl)phenyl)amino)-6-oxohexanoic acid (S22):

The compound was prepared according to the general procedure B using 4-(5-nitro-1H-benzo[d]imidazol-2-yl)aniline 3d (0.2 g, 0.79 mmol), adipic anhydride (0.1 g, 0.79 mmol) to afford 22 (0.21 g, 66% yield) as yellow solid. M.P - 298 – 300 °C. ¹H NMR (DMSO-d₆): δH 1.42 -2.34 (m, 8H), 7.67 - 8.58 (m, 7H), 10.16 (s, 1H), 12.65 (b, 1H). ¹³C NMR (DMSO-d₆): δc 180.1, 178.6, 153.1, 148.2, 144.5, 140.1, 138.8, 128.3, 122.2, 120.2, 118.8, 116.2, 113.2, 38.2, 33.6, 27.2, 23.9. EI-MS m/z: 383.3 (M+H)⁺. Anal Calcd for C₁₉H₁₈N₄O₅: C, 59.68; H, 4.74; N, 14.65; Found: C, 59.66; H, 4.77; N, 14.68.

4.2.18. 4-((4-(5-Methoxy-1H-benzo[d]imidazol-2-yl)phenyl)amino)-4-oxobutanoic acid (S24):

The compound was prepared according to the general procedure B using 4-(5-methoxy-1H-benzo[d]imidazol-2-yl)aniline 3e (0.2 g, 0.84 mmol), succinic anhydride (0.084 g, 0.84 mmol) to afford 24 (0.169 g, 60% yield) as pale brown solid. M.P – 180 – 182 °C. ¹H NMR (DMSO-d₆): δH 2.36 - 2.62 (m, 4H), 3.87 (s, 3H), 7.02 - 8.33 (m, 7H), 10.13 (s, 1H), 12.61 (b, 1H). ¹³C NMR (DMSO-d₆): δc 177.8, 174.3, 156.5, 153.2, 140.3, 138.7, 134.2, 128.3, 122.3,

120.2, 116.7, 112.2, 100.9, 56.5, 30.7, 28.8. EI-MS m/z : 340.45(M+H)⁺. Anal Calcd for C₁₈H₁₇N₃O₄: C, 63.71; H, 5.05; N, 12.38; Found: C, 63.75; H, 5.01; N, 12.40.

4.2.19. 5-((4-(5-Methoxy-1H-benzo[d]imidazol-2-yl)phenyl)amino)-5-oxopentanoic acid (S25): The compound was prepared according to the general procedure B using 4-(5-nitro-1H-benzo[d]imidazol-2-yl)aniline 3e (0.2 g, 0.84 mmol), glutaric anhydride (0.095 g, 0.84 mmol) to afford 25 (0.186 g, 63% yield) as brown solid. M.P - 212 – 214 °C. ¹H NMR (DMSO-*d*₆): δ_H 1.66 - 2.33 (m, 6H), 3.94 (s, 3H), 7.05 - 8.26 (m, 7H) 10.11 (s, 1H), 12.73(b, 1H). ¹³C NMR (DMSO-*d*₆): δ_C 180.3, 177.6, 156.5, 153.6, 139.2, 138.5, 134.4, 128.7, 122.3, 120.5, 116.8, 112.3, 100.9, 56.5, 37.2, 33.2, 20.9. EI-MS m/z : 354.4 (M+H)⁺. Anal Calcd for C₁₉H₁₉N₃O₄: C, 64.58; H, 5.42; N, 11.89; Found: C, 64.54; H, 5.45; N, 11.91.

4.2.20. 6-((4-(5-Methoxy-1H-benzo[d]imidazol-2-yl)phenyl)amino)-6-oxohexanoic acid (S27): The compound was prepared according to the general procedure B using 4-(5-methoxy-1H-benzo[d]imidazol-2-yl)aniline 3e (0.2 g, 0.84 mmol), adipic anhydride (0.107 g, 0.84 mmol) to afford 27 (0.218 g, 71% yield) as reddish brown solid. M.P – 171 – 173 °C. ¹H NMR (DMSO-*d*₆): δ_H 1.39 - 2.35 (m, 8H), 3.86 (s, 3H), 7.04 - 8.26 (m, 7 H) 10.16 (s, 1H), 12.66 (b, 1H). ¹³C NMR (DMSO-*d*₆): δ_C 180.2, 178.5, 156.7, 153.2, 140.2, 138.7, 133.8, 128.3, 121.7, 120.3, 116.7, 112.2, 100.6, 56.2, 38.2, 33.5, 27.6, 24.5. EI-MS m/z : 368.5 (M+H)⁺. Anal Calcd for C₂₀H₂₁N₃O₄: C, 65.38; H, 5.76; N, 11.44; Found: C, 65.35; H, 5.78; N, 11.46.

4.2.21. 4-((4-(1H-Imidazo[4,5-*b*]pyridin-2-yl)phenyl)amino)-4-oxobutanoic acid (S29): The compound was prepared according to the general procedure B using 4-(3H-imidazo[4,5-*b*]pyridin-2-yl)aniline 3e (0.2 g, 0.95 mmol), succinic anhydride (0.095 g, 0.95 mmol) to afford 29 (0.211 g, 71% yield) as off white solid. M.P – 233 – 235 °C. ¹H NMR (DMSO-*d*₆): δ_H 2.36 -

2.68 (s, 4H), 7.05 - 8.32 (m, 7H) 10.15 (s, 1H), 12.68 (b, 1H). ¹³C NMR (DMSO-d₆): δ_c 177.8, 174.2, 161.7, 150.6, 145.3, 138.6, 130.6, 128.1, 123.8, 122.6, 120.1, 30.2, 28.6. EI-MS m/z: 311.3 (M+H)⁺. Anal Calcd for C₁₆H₁₄N₄O₃: C, 61.93; H, 4.55; N, 18.06; Found: C, 61.95; H, 4.58; N, 18.01.

4.2.22. 5-((4-(1H-Imidazo[4,5-b]pyridin-2-yl)phenyl)amino)-5-oxopentanoic acid (S30): The compound was prepared according to the general procedure B using 4-(3H-imidazo[4,5-b]pyridin-2-yl)aniline 3e (0.2 g, 0.95 mmol), glutaric anhydride (0.108 g, 0.95 mmol) to afford 30 (0.191 g, 62% yield) as pale brown solid. . M.P – 271 – 273 oC. ¹H NMR (DMSO-d₆): δ_H 1.71 - 2.39 (m, 6H), 7.03 -8.25 (m, 7H) 10.16 (s, 1H), 12.6 (b, 1H). ¹³C NMR (DMSO-d₆): δ_c 180.1, 178.5, 161.8, 150.6, 145.8, 138.7, 130.5, 128.2, 123.8, 122.7, 120.3, 37.5, 32.5, 20.4. EI-MS m/z: 325.5 (M+H)⁺. Anal Calcd for C₁₇H₁₆N₄O₃: C, 62.95; H, 4.97; N, 17.27; Found: C, 62.98; H, 4.96; N, 17.26.

4.2.23. 6-((4-(1H-Imidazo[4,5-b]pyridin-2-yl)phenyl)amino)-6-oxohexanoic acid (S32): The compound was prepared according to the general procedure B using 4-(3H-imidazo[4,5-b]pyridin-2-yl)aniline 3e (0.2 g, 0.95 mmol), adipic anhydride (0.122 g, 0.95 mmol) to afford 32 (0.22 g, 69% yield) as buff coloured solid. M.P – 259 - 261 oC. ¹H NMR (DMSO-d₆): δ_H 1.42 - 2.32 (m, 8H), 7.03 - 8.30 (m, 7H) 10.16 (s, 1H), 12.65 (b, 1H). ¹³C NMR (DMSO-d₆): δ_c 180.2, 178.7, 161.8, 150.6, 145.3, 138.9, 130.6, 128.2, 123.6, 122.8, 120.2, 38.2, 33.8, 27.5, 23.9. EI-MS m/z: 339.5 (M+H)⁺. Anal Calcd for C₁₈H₁₈N₄O₃: C, 63.89; H, 5.36; N, 16.56; Found: C, 63.92; H, 5.34; N, 16.57.

General procedure for the synthesis of ester derivatives (S6, S11, S16, S21, S26, and S31),

Procedure C: To a well stirred solution of the corresponding carboxylic acid analogues (S1, S10,

S20, S25 and S30) in methanol at 0oC was added catalytic amount of H₂SO₄. The reaction was then heated to reflux for about 5-6 h (monitored by TLC and LCMS for completion). The solvent was removed under vacuum, diluted with water and neutralised with 10% sodium bicarbonate solution to a pH of 7, and extracted repeatedly with ethyl acetate, (any trace amount of acid, if left over was removed by sodium bicarbonate washings) The combined organic layer was then dried over anhydrous sodium sulphate and concentrated under reduced pressure to afford the desired product in good yield and purity as described below.

4.2.24. Methyl 5-((4-(1H-benzo[d]imidazol-2-yl)phenyl)amino)-5-oxopentanoate (S6): The compound was prepared according to the general procedure C using 5-((4-(1H-benzo[d]imidazol-2-yl)phenyl)amino)-5-oxopentanoic acid 1 (0.1 g, 0.31 mmol), to afford 7 (0.23 g, 69% yield) as pale brown solid. M.P – 218 – 220 oC. ¹H NMR (DMSO-d₆): δH 3.82 (s, 3H), 1.77 - 2.37 (m, 6H), 7.25 - 8.21 (m, 8H), 10.14 (s, 1H). ¹³C NMR (DMSO-d₆): δc 173.8, 153.1, 141.6, 139.5, 128.5, 123.8, 121.6, 120.2, 115.8, 52.3, 33.2, 20.5. EI-MS m/z: 338.45 (M+H)⁺. Anal Calcd for C₁₉H₁₉N₃O₃: C, 67.64; H, 5.68; N, 12.46. Found: C, 67.62; H, 5.72; N, 12.45.

4.2.25. Methyl 5-((4-(5-fluoro-1H-benzo[d]imidazol-2-yl)phenyl)amino)-5-oxopentanoate (S11): The compound was prepared according to the general procedure C using 5-((4-(5-fluoro-1H-benzo[d]imidazol-2-yl)phenyl)amino)-5-oxopentanoic acid 10 (0.1 g, 0.29 mmol), to afford 11 (0.2 g, 63% yield) as off white solid. M.P – 244 – 246 oC. ¹H NMR (DMSO-d₆): δH 1.61 – 2.31 (m, 6H), 3.75 (s, 3H), 7.06 - 8.28 (m, 7H) 10.18 (s, 1H). ¹³C NMR (DMSO-d₆): δc 180.2, 173.5, 156.8, 153.2, 140.9, 138.8, 137.6, 128.3, 122.2, 119.6, 117.1, 110.3, 102.2, 52.3, 36.5, 33.1, 20.8. EI-MS m/z: 356.5 (M+H)⁺. Anal Calcd for C₁₉H₁₈FN₃O₃: C, 64.22; H, 5.11; N, 11.82; Found: C, 64.28; H, 5.07; N, 11.80.

4.2.26. Methyl 5-((4-(5-chloro-1H-benzo[d]imidazol-2-yl)phenyl)amino)-5-oxopentanoate

(S16): The compound was prepared according to the general procedure C using 5-((4-(5-chloro-1H-benzo[d]imidazol-2-yl)phenyl)amino)-5-oxopentanoic acid 15 (0.1 g, 0.28 mmol), to afford 16 (0.21 g, 68% yield) as off white solid. M.P – 263 – 265 oC. ¹H NMR (DMSO-d₆): δH 1.82 - 2.32 (m, 6H), 3.85 (s, 3H), 7.21 - 8.43 (m, 7H) 10.19 (s, 1H). ¹³C NMR (DMSO-d₆): δc 180.3, 173.3, 153.4, 138.7, 133.2, 131.2, 129.6, 128.4, 124.3, 122.4, 120.3, 116.7, 115.9, 52.3, 37.3, 32.7, 20.8. EI-MS m/z: 372.4 (M+H)⁺. Anal Calcd for C₁₉H₁₈ClN₃O₃: C, 61.38; H, 4.88; N, 11.30; Found C, 61.42; H, 4.85; N, 11.29.

4.2.27. Methyl 5-((4-(5-nitro-1H-benzo[d]imidazol-2-yl)phenyl)amino)-5-oxopentanoate

(S21): The compound was prepared according to the general procedure C using 5-((4-(5-nitro-1H-benzo[d]imidazol-2-yl)phenyl)amino)-5-oxopentanoic acid 20 (0.1 g, 0.27 mmol), to afford 21 (0.218g, 73% yield) as yellow solid. The compound was prepared according to the general procedure C using 5-((4-(5-nitro-1H-benzo[d]imidazol-2-yl)phenyl)amino)-5-oxopentanoic acid 20 (0.1g, mmol), to afford 21 (0.218 g, 73% yield) as yellow solid. M.P – 275 - 277 oC. ¹H NMR (DMSO-d₆): δH 1.63 - 2.35 (m, 6H), 3.8 3(s, 3H), 7.69 - 8.57 (m, 7H) 10.19 (s, 1H). ¹³C NMR (DMSO-d₆): δc 180.2, 173.3, 153.3, 148.6, 144.6, 140.2, 138.7, 128.3, 122.3, 120.2, 118.9, 116.3, 113.2, 52.3, 37.5, 32.8, 20.8. EI-MS m/z: 383.4 (M+H)⁺. Anal Calcd for C₁₉H₁₈N₄O₅: C, 59.68; H, 4.74 N, 14.65; Found: C, 59.69; H, 4.77 N, 14.62.

4.2.28. Methyl 5-((4-(5-methoxy-1H-benzo[d]imidazol-2-yl)phenyl)amino)-5-oxopentanoate

(S26): The compound was prepared according to the general procedure C using 5-((4-(5-methoxy-1H-benzo[d]imidazol-2-yl)phenyl)amino)-5-oxopentanoic acid 25 (0.1 g, 0.28 mmol), to afford 26 (0.188 g, 61% yield) as brown solid. M.P – 251 – 253 oC. ¹H NMR (DMSO-d₆): δH 1.74 - 2.35 (m, 6H), 3.72 (s, 3H), 3.95 (s, 3H), 7.02 - 8.21 (m, 7H) 10.16 (s, 1H). ¹³C NMR

(DMSO-d₆): δ_c 180.1, 156.7, 153.4, 139.5, 138.6, 134.5, 128.4, 122.3, 120.2, 116.8, 112.1, 100.6, 56.3, 51.5, 37.1, 33.3, 21.2. EI-MS m/z : 368.3 (M+H)⁺. Anal Calcd for C₂₀H₂₁N₃O₄: C, 65.38; H, 5.76; N, 11.44; Found: C, 65.42; H, 5.72; N, 11.46.

4.2.29. Methyl 5-((4-(3H-imidazo[4,5-b]pyridin-2-yl)phenyl)amino)-5-oxopentanoate (S31):

The compound was prepared according to the general procedure C using 5-((4-(3H-imidazo[4,5-b]pyridin-2-yl)phenyl)amino)-5-oxopentanoic acid 30 (0.1 g, 0.31 mmol), to afford 31 (0.23 g, 72% yield) as pale brown solid. M.P – 230 – 232 °C. ¹H NMR (DMSO-d₆): δ_H 1.69 -2.32 (m, 6H), 3.43 (s, 3H), 7.03 - 8.26 (m, 7H) 10.14 (s, 1H). ¹³C NMR (DMSO-d₆): δ_c 180.3, 173.8, 162.3, 150.7, 145.6, 138.7, 130.5, 128.3, 123.9, 122.8, 120.3, 52.4, 37.3, 32.8, 20.8. EI-MS m/z : 339.3 (M+H)⁺. Anal Calcd for C₁₈H₁₈N₄O₃: C, 63.89; H, 5.36; N, 16.56; O, 14.19; Found: C, 63.86; H, 5.39; N, 16.54.

General procedure for the synthesis of oxygen and thio-substituted acyl derivatives (S33 - S44), Procedure D: To a well stirred solution of the corresponding 4-(sub:-1H-benzo[d]imidazol-2-yl)aniline /4-(3H-imidazo[4,5-b]pyridin-2-yl)aniline (3a-f) (1 equiv) and triethylamine (2.5 equiv) in dichloromethane was added the appropriate dicarboxylic acid (1 equiv) followed by propylphosphonic anhydride solution (2.5 equiv; 50% solution in ethyl acetate) at 0°C. The reaction mixture was warmed to room temperature and stirred at room temperature for 8h (monitored by TLC and LCMS for completion). The reaction mixture was then washed with water, brine dried over anhydrous sodium sulphate and concentrated under reduced pressure. The residue obtained was then purified by flash chromatography to afford the desired product in good yield and purity as described below.

4.2.30. 2-(2-((4-(1H-Benzo[d]imidazol-2-yl)phenyl)amino)-2-oxoethoxy)acetic acid (S33):

The compound was prepared according to the general procedure D using 4-(1H-benzo[d]imidazol-2-yl)aniline 3a (0.1 g, 0.48 mmol), triethylamine (0.121 g, 1.2 mmol), 2,2'-oxydiacetic acid (0.064 g, 0.048 mmol) and propylphosponic anhydride solution (0.38 g, 1.2 mmol) to afford 33 (0.188 g, 61% yield) as off white solid. M.P – 244 - 246 oC. ¹H NMR (DMSO-d₆): δH 4.25 (m, 4H), 7.32 - 8.14 (m, 8H), 10.16 (s, 1H), 12.83 (b, 1H). ¹³C NMR (DMSO-d₆): δc 173.2, 170.1, 153.3, 141.5, 139.2, 127.6, 123.3, 122.2, 120.2, 115.5, 69.2, 68.6. EI-MS m/z: 326.4 (M+H)⁺. Anal Calcd for C₁₇H₁₅N₃O₄: C, 62.76; H, 4.65; N, 12.92 Found: C, 62.79; H, 4.64; N, 12.91.

4.2.31. 2-((2-((4-(1H-Benzo[d]imidazol-2-yl)phenyl)amino)-2-oxoethyl)thio)acetic acid (S34):

The compound was prepared according to the general procedure D using 4-(1H-benzo[d]imidazol-2-yl)aniline 3a (0.1 g, 0.48 mmol), triethylamine (0.121 g, 1.2 mmol), 2,2'-thiodiacetic acid (0.072 g, 0.048 mmol) and propylphosponic anhydride solution (0.38 g, 1.2 mmol) to afford 34 (0.231 g, 70% yield) as pale brown solid. M.P – 184 - 186 oC. ¹H NMR (DMSO-d₆): δH 3.22 (s, 2H), 3.6 (s, 2H), 7.54 - 8.34 (m, 8H), 10.15 (s, 1H), 12.93 (b, 1H). ¹³C NMR (DMSO-d₆): δc 175.2, 169.1, 153.2, 141.5, 139, 128.1, 123.2, 121.6, 119.5, 115.7, 44, 42.2. EI-MS m/z: 342.3 (M+H)⁺. Anal Calcd for C₁₇H₁₅N₃O₃S: C, 59.81; H, 4.43; N, 12.31; Found: C, 59.78; H, 4.45

4.2.32. 2-(2-((4-(5-Fluoro-1H-benzo[d]imidazol-2-yl)phenyl)amino)-2-oxoethoxy)acetic acid (S35):

The compound was prepared according to the general procedure D using 4-(5-fluoro-1H-benzo[d]imidazol-2-yl)aniline 3b (0.1 g, 0.44 mmol), triethylamine (0.111 g, 1.1 mmol), 2,2'-oxydiacetic acid (0.059 g, 0.44 mmol) and propylphosponic anhydride solution (0.35 g, 1.1 mmol) to afford 35 (0.186 g, 62% yield) as pale brown solid. M.P – 247 - 249 oC. ¹H NMR

(DMSO-d₆): δH 4.23 (s, 4H), 7.00 - 8.11 (m, 7H) 10.15 (s, 1H), 12.94 (b, 1H). ¹³C NMR (DMSO-d₆): δc 173.3, 170.2, 153.3, 141.1, 139.1, 137.8, 128.2, 122.3, 119.5, 117.2, 110.3, 101.9, 69.2, 68.5. EI-MS m/z: 344.02 (M+H)⁺. Anal Calcd for C₁₇H₁₄FN₃O₄: C, 59.47; H, 4.11; N, 12.24; Found: C, 59.50 H, 4.10; N, 12.25.

4.2.33. 2-((2-((4-(5-Fluoro-1H-benzo[d]imidazol-2-yl)phenyl)amino)-2-oxoethyl)thio)acetic acid (S36): The compound was prepared according to the general procedure D using 4-(5-fluoro-1H-benzo[d]imidazol-2-yl)aniline 3b (0.1 g, 0.44 mmol), triethylamine (0.111 g, 1.1 mmol), 2,2'-thiodiacetic acid (0.066 g, 0.44 mmol) and propylphosponic anhydride solution (0.35 g, 1.1 mmol) to afford 36 (0.203 g, 64% yield) as pale brown solid. M.P – 159 -161 °C. ¹H NMR (DMSO-d₆): δH 3.2 (s, 2H), 3.41 (s, 2H), 7.06 -8.33 (m, 7H) 10.18 (s, 1H), 12.59 (b, 1H). ¹³C NMR (DMSO-d₆): δc 175.1, 168.8, 156.8, 153.2, 140.7, 139.1, 137.5, 128.4, 122.3, 120.2, 117.3, 110.3, 102.8, 44.1, 41.7. EI-MS m/z: 360.6 (M+H)⁺. Anal Calcd for C₁₇H₁₄FN₃O₃S: C, 56.82; H, 3.93; N, 11.69; Found: C, 56.85; H, 3.89; N, 11.71.

4.2.34. 2-(2-((4-(5-Chloro-1H-benzo[d]imidazol-2-yl)phenyl)amino)-2-oxoethoxy)acetic acid (S37): The compound was prepared according to the general procedure D using 4-(5-chloro-1H-benzo[d]imidazol-2-yl)aniline 3c (0.1 g, 0.41 mmol), triethylamine (0.104 g, 1.03 mmol), 2,2'-oxydiacetic acid (0.055 g, 0.41 mmol) and propylphosponic anhydride solution (0.326 g, 1.03 mmol) to afford 37 (0.207 g, 70% yield) as off white solid. M.P – 278 - 280 °C. ¹H NMR (DMSO-d₆): δH 4.26 (s, 4H), 7.26 - 8.48 (m, 7H) 10.11 (s, 1H), 12.80 (b, 1H). ¹³C NMR (DMSO-d₆): δc 173.2, 169.5, 153.4, 138.8, 133.1, 131.5, 129.5, 127.9, 124.5, 122.2, 120.2, 116.8, 115.9, 69.3 67.8. EI-MS m/z: 360.7 (M+H)⁺. Anal Calcd for C₁₇H₁₄ClN₃O₄: C, 56.75; H, 3.92 N, 11.68; Found C, 56.79; H, 3.88 N, 11.69.

4.2.35. 2-((2-((4-(5-Chloro-1H-benzo[d]imidazol-2-yl)phenyl)amino)-2-oxoethyl)thio)acetic acid (S38): The compound was prepared according to the general procedure D using 4-(5-chloro-1H-benzo[d]imidazol-2-yl)aniline 3c (0.1 g, 0.41 mmol), triethylamine (0.104 g, 1.03 mmol), 2,2'-thiodiacetic acid (0.062 g, 0.41 mmol) and propylphosponic anhydride solution (g, 1.03 mmol) to afford 38 (0.227 g, 74% yield) as off white solid. M.P – 278 - 280 oC. ¹H NMR (DMSO-d₆): δH 3.21 (s, 2H), 3.40 (s, 2H), 7.24 - 8.39 (m, 7H) 10.18 (s, 1H), 12.65 (b, 1H). ¹³C NMR (DMSO-d₆): δc 174.8, 168.6, 153.2, 138.7, 133.2, 131.2, 129.4, 128.2, 124.5, 122.2, 120.3, 116.8, 115.9, 43.8, 41.4. EI-MS m/z: 376.3 (M+H)⁺. Anal Calcd for C₁₇H₁₄ClN₃O₃S: C, 54.33; H, 3.75 N, 11.18; Found: C, 54.35; H, 3.77 N, 11.14.

4.2.36. 2-(2-((4-(5-Nitro-1H-benzo[d]imidazol-2-yl)phenyl)amino)-2-oxoethoxy)acetic acid (S39): The compound was prepared according to the general procedure D using 4-(5-chloro-1H-benzo[d]imidazol-2-yl)aniline 3d (0.1 g, 0.39 mmol), triethylamine, (0.1 g, 0.98 mmol), 2,2'-oxydiacetic acid (0.053 g, 0.39 mmol) and propylphosponic anhydride solution (0.313 g, 0.98 mmol) to afford 39 (0.173 g, 59% yield) as yellow solid. M.P – 251 – 253 oC. ¹H NMR (DMSO-d₆): δH 4.23 (s, 4H), 7.72 - 8.55 (m, 7H), 10.15 (s, 1H), 12.58 (b, 1H). ¹³C NMR (DMSO-d₆): δc 173.2, 169.8, 153.2, 147.9, 144.6, 140.2, 138.1, 122.2, 128.3, 119.9, 118.7, 116.5, 113.2, 69.2, 68.2. EI-MS m/z: 371.3 (M+H)⁺. Anal Calcd for C₁₇H₁₄N₄O₆: C, 55.14; H, 3.81; N, 15.13; Found: C, 55.16; H, 3.79; N, 15.12

4.2.37. 2-((2-((4-(5-Nitro-1H-benzo[d]imidazol-2-yl)phenyl)amino)-2-oxoethyl)thio)acetic acid (S40): The compound was prepared according to the general procedure D using 4-(5-chloro-1H-benzo[d]imidazol-2-yl)aniline 3d (0.1 g, 0.39 mmol), triethylamine (0.1 g, 0.98 mmol), 2,2'-thiodiacetic acid (0.059 g, 0.39 mmol) and propylphosponic anhydride solution (0.313 g, 0.98 mmol) to afford 40 (0.173 g, 57% yield) as yellow solid. M.P – 231 – 233 oC. ¹H

NMR (DMSO-d₆): δ_H 3.25 (s, 2H), 3.39 (s, 2H), 7.69 -8.52 (m, 7H), 10.14 (s, 1H), 12.68 (b, 1H). ¹³C NMR (DMSO-d₆): δ_c 174.8, 168.5, 153.2, 148.2, 144.5, 140.1, 138.8, 128.1, 122.3, 120.2, 118.7, 116.5, 113.3, 43.8, 41.5. EI-MS m/z: 387.6 (M+H)⁺. Anal Calcd for C₁₇H₁₄N₄O₅S: C, 52.84; H, 3.65; N, 14.50; Found C, 52.86; H, 3.63; N, 14.52.

4.2.38. 2-(2-((4-(5-Methoxy-1H-benzo[d]imidazol-2-yl)phenyl)amino)-2-oxoethoxy)acetic acid (S41): The compound was prepared according to the general procedure D using 4-(5-methoxy-1H-benzo[d]imidazol-2-yl)aniline 3e (0.1 g, 0.42 mmol), triethylamine (0.11 g, 1.05 mmol), 2,2'-oxydiacetic acid (0.056 g, 0.42 mmol) and propylphosponic anhydride solution (0.332 g, 1.05 mmol) to afford 41 (0.208 g, 70% yield) as buff coloured solid. M.P - 234 – 236 °C. ¹H NMR (DMSO-d₆): δ_H 4.26 (s, 4H), 3.91 (s, 3H), 7.03 - 8.24 (m, 7H) 10.15 (s, 1H), 12.65 (b, 1H). ¹³C NMR (DMSO-d₆): δ_c 171.3, 165.8, 155.8, 153.2, 139.8, 138.2, 134.8, 128.3, 122.3, 119.8, 115.8, 112.2, 100.3, 68.5, 56.8. EI-MS m/z: 356.3 (M+H)⁺. Anal Calcd for C₁₈H₁₇N₃O₅: C, 60.84; H, 4.82; N, 11.83; Found: C, 60.87; H, 4.79; N, 11.85

4.2.39. 2-((2-((4-(5-Methoxy-1H-benzo[d]imidazol-2-yl)phenyl)amino)-2-oxoethyl)thio)acetic acid (S42): The compound was prepared according to the general procedure D using 4-(5-methoxy-1H-benzo[d]imidazol-2-yl)aniline 3e (0.1 g, 0.42 mmol), triethylamine (0.11 g, 1.05 mmol), 2,2'-thiodiacetic acid (0.063 g, 0.42 mmol) and propylphosponic anhydride solution (0.332 g, 1.05 mmol) to afford 42 (0.189 g, 61% yield) as dark brown solid. M.P - 250 – 252 °C. ¹H NMR (DMSO-d₆): δ_H 3.26 (s, 2H), 3.39 (s, 2H), 3.92 (s, 3 H), 7.09 - 8.29 (m, 7H) 10.11 (s, 1H), 12.81 (b, 1H). ¹³C NMR (DMSO-d₆): δ_c 174.8, 169.1, 156.7, 153.1, 140.2, 138.7, 133.9, 128.2, 122.3, 120.2, 115.9, 111.8, 101.3, 56.3, 44.2, 41.8. EI-MS m/z: 372.5 (M+H)⁺. Anal Calcd for C₁₈H₁₇N₃O₄S: C, 58.21; H, 4.61; N, 11.31; Found: C, 58.25; H, 4.65; N, 11.30.

4.2.40. 2-(2-((4-(3H-Imidazo[4,5-b]pyridin-2-yl)phenyl)amino)-2-oxoethoxy)acetic acid

(S43): The compound was prepared according to the general procedure D using 4-(3H-imidazo[4,5-b]pyridin-2-yl)aniline 3f (0.1 g, 0.48 mmol), triethylamine, acid (0.12 g, 1.2 mmol), 2,2'-oxydiacetic acid (0.063 g, 0.48 mmol) and propylphosponic anhydride solution (0.38 g, 1.2 mmol) to afford 43 (0.228 g, 73% yield) as pale brown solid. M.P – 273 – 275 oC. ¹H NMR (DMSO-d₆): δH 4.21 (s, 4H), 7.03 - 8.26 (m, 7H) 10.16 (s, 1H), 12.61 (b, 1H). ¹³C NMR (DMSO-d₆): δc 173.4, 169.8, 162.2, 150.7, 145.6, 138.8, 130.8, 128.9, 123.8, 122.6, 120.3, 70.2, 67.8. EI-MS m/z: 327.4 (M+H)⁺. Anal Calcd for C₁₆H₁₄N₄O₄: C, 58.89; H, 4.32; N, 17.17; Found: C, 58.91; H, 4.30; N, 17.19.

4.2.41. 2-((2-((4-(3H-Imidazo[4,5-b]pyridin-2-yl)phenyl)amino)-2-oxoethyl)thio)acetic acid

(S44): The compound was prepared according to the general procedure D using 4-(3H-imidazo[4,5-b]pyridin-2-yl)aniline 3f (0.1 g, 0.48 mmol), triethylamine, acid (0.12 g, 1.2 mmol), 2,2'-thiodiacetic acid (0.071 g, 0.48 mmol) and propylphosponic anhydride solution (0.38 g, 1.2 mmol) to afford 44 (0.232 g, 71% yield) as brown solid. M.P – 250 – 252 oC. ¹H NMR (DMSO-d₆): δH 3.26 (s, 2H), 3.39 (s, 2H), 7.02 - 8.27 (m, 7H) 10.14 (s, 1H), 12.73 (b, 1H). ¹³C NMR (DMSO-d₆): δc 174.8, 168.5, 161.8, 150.6, 145.3, 138.8, 130.8, 128.5, 123.8, 122.6, 120.2, 43.8, 41.5. EI-MS m/z: 343.5 (M+H)⁺. Anal Calcd for C₁₆H₁₄N₄O₃S: C, 56.13; H, 4.12; N, 16.36; Found: C, 56.16; H, 4.09; N, 16.38.

Annexure-III

Experimental Procedure for lead molecule (B1):

General procedure for the preparation of tert-Butyl 4-aminophenylcarbamate (T2): To a stirred solution of compound T1 (10 g, 92 mmol) and triethylamine (Et₃N) (22 ml, 157 mmol) in 100 mL of N,N dimethyl formamide (DMF), Boc-anhydride (15.4 ml, 0.070 mol) was added slowly at room temperature and allowed to stir at room temperature for 6 h. Reaction completion was monitored by TLC after completion, DMF was removed by high vacuum pump and diluted with ice cold water (150 mL) and extracted with dichloromethane (DCM), organic layer was concentrated under reduced pressure obtained pale brown solid further purified by flash column chromatography by silica gel [230-400 mesh] using ethyl acetate (15- 25 %) in petroleum ether as eluent to afford an off-white solid (6.5 g, 70 %). ESI-MS was found 209.34 [M+H] and carried to next step.

General procedure for the preparation of tert-Butyl 4-(5-substituted-5-membered heterocyclic-2-carboxamido)phenylcarbamates (3a-h): Procedure A: To a solution of compound T2 (1 equiv) and Et₃N (3 equiv) in DCM (20 mL) at 0°C, corresponding heterocyclic acid chloride (I-VIII) was added slowly over a period of 10 min under N₂↑, TLC analysis indicated that the reaction was complete, to the reaction mass ice cold water (15 mL) was added. The organic layer was separated, washed with brine (15 mL) and dried over anhydrous sodium sulphate. The organic layer was concentrated under reduced pressure to afford crude solid, which was purified by flash column chromatography by silica gel [230-400 mesh] using ethyl acetate (15- 40 %) in petroleum ether as eluent to afford compound T3 as solid in good yields. Further Boc de-protection of compound 3 by trifluoroacetic acid (TFA) (15 mL) in DCM (10 mL)

at 0 °C to room temperature for 4h. After completion of reaction, TFA was removed under reduced pressure, to this crude crushed ice was added and basified with 5% sodiumhydroxide solution (10 mL) and extracted with dry DCM to get the corresponding amine compound and proceeded to further step without any purification.

Preparation of tert-Butyl (4-(furan-2-carboxamido)phenyl)carbamate (3a): The compound was prepared according to the general procedure A using compound 2 (1g, 4.8 mmol), Et₃N (2 mL, 14.4 mmol) and furan-2-carbonyl chloride (I) (0.66g, 5 mmol) as an off-white solid; Yield (1.11g, 77%); ESI-MS was found at m/z 303.21 [M+H]⁺. ¹H NMR (CDCl₃-300 MHz) δ_H. 10.12 (s, 2H), 8.07 (m, 1H), 7.62-7.57 (m, 4H), 7.26-6.80 (m, 2H), 1.34 (s, 9H).

Preparation of tert-Butyl (4-(5-methylfuran-2-carboxamido)phenyl)carbamate (3b): The compound was prepared according to the general procedure A using compound 2 (1g, 4.8 mmol), Et₃N (2 mL, 14.4 mmol) and 5-methylfuran-2-carbonyl chloride (0.73g, 5 mmol) as an off-white solid; Yield (1.06g, 70%); ESI-MS was found at m/z 317.42 [M+H]⁺. ¹H NMR (CDCl₃-300 MHz) δ_H. 10.01 (s, 2H), 7.61-7.56 (m, 4H), 7.24-6.78 (m, 2H), 2.36 (s, 3H), 1.38 (s, 9H).

Preparation of tert-Butyl (4-(5-nitrofuran-2-carboxamido)phenyl)carbamate (3c): The compound was prepared according to the general procedure A using compound 2 (1g, 4.8 mmol), Et₃N (2 mL, 14.4 mmol) and 5-nitrofuran-2-carbonyl chloride (II) (0.88g, 5 mmol) as Pale yellow solid; Yield (1.2g, 72%); ESI-MS was found at m/z 346.36 [M-H]⁺. ¹H NMR (CDCl₃-300 MHz) δ_H. 10.23 (s, 2H), 7.69-7.58 (m, 4H), 7.28-6.81 (m, 2H), 1.33 (s, 9H).

Preparation of tert-Butyl (4-(thiophene-2-carboxamido)phenyl)carbamate (3d): The compound was prepared according to the general procedure A using compound 2 (1g, 4.8 mmol), Et₃N (2 mL, 14.4 mmol) and thiophene-2-carbonyl chloride (III) (0.74g, 5 mmol) as Pale

brown solid; Yield (1.2g, 76%); ESI-MS was found at m/z 319.14 $[M+H]^+$. 1H NMR ($CDCl_3$ -300 MHz) δ_H . 10.11 (s, 2H), 8.28-8.16 (m, 2H), 7.67-7.55 (m, 4H), 7.28 (m, 1H), 1.37 (s, 9H).

Preparation of tert-Butyl (4-(5-methylthiophene-2-carboxamido)phenyl)carbamate (3e):

The compound was prepared according to the general procedure A using compound **2** (1g, 4.8 mmol), Et_3N (2 mL, 14.4 mmol) and 5-methylthiophene-2-carbonyl chloride (IV) (0.81g, 5 mmol) as an off-white solid; Yield (1.2g, 75%); ESI-MS was found at m/z 333.34 $[M+H]^+$. 1H NMR ($CDCl_3$ -300 MHz) δ_H . 10.13 (s, 2H), 7.78 (m, 1H), 7.62-7.58 (m, 4H), 7.03 (m, 1H), 2.38 (s, 3H), 1.35 (s, 9H).

Preparation of tert-Butyl (4-(5-nitrothiophene-2-carboxamido)phenyl)carbamate (3f):

The compound was prepared according to the general procedure A using compound **2** (1g, 4.8 mmol), Et_3N (2 mL, 14.4 mmol) and 5-nitrothiophene-2-carbonyl chloride (V) (0.96g, 5 mmol) as pale yellow solid; Yield (1.3g, 78%); ESI-MS was found at m/z 364.34 $[M+H]^+$. 1H NMR ($CDCl_3$ -300 MHz) δ_H . 10.15 (s, 2H), 8.17-7.81 (m, 2H), 7.68-7.60 (m, 4H), 1.38 (s, 9H).

Preparation of tert-Butyl (4-(1H-pyrrole-2-carboxamido)phenyl)carbamate (3g):

The compound was prepared according to the general procedure A using compound **2** (1g, 4.8 mmol), Et_3N (2 mL, 14.4 mmol) and 1H-pyrrole-2-carbonyl chloride (VI) (0.65g, 5 mmol) as brown solid; Yield (1g, 68%); ESI-MS was found at m/z 302.24 $[M+H]^+$. 1H NMR ($CDCl_3$ -300 MHz) δ_H . 10.06 (s, 2H), 7.70-7.59 (m, 4H), 7.56-6.43 (m, 3H), 4.98 (s, 1H), 1.36 (s, 9H).

Preparation of tert-Butyl (4-(tetrahydrofuran-2-carboxamido)phenyl)carbamate (3h):

The compound was prepared according to the general procedure A using compound **2** (1g, 4.8 mmol), Et_3N (2 mL, 14.4 mmol) and tetrahydrofuran-2-carbonyl chloride (VII) (0.68g, 5 mmol) as brown solid; Yield (1g, 66%); ESI-MS was found at m/z 307.43 $[M+H]^+$. 1H NMR ($CDCl_3$ -

300 MHz) δ_{H} . 10.06 (s, 1H), 7.64-7.56 (m, 4H), 7.21 (s, 1H), 4.68-3.72 (m, 3H), 2.25-1.93 (m, 4H), 1.37 (s, 9H).

General procedure for the preparation of 4-((4-(5-Substituted-5-membered heterocyclic -2-carboxamido)phenyl)amino)-4-oxobutanoic acid (T5-T12): Procedure B: Compound 3 (1 equiv) was taken in anhydrous tetrahydrofuran (THF) (15 mL) to this succinic anhydride (1 equiv), 4 Å molecular sieves (2 equiv/wt) were added and subjected to microwave irradiation in Biotage microwave initiator with stirring at 165 °C for 0.5h. After completion of reaction (monitored by TLC) organic layer was filtered through celite bed and removed under reduced pressure, diluted with water (15 mL) to this solid bicarbonate was added until the P^{H} reaches to ~9. The aqueous layer washed with DCM (2*20 mL) to remove impurities then acidified with 2N HCl until the P^{H} reaches to 3-5 to get solid which was recrystallized from ethanol to afford the desired acid derivative in moderate yield.

Preparation of 4-((4-(Furan-2-carboxamido)phenyl)amino)-4-oxobutanoic acid (T5): The compound was prepared according to the general procedure B using N-(4-aminophenyl)furan-2-carboxamide (4a) (1g, 5 mmol), succinic anhydride (0.5g, 5 mmol), 2g of 4 Å molecular sieves as an off-white solid; Yield (0.97g, 65%); ^1H NMR (DMSO- d_6): δ_{H} . 2.52-2.56 (m, 4H), 6.70-6.78 (m, 1H), 7.12 ($J = 2.0$ Hz, d, 1H), 7.58-7.62 (m, 4H), 7.91 (2.2 Hz, d, 1H), 10.1 (s, 2H), 12.1 (b, 1H). ^{13}C NMR (DMSO- d_6): δ_{C} . 177.5, 173.5, 162.2, 148.1, 143.3, 134.4, 133.2, 122.1 (2C), 121.5 (2C), 115.4, 111.6, 30.4, 28.2. EI-MS m/z (Calcd. for $\text{C}_{15}\text{H}_{14}\text{N}_2\text{O}_5$: 302.09); Found: 301.13 (M-H) $^-$. Anal Calcd. for $\text{C}_{15}\text{H}_{14}\text{N}_2\text{O}_5$ C, 59.60; H, 4.67; N, 9.27; Found: C, 60.00; H, 4.57; N, 9.23.

Preparation of 4-((4-(5-Methylfuran-2-carboxamido)phenyl)amino)-4-oxobutanoic acid

(T6): The compound was prepared according to the general procedure B using N-(4-aminophenyl)-5-methylfuran-2-carboxamide (**4b**) (1g, 4.6 mmol), succinic anhydride (0.46g, 4.6 mmol), 2g of 4 Å molecular sieves as an off-white solid; Yield (0.96g, 66%); ¹H NMR (DMSO-d₆): δ_H. 2.37 (s, 3H), 2.52-2.54 (m, 4H), 6.3 (*J* = 2.4 Hz, d, 1H), 7.2 (*J* = 2.1 Hz, d, 1H), 7.5 (*J* = 2.9 Hz, d, 2H), 7.6 (*J* = 3.9 Hz, d, 2H), 9.92-9.94 (s, 2H), 12.1 (s, 1H). ¹³C NMR (DMSO-d₆): δ_C. 177.6, 173.6, 162.0, 157.3, 145.0, 134.0, 133.0, 122.5 (2C), 121.8 (2C), 114.0, 108.1, 30.5, 28.1, 13.1. EI-MS *m/z* (Calcd. for C₁₆H₁₆N₂O₅: 316.11); Found: 317.45 (M+H)⁺. Anal Calcd for C₁₆H₁₆N₂O₅: C, 60.75; H, 5.10; N, 8.86; Found: C, 60.81; H, 5.11; N, 8.85.

Preparation of 4-((4-(5-Nitrofuran-2-carboxamido)phenyl)amino)-4-oxobutanoic acid (T7):

The compound was prepared according to the general procedure B using N-(4-aminophenyl)-5-nitrofuran-2-carboxamide (**4c**) (1g, 4 mmol), succinic anhydride (0.4g, 4 mmol), 2g of 4 Å molecular sieves as an off-white solid; Yield (0.91g, 65%); ¹H NMR (DMSO-d₆): δ_H. 2.52-2.56 (m, 4H), 7.54-7.66 (m, 4H), 7.91-8.03 (m, 2H), 9.92-9.99 (s, 2H), 11.57 (s, 1H). ¹³C NMR (DMSO-d₆): δ_C. 177.7, 174.1, 165.3, 154.2, 134.8, 133.3, 122.9 (2C), 122.3 (2C), 116.3, 115.8, 30.3, 28.4. EI-MS *m/z* (Calcd. For C₁₅H₁₃N₃O₇: 347.08); Found: 348.27 (M+H)⁺. Anal Calcd for C₁₅H₁₃N₃O₇: C, 51.88; H, 3.77; N, 12.10; Found: C, 51.57; H, 3.82; N, 12.19.

Preparation of 4-oxo-4-((4-(Thiophene-2-carboxamido)phenyl)amino)butanoic acid (T8):

The compound was prepared according to the general procedure B using N-(4-aminophenyl)thiophene-2-carboxamide (**4d**) (1g, 4.6 mmol), succinic anhydride (0.46g, 4.6 mmol), 2g of 4 Å molecular sieves as an off-white solid; Yield (0.92g, 63%); ¹H NMR (DMSO-d₆): δ_H. 2.51-2.54 (m, 4H), 7.26-7.28 (m, 1H), 7.51 (*J* = 2.5 Hz, d, 2H), 7.56 (*J* = 2.9 Hz, d, 2H), 8.13-8.21 (m, 2H), 9.95 (s, 2H), 12.0 (s, 1H). ¹³C NMR (DMSO-d₆): δ_C. 177.6, 172.7,

161.4, 140.0, 134.6, 133.2, 131.7, 130.2, 129.1, 122.7 (2C), 122.0 (2C), 30.3, 28.6. EI-MS m/z (Calcd. For $C_{15}H_{14}N_2O_4S$: 318.07; Found: 319.20 (M+H)⁺. Anal Calcd for $C_{15}H_{14}N_2O_4S$: C, 56.59, H, 4.43; N, 8.80; Found: C, 56.60; H, 4.37; N, 8.84.

Preparation of 4-((4-(5-Methylthiophene-2-carboxamido)phenyl)amino)-4-oxobutanoic acid (T9): The compound was prepared according to the general procedure B using N-(4-aminophenyl)-5-methylthiophene-2-carboxamide (**4e**) (1g, 4.3 mmol), succinic anhydride (0.43g, 4.3 mmol), 2g of 4 Å molecular sieves as an off-white solid; Yield (0.96g, 67%); ¹H NMR (DMSO- d_6): δ_H . 2.56 (s, 3H), 2.57-2.73 (m, 4H), 6.97 ($J = 2.7$ Hz, d, 1H), 7.55-7.68 (m, 4H), 7.80 ($J = 2.9$ Hz, d, 1H), 9.98 (s, 2H), 12.0 (s, 1H). ¹³C NMR (DMSO- d_6): δ_C . 177.8, 173.9, 161.9, 160.1, 162.3, 134.8, 133.2, 129.7, 128.6, 122.8 (2C), 122.2 (2C), 30.7, 28.8, 15.6. EI-MS m/z (Calcd. For $C_{16}H_{16}N_2O_4S$: 332.37) ; Found: 333.39 (M+H)⁺. Anal Calcd for $C_{16}H_{16}N_2O_4S$: C, 57.82; H, 4.85; N, 8.43; Found: C, 57.84; H, 4.76; N, 8.53.

Preparation of 4-((4-(5-Nitrothiophene-2-carboxamido)phenyl)amino)-4-oxobutanoic acid (T10): The compound was prepared according to the general procedure B using N-(4-aminophenyl)-5-nitrothiophene-2-carboxamide (**4f**) (1g, 3.8 mmol), succinic anhydride (0.38g, 3.8 mmol), 2g of 4 Å molecular sieves as an off-white solid; Yield (0.94g, 68%); ¹H NMR (DMSO- d_6): δ_H . 2.56-2.68 (m, 4H), 7.57-7.83 (m, 4H), 7.89 ($J = 2.7$ Hz, d, 1H), 8.21 ($J = 2.5$ Hz, d, 1H), 10.22 (s, 2H), 12.10 (s, 1H). ¹³C NMR (DMSO- d_6): δ_C . 177.9, 173.5, 161.8, 161.3, 145.7, 138.9, 134.6, 133.3, 130.3, 122.8 (2C), 122.3 (2C), 30.6, 28.9. EI-MS m/z (Calcd. $C_{15}H_{13}N_3O_6S$: 363.05; Found: 364.13 (M+H)⁺. Anal Calcd for $C_{15}H_{13}N_3O_6S$: C, 49.58; H, 3.61; N, 11.56; Found: C, 49.62; H, 3.53; N, 11.47.

Preparation of 4-((4-(1H-Pyrrole-2-carboxamido)phenyl)amino)-4-oxobutanoic acid (T11):

The compound was prepared according to the general procedure B using N-(4-aminophenyl)-1H-pyrrole-2-carboxamide (**4g**) (1g, 5 mmol), succinic anhydride (0.5g, 5 mmol), 2g of 4 Å molecular sieves as an off-white solid; Yield (0.91g, 61%); ¹H NMR (DMSO-d₆): δ_H. 2.56-2.78 (m, 4H), 6.42-6.49 (m, 1H), 7.47 (*J* = 2.6 Hz, d, 1H), 7.58 (*J* = 3.0 Hz, d, 1H), 7.60-7.68 (m, 4H), 9.98 (s, 2H), 11.50 (s, 1H), 12.06 (s, 1H). ¹³C NMR (DMSO-d₆): δ_C. 177.6, 173.8; 162.4, 134.7, 133.6, 127.5, 122.5 (2C), 121.6 (3C), 110.6, 110.0, 30.6, 28.6. EI-MS *m/z* (Calcd. for C₁₅H₁₅N₃O₄: 301.11; Found: 302.46 (M+H)⁺. Anal Calcd for C₁₅H₁₅N₃O₄; C, 59.79; H, 5.02; N, 13.95; Found: C, 59.82; H, 5.03; N, 13.89.

Preparation of 4-oxo-4-((4-(Tetrahydrofuran-2-carboxamido)phenyl)amino)butanoic acid (T12):

The compound was prepared according to the general procedure B using N-(4-aminophenyl)tetrahydrofuran-2-carboxamide (**4h**) (1g, 4.8 mmol), succinic anhydride (0.48g, 4.8 mmol), 2g of 4 Å molecular sieves as an off-white solid; Yield (0.97g, 65%); ¹H NMR (DMSO-d₆): δ_H. 1.81-1.92 (m, 2H), 2.04-2.32 (m, 2H), 2.58-2.82 (m, 4H), 3.70-3.82 (m, 2H), 4.71 (m, 1H), 7.62-7.69 (m, 4H), 10.03 (s, 2H), 12.17 (s, 1H). ¹³C NMR (DMSO-d₆): δ_C. 177.6, 173.7, 171.1, 134.3, 122.6 (2C), 122.2 (2C), 84.7, 67.7, 31.8, 30.1, 28.7, 24.8. EI-MS *m/z* (Calcd. for C₁₅H₁₈N₂O₅: 306.12; Found: 307.26 (M+H)⁺. Anal Calcd for C₁₅H₁₈N₂O₅; C, 58.82; H, 5.92; N, 9.15; Found: C, 58.84; H, 5.94; N, 9.17.

General procedure for the preparation of Methyl 4-((4-(5-substituted-5-membered heterocyclic -2-carboxamido)phenyl)amino)-4-oxobutanoate (T13-T20): Procedure C: The

compound **5** (0.5g) was taken in methanol (20 ml) and kept at 0 °C to this catalytic amount of sulphuric acid (1-3 drops) was added and refluxed for 5-6h (monitored by TLC). After completion of the reaction the solvent was removed under vacuum, diluted with water and

neutralised with 10% sodium bicarbonate solution to a pH of 7, and extracted with ethyl acetate (3*20 mL). The combined organic layer was then dried over anhydrous sodium sulphate and concentrated under reduced pressure to afford the desired product in good yield.

Preparation of Methyl 4-((4-(Furan-2-carboxamido)phenyl)amino)-4-oxobutanoate (T13):

The compound was prepared according to the general procedure C using **5a** (0.5g, 1.6 mmol) to get an off-white solid. Yield (0.35g, 68%); ¹H NMR (DMSO-d₆): δ_H. 2.52-2.54 (m, 4H), 3.65 (s, 3H), 6.69-6.71 (m, 1H), 7.02 (*J* = 2.2 Hz, d, 1H), 7.41-7.50 (m, 4H), 7.89 (*J* = 2.1 Hz, d, 1H), 10.10-10.17 (s, 2H). ¹³C NMR (DMSO-d₆): δ_C. 177.3, 173.2, 162.1, 147.8, 143.2, 134.2, 133.4, 122.3 (2C), 121.8 (2C), 115.4, 112.1, 50.9, 32.4, 28.7. EI-MS *m/z* (Calcd. for C₁₆H₁₆N₂O₅: 316.11); Found: 317.33 (M+H)⁺. Anal Calcd. for C₁₆H₁₆N₂O₅: C, 60.75; H, 5.10; N, 8.86; Found; C, 60.68; H, 5.09; N, 8.78.

Preparation of Methyl 4-(4-(5-Methylfuran-2-carboxamido)phenylamino)-4-oxobutanoate (T14):

The compound was prepared according to the general procedure C using **5b** (0.5g, 1.6 mmol) to get an off-white solid. Yield (0.35g, 67%); ¹H NMR (DMSO-d₆): δ_H. 2.29 (s, 3H), 2.53-2.54 (m, 4H), 3.67 (s, 3H), 6.27 (*J* = 2.5 Hz, d, 1H), 7.21 (*J* = 2.6 Hz, d, 1H), 7.42 (*J* = 2.6 Hz, d, 2H), 7.51 (*J* = 3.7 Hz, d, 2H), 9.94-10.1 (s, 2H). ¹³C NMR (DMSO-d₆): δ_C. 178.1, 172.8, 163.8, 158.1, 145.2, 134.5, 133.2, 122.3 (2C), 121.6 (2C), 115.1, 107.8, 60.3, 32.4, 28.6, 16.0. EI-MS *m/z* (Calcd. for C₁₇H₁₈N₂O₅ 330.13); Found: 331.16 (M+H)⁺. Anal Calcd. for C₁₇H₁₈N₂O₅: C, 61.81; H, 5.49; N, 8.48; Found; C, 61.94; H, 5.42; N, 8.52.

Preparation of Methyl 4-(4-(5-Nitrofuran-2-carboxamido)phenylamino)-4-oxobutanoate (T15):

The compound was prepared according to the general procedure C using **5c** (0.5g, 1.4 mmol) to get an yellow solid; Yield (0.37g, 72 %); ¹H NMR (DMSO-d₆): δ_H. 2.52-2.53 (m, 4H),

3.55 (s, 3H), 7.57 ($J = 3.1$ Hz, d, 2H), 7.64 ($J = 2.3$ Hz, d, 1H), 7.91-8.02 (m, 2H), 9.82-9.90 (s, 2H). ^{13}C NMR (DMSO- d_6): δ_{C} . 177.5, 173.5, 162.8, 154.2, 151.1, 134.0, 133.2, 122.4 (2C), 121.9 (2C), 116.4, 116.0, 52.3, 31.5, 28.7. EI-MS m/z (Calcd. For $\text{C}_{16}\text{H}_{15}\text{N}_3\text{O}_7$: 361.01); Found: 362.05 (M+H) $^+$. Anal Calcd for $\text{C}_{16}\text{H}_{15}\text{N}_3\text{O}_7$: C, 53.19; H, 4.18; N, 11.63; Found: C, 53.24; H, 4.22; N, 11.67.

Preparation of Methyl 4-oxo-4-((4-(Thiophene-2-carboxamido)phenyl)amino)butanoate (T16): The compound was prepared according to the general procedure C using **5d** (0.5g, 1.6 mmol) to get an off white solid; Yield (0.36g, 70 %); ^1H NMR (DMSO- d_6): δ_{H} . 2.51-2.55 (m, 4H), 3.68 (s, 3H), 7.28 (m, 1H), 7.51 ($J = 3.1$ Hz, d, 2H), 7.6 ($J = 3.7$ Hz, d, 2H), 8.16 ($J = 2.4$ Hz, d, 1H), 8.31 ($J = 2.7$ Hz, d, 1H), 9.8 (s, 2H). ^{13}C NMR (DMSO- d_6): δ_{C} . 177.6, 173.6, 161.9, 139.6, 134.1, 133.4, 132.0, 130.3, 129.1, 122.9 (2C), 122.4 (2C), 52.0, 31.8, 29.0. EI-MS m/z (Calcd. For $\text{C}_{16}\text{H}_{16}\text{N}_2\text{O}_4\text{S}$: 332.38; Found: 333.09 (M+H) $^+$). Anal Calcd for $\text{C}_{16}\text{H}_{16}\text{N}_2\text{O}_4\text{S}$: C, 57.82; H, 4.85; N, 8.43; Found: C, 57.81; H, 4.82; N, 8.41.

Preparation of Methyl 4-(4-(5-Methylthiophene-2-carboxamido)phenylamino)-4-oxobutanoate (T17): The compound was prepared according to the general procedure C using **5e** (0.5g, 1.5 mmol) to get pale brown solid; Yield (0.35g, 68 %); ^1H NMR (DMSO- d_6): δ_{H} . 2.34 (s, 3H), 2.56-2.64 (m, 4H), 3.59 (s, 3H), 7.0 ($J = 2.6$ Hz, d, 1H), 7.58-7.67 (m, 4H), 7.79 ($J = 2.7$ Hz, d, 1H), 10.11 (s, 2H). ^{13}C NMR (DMSO- d_6): δ_{C} . 177.8, 173.7, 162.0, 152.8, 135.8, 134.7, 133.2, 130.1, 128.5, 122.5 (2C), 121.9 (2C), 60.2, 31.6, 28.9, 15.0. EI-MS m/z (Calcd. For $\text{C}_{17}\text{H}_{18}\text{N}_2\text{O}_4\text{S}$: 346.10); Found: 347.23 (M+H) $^+$. Anal Calcd for $\text{C}_{17}\text{H}_{18}\text{N}_2\text{O}_4\text{S}$: C, 58.94; H, 5.24; N, 8.09; Found: C, 58.82; H, 5.26; N, 8.10.

Preparation of Methyl 4-(4-(5-Nitrothiophene-2-carboxamido)phenylamino)-4-oxobutanoate (T18): The compound was prepared according to the general procedure C using **5f** (0.5g, 1.4 mmol) to get an yellow solid; Yield (0.30g, 65 %); ^1H NMR (DMSO- d_6): δ_{H} . 2.59-2.65 (m, 4H), 3.71 (s, 3H), 7.65-7.78 (m, 4H), 8.01 ($J = 2.6$ Hz, d, 1H), 8.21 ($J = 3.0$ Hz, d, 1H), 10.11-10.27 (s, 2H). ^{13}C NMR (DMSO- d_6): δ_{C} . 177.8, 173.6, 161.9, 160.8, 146.2, 138.9, 134.9, 133.4, 130.8, 122.5 (2C), 121.9 (2C), 59.9, 32.2, 29.0. EI-MS m/z (Calcd. For $\text{C}_{16}\text{H}_{15}\text{N}_3\text{O}_6\text{S}$: 377.07; Found: 378.28 (M+H) $^+$. Anal Calcd for $\text{C}_{16}\text{H}_{15}\text{N}_3\text{O}_6\text{S}$: C, 50.92; H, 4.01; N, 11.13; Found: C, 50.98; H, 4.04; N, 11.15.

Preparation of Methyl 4-(4-(1H-Pyrrole-2-carboxamido)phenylamino)-4-oxobutanoate (T19): The compound was prepared according to the general procedure C using **5g** (0.5g, 1.6 mmol) to get an off white solid; Yield (0.34g, 65 %); ^1H NMR (DMSO- d_6): δ_{H} . 2.60-2.65 (m, 4H), 3.78 (s, 3H), 6.46-6.49 (m, 1H), 7.48 ($J = 2.6$ Hz, d, 1H), 7.58 ($J = 2.8$ Hz, d, 1H), 7.61-7.68 (m, 4H), 10.12 (m, 2H), 11.28 (s, 1H). ^{13}C NMR (DMSO- d_6): δ_{C} . 177.8, 174.1, 163.1, 134.8, 133.2, 126.8, 122.2 (3C), 121.7 (2C), 110.9, 109.6, 52.8, 32.7, 28.7. EI-MS m/z (Calcd. for $\text{C}_{16}\text{H}_{17}\text{N}_3\text{O}_4$: 315.12; Found: 316.14 (M+H) $^+$. Anal Calcd for $\text{C}_{16}\text{H}_{17}\text{N}_3\text{O}_4$: C, 60.94; H, 5.43; N, 13.33; Found: C, 60.99; H, 5.47; N, 13.35.

Preparation of Methyl 4-oxo-4-(4-(Tetrahydrofuran-2-carboxamido)phenylamino)butanoate (T20): The compound was prepared according to the general procedure C using **5h** (0.5g, 1.6 mmol) to get an off white solid, Yield (0.36g, 70 %) ^1H NMR (DMSO- d_6): δ_{H} . 1.79-1.92 (m, 2H), 2.04-2.35 (m, 2H), 2.58-2.68 (m, 4H), 3.65 (s, 3H), 3.69-3.82 (m, 2H), 4.70 (m, 1H), 7.62-7.69 (m, 4H), 10.13 (s, 2H). ^{13}C NMR (DMSO- d_6): δ_{C} . 177.6, 173.1, 171.7, 134.4, 122.4 (2C), 122.0 (2C), 84.6, 67.8, 60.3, 32.3, 31.9, 28.8, 24.7. EI-MS m/z

(Calcd. for $C_{16}H_{20}N_2O_5$: 320.14; Found: 321.34 (M+H)⁺. Anal Calcd for $C_{16}H_{20}N_2O_5$: C, 59.99; H, 6.29; N, 8.74; Found: C, 60.02; H, 6.27; N, 8.76.

General procedure for the preparation of N-(4-(4-Hydrazinyl-4-oxobutanamido)phenyl) 5-membered heterocyclic -2-carboxamide (T21-T28): Procedure D: To a stirred solution of compound T6 (0.2g) in ethanol (15 ml) 30% hydrazine hydrate (0.5 mL) was added and refluxed for 4h (monitored by TLC) to get a solid which was filtered and recrystallized from ethanol to afford the corresponding desired hydrazine derivative in moderate yield.

Preparation of N-(4-(4-Hydrazinyl-4-oxobutanamido)phenyl)furan-2-carboxamide (T21):

The compound was prepared according to the general procedure D using 6a (0.2g, 1.6 mmol) to get brown gammy; Yield (0.13g, 65%); ¹H NMR (DMSO-d₆): δ_H. 1.98(s, 2H), 2.50-2.52 (m, 4H), 6.79-6.88 (m, 1H), 7.12 (*J* = 2.3 Hz ,d ,1H), 7.41 (*J* = 2.7 Hz, d, 2H), 7.50 (*J* = 3.8 Hz ,d, 2H), 7.82 (*J* = 2.2 Hz, d, 1H), 8.0 (s, 1H), 10.12 (s, 2H). ¹³C NMR (DMSO-d₆): δ_C. 177.7, 177.6, 164.2, 148.1, 143.2, 135.2, 134.2, 122.8 (2C), 122.2 (2C), 116.2, 111.9, 34.3, 32.1. EI-MS m/z (Calcd. for $C_{15}H_{16}N_4O_4$: 316.12); Found: 315.33 (M-H)⁻. Anal Calcd. for $C_{15}H_{16}N_4O_4$: C, 56.96; H, 5.10; N, 17.71; Found; C, 56.90; H, 5.11; N, 17.67.

Preparation of N-(4-(4-Hydrazinyl-4-oxobutanamido)phenyl)-5-methylfuran-2-carboxamide (T22): The compound was prepared according to the general procedure D using 6b (0.2g, 1.6 mmol) to get brown gammy; Yield (0.12g, 62%); ¹H NMR (DMSO-d₆): δ_H. 2.01 (s, 2H), 2.29 (s, 3H), 2.52-2.54 (m, 4H), 6.4 (*J* = 2.4 Hz, d, 1H), 7.0 (*J* = 2.0 Hz, d, 1H), 7.4 (*J* = 3.0 Hz , d, 2H), 7.6 (*J* = 3.8 Hz, d, 2H), 8.92 (s, 1H), 9.93-9.95 (s, 2H). ¹³C NMR (DMSO-d₆): δ_C. 177.5, 177.2, 162.5, 156.8, 143.1, 134.0, 133.1, 122.6 (2C), 122.1 (2C), 115.1, 107.2, 33.5,

31.0, 14.1. EI-MS m/z (Calcd. For $C_{16}H_{18}N_4O_4$: 330.14); Found: 329.12 (M-H)⁻. Anal Calcd for $C_{16}H_{18}N_4O_4$: C, 58.17; H, 5.49; N, 16.96; Found: C, 58.10; H, 5.37; N, 16.83.

Preparation of N-(4-(4-Hydrazinyl-4-oxobutanamido)phenyl)-5-nitrofur-2-carboxamide

(T23): The compound was prepared according to the general procedure D using **6c** (0.2g, 1.6 mmol) to get brown gammy; Yield (0.13g, 65 %); ¹H NMR (DMSO- d_6): δ_H . 2.52-2.54 (m, 4H), 4.23 (s, 2H), 7.59 (J = 3.1 Hz, d, 2H), 7.63 (J = 3.8 Hz, d, 2H), 7.90 (J = 2.6 Hz, d, 1H), 8.1 (J = 2.2 Hz, d, 1H), 8.86 (s, 1H), 10.1 (s, 2H), 11.98 (s, 1H). ¹³C NMR (DMSO- d_6): δ_C . 177.6, 177.3, 162.8, 154.1, 150.7, 134.0, 133.2, 122.5 (2C), 121.9 (2C), 116.5, 116.1, 33.5, 31.8. EI-MS m/z (Calcd. For $C_{15}H_{15}N_5O_6$: 361.10); Found: 362.31 (M+H)⁺. Anal Calcd for $C_{15}H_{15}N_5O_6$: C, 49.86; H, 4.18; N, 19.38; Found: C, 49.91; H, 4.20; N, 19.34.

Preparation of N-(4-(4-Hydrazinyl-4-oxobutanamido)phenyl)thiophene-2-carboxamide

(T24): The compound was prepared according to the general procedure D using **6d** (0.2g, 1.6 mmol) to get brown solid; Yield (0.14g, 70 %); ¹H NMR (DMSO- d_6): δ_H . 2.50-2.55 (m, 4H), 4.10 (s, 2H), 7.22-7.28 (m, 1H), 7.58-7.61 (m, 4H), 7.92 (J = 2.5 Hz, d, 1H), 8.27 (J = 2.4 Hz, d, 1H), 8.82 (s, 1H), 10.12 (s, 2H). ¹³C NMR (DMSO- d_6): δ_C . 177.8, 177.5, 160.7, 140.0, 134.2, 133.5, 132.9, 130.6, 128.7, 122.1 (2C), 121.6 (2C), 33.6, 30.9. EI-MS m/z (Calcd. For $C_{15}H_{16}N_4O_3S$: 332.09); Found: 333.11 (M+H)⁺. Anal Calcd for $C_{15}H_{16}N_4O_3S$: C, 54.20; H, 4.85; N, 16.86; Found: C, 54.27; H, 4.73; N, 16.89.

Preparation of N-(4-(4-Hydrazinyl-4-oxobutanamido)phenyl)-5-methylthiophene-2-

carboxamide (T25): The compound was prepared according to the general procedure D using **6e** (0.2g, 1.6 mmol) to get brown solid; Yield (0.13g, 69 %); ¹H NMR (DMSO- d_6): δ_H . 2.37 (s, 3H), 2.53-2.60 (m, 4H), 4.12 (s, 2H), 6.95 (J = 2.5 Hz, d, 1H), 7.52-7.69 (m, 4H), 7.78 (J = 2.8

Hz, d, 1H), 8.81 (s, 1H), 10.2 (s, 2H). ^{13}C NMR (DMSO- d_6): δ_{C} . 177.6, 177.1, 161.9, 153.1, 135.7, 133.9, 133.0, 129.3, 128.3, 122.6 (2C), 121.9 (2C), 33.8, 32.0, 14.9. EI-MS m/z (Calcd. For $\text{C}_{16}\text{H}_{18}\text{N}_4\text{O}_3\text{S}$: 346.11; Found: 347.23 (M+H) $^+$. Anal Calcd for $\text{C}_{16}\text{H}_{18}\text{N}_4\text{O}_3\text{S}$: C, 55.48; H, 5.24; N, 16.17; Found: C, 55.50; H, 5.26; N, 16.20.

Preparation of N-(4-(4-Hydrazinyl-4-oxobutanamido)phenyl)-5-nitrothiophene-2-carboxamide (T26): The compound was prepared according to the general procedure D using **6f** (0.2g, 1.6 mmol) to get yellow solid; yield (0.12g, 63 %); ^1H NMR (DMSO- d_6): δ_{H} . 2.58-2.61 (m, 4H), 4.18 (s, 2H), 7.58-7.69 (m, 4H), 7.98 ($J = 2.8$ Hz, d, 1H), 8.21 ($J = 3.0$ Hz, d, 1H), 8.89 (s, 1H), 10.21 (s, 2H). ^{13}C NMR (DMSO- d_6): δ_{C} . 177.7, 177.4, 168.6, 161.0, 146.8, 138.9, 134.6, 133.4, 130.9, 122.4 (2C), 121.9 (2C), 33.8, 32.0. EI-MS m/z (Calcd. $\text{C}_{15}\text{H}_{15}\text{N}_5\text{O}_5\text{S}$: 377.08; Found: 378.13 (M+H) $^+$. Anal Calcd for $\text{C}_{15}\text{H}_{15}\text{N}_5\text{O}_5\text{S}$: C, 47.74; H, 4.01; N, 18.56; Found: C, 47.84; H, 4.03; N, 18.46.

Preparation of N-(4-(4-Hydrazinyl-4-oxobutanamido)phenyl)-1H-pyrrole-2-carboxamide (T27): The compound was prepared according to the general procedure D using **6g** (0.2g, 1.6 mmol) to get brown solid; Yield (0.12g, 60 %); ^1H NMR (DMSO- d_6): δ_{H} . 2.56-2.65 (m, 4H), 4.20 (s, 2H), 6.44-6.48 (m, 1H), 7.46 ($J = 2.4$ Hz, d, 1H), 7.57 ($J = 3.0$ Hz, d, 1H), 7.59-7.64 (m, 4H), 8.86 (s, 1H), 10.01 (s, 2H), 11.45 (s, 1H). ^{13}C NMR (DMSO- d_6): δ_{C} . 178.0, 177.4, 162.8, 134.7, 133.3, 126.9, 121.9 (3C), 121.4 (2C), 110.6, 109.2, 33.8, 32.1. EI-MS m/z (Calcd. for $\text{C}_{15}\text{H}_{17}\text{N}_5\text{O}_3$: 315.13; Found: 316.13 (M+H) $^+$. Anal Calcd for $\text{C}_{15}\text{H}_{17}\text{N}_5\text{O}_3$: C, 57.13; H, 5.43; N, 22.21; Found: C, 57.16; H, 5.42; N, 22.24.

Preparation of N-(4-(4-Hydrazinyl-4-oxobutanamido)phenyl)tetrahydrofuran-2-carboxamide (T28): The compound was prepared according to the general procedure D using **6h** (0.2g, 1.6 mmol) to get brown solid; Yield (0.13g, 68 %); ^1H NMR (DMSO- d_6): δ_{H} . 1.81-1.92 (m, 2H), 2.06-2.32 (m, 2H), 2.55-2.64 (m, 4H), 3.71-3.80 (m, 2H), 4.18 (s, 2H), 4.70 (m, 1H), 7.62-7.69 (m, 4H), 8.86 (s, 1H), 10.03 (s, 2H). ^{13}C NMR (DMSO- d_6): δ_{C} . 177.5, 176.9, 171.3, 134.3, 122.3 (2C), 121.9 (2C), 84.5, 67.5, 33.9, 32.1, 25.1. EI-MS m/z (Calcd. for $\text{C}_{15}\text{H}_{20}\text{N}_4\text{O}_4$: 320.15; Found: 321.32 (M+H) $^+$). Anal Calcd for $\text{C}_{15}\text{H}_{20}\text{N}_4\text{O}_4$: C, 56.24; H, 6.29; N, 17.49; Found: C, 56.26; H, 6.30; N, 17.50.

APPENDIX

LIST OF PUBLICATIONS

FROM THESIS WORK

1. Structure-guided design and development of novel benzimidazole class of compounds targeting DNA gyraseB enzyme of *Staphylococcus aureus*. **Janupally Renuka.**, Jeankumar V.U., Bobesh K.A., Soni V., Devi P.B., Pulla V.K., Suryadevara P., Chennubhotla K.S., Kulkarni P., Yogeeswari P., Sriram D. *Bioorg Med Chem.* **2015**, 23, 1661-3
2. Design and Biological Evaluation of Furan/Pyrrole/Thiophene-2-carboxamide Derivatives as Efficient DNA GyraseB Inhibitors of *Staphylococcus aureus*. **Janupally Renuka.**, Medepi B., Brindha Devi P., Suryadevara P., Jeankumar V.U., Kulkarni P., Yogeeswari P., Sriram D. *Chem Biol Drug Des.* **2015**, 125-29.

OTHER PUBLICATIONS

1. Design, synthesis, biological evaluation of substituted benzofurans as DNA gyrase B inhibitors of Mycobacterium tuberculosis. **Janupally Renuka** , Kummetha Indrasena Reddy, Konduri Srihari, Variam Ullas Jeankumar *et.al Bioorganic and Medicinal Chemistry*, **2014**, *22*, 6552-63.
2. Extending the N-linked aminopiperidine class to the mycobacterial gyrase domain: pharmacophore mapping from known antibacterial leads. Bobesh K.A, **Renuka Janupally**, Jeankumar V.U, Shruti S.K, Sridevi J.P, Yogeeswari P, Sriram D. *Eur J Med Chem.* **2014**, *6*, 593-604.
3. Thiazole-Aminopiperidine hybrid analogues: Design and synthesis of novel Mycobacterium tuberculosis Gyr B inhibitors Variam Ullas Jeankumar, **Janupally Renuka**, *et al.*, *Eur J Med Chem.* **2013**, *70*, 143-53.
4. Synthesis and evaluation of 1-cyclopropyl-6-fluoro-1,4-dihydro-4-oxo-7-(4-(2-(4-substitutedpiperazin-1-yl)acetyl)piperazin-1-yl)quinoline-3-carboxylic acid derivatives as anti-tubercular and antibacterial agents. Suresh N., Nagesh H.N., **Renuka Janupally**, Rajput V., Sharma R., Khan *et al.*, *Eur J Med Chem.* **2014**, *71*, 324-32.
5. Development of Novel N-linked Aminopiperidine based Mycobacterial DNA Gyrase B inhibitors: Scaffold hopping from known Antibacterial lead. Variam Ullas Jeankumar, **Renuka Janupally**, Venkat Koushik Pulla, *et al.*, *Int J Antimicrob Agents.* **2014**, *43*, 269-78.

6. Gyrase ATPase domain as an antitubercular drug discovery platform: Structure based design and lead optimization of nitrothiazolyl-carboxamides analogues . Variam Ullas Jeankumar, **Janupally Renuka**, Sonali Kotagiri, *et al.*, *Chemmedchem*, **2015**, 23, 588-601.

7. Mycobacterial DNA Gyr B inhibitors: Ligand based pharmacophore modelling and in vitro enzyme inhibition studies. Shalini Saxena, **Renuka Janupally**, Variam Ullas Jeankumar, *et al.*, *Curr Top Med Chem*. **2014**, 14, 1990-2005.

Discovery of novel mycobacterial DNA gyrase B inhibitors: In silico and *in vitro* biological evaluation. Shalini Saxena, **Janupally Renuka et al.**, *Molecular informatics*, **2014**.

8. Development of benzo[d]oxazol-2(3H)-ones derivatives as novel inhibitors of Mycobacterium tuberculosis InhA. Pedgaonkar G.S, Sridevi JP, Jeankumar V.U, Saxena S, Devi P.B, **Renuka Janupally**, Yogeeswari P, Sriram D., *Bioorg Med Chem*. **2014**, 22, 6134-45

9. Development of 2-(4-oxoquinazolin-3(4H)-yl)acetamide derivatives as novel enoyl-acyl carrier protein reductase (InhA) inhibitors for the treatment of tuberculosis. Pedgaonkar G.S, Sridevi J.P, Jeankumar V.U, Saxena S, Devi P.B, **Renuka Janupally**, Yogeeswari P, Sriram D. *Eur J Med Chem*. **2014**, 30;86:613-27.

10. An efficient synthesis and biological screening of benzofuran and benzo[d]isothiazole derivatives as Mycobacterium tuberculosis DNA Gyr B inhibitors. Kummetha Indrasena Reddy, Konduri Srihari, **Janupally Renuka**, Variam Ullas Jeankumar *et al.*, *Eur J Med Chem*. **2014**, 22, 6552-63.

PAPERS PRESENTED AT NATIONAL/INTERNATIONAL CONFERENCES

1. **Renuka, J***, JeanKumar, V., Bobesh, A., Vijay, S., Devi, P.B., Venkat, K.P., Priyanka, S., Keerthana, S., Pushkar, K., Yogeewari, P., Sriram, D., Design and biological evaluation of novel antibacterial inhibitors against DNA Gyr B from clinical isolates of *Staphylococcus aureus*. Gordon Research Conferences, 10-15th August 2014, Maine, USA.

2. **J Renuka***, P. Yogeewari, D. Sriram, Insilico design and invitro assay of inhibitors for pathogenic *Staphylococcus aureus* DNA Gyrase, 3rd World Congress on Biotechnology, 13-15 September 2012, Hyderabad, India.

3. **J. Renuka***, M. Shravan*, P. Yogeewari, D. Sriram, Design and biological evaluation of novel *Staphylococcus aureus* DNA gyrase inhibitors. International Conference on "Drugs for the Future: Infectious Diseases", Antimicrobial Drug Discovery: Challenges and Perspectives, 27-28 March 2014, NIPER, Hyderabad, India.

4. **J. Renuka ***, P. Yogeewari, D. Sriram, Insilico design and Biological evaluation of novel inhibitors for pathogenic *Staphylococcus aureus* DNA Gyrase, Current trends in pharmaceutical Sciences, 17 November, 2012, Hyderabad, India.

BIOGRAPHY OF RENUKA J

Mrs. Renuka J completed her Bachelor of Science from Nizam college, Hyderabad and Master of Science in Biotechnology from Osmania University, Hyderabad. She has about 6 months training experience from Biological e-limited as a part of BCIL trainee in R&D department.. She has been appointed as a Junior Research Fellow at Birla Institute of Technology and Science, Pilani, Hyderabad campus from 2012-2013 under the supervision of D. Sriram. She has later qualified for CSIR-SRF fellowship sponsored by Council of Scientific and Industrial Research and Industrial, Delhi. She as published twenty scientific publications in well-renowned international journals and presented papers at various national and international conferences

BIOGRAPHY OF PROFESSOR. D. SRIRAM

D. Sriram is presently working in the capacity of Professor at Department of Pharmacy, Birla Institute of Technology and Science, Pilani, Hyderabad campus. He received his Ph.D. in 2000 from Banaras Hindu University, Varanasi. He has been involved in teaching and research for last 14 years. He has 250 peer-reviewed research publications to his credit. He has collaborations with various national and international organizations such as Karolinska institute, Sweden; the Indian Institute of Science, Bangalore and National Institute of Immunology, New Delhi. He was awarded the Young Pharmacy Teacher of the year award of 2006 by the Association of Pharmacy Teachers of India. He received ICMR Centenary year award in 2011. He has guided 8 Ph.D. students and 13 students are pursuing Ph.D currently. His research is funded by agencies like the UGC, CSIR, ICMR, DBT and DST.